ADHESIVE BONDING OF ALUMINIUM

by Anthony Maddison

Submitted for the degree of Ph.D., August, 1983.

at The University of Aston in Birmingham

The University of Aston in Birmingham

ADHESIVE BONDING OF ALUMINIUM

By Anthony Maddison

Submitted for the degree of Ph.D., 1983.

Summary

Adhesive bonding of aluminium is widely used in the aerospace industry. High initial bond strengths can be obtained, but bond failure occurs after prolonged exposure to humid environments. The thesis contains details of a test procedure which has been designed and developed for the assessment of different alloys, pretreatments, and adhesives which will give adhesively bonded aluminium joints of high strength coupled with long term durability. The test involves assembly of lap shear specimens in a precision jig using 250μm ballotini spacers in the adhesive to control the bond line thickness. The test is modified by drilling three accurately located holes through the bonded area after assembly of the joint and curing of the adhesive. Further important features of the test, such as fillet control, are detailed. The test was assessed, modified and developed to give a reliable and reproducible method which would discriminate amongst different bonding systems after exposure to humid test environments. This is the first test to have achieved the discrimination necessary for short term assessment of bond systems where long term durability is required. Even better discrimination has been obtained by applying stress in a stress humidity test.

Having established accurate, reliable and discriminating test methods they were used to study the durability of structural epoxy adhesive bonds to aluminium as a function of alloy, pretreatment, adhesive and environment. It was established that the long term durability of adhesively bonded aluminium was directly related to the influence of water migrating within the adhesive. Pretreatments differed in their ability to prevent hydration of the aluminium oxide by the water absorbed within the adhesive.

Key words: adhesive bonding, aluminium, environmental testing.

Dedicated to Mary and Albert, Robert and James

CONTENTS

List of figures and tables

CHAPTER 2

CHAPTER 3

CHAPTER 4

CHAPTER 5

Acknowledgements

I wish to express my sincere gratitude to Dr. D.J. Arrowsmith of Aston University for his enthusiastic supervision of this project and to the SERC and B.L. Technology for granting an Industrial Studentship.

I am also indebted to Mr. P.G. Selwood and Dr. D. Kewley for external supervision and support, and to my colleagues in the B.L. Technology Laboratory at Solihull.

I much appreciate the assistance of Messrs. H. Mills and G. Stokes of the photographic department of B.L.T. at Webb Lane, Mrs. C. Catton of Pyrene Ltd., Dr. J. Treverton of Alcan Research Laboratories, and Dr. J. Comyn of Leicester Polytechnic.

Finally, I would like to sincerely thank Mrs. P. Darling for typing this thesis.

CHAPTER 1

INTRODUCTION

In 1944 a new twin engine fighter, the de Havilland Hornet, came into service. It was the fastest combat aircraft that the R.A.F. had then received. It was also the first to use structural adhesive bonding of metals. The airframe was mainly constructed of wood but the tension flanges in the spars were made of bonded aluminium alloy and the joint between the wood and the aluminium was bonded with vinyl-phenolic adhesive. Some metal-to-metal adhesive bonding was also used to build up sheet thickness at points of attachment such as that of the tail wheel bracket.(1) The success of adhesive bonding in the Hornet led to its adoption in the stringer-skin joints in the all-metal Dove and then in the Comet.(2) To-day, in 1983, after progressive development and proven performance of adhesive bonding of aircraft in service, the design of the latest British Aerospace jet aircraft, the B.Ae. 146, is based on the use of metal-to-metal adhesive bonded structures throughout and incorporates the largest bonded wing panels in production.(3)

Structural adhesive bonding is now widely used in the aircraft and aerospace industries where the cost of production, though always important is often not as important as weight-saving. Only since the mid-1970's has weight-saving become important in the motor industry.

In 1982, BL Technology Ltd. demonstrated an experimental vehicle ECV3 designed to give exceptionally good fuel economy.(4) A reduction in body weight was achieved by using aluminium instead of steel for the basic structure of the car. The design of the

aluminium monocoque base was achieved with the help of finite element computer modelling to optimize the stiffnesss-to-weight ratio. The stiffness was enhanced by the use of adhesive bonding to supplement the mechanical fixing of joints. Adhesive bonding was also used to overcome the problem associated with the welding of aluminium. However, no details of the surface preparation prior to bonding, nor of the adhesive used were given.

B.L. stated that the ECV3 was not a production prototype but an experimental car to test and evaluate ideas, components, materials and processes."

The aim of the work described in this thesis was to develop reproducible and discriminating techniques to assess the durability of adhesively bonded aluminium joints and thereby enable a better understanding of the scientific mechanisms involved. The thesis contains results of experiments carried out as part of an on-going research programme developing the technology for the mass production by the motor industry of adhesively bonded aluminium joints which have long term durability in the range of environments encountered by vehicles in service.

CHAPTER 2 LITERATURE SURVEY

2. Introduction

Kinloch [5] defined an adhesive as a material which when applied to substrate surfaces can join them together and resist separation. As a means of joining materials, the use of adhesives offers many advantages when compared with other more conventional methods such as welding, riveting, bolting, etc. The advantages include:

(a) the ability to join dissimilar materials,

(b) the ability to join thin sheet materials efficiently,

(c) an improved stress distribution in the joint which imparts, for example, an increase in fatigue resistance to the bonded component,

(d) an increase in the design flexibility,

(e) it is often the most convenient and cost effective technique.

These advantages have led to a continuing increase in the use of adhesives. However, a fundamental knowledge of the nature of the forces of attraction between bodies, determination of the magnitude of such intrinsic forces, and their relation to measured adhesive joint strengths has lagged behind the applied technology. Indeed, for many adhesive/substrate interfaces of considerable practical importance there are still unresolved debates concerning the detailed mechanisms of adhesion and the mechanics of joint rupture. One of the main reasons why the theory has followed behind the technology is that the science of adhesion is a truly multi-disciplinary subject. Surface chemistry and physics, rheology, polymer chemistry and physics, stress analysis and fracture analysis have all to be considered in the interpretation of adhesion experiments.

The many books and publications [5-18] on the topic of adhesion and adhesives illustrate this point. Kinloch [5,6] has published a critical assessment of recent published works on those aspects of adhesion science which are relevant to the adhesive joining of materials. Much of the literature survey in this thesis is based on Kinloch's review.

2.1.1. Interfacial Contact

The establishment of intimate molecular contact at the interface is a necessary, though sometimes insufficient, requirement for developing strong adhesive joints. The adhesive needs to be able to be spread over the solid substrate surface, and needs to displace air and any other contaminants that may be present on the surface. An adhesive which conforms ideally to these conditions must [19]:-

(a) when liquid, exhibit a zero or near zero contact angle,

(b) at some time during the bonding operation have a viscosity that should be relatively low, e.g. no more than a few centipoises,

(c) be brought together with the substrate with a rate and manner that should assist the displacement of any trapped air.

In order to assess the ability of a given adhesive/substrate combination to meet these criteria it is necessary to consider wetting equilibria, to ascertain values of the surface free energies of the adhesive and substrate and the free energy of the adhesive/substrate interface and to examine the kinetics of the wetting process.

2.1.2. Wetting Equilibria

Surface tension is a direct measurement of intermolecular forces. The tension in surface layers is the result of the attraction of the bulk material for the surface layer and this attraction tends to reduce the number of molecules in the surface region resulting in an increase in the intermolecular distance. This increase requires work to be done, and returns work to the system upon a return to a normal configuration. This explains why tension exists and why there is a surface free energy. The most common type of physical surface attractive forces are the van der Waals forces resulting from (a) dispersion (or London) forces arising from internal electron motions which are independent of dipole moments and (b) polar (or Keesom) forces arising from the orientation of permanent electric dipoles and the induction effect of permanent dipoles or polarizable molecules. The dispersion forces are usually weaker than the polar forces but they are universal and all materials exhibit them. Another type of force that may operate is the hydrogen bond, formed as a result of the attraction between a hydrogen atom and a second, small and strongly electronegative atom such as a fluorine, oxygen or nitrogen.

Wetting may be quantitatively defined by reference to a liquid drop resting in equilibrium on a solid surface as shown in Fig 2.1.

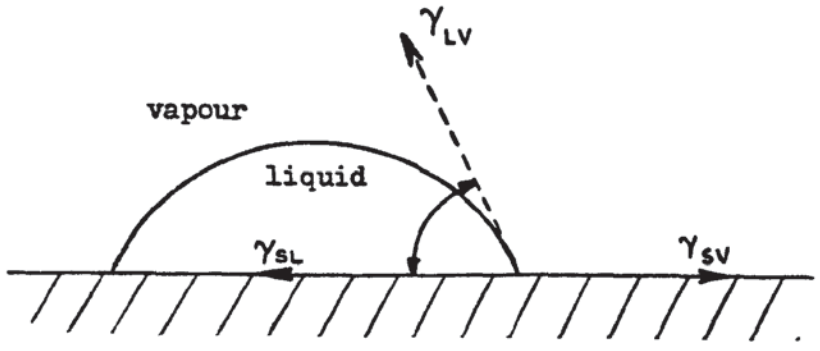

Fig 2.1. A liquid drop resting at equilibrium on a solid surface.

The tensions at the three phase contact point are indicated such that LV is the liquid/vapour point, SL is the solid/liquid point and SV is the solid/vapour point. The Young equation relating these tensions to the equilibrium contact angle θ may be written as

$$\gamma_{SV} = \gamma_{SL} + \gamma_{LV} \cos\theta \qquad (1)$$

The term γ_{SV} represents the surface free energy of the solid substrate resulting from adsorption of vapour from the liquid and may be considerably lower in value than the surface free energy of the solid in vacuo γ_S. This reduction in the surface free energy of the solid when covered by a layer of vapour has been defined by the concept of equilibrium spreading pressure, π_S, where,

$$\pi_S = \gamma_S - \gamma_{SV} \qquad (2)$$

Thus Equation 1 may be re-written as

$$\gamma_S = \gamma_{SL} + \gamma_{LV} \cos\theta + \pi_S \qquad (3)$$

When $\theta > 0^\circ$ the liquid is nonspreading but when $\theta = 0^\circ$ the liquid wets the solid completely and spontaneously and spreads freely over the surface at a rate depending on the liquid viscosity and solid surface roughness. Thus for spontaneous wetting to occur $\gamma_{SV} \geq \gamma_{SL} + \gamma_{LV}$ (4)

$$\gamma_S \geq \gamma_{SL} + \gamma_{LV} + \pi_S \qquad (5)$$

It is also possible for a liquid to spread and wet a solid surface even when $\theta > 0^\circ$ but this requires the application of a pressure or force to the liquid to forcibly spread it over the solid surface.

2.2. Surface and interfacial free energies

A distinction may be made between low-energy and high-energy solid surfaces. Organic compounds, such as polymers, belong to the first group and their surface free energies are usually less than 100 $mJm.^{-2}$ Metals, metal oxides, and ceramics belong to the second group and their surface free energies are typically greater than 500 $mJm.^{-2}$

Sharpe and Schonhorn [20] have emphasised the importance of wetting and proposed that the single most important factor influencing adhesive joint strength is the ability of the adhesive to spread spontaneously on the substrate when the joint is initially formed. They developed a criterion from Equation (4) for the case when the adhesive will spontaneously spread on the substrate and, by ignoring the interfacial free energy, proposed that the γ_c of the adhesive must be less than that of the substrate where γ_c is the critical surface tension of a liquid which will just spread on the surface giving a zero contact angle. They showed, for example, that high joint strength should not result, and has been observed not to result, when polyethylene substrates are bonded using an epoxy-amine adhesive but that polyethylene should, and does, adhere strongly when melted against a cured epoxy-amine solid substrate. This arises because , in the former case

γ_{LV} (epoxy-amine adhesive) $> \gamma_c$ (polyethylene substrate)

and hence wetting is limited, while in the latter case

γ_{LV} (polyethylene adhesive) $< \gamma_c$ (cured epoxy-amine substrate)

and so spontaneous wetting occurs. Indeed, the requirement

for the low surface free energy of polyethylene and similar substrates to be increased is a major reason why surface modification of such materials is often necessary prior to bonding [21]. Thus the Sharpe and Schonhorn [20] criterion essentially proposes that a mobile, liquid adhesive with small or zero contact angle, which will spread readily, flow into crevices, and achieve true contact with little opportunity for the voids which may act as stress concentrators, is of prime importance. Further work has since suggested that an additional requirement is that the interfacial free energy, γ_{SL} should be as low as possible.[22-25]

Schonhorn has since considerably modified his views (see Section 2.6.5.)and Huntsberger's [26] analysis indicates that good adhesives are not necessarily those which exhibit low or zero contact angle with the substrate. Huntsberger's analysis stresses the importance of wetting as a kinetic process for, although the thermodynamics may indicate the establishment of intimate molecular contact, the kinetics of wetting may be the determining factor.

2.3. Kinetics of wetting

Bascom et al [27, 28] have shown that if the contact angle is zero, surface tension gradients may exist at the spreading front which may assist or hinder spreading depending upon their direction. These surface tension gradients arise from thermal gradients or, in the case of liquids containing a more volatile

component of different surface free energy, such as a trace impurity, they may arise from a concentration gradient. This effect is illustrated in Fig 2.2 and at the leading edge of the spreading liquid there is a thin (either 1 or 2 monomolecular layers) primary film which is followed by a transition region in which thermal or concentration gradients create a surface tension gradient and thereby a surface flow that drags the underlying liquid forward.

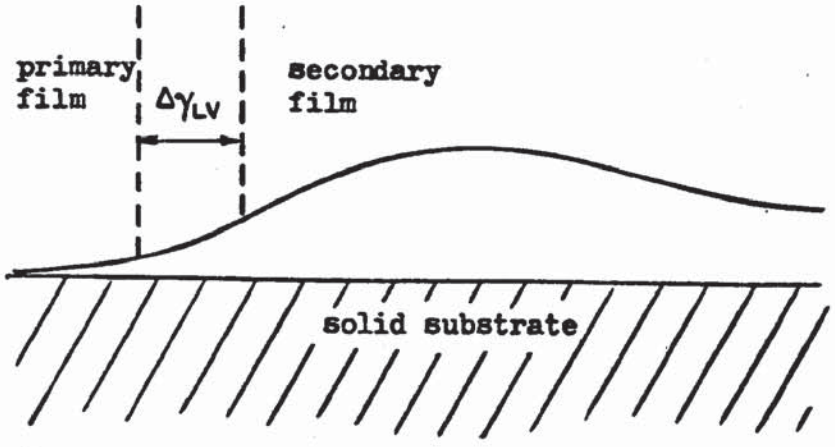

Fig 2.2. Schematic diagram of the surface and bulk flow patterns at the leading edge of a spontaneously spreading film, after Bascom and Patrick [27]

The rate of flow in the transition region may exceed the rate of gravity flow in the much thicker secondary film so that a ridge of liquid develops. Spreading rates resulting from this gradient effect are relatively low.

The topography of the substrate surface may also influence the kinetics of wetting.

Firstly, a liquid forming a contact angle of less than 90^{o} with a solid surface may spread along fine pores, scratches and other inhomogeneities by capillary action, even though it may be non-wetting on a planar surface. Bascom et al [28] have reported that random surface scratches increased the spreading rate of some liquids by as much as fifty per cent and that open capillaries filled well ahead of the diffusional advance of the primary film. Similar observations have been recorded by Cottington et al [29]. Cheever [30] has studied zinc phosphate conversion coatings and treated the situation theoretically as a capillary matrix in which the capillaries assume the particular shape of slits. A mathematical and physical model was derived from Poiseuille's equation which adequately described the flow of liquid in zinc phosphated steel substrates, and gave the capillary pressure which was generated in the zinc phosphate coating to be about 0.7MPa. However, spreading rates from this effect and surface tension gradients are not high and may be overshadowed when a liquid adhesive is forcibly spread over such a surface. Nevertheless Bascom and Patrick [27] have suggested that such effects may

play a role in the redistribution of the adhesive after its initial application. Secondly, Wenzel [31] has shown that another effect of surface roughness is to change the apparent contact angle, θ', observed for the rough solid, compared to the same angle, θ, observed for the smooth surface. This change in the apparent contact angle can be expressed by

$$\cos \theta' = r \cos \theta \qquad (6)$$

where r is the roughness factor or the ratio of the actual area to the projection area of the solid. On a smooth surface, if θ is less than 90° roughening the surface will result in θ' being even smaller, thus increasing the apparent surface free energy of the solid surface and consequently also the extent of wetting. However, if θ is greater than 90° on a smooth surface roughening the surface will increase the contact angle θ' still further and decrease the degree of wetting. Other, more sophisticated models of substrate surface topography have since been developed [32-37] to take account of advancing and receding contact angles and contact angle hysteresis (i.e. the difference often observed in the value of these two angles). Thirdly, de Bruyne [38] has modelled various types of substrate surface topography and obtained quantitative expressions for the relationship between the extent of wetting and the driving pressure. Fig. 2.3. shows the capillary penetration to be expected, under atmospheric pressure and against the back pressure of trapped air, as a function of the contact angle made on the solid by the penetrating liquid. The limited penetration

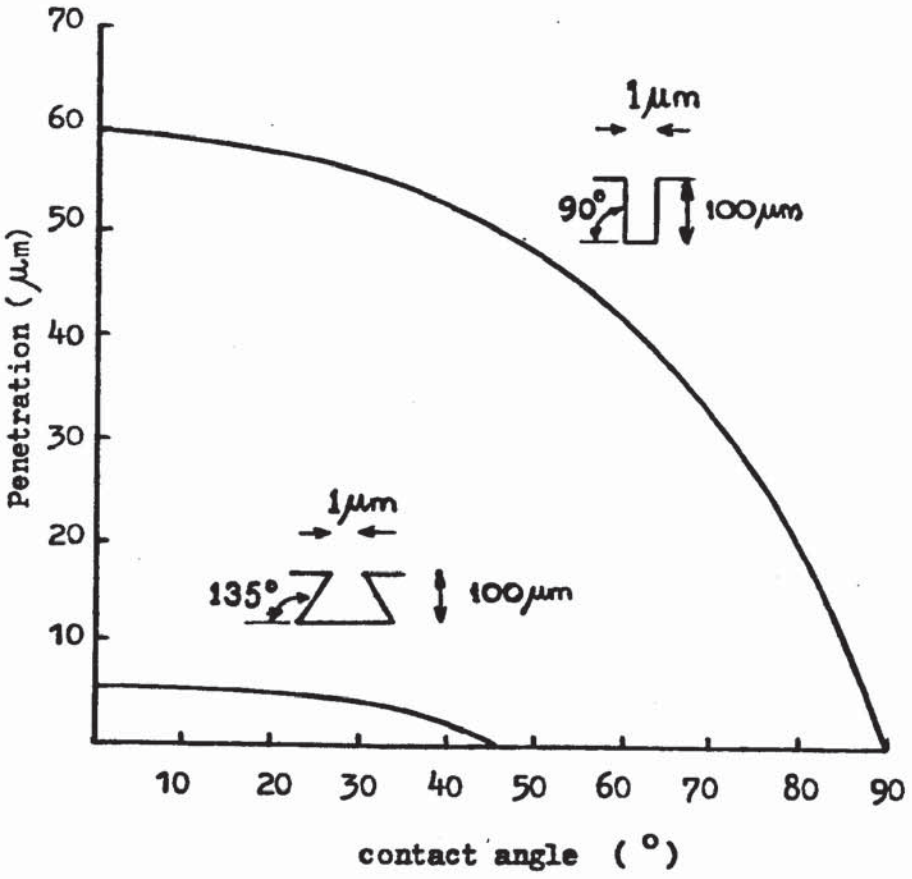

Fig 2.3. Comparison of the penetration of a film into cylindrical and "ink-bottle" pits, after De Bruyne (38)

into the "ink-bottle" pits is expecially marked and this effect will be heightened if the liquid has a viscosity greater than a few tens of centipoises and is forced rapidly across the substrate surface. Under such circumstances the liquid near the surface cannot keep up with the advancing front so that a higher dynamic contact angle develops [27,39,40]. Various workers [41-43] have examined the kinetics of wetting of molten polymers on substrates by following the change in the contact angle of molten polymers as a function of time at different temperatures. Schonhorn et al [41] have demonstrated that the ratios of the cosine of the contact angle, θ_t, at a time, t, to the cosine of the contact angle, θ_∞ at an infinite time, could be superimposed, using a time-temperature equivalence, to give a single master curve. Newman [44] and Cherry and Holmes [42] have reported that this time-temperature dependence may be expressed by

$$\cos\theta_t = \cos\theta_\infty \left[1 - \alpha e^{-ct}\right]$$

where α and c are constants and where [41] $c = \gamma_{LV}/\eta L$

where η is the viscosity of the polymer and L a parameter with dimensions of length [42,45] and related to the adhesive/substrate interaction.

Cherry and Holmes also concluded that the spreading of a molten polymer across a metal surface could be described in terms of an activated rate process in which the activation energy barriers were the same as those which oppose viscous flow, and the

driving force for this derives from the action of surface forces during the replacement of a solid/vapour interface by the solid/liquid interface. In subsequent work [45] the parameter **C** was termed the "wetting constant" and joint strengths were thought to correlate better with a high wetting constant (except for very low values) than with a low contact angle.

2.4. The bonding operation.

2.4.1. Air entrapment.

Bascom and Cottington [46] have studied the mechanism and effects of air entrapment during the preparation of joints with structural film adhesives. Optical microscopy studies on glass/adhesive joints revealed that initially a thin film of air was trapped between the adhesive and glass substrate which usually extended over about half of the interfacial area. As the temperature was raised, to effect cure of the adhesive, this air drew up into bubbles that were eventually displaced into the adhesive layer. However, incomplete displacement occurred if the adhesive had a contact angle greater than zero on the substrate surface or did not become sufficiently fluid during the heat cure. Such air voids may be eliminated if the joint is bonded in any autoclave, where there is a hydrostatic pressure high enough to compress entrapped air to a negligible volume, or by employing a "vacuum release" technique [46]. This latter method simply involves starting the cure in vacuum (about 650 Pa) and subsequently releasing

the vacuum at the temperature at which the resin's viscosity is at a minimum. Air voids may obviously act as stress raisers and, indeed, increases in the peel strength of aluminium epoxy adhesive joints of up to thirty per cent were reported upon complete void removal using the vacuum release technique.

2.4.2. The bonding environment

Other aspects of the bonding operation are the environmental conditions employed and these are particularly important when bonding metallic substrates. Metals and metal oxides are usually classed as high-energy solids since in the ultra-clean state they have surface free energies, γ_s, typically greater than 500 mJm^{-2}. Thus, it would seem, at first, that such a surface would be readily wetted by organic adhesives having low surface free energies (typically less than about 70 mJm^{-2}) once any machine oil, protective greases or other contaminants remaining from the materials production had been removed. However, even in the absence of these obvious impurities a high-energy surface adsorbs water vapour from the atmosphere [47 48] and other contaminants such as nitrogen and organic adsorbates, such as hydrocarbons [49] which lower the surface free energy of the substrate and may prevent spreading of the adhesive. Indeed Bernett and Zisman [50] determined the critical surface tensions, γ_c, of various "clean" hydrophilic, high-energy surfaces at two extreme values of relative humidity, 0.6% r.h. and 95% r.h. and found that the surfaces were converted to

ones of low γ_c (about 46 and 38 mJm $^{-2}$ respectively) and, further, that the γ_c values were almost independent of the actual underlying solid substrate.

Gledhill et al. [50] have recently extended this earlier work by examining the effect of a range of relative humidities on the wettability of the mild-steel surfaces of different roughness and have considered the implications of such data on the strength of joints prepared under different humidities. From the contact angle measurements, the value of γ_{sv} for a polished and grit blasted steel surface was deduced as a function of relative humidity. For the polished surface there was a linear correlation and the results were in good agreements with values previously reported by Bernett and Zisman [50]. For the rougher, grit-blasted surfaces there was a considerably greater variation in the value of γ_{sv} with humidity and, as might be expected from Section 2.3. the value of γ_{sv}(rough) was greater than γ_{sv}(polished). Therefore it is important to ensure that the bonding environment is such that adsorbed contamination is kept to a minimum, the lower the extent of such contamination, the more readily will it be displaced by the adhesive which may then achieve intimate molecular contact with the solid substrate surface. If multilayer contamination is not displaced by the adhesive it will act as a "weak boundary layer" (see Section 2.6.5.) and low joint strengths will result. Finally, it is of interest to note that the presence of

adsorbed hydrocarbons probably assists this displacement process since the common adhesives are usually relatively polar in character and thus will have a thermodynamic tendency to displace such non-polar contamination, especially if only physisorbed. This is particularly significant when considering the adhesive bonding of aluminium sheet in the presence of forming lubricants.

2.5. Orientation at interfaces

Schonhorn [52] has shown that orientated monolayers of amphipathic molecules, such as stearic acid, may be employed as extremely effective adhesives in the bonding of polyethylene to aluminium; indeed, so effective are these adhesives, that joint strengths may exceed the cohesive strength of the polyethylene. Multi-layer adsorption lowered the joint strengths not because of less intrinsic adhesion of the amphipathic molecule to the substrate surface, but because the relatively thick layer possessed low cohesive strength and thus behaved as a weak boundary layer. While chemisorption was thought to occur for the stearic acid on the aluminium oxide [53,54] Wake [55] has speculated that some diffusion occurs across the interface between the alkane chains of the acid and the polyethylene.

Recent elegant work by Baszkin, Nishino and Ter-Minassian-Saraga [56,57,58] has also demonstrated the effect that orientation at the interface may have upon measured joint strengths. They have quantitatively determined the surface densities

of the polar sites on a polyethylene substrate as the surface is oxidised. They showed that as the temperature is raised to between about 80°C and 85°C there is a decrease in wettability, due to the increase of chain mobility, leading to the redistribution of polar groups into the bulk, and that the remaining surface density of polar groups depended upon the nature of the liquid in contact with the polyethylene. This loss of polar groups at elevated temperatures was mirrored by a loss in joint strength.

2.6. Mechanisms of adhesion

Many theories of adhesion are to be found in the current literature. Often, the proponents of each theory offer their hypothesis as a comprehensive explanation of all adhesion phenomena and exclude all the alternative explanations. Much of this confusion undoubtedly arises because the test methods commonly employed to measure the strengths of adhesive joints are not well suited to theoretical analysis. They introduce geometrical factors and loading factors which are difficult to analyse and the measured joint strength includes indeterminate contributions from rheological energy losses in the adhesive and substrate. Thus, although the intrinsic adhesion forces acting across the adhesive/substrate interface may affect joint strength they are usually completely obscured by other contributions, and information concerning the magnitude of such forces may only be indirectly obtained.

This inability to measure the interfacial interactions has been the main obstacle to the development of a comprehensive theory of adhesion.

The four main mechanisms of adhesion which have been proposed are:-

(a) mechanical interlocking

(b) diffusion theory

(c) electronic theory

(d) adsorption theory

2.6.1. Mechanical interlocking

This theory proposes that mechanical interlocking of the adhesive into the irregularities of the substrate surface is the major source of intrinsic adhesion. The attainment of good adhesion between smooth surfaces exposes this theory as not being of general applicability and the results shown in Fig. 2.3. must raise doubts as to whether any significant penetration of adhesive into some configurations of irregular cavities suitable for forming a mechanical key, for example an "ink-pot" type cavity, would normally occur. However, there are some instances where mechanical interlocking has been demonstrated to contribute significantly to the intrinsic adhesion forces. The most notable example of such a significant contribution is the adhesion of polymers to textiles. Borroff and Wake [59-61] convincingly demonstrated that the most important single feature in the adhesion of a simple rubber to an uncoated fabric is the penetration of the protruding fibre ends of the spun yarn into the rubber.

The degree of penetration necessary is such that, upon the rubber-textile structure being stressed, the length of fibre embedded is sufficient for the total shearing force on the fibre/rubber interface to exceed the breaking strength of the fibre. The intrinsic adhesion between fibre and rubber arises from primary or secondary forces, either chemical or van der Waals bonds, but is only of indirect importance since it will simply determine the length of fibre which is needed to be embedded before the interfacial shear strength exceeds the tensile strength of the fibre. If the fibre ends are removed by employing a fabric woven from continuous filament yard then this mechanical interlocking mechanism can no longer operate. Hence when using rayon, nylon or other continuous filament textiles, pre-treatments typically based upon isocyanates or resorcinol-formaldehyde are necessary to increase the contribution from primary and secondary interfacial forces to the intrinsic adhesion [42]

Another example of where mechanical interlocking may contribute significantly to the intrinsic adhesion is the metal plating of polymers where a chemical pre-treatment of the polymeric substrate is employed prior to plating. Some workers[63-67] have argued that the adhesion of metal plating to polymeric substrates is a function of the surface topography. Others [67-70] have emphasised the role that increased oxidation of the polymer surface, commonly induced by the pre-treatments employed prior to plating, plays and thus the importance of surface force interactions. A balanced view emerges from the quantitative experiments of Perrins and Pettett [71] which enabled the contributions to the intrinsic adhesion arising from mechanical interlocking and surface force components to be separated

out for the adhesion of electroplated copper to polypropylene. Similarly Arrowsmith [72] compared quantitatively the contributions of mechanical interlocking and chemical bonding to the adhesion of electroformed copper and nickel to glass fibre reinforced epoxy laminates.

Following the theories of Andrews and Kinloch [73, 74] and Gent and Schultz [75], Wake [76] has suggested that the effects of mechanical interlocking and surface force components could be multiplied to give a result for the measured joint strength:

$$\text{Joint strength} = k.M.S$$

where k = constant
M = mechanical component
S = surface force component

This equation reveals that the substrate should possess, simultaneously, the topography and surface chemistry necessary to produce the highest extent of mechanical interlocking and surface force contribution. Thus, this interaction results in the highest joint strengths. Recent work by Packham and co-workers [77-82] provides further evidence for the importance of substrate surface topography when considering the strength of certain interfaces. In their studies on the adhesion of polyethylene to metallic substrates they found that high peel strengths were obtained when a very rough, fibrous-type oxide surface was formed on the substrate. When the fibres were damaged to reduce the surface roughness, without detectably having changed the chemical nature of the substrate, the joint strength dropped markedly. However, if the chemical nature of the oxide was changed by electrolytic reduction, with a minimum change in topography, the strength was still substantial.

The enhancement of joint strength that may result from increasing the rugosity of the substrate surface, as detailed above by Packham and co-workers and previously by Jennings [83,84] Bascom et al [85] and Mulville and Vaishnav [86] need not necessarily arise either from a mechanical interlocking mechanism or indeed from an increase in surface area for bonding or from improved kinetics of wetting (see Section 2.3.)

The measured adhesive joint strength almost always reflects the value of two parameters: (a) the intrinsic adhesion and (b) the energy dissipated viscoelastically and plastically in the highly strained volume around the tip of the propagating crack and in the bulk of the joint. The latter term usually dominates the measured joint strength, and also gives rise to the rate and temperature dependence of joint strengths (see Section 2.6.4.) Several workers [82,87,88] have suggested that the importance of high surface rugosity is to increase the energy dissipated viscoelastically and plastically during joint failure, and Evans and Packham [82] and Wang and Vazirani [88] have applied the theory of the strength of fibre reinforced composite material to the problem. Evans and Packham treated the polyethylene/fibrous oxide interfaces as a composite with discontinuous fibres in a resin matrix. When such a composite is stressed so that fibres and matrix are deformed elastically, stress is transferred from the fibres to the matrix in the region of the fibre ends and this leads to the build-up of high shear stresses at the fibre ends. Thus, by analogy, it is to be expected that the presence of fibres on the substrate would lead to high shear stresses around the fibre ends,

giving failure by plastic deformation of the polymer, initially around the fibre tips, and then, as the stress concentration is relieved, further into the bulk of the polymer.

Thus, a much larger volume of polymer will be plastically deformed during fracture, compared to that volume deformed when bonding to a chemically similar but smooth surface, and this large amount of plastic deformation accounts for the high joint strength.

Therefore, although in certain instances mechanical interlocking may contribute to the intrinsic adhesion forces, the frequently observed increase in measured joint strength with increasing surface rugosity may be attributable to other mechanisms.

2.6.2. Diffusion theory

Voyutskii [89] is the chief advocate of the diffusion theory of adhesion which states that the intrinsic adhesion of high polymers to themselves (autohesion) and to each other, is due to mutual diffusion of polymer molecules across the interface. This requires that the macromolecules or chain segments of the polymers (adhesive and substrate) possess sufficient mobility and are mutually soluble. Voyutskii's experimental evidence for his proposals are the effects of contact time, temperature, polymer type, molecular weight and viscosity on the measured joint strength. He argues that the functional dependence of joint strength on some of these parameters is similar to that expected for a diffusion process and therefore that adhesion is a result of diffusion. However, the dependence of measured joint strengths on parameters such as time-of-contact and polymer molecular weight, may be readily explained either by their

effect on the kinetics of the wetting process in which intimate molecular contact is established between adhesive and substrate [90-94] or on the energy dissipative processes which may occur in the adhesive and the substrate during joint fracture. Vasenin [95-97] has adopted a more fundamental approach to the diffusion theory and has derived an equation relating molecular characteristics of the polymer chain to measured joint strengths. With the autohesion of polyisobutylene, experimental and theoretical relations for the measured joint strength as a function of the time-of-contact and polymer molecular weight were compared. The agreement between the experimental results and the theoretical predictions was good although it should be noted that since the values of two parameters in the theory could not be calculated, they were obtained by fitting to the experimental data. It is worthwhile to consider that, if the coefficient of diffusion is taken to be 10^{-14} $cm^2 s^{-1}$. Vasenin's theory predicts, for instance, that it takes one hundred hours (3.6×10^5 secs) for the molecular segments of one polyisobutylene sheet to penetrate 10μm into the other. However, Voyutskii and Vasenin point out that a much smaller penetration can still result in high joint strengths and for example, that an interpenetration of macromolecules between 10 and 20 Å may result in a five to nine-fold increase in joint strength. One criticism of this work is that, since peel tests introduce various geometric considerations and usually involve rheological properties of the adhesive and substrate, the results from such tests may be ambiguous. Campion [98,99] has shown that the degree of autohesion of various elastomers may be correctly ranked from a consideration of the

polymer's microstructure since this controls the ease with which cavities of space may form between chains, which directly affect the diffusion rate across the interface.

Direct evidence for inter-diffusion in compatible polymers does exist. Radiometric studies [100,101] have demonstrated the presence of macromolecule diffusion. The diffusion constants were found to be in the order of 10^{-10} to 10^{-14} cm^2s^{-1} which Voyutskii argues is completely adequate for the formation of an intrinsically strong interface between the polymers after a contact time of only a few seconds, as discussed above. Further work [103,104] using techniques of optical microscopy, including some under ultraviolet light employing luminescence analysis [105] has indicated that in compatible non-polar polymers the zone of interfacial boundary dissolution due to diffusion may be about 10μm deep.

In summary, the inter-diffusion of polymer chains across an interface requires the polymers (adhesive and substrate) to be mutually soluble and the macromolecules or segments to have sufficient mobility. These conditions are usually met in the autohesion of elastomers and and in the solvent welding of compatible, amorphous plastics.

In both these examples inter-diffusion does significantly contribute to the intrinsic adhesion. However, where the solubility parameters of the materials are not similar, or where one polymer is highly crosslinked, is crystalline or is above its glass transition temperature, then inter-diffusion is an unlikely mechanism.

2.6.3. Electronic theory

If the adhesive and substrate have different electronic band structures there is likely to be some electron transfer on contact to balance Fermi levels which will result in the formation of a double

layer of electrical charge at the interface. The electronic theory of adhesion is due primarily to Deryaguin and co-workers [106,107] and they have suggested that the electrostatic forces arising from such contact or junction potentials may contribute significantly to the intrinsic adhesion. The controversy this theory has caused is due to this final statement that electrostatic forces are an important cause, rather than merely a result, of high joint strength.

Deryaguin's theory essentially treats the adhesive/substrate system as a capacitor which is charged due to the contact of the two different materials. Separation of the parts of the capacitor, as during interface rupture, leads to a separation of charge and to a potential difference which increases until a discharge occurs. Adhesion is presumed to be due to the existence of these attractive forces across the electrical double-layer.

Skinner, Savage and Rutzler [108] have calculated the tensile strength of a metal/polymer/metal joint due to the existence of electrical double layers at the interfaces as a function of the volume charge density. For boundary charge densities of 10^{17}, 10^{19} and 10^{21} electrons $cm.^{-3}$ corresponding values of joint strength of 0.4kPa, 40kPa and 4 MPa were deduced, while the experimental measurements indicated that the maximum charge density was of the order of 10^{19} electrons cm^{-3} and the joint strength was of the order of 7 MPa. Roberts[109] has concluded that the maximum contribution to the thermodynamic work of adhesion for a natural rubber/glass interface is about 10^{-5} $mJm.^{-2}$ which is negligible compared to the contribution from van de Waals forces of about 60 mJ $m.^{-2}$

Several groups of workers [110,113] have investigated the improvement in the adhesion of thin metal films which is recorded if the insulator substrate is subjected to a low-pressure glow discharge prior to coating. Stoddart et al [111] found no net surface electric charge on the substrate but found that the electron emission was altered, indicating that the surface electronic states of the substrate had been changed. The mechanisms of adhesion, and the relative importance of any electrostatic contribution, remain therefore somewhat vague. Recognising this, Wake [114] has recently suggested that, while the nature of the charge-carrying bodies in polymers is obscure, it is known that additives and impurities may drastically affect their ability to form electrical double layers and thus it would be extremely worthwhile to generate data on radiation polymerized material made from a highly purified monomer.

Finally, however, an interface where the influence of an electrostatic double layer has been clearly demonstrated is Zr coated gold spheres on CdS single crystal substrates [115,116]. The adhesive force was measured by a centrifuge technique as the intensity of the illumination on the adhesive system was varied. This changed the electronic properties of the photoconducting CdS substrates, and hence the electrostatic double layer force at the interfaces could be varied leaving the other forces, e.g. van der Waals forces, unaffected. Qualitatively the experimental results were in agreement with a simple model of the metal-semiconductor contact.

It should be noted that most workers have described their results in terms of the bulk electronic properties of the materials.

However, since, for example, most metals are covered by an oxide layer which has its own electronic states which may well influence the electron transfer mechanisms, the possibly greater relevance of the surface electronic states should not be overlooked.

2.6.4. Adsorption theory

The adsorption theory of adhesion is the most generally accepted theory and has been discussed in depth by Kemball [117] Huntsberger [26] Staverman [118] and Wake [119] This theory proposes that, provided sufficiently intimate intermolecular contact is achieved at the interface, the materials will adhere because of the surface forces acting between the atoms in the two surfaces, the most common such forces are van der Waals forces and are referred to as secondary bonds. In addition, chemisorption may well occur and thus ionic, covalent and metallic bonds may operate across the interface; these types of bonds are referred to as primary bonds. The terms primary and secondary are in a sense a measure of the relative strength of the bonds as may be seen from Table 2.1 where the types of bonds are shown with estimates of the range of magnitude of their respective bond energies.

2.6.4.1. Secondary force interactions

Huntsberger [26,120] and others [121,122] have calculated the attractive forces between two planar bulk phases due solely to dispersion forces and have showed, for example, that even at a separation of one nanometre the attractive force would be approximately 100 MPa. This is considerably higher than the experimental strength of most joints. This discrepancy between theoretical and experimental joint strengths is attributed to air voids, cracks,

Table 2.1. Bond types and typical bond energies (127, 128)

Type	Bond energy ($KJ.Mol^{-1}$)
Ionic	590 - 1050
Covalent	63 - 710
Metallic	113 - 347
Permanent dipole-dipole interactions:	
Hydrogen bonds involving fluorine	Up to 42
Hydrogen bonds excluding fluorine	10 - 26
Other dipole-dipole (excluding hydrogen bonds)	4 - 21
Dipole - induced dipole	Less than 2
Dispersion (London) forces	0.08 - 42

defects or geometric features acting as stress raisers when the joint is loaded, causing rupture of the joint at stresses very much below the theoretical value. However, this calculation does indicate that high joint strengths may result from the intrinsic adhesion arising from solely dispersion force interactions.

By adopting a continuum fracture mechanics approach the work of Andrews and Kinloch [73,74,123,124] and Gent and Kinloch [125] defined a geometry independent measure of joint strength, the adhesive failure energy, P.

Experimental and theoretical considerations [73,74,75,124] demonstrated that the adhesive failure energy, P, for a crosslinked rubbery adhesive/rigid plastic substrate interface could be divided into two major components:

(a) The energy required to propagate a crack through unit area of interface in the absence of viscoelastic energy losses, i.e. an intrinsic adhesive failure energy,

(b) The energy dissipated viscoelastically within the rubbery adhesive at the propagating crack, again referred to unit area of interface.

The intrinsic adhesive failure energy, P_o, was evaluated and found to be virtually independent of rate and temperature, since its value depended upon the type and strength of bonding forces at the interface (or in the adhesive or substrate depending upon the locus of failure). The energy dissipated viscoelastically was usually the dominant term and was, by definition, rate, $\dot{C}$, and temperature, T,

dependent. Thus, it was shown that

$$P = P_o F (\dot{C}, T)$$

where F is a viscoelastic loss function dependent upon the rate and temperature (and strain at points remote from the crack [126]). P_o was then expressed as a weighted average of the various failure modes,

$$P_o = i I_o + r \mathcal{T}_o + s S_o$$

where I_o, $\mathcal{T}_o$ and S_o are the intrinsic failure energies for interfacial, cohesive-in-rubber and cohesive-in-substrate failure respectively, and i, r and s are the respective area fractions of interfacial failure, failure in adhesive and failure in substrate. For those joints which exhibited a solely interfacial locus of failure and in which only secondary bonding was established across the interface then $i = 1$, $I_o = W_A$ and therefore P_o should be equal to the thermodynamic work of adhesion, W_A The value of P_o was ascertained from these mechanical property studies and compared with calculated values of W_A and the two parameters were found to be in good agreement.

The strength of the hydrogen bond lies between that of the van der Waals forces and the primary bonds, and the formation of hydrogen bonds across the interface may certainly increase the intrinsic adhesion as has been discussed by Pritchard [129]. He cites the dipping of nylon cords into a complex adhesive mixture of rubber and resorcinol-formaldehyde, as used in the production of tyres, as an example where hydrogen bonding may play an important role; the resorcinol-formaldehyde being adsorbed onto the nylon surface via hydrogen bonds through the phenolic groups.

Another example where hydrogen bonding has been shown to play an important role is in the autohesion of polymers which have been subjected to surface oxidation by immersion in certain acids [130,131] or exposure to an electrical ("corona") discharge [132,134]. In the case of polyethylene, the formation of hydrogen bonds has been suggested to be the result of tautomerization.

Here the carbonyl group at the surface of the oxidized polyethylene may first undergo the tautomerization of the ketone to the enolic form. The enolic form then exhibits an acidic character and may form a hydrogen bond with a carbonyl group of adjacent surface.

A second possible mechanism of hydrogen bond formation is between carbonyl groups on adjacent polymer chains via a water molecule [135] Some supporting evidence comes from the studies of Blythe et al. [134] who have employed X-ray photoelectron spectroscopy to analyse the surface of oxidized polyethylene. However, their results also indicate that several other hydrogen bonding mechanisms should be considered.

It has also been suggested [136,137] that acid-base interactions across an interface may contribute to intrinsic adhesion forces. The analysis presented by Bolger and Michaels [137] attempts to identify many of the distinguishing features of acid-base interactions in terms of the ionic character of a hydroxylated metal oxide substrate and the organic functional group provided by the adhesive.

2.6.4.2. The role of primary interfacial bonding.

Although intrinsic adhesion arising from secondary bonding forces alone may result in adequate and high joint strengths, many adhesion scientists believe that the additional presence of primary bonding may often increase the measured joint strength and is certainly a

necessary requirement for securing environmentally stable interfaces. However, although there is considerable indirect evidence [124,138,149] emphasizing the importance of interfacial chemical bonding, studies which directly confirm its role are scarce. The use of sophisticated, surface-specific, analytical techniques such as Laser-Raman spectroscopy [150] X-ray photoelectron spectroscopy [151] and secondary-ion mass spectroscopy [152,153] has produced definitive evidence that primary interfacial bonding may occur in certain circumstances and may make a significant, indeed often vital, contribution to the intrinsic adhesion.

One of the most controversial areas for the role of primary interfacial bonds has been when adhesion promotors or coupling agents, are employed to enhance the joint strength or, more commonly to enhance the environmental resistance of the interface to attack by moisture.

The various types of adhesion promotors that have been employed have been the subject of many papers [154 161] and it is sufficient to note here that the most common type are the silane coupling agents which have the general structure $X_3Si(CH_2)_nY$, where n=0 and 3, X is a hydrolysable group on silicon and Y is an organo-functional group selected for compatibility with a given resin. They are widely used as a surface finish on glass fibres prior to forming a glass fibre reinforced composite, as an additive in adhesive formulations and as a primer applied to the substrate prior to adhesive bonding.

The silane films usually employed on the substrate have been shown to be polymeric,[162,163] indeed, the films were found to be much thicker than a monolayer of silane monomer and appeared to be composed of a strongly held polysiloxane network along with some hydrolysed or partially hydrolysed silane and small polysiloxane molecules.

Until recently there has been little known of the mechanism by which the intrinsic adhesion of the interface is enhanced, especially with respect to environmental attack. The generally, but not universally, accepted mechanism by which the durability of the joint is increased is the formation of strong, primary interfacial bonds. For the polysiloxane/substrate interface this arises from formation of Si-O-substrate bonds. For the adhesive/silane interface this arises from the reaction of the Y-group on the silane with reactive groups in the adhesive. Alternatively, other features such as wetting [156] and the possible formation of a boundary layer in the adhesive differing in chemical and physical properties to that of the bulk resin [19] have been suggested to be of importance.

Recent studies by Koenig and Shih [150] employing Laser-Raman spectroscopy have clearly established the presence of ≡Si-O-Si bonding across a polysiloxane/glass interface, and the presence of such bonds most probably accounts for the increased water resistance of glass fibre composites and glass joints, bonded with structural adhesives [164] when a silane primer is present. Also Gettings and Kinloch [152,153] have employed secondary ion mass spectroscopy (SIMS) to investigate the interfacial interactions between a

γ- glycidoxypropyltri-methoxy silane primer deposited onto a mild or stainless steel substrate. Good interface stability was associated with the presence of $FeOSi^+$ radicals from the primer coated mild steel surface and $FeOSi^+$ and $CrOSi^+$ radicals from the coated stainless steel surface. This was firm evidence for the formation of primary interfacial bonding, probably -Fe-O-Si≡ and -Cr-O-Si≡ respectively between the metal oxide and polysiloxane primer.

Somewhat different examples of instances where strong interfacial bonding has been confirmed come from the use of inelastic electron tunneling spectroscopy [165,167] and attenuated total reflectance infra-red spectroscopy [168]. In these studies organic molecules were found to chemisorb onto metal oxides and the bonding was found to be almost purely ionic in character. Chu et al [165] examined the adsorption of 4-hydroxybenzoic acid on aluminium oxide and concluded that the bonding was ionic in character ($-COO^-Al^+$) with the phenyl ring orientated perpendicular to the surface. These new, surface-specific techniques should provide much interesting information on the nature of interfacial bonding and considerably assist in the identification of mechanisms of adhesion.

2.6.5. Weak boundary layers

The topic of weak boundary layers has been the subject of considerable controversy in discussion of the mechanisms of adhesion, especially with respect to low-energy substrates which are usually subjected to various surface pretreatments prior to bonding in order

to improve their adhesion.

Bikerman [11] initiated the debate when he stated that even though failure might appear to be interfacial, with the separation appearing to be exactly along the adhesive/substrate interface, a cohesive break of a weak boundary layer is the real event. Bikerman has proposed many classes of weak layers and offered two basic premises to explain why joints never fail interfacially.

Firstly, he considered the probability of a crack situated at the interface, between an adhesive molecule and a substrate molecule, proceeding along the interface. Considering a two-dimensional structure, the crack must propagate either between two molecules of the adhesive or between two molecules of the substrate, or between a molecule of the adhesive and a molecule of the substrate. If these three paths are equally probable, the probability of the crack propagating along the interface is $\frac{1}{3}$. Thus the probability of the crack propagating along the interface between $(n + 1)$ pairs of dissimilar molecules is $(\frac{1}{3})^n$ and this probability of course decreases even further if a three-dimensional structure is considered. Therefore, when the formation of a crack between any two molecules is equally probable, the fracture can never occur only along the adhesive/substrate interface for purely statistical reasons. Secondly, he considered the forces of attraction between two dissimilar gases and showed that the attraction between two dissimilar molecules is smaller than between two identical "strong" molecules, but greater than between two "weak" molecules. Thus, by analogy to adhesive systems, molecules favour rupture in cohesion in the weaker phase.

Huntsberger [166] and Voyutskii [167] have critically examined these premises and have shown that the simplifying assumptions made by Bikerman do not hold for most practical systems. They have pointed out that Bikerman has failed to take into account the structure of real adhesives which are invariably polymeric. Structural features such as chain entanglements, crystallinity, and orientation of chains and cross-links will result in the cohesive fracture stress often being much greater than that required for interfacial failure where often only secondary intermolecular forces are involved. Experimentally, also, much evidence [74,166,168,172] has been published to show that interfacial failure can occur and does so fairly frequently. The new techniques of Auger and X-ray photoelectron spectroscopy have confirmed instances of interfacial failure beyond any doubt [49,173,174] Further, even if the locus of joint failure is cohesive in the adhesive or substrate close to the interface, this does not necessarily imply the presence of a weak boundary layer. Several authors [85,175] have recently suggested that the stress distribution in the joint and around the tip of a crack propagating close to the interface causes "mechanical focusing" of the failure path close to the interface. More recently Bikerman's ideas on weak boundary layers have been revitalised by the conclusions drawn by Schonhorn and co-workers. In 1966 Schonhorn and Hansen [176] reported a highly effective treatment for the surface preparation of low surface energy polymers to enhance adhesive bonding. Essentially the technique consisted of exposing the polymer surface to an inert gas plasma at reduced

pressure generated by an electrodeless glow discharge (i.e. radio-frequency field). For polyethylene only very short treatment times were necessary and Schonhorn and co-workers [176,179] reported that, whilst this treatment did not change the wettability of the polyethylene, as measured by the critical surface tension, gel permeation chromatography showed that some highly cross linked polymer was formed after treatment and the weight- and number-average molecular weights, M_w and M_n increase from 86000 to 135000 and from 1800 to 4000 respectively. Also attenuated total reflectance infra-red spectroscopy showed only the formation of transethylenic unsaturation after treatment and a thin intractable skin was readily observed by melting the polymer. However, attenuated total reflectance infra-red spectroscopy is not a true surface technique. The technique has a sampling depth, typically about 1μm that is relatively large compared to the likely depth of affected polymer, and care must therefore be taken to avoid possible misinterpretation of the results. Notwithstanding this, Schonhorn concluded that wettability was not the sole criterion for the formation of an adhesive joint and that the enhancement of the cohesive strength of a weak surface might be a factor of greater importance. He suggested that many melt-crystallized polymers possess an inherently weak boundary layer, between about 0.02 and 0.10μm thick, which is composed of amorphous low molecular-weight materials rejected by the crystallization process. (The crystallization process is assumed to start in the bulk and proceeds outwards)

It was therefore concluded that the increases in joint strength achieved by this technique were primarily due to increasing the cohesive strength of the polymer in the surface regions by the introduction of crosslinks.

Schonhorn and co-workers [180,182] have examined the effect of similar gas plasma treatment on improving the joint strengths of many polymeric substrates and have also investigated other methods [181,183,186] for increasing the strength of any weak boundary layer which may be present.

A major criticism of Schonhorn's proposal that a weak amorphous surface is produced when polymeric films are melt crystallized in air is that his evidence is mainly inferred. Indeed recent work by Briggs and co-workers [173,174] using X-ray photoelectron spectroscopy found no evidence of joint failure occurring in the surface regions of a polyethylene substrate. Furthermore, many workers [21,73,187,194] have established that the surface free energy of the polymer substrate may be increased by the glow discharge treatment, and by some of the other treatments, investigated by Schonhorn. Thus, surface energetics and the production of chemically active species, to which grafting may occur, may account for the observed increased adhesion.

Therefore, while certain classes of weak boundary layers are well established, for example surface contamination (Section 2.6.4.2.) their presence in joints where low strengths are recorded should not be automatically assumed.

2.7. Stresses in adhesive joints

To predict the strength of adhesive joints, a knowledge of the stress distribution must be coupled with a knowledge of the relevant mechanical properties of the adhesive and substrate and a suitable failure criterion. Such criteria are not well established for adhesive joints but are discussed in section 2.7.3.

2.7.1. Single-lap joints

Of all the various geometries and methods of loading the single-lap joint loaded in tension has undoubtedly received the most attention from the stress analysts [195,217] There are two main reasons for this interest. First, it is a convenient and thus frequently used test geometry for evaluating adhesives and, second, it is the basis for many joint designs employed in industry.

The single-lap joint loaded in tension is shown schematically in Fig 2.4. The stresses in the adhesive layer are not, in practice, uniform and stress concentrations arise from the differential straining of the bonded substrates and from the eccentricity of the loading path.

The stresses arising from the differential straining of the bonded substrates were first studied by Volkersen [198] and may be understood [218] by reference to Fig 2.4. In the case of the loaded joint with inextensible substrates, see Fig 2.4.b., the non-deformable substrates will move as solid blocks and the adhesive will suffer a uniform shear strain, γ_{yz}. However, each substrate bears the full load just before the joint and transmits it gradually to the other through the adhesive. Thus, the stress in Substrate 1 will be highest at A

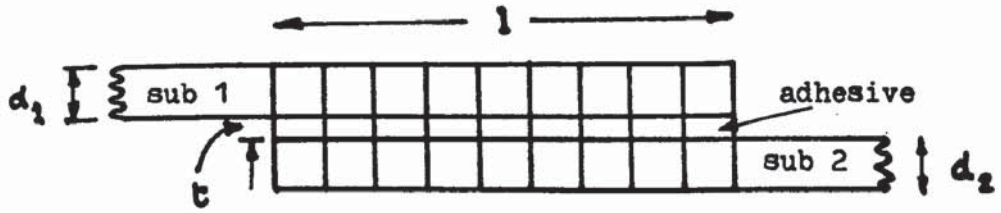

(a) Unloaded

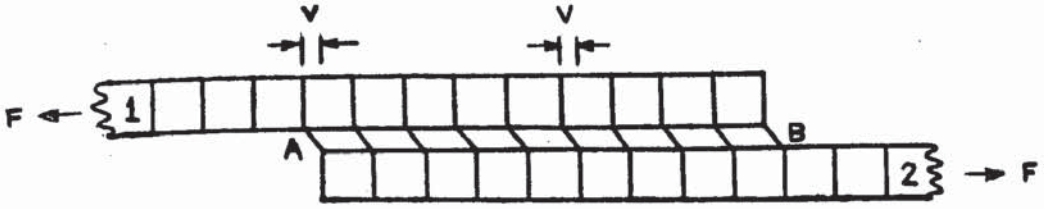

(b) Loaded, inextensible substrates

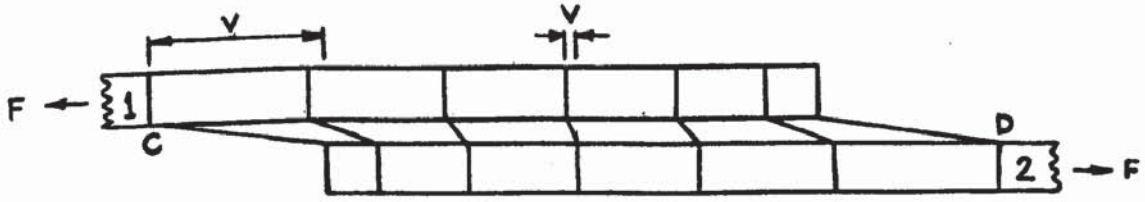

(c) Loaded, elastic substrates

Fig. 2.4. Schematic representation of a single-lap shear joint. (v is the extension of the adhesive)

and gradually diminish towards B where it will be zero and the converse will hold for Substrate 2. This variation in stress is not important if the substrates are inextensible but in practice, of course, they behave at least as elastic materials. Therefore, the picture of the deformation will be as in Fig. 2.4c and the largest deformations and shear strains, and hence stresses, in the adhesive will occur at the very ends of the overlap, at points C and D. (This cannot occur in practice since it implies a complementary shear stress on a free surface and no shear stress can exist on a free surface. Allowing for such end-effects appears to decrease the maximum shear-stress concentration, from that predicted for materials of Hookean elasticity, by a small amount [205]). For materials of Hookean elasticity the stress concentration factor n is given by:

$$n = \frac{\text{maximum shear stress}}{\text{applied shear stress}} = \frac{\tau_{yx}(\max)}{\tau_o}$$

$$= \left(\frac{\Delta}{W}\right)^{\frac{1}{2}} \left(\frac{W - 1 + \cosh \sqrt{\Delta W}}{\sinh \sqrt{\Delta W}} \right) \qquad (10)$$

where

$$\Delta = \frac{G_a l^2}{E_{S2} d_2 t} \qquad (11)$$

and

$$W = \left(\frac{E_{S1} d_1 + E_{S2} d_2}{E_{S1} d_1} \right) \qquad (12)$$

if $E_{S1}d_1 > E_{S2}d_2$, and τ_{yx} (max) is the maximum shear stress, τ_o is

the applied stress $\left[\tau_o = F/(\text{bonded area}) = F/(\text{overlap length x width})\right]$, G_a is the shear modulus of the adhesive, l is the overlap length, E_{S1} and E_{S2} are the Young's moduli of substrate 1 and substrate 2 respectively, d_1 and d_2 are the thicknesses of substrate 1 and substrate 2 respectively and t is the thickness of the adhesive layer. For substrates for which $E_{S1}.d_1$ and $E_{S2}.d_2$ are equal then W reduces to a value of 2 and equation 10 becomes (218):

$$n = \left(\frac{\Delta}{2}\right)^{\frac{1}{2}} \coth\left(\frac{\Delta}{2}\right)^{\frac{1}{2}} \qquad (13)$$

Thus, the stress concentration factor becomes simply a function of a single dimensionless coefficient, Δ. It can, therefore, be readily appreciated that the theory of Volkersen predicts that decreasing the overlap- length or shear modulus of the adhesive, or increasing the stiffness of the substrate or the thickness of the adhesive layer, will decrease the shear stress concentration in the adhesive layer. However, whether these changes result in stronger joints will often depend upon other factors. For example, a decrease in G_a possibly by plasticizing the adhesive, is usually accompanied by a decrease in shear strength of the adhesive, so little improvement may result from such a change in adhesive formulation.

The situation examined by Volkersen, whilst it indicates the importance of various parameters on the potential strength of a single-lap joint, is incomplete in that it takes no account of the tensile, or "tearing" stresses generated in the adhesive as a result of the eccentricity of the loading of the joint. This additional feature was first considered by Goland and Reissner (199) who recognized from laboratory experiments with lap joints that the bending of the

substrates outside of the joint region has a pronounced effect upon the stress distribution in the joint itself. This effect they expressed in their bending moment factor, k, and associated rotation factor, k'. These parameters k and k' are not independent of one another but k is usually the dominant term; k is dimensionless and is the ratio of the existing bending moment just before the bonded overlap to the value of this moment for inflexible substrates:

$$\frac{1}{k} = 1 + 2(2)^{\frac{1}{2}} \tanh\left\{\left[\frac{3}{2}\left(1-\nu_s^2\right)\right]^{\frac{1}{2}} \frac{1}{2d}\left(\frac{\sigma_s}{E_s}\right)^{\frac{1}{2}}\right\}, \quad (14)$$

where ν_s and σ_s are the Poisson's ratios and applied stress for the substrate away from the overlap. Thus, k, depends upon the geometry of the joint, the elastic properties of the substrates and the stress on the substrates. The value of k is unity for undeformed substrates but, for increasing flexibility or load, k will diminish towards zero as a limit, although in practice it remains above about 0.35. Thus, as the substrates bend the value of k falls and the predicted stress concentrations in the joint decrease. Goland and Reissner [199] considered two cases:

(a) where the adhesive layer is extremely thin and of similar elastic stiffness to the substrates, so that its deformations are of little importance, for example, adhesive-bonded wooden joints, and

(b) where the layer is thin but its deformation makes a significant contribution to the stress distribution in the joint, as in bonded metal-to-metal joints.

Goland and Reissner [199] established the quantitative limits for these assumptions from strain-energy considerations.

For their first case, the stress distributions are shown in Fig. 2.5 and the variations of the maximum stresses with the bending moment factor k are shown in Fig. 2.6 As may be seen, the tensile (or tearing stress), σ_{yy} is very high at the edge of the joint and all the stresses decrease as the bending moment factor, k, decreases, i.e. as the substrates bend.

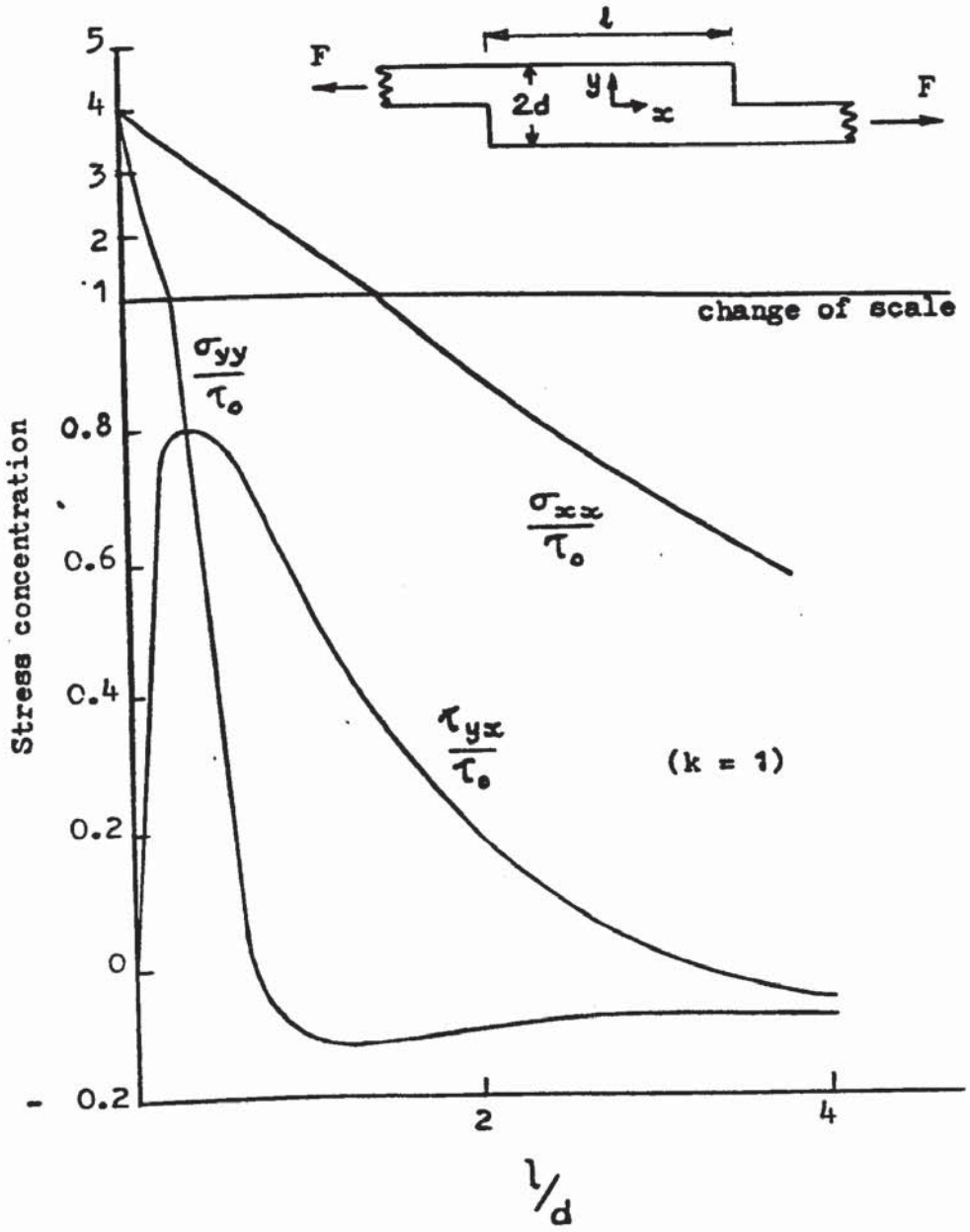

Fig 2.5. Stress distribution along the shear plane as a function of distance from the edge of the overlap (bending moment factor k equal to one) after Goland and Reissner (199)

For their second case,

$$\frac{\tau_{yx}(max)}{\tau_o} = \frac{1+3k}{4}(2\Delta)^{\frac{1}{2}}\coth(2\Delta)^{\frac{1}{2}} + \frac{3}{4}(1-k) \qquad (15)$$

and tensile stresses are also present in the adhesive layer. Thus, for relatively long overlaps and $k = 1$, Equations 10 and 15 reveal that the shear stress concentration factor predicted by Goland and Reissner will be twice as large as that predicted from the analysis of Volkersen. This arises, of course, because the latter takes no account of the stress concentrations caused by eccentricity of the loading path.

Ishai et al [219] have confirmed that for joints which exhibit essentially only elastic behaviour the analytical solutions of Goland and Reissner [199] are in good agreement with the experimental results for both the shear and tensile-stress distributions in the adhesive layer.

So far only the stresses acting in two dimensions have been considered, but Adams and co-workers [203, 204] have approached the problem of examining the transverse stresses by experimental modelling and theoretical analytical and finite-element analysis solutions of the Volkersen theory considered in three dimensions. They demonstrated that Poisson's ratio strains generated in the substrates cause shear stresses in the adhesive layer and tensile stresses in the substrate acting perpendicular to the direction of the applied load. For metal-to-metal joints the transverse shear

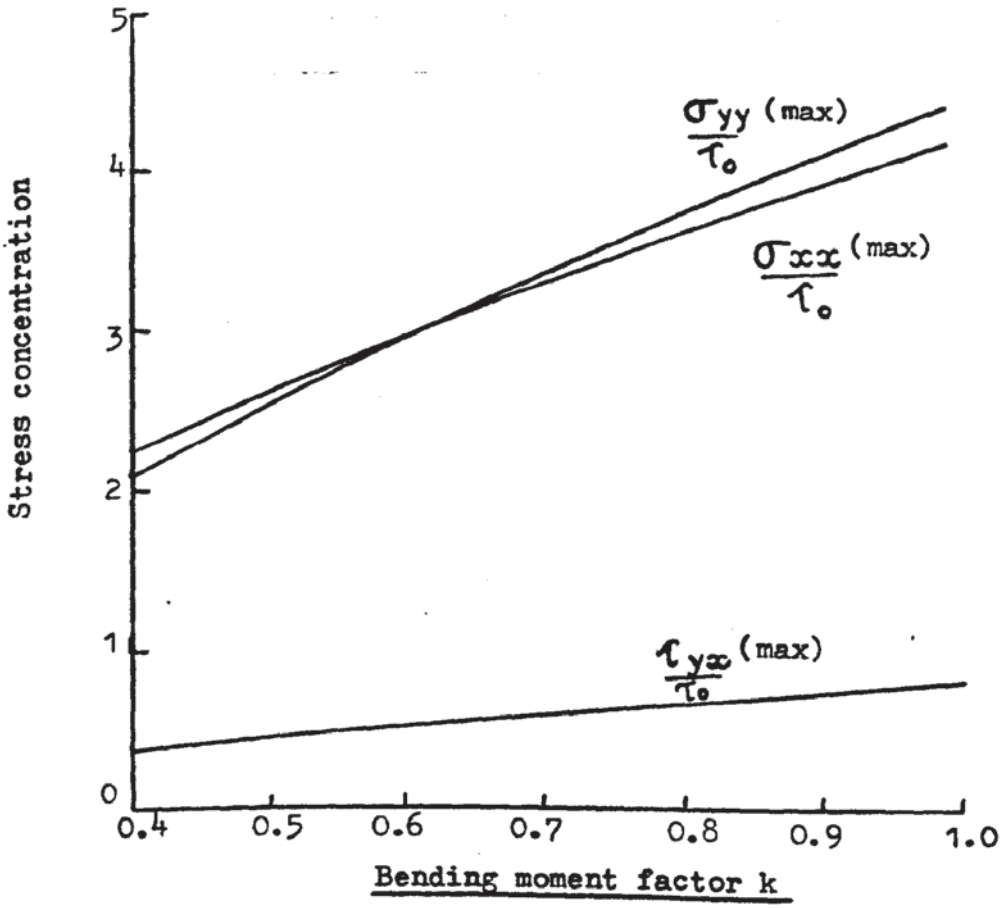

Fig. 2.6 Reduction of the maximum stresses in the shear plane at a single lap joint resulting from bending of the substrates (i.e. diminishing value of k) after Goland and Reissner (199)

stress has a maximum value of about one-third of the minimum longitudinal shear stress, and this occurs at the corners of the overlap. This, therefore, enhances the shear-stress concentration which exists at this point due to the effects described above. Bonding substrates of dissimilar stiffness produces greater stress concentrations in the adhesive than when similar substrates are employed.

The above analyses all consider the substrates and adhesive to behave as elastic materials, however, most of the adhesives commonly employed exhibit elastic-plastic behaviour. Several groups of workers [195, 196, 206, 212, 217, 220] have recently sought to include this behaviour in their calculations. The most extensive studies have been conducted by Hart-Smith [195, 212, 216] who has used closed-form analytical solutions, employing iterative solutions on a digital computer for the more complicated joint configurations. These studies show that inclusion of adhesive plasticity under shear loading in the analysis may decrease the stress concentrations substantially and thus increase the predicted joint strengths quite significantly, compared with a solely elastic analysis.

2.7.2. Internal stresses

Adhesives are often subject to additional stresses in the joint arising from shrinkage of the adhesive relative to the substrates. The main reason for the shrinkage comes from equilibrium contact between the adhesive and substrates being established at temperatures above the subsequent operating temperature of the joint. Thus, since the adhesive and substrates usually have different coefficients of thermal expansion, thermal strains are introduced upon cooling. Other events such as polymerization reaction, cross-linking, loss of solvent, etc., may also be accompanied by volume contractions but are usually considered to be of secondary importance.

Experimental work [221, 226] especially that using photoelastic techniques, has established the presence of residual stresses in joints but the results have often not been quantitative. For the simpler case of polymeric films coated onto metallic substrates, photoelastic techniques and a method based upon the bi-metallic strip principle have often been employed [227, 232] Using the latter method Danneberg [231] showed that for a wide range of epoxy-based coatings on an aluminium substrate thermal contraction was the major cause of internal stress and that the stresses generated were of the order of 0.08 $MPa\,^{o}C^{-1}$.

The theoretical analysis of the internal stresses in an adhesive joint is beset with great difficulties even if it is assumed that the adhesive is perfectly elastic. Bikerman, [233] Wake, [234] Harrison and Harrison [197], Carlson and Sapetta [235], and Inoue and Kobatake [226] have made this assumption and attempted theoretical predictions. The maximum value of τ_{yx} occurs at, or near, an interface and near the ends of the joint, being zero in the centre. Harrison and Harrison have also concluded that $\tau_{yx}(max)$ is much higher for an adhesive possessing a Poisson's ratio of 0.33, as opposed to 0.49. Near the edges σ_{yy} is compressive while σ_{xx} falls below its value in the uniform stress region. However, these analyses all assume elastic behaviour and whilst the results from Inoue and Kabatake [226] appear intuitively to be of the expected magnitude, and were confirmed by photoelasticity techniques, the results from Carlson and Sapetta [235] appear to be unduly pessimistic. Indeed $\tau_{yx}(max)$ values calculated [236] from

the Carlson and Sapetta analysis for an aluminium-epoxy-cfrp joint would readily fail solely because of the high internal stresses arising from thermal contraction. In practice, the joint possessed a relatively high strength. A more realistic but still somewhat pessimistic, prediction of these experimental results is achieved if the analysis of Hart-Smith [212] is employed. This assumes elastic-plastic behaviour of the adhesive but makes no allowance for stress relaxation. Increased adhesive plasticity or adhesive layer thickness results in lower internal stresses.

Thus, to summarize, the magnitude and importance of internal stresses in adhesive joint is a frequently discussed topic and one which would certainly benefit from further studies.

2.7.3. Failure criteria

In order to predict the strength of adhesive joints a knowledge of the stress distribution in the joint must be coupled with a suitable failure criterion and the relevant mechanical properties of the adhesive. Greenwood, Boag and McLaren [237] have suggested that the failure of lap joints occurs when the maximum shear stress in the adhesive layer attains the same value as the shear strength of the adhesive. Experimental results, using both a rigid, thermosetting adhesive and a flexible elastomeric adhesive were very encouraging but subsequent work [195, 196, 206, 212, 213, 220] has indicated that this criterion cannot be generally applied. These subsequent studies revealed that a criterion based upon maximum shear stress is insufficient since the strain capability of the adhesive, especially if it exhibits extensive

plasticity when tested in shear, must be taken into account. Adhesives exhibiting elastic-plastic behaviour, rather than solely elastic behaviour, result in joints possessing lower stress concentrations, as discussed above, and do not fracture under shear loading as soon as the load corresponding to their shear strength is attained. Thus, current practice is to use the maximum shear strain or maximum adhesive strain-energy in shear as the appropriate failure criterion. However, it should be noted that failure in lap joints may occur by modes other than shear failure of the adhesive. For example, the tearing stress, σ_{yy} may exceed the tensile strength of the adhesive or the transverse strength of the fibrecomposite substrate before any of the above conditions are met.

The difficulty in defining adequate failure criteria, even when equipped with a full knowledge of the stress distribution had led to the application of fracture mechanics to adhesive joint failure.

2.8. Lap joints

As predicted in Sections 2.7.1. for an essentially elastic adhesive the breaking load, F_b, increases up to an approximately constant value and the average applied stress, τ_b at failure decreases as the overlap-length, l, of a lap-joint is increased. This is illustrated in Fig. 2.7. However, if too short an overlap is employed high stresses will exist in the centre of the overlap upon loading and thus make the joint more susceptible to creep and environmental attack The overlap should therefore be sufficiently long to ensure these

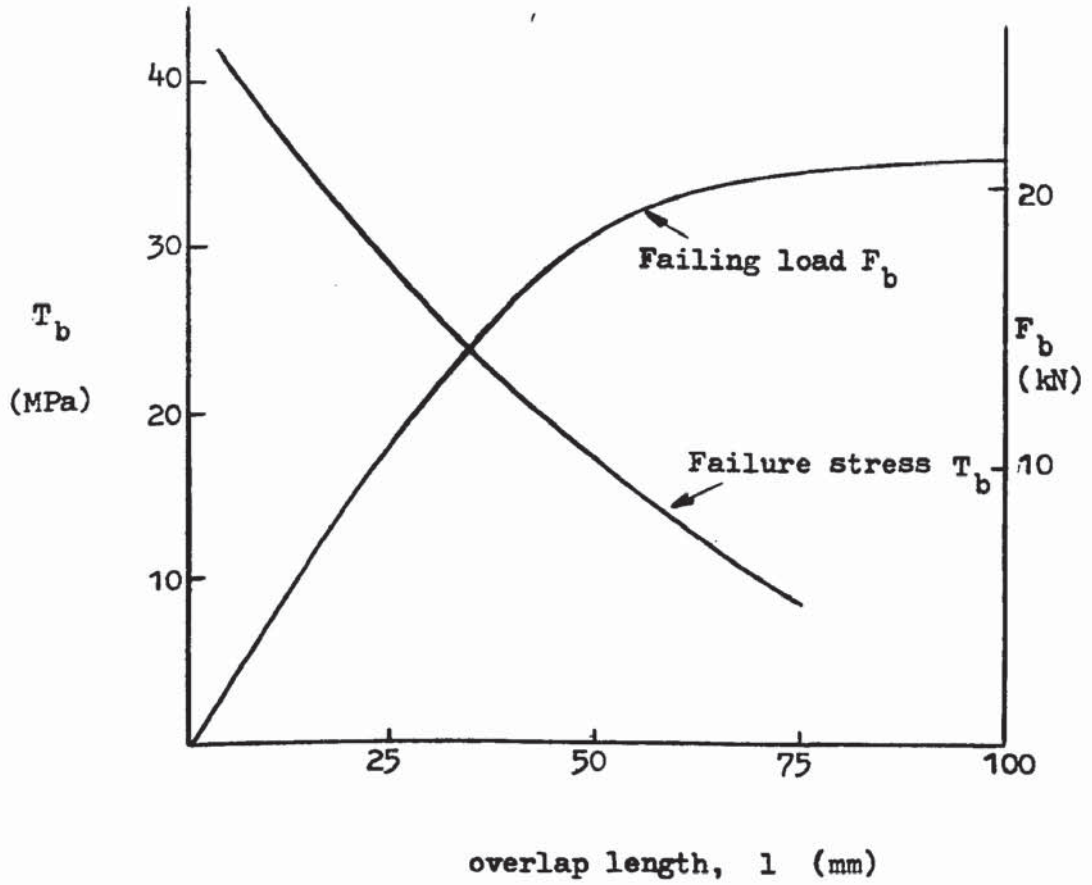

Fig 2.7. Failing load, F_b and stress T_b of single overlap joint of modified phenolic-aluminium alloy as a function of overlap length, l, after De Bruyne (218, 238)

stresses are elastic in nature and low in magnitude. Further, if a ductile adhesive is used then a relatively long overlap (e.g. $l:d$ of about 80:1) will reduce [195] the eccentricity of the load path, and hence the tearing stresses, σ_{yy} and so the breaking load F_b will continue to rise somewhat with increasing l. Increasing the thickness of the substrates results in a lower shear stress concentration but may increase the tensile, or tearing stress σ_{yy}. [213] Thus increasing the thickness of the substrates results in higher joint strengths, up to a certain limit.

The theoretical analyses outlined in Section 2.7.1. predict that the breaking stress τ_b of lap joints will increase as the thickness, t, of the adhesive layer increases. Generally, if all other joint parameters are held constant the value of τ_b is predicted to be proportional to the reciprocal of the square-root of the thickness, t, provided the thickness is relatively small. Fig. 2.8. taken from the work of Adams and Peppiatt [205] shows the predictions for three different analyses for an epoxy-aluminium-alloy single-lap joint and all suggest that the breaking load will increase as the value of t increases. However, the experimental results for the joints, in accord with other work [206, 238, 241] show that the actual breaking load does not increase with increasing t and may even fall slightly.

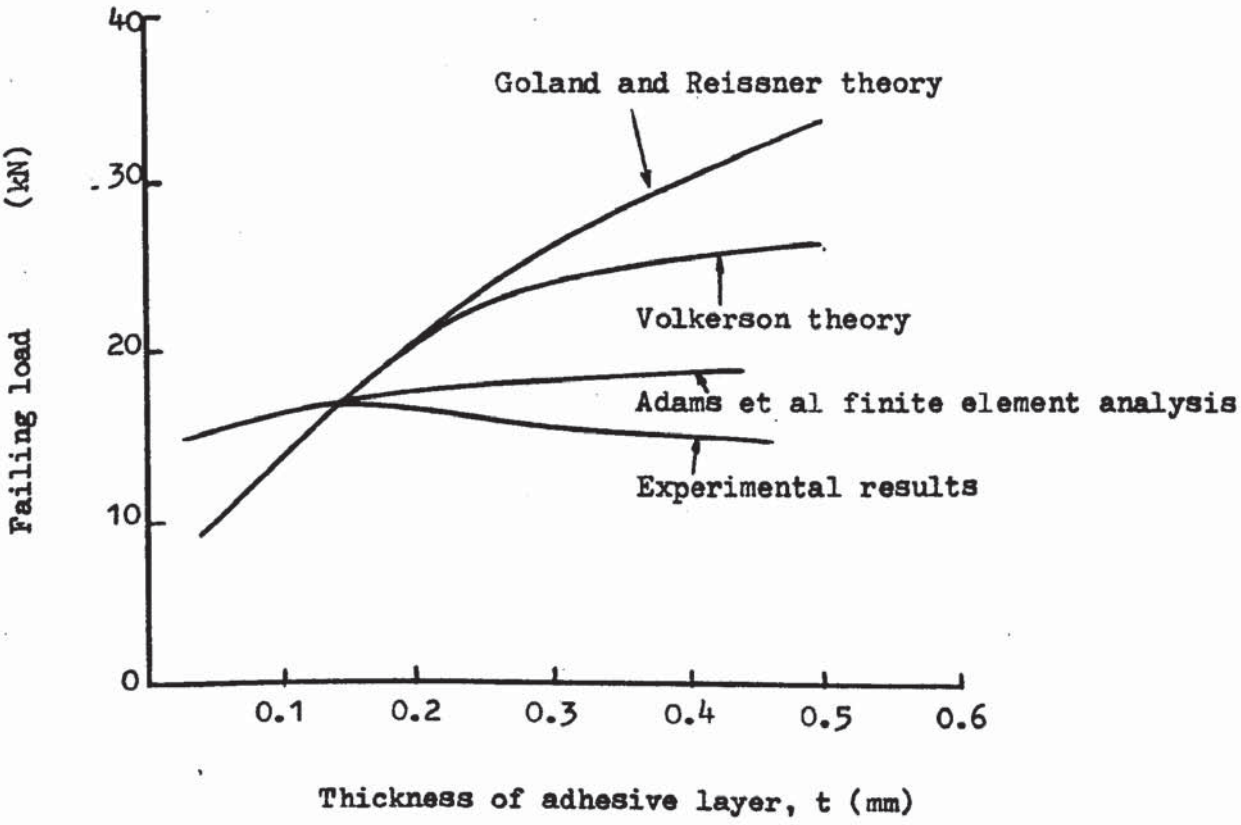

Fig 2.8. Influence of thickness, t, of adhesive layer upon experimental and theoretical failing loads of epoxy-aluminium alloy single-lap joints, after Adams and Peppiatt[205]

2.9. Effect of test temperature and rate

First, considering adhesives tested above their glass transition temperature, Tg,then it is well established [242, 252] that the measured tensile strengths of elastomeric adhesive joints obtained over a wide range of test temperatures and rates may be plotted to yield a single master curve when normalized to a reference temperature by means of the Williams-Landel-Ferry [253] rate-temperature equivalence for viscoelastic materials. The relationship is relatively simple resulting in a monotonic increase of tensile strength with increasing rate and decreasing temperature but the relation for the peel strength of an uncross-linked elastomeric adhesive may be extremely complex [250, 254] Gent and Petrich [250] reported two main features for such a master curve: a sharp maximum occurring at low rates and high temperatures, which may in some instances be accompanied by a transition from cohesive-in-adhesive to interfacial failure, and a sharp decrease in peel strength at high rates and low temperatures. The former feature was shown to arise from a change in the deformation process in the adhesive from a liquid-like to a rubber-like response and Gent and Petrich proposed an approximate relation between peel strength and the tensile stress-strain behaviour of the bulk adhesive using a single empirically determined parameter, namely the interfacial bond strength. The second effect was due to the transition from a rubber-like to glass-like response of the adhesive and to the exact peel geometry employed. Second, considering adhesives tested largely below their glass transition temperatures, Fig. 2.9 illustrates some typical results for various adhesives

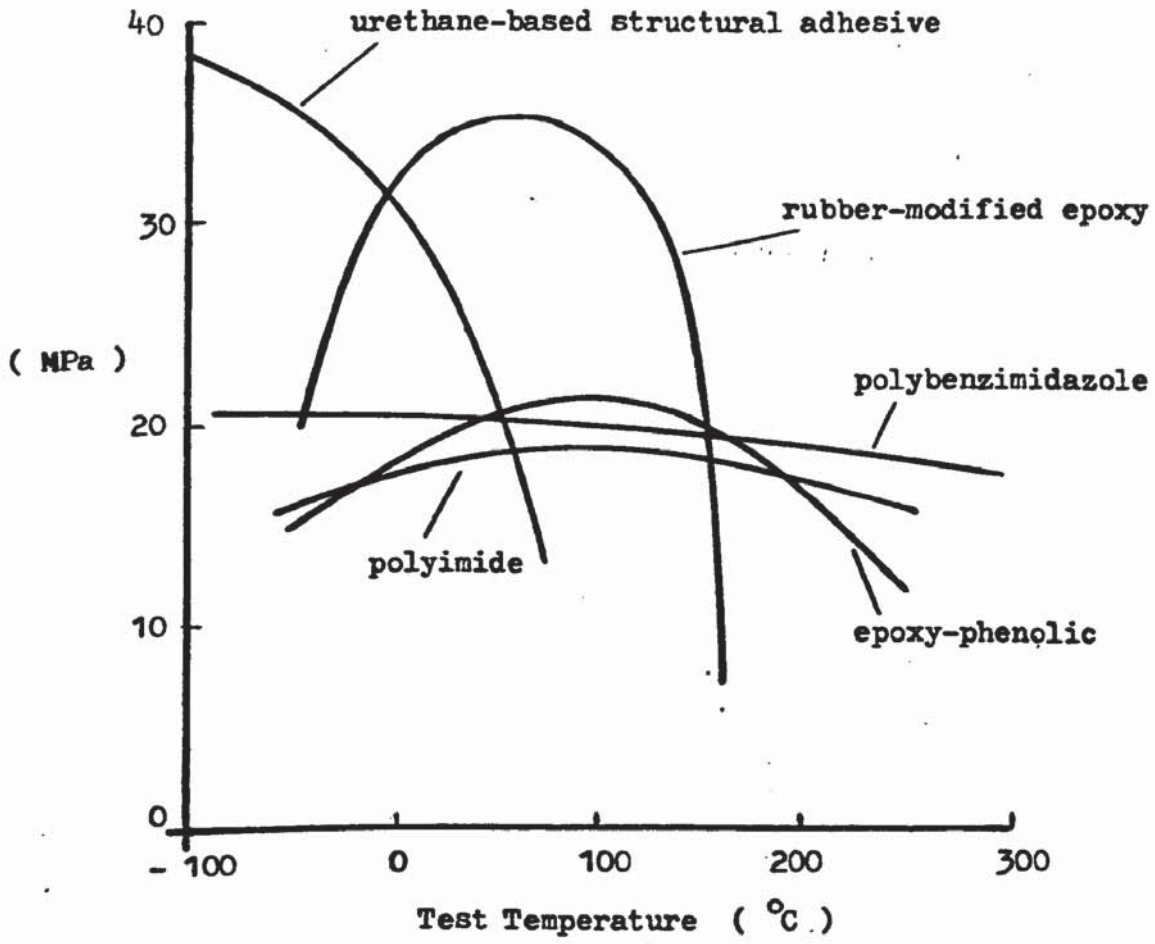

Fig 2.9 Typical strengths of single-lap joints loaded in tension using various structural adhesives as a function of test temperature after Cotter and Bolger (255, 259)

compositions. The epoxy-phenolic, polyimide and polybenzimidazole exhibit the best high-temperature strengths of those shown. In a recent review Cotter [255] concluded that the former formulations are available for long-term use to about 175°C and are capable of short excursions to temperatures as high as 250°C. The polyimide compositions may be used for very long times at 260°C and maintain a useful strength at 425°C for about 1h. Polybenzimidazole adhesives have a higher temperature ceiling than polyimide formulations in inert atmospheres but are markedly susceptible to oxidative degradation above 260°C. The relationship between low-temperature performance and the structure and formulation of the adhesive have also been considered [256, 257] Increasing the rate of loading structural adhesive joints is generally equivalent to decreasing the test temperature, as would be expected.

The creep and stress rupture of adhesive joints under static [258, 267] and dynamic [268, 274] loadings have been the subject of many investigations. The failure behaviour of epoxy adhesives when subjected to a constant applied load is particularly intriguing. It has been reported [258] that some epoxy adhesive joints, tested in a tapered-double-cantilever-beam geometry, do not appear to suffer from static fatigue, even when stressed to a relatively high level. This arises because severe crack-tip blunting reduces the stress concentration at the crack tip to such an extent that the tip stress level [260, 261] necessary for crack extension is not attained and thus this mechanism forestalls static-fatigue. However, in compositions where the capacity for crack-tip blunting during the static fatigue

test is limited, delayed failure is observed. Gledhill and Kinloch [267] have studied one such epoxy adhesive composition and a linear relationship was found to exist between the applied fracture energy, G_{1c} and the logarithmic failure time, the failure time decreasing as the value of G_{1c} was increased.

2.10. Environmental attack

2.10.1. Introduction

A serious limitation that has been encountered in the use of adhesives, especially for structural engineering applications, is the deleterious effect that moisture may have upon the strength of a bonded component [268, 273]. Such effects are particularly pronounced when the component is also subjected to conditions of relatively high stress and temperature. The mechanisms and kinetics of such environmental failure will be first discussed, followed by a consideration of the methods which have been developed to increase the service-life of adhesive joints.

2.10.2. Mechanisms of failure

2.10.2.1. Stability of the adhesive

It is an obvious statement that if the service environment physically or chemically attacks the adhesive to any significant extent then the joint may well be appreciably weakened. However, assuming a degree of common-sense has been exercised in adhesive selection, then loss

of strength in the adhesive is not usually a major mechanism of attack in aqueous environments. This is evident from the frequent observation that, while the locus of failure of well prepared joints is invariably by cohesive fracture in the adhesive layer, after environmental attack it is usually via "apparent" interfacial failure between the adhesive (or primer) and substrate.

2.10.2.2. Stability of the interface

The above observation highlights the importance of the interface when considering environmental failure mechanisms. The thermodynamic work of adhesion, W_A, required to separate unit area of two phases forming an interface may be related to the surface free energies. In the absence of chemisorption, interdiffusion and mechanical interlocking, the reversible work of adhesion, W_A in an inert medium may be expressed by

$$W_A = \gamma_a + \gamma_b - \gamma_{ab} \quad (16)$$

where γ_a and γ_b are the surface energies of the two phases and γ_{ab} is the interfacial free energy. In the presence of a liquid (denoted by the subscript L), the work of adhesion, W_{AL} is

$$W_{AL} = \gamma_{aL} + \gamma_{bL} - \gamma_{ab} \quad (17)$$

For an adhesion-substrate interface the work of adhesion, W_A in an inert atmosphere, for example dry air, usually has a positive value, indicating thermodynamic stability of the interface. However, in the presence of a liquid the thermodynamic work of adhesion, W_{AL} may well have a negative value indicating the interface is now unstable and will dissociate. Thus calculation of the terms W_A and W_{AL} may enable the environmental stability of the interface to be

predicted. The values of W_A and W_{AL} may be calculated [274, 275]

$$W_A = 2\left(\gamma_a^D \gamma_b^D\right)^{\frac{1}{2}} + 2\left(\gamma_a^P \gamma_b^P\right)^{\frac{1}{2}} \quad (18)$$

$$W_{AL} = 2\gamma_L - \left(\gamma_a^D \gamma_L^D\right)^{\frac{1}{2}} - \left(\gamma_a^P \gamma_L^P\right)^{\frac{1}{2}} - \left(\gamma_b^D \gamma_L^D\right)^{\frac{1}{2}} - \left(\gamma_b^P \gamma_L^P\right)^{\frac{1}{2}} + \left(\gamma_a^D \gamma_b^D\right)^{\frac{1}{2}} + \left(\gamma_a^P \gamma_b^P\right)^{\frac{1}{2}} \quad (19)$$

where γ^D and γ^P are the dispersion and polar force components, respectively, of the surface free energy, γ.

Some examples of values of W_A and W_{AL} are shown in Table 2.2. and the generality of this concept is illustrated by reference to environments other than water.

For those interfaces where there is a change from positive to negative work-of-adhesion then this provides a driving force for the displacement of adhesive on the substrate surface by the liquid. It is therefore to be expected that, if the joint is subjected to such an environment there will be a progressive encroachment into the joint of de-bonded interface. This will have the effect of progressively reducing the joint strength and also of progressively changing the locus of failure to interfacial between adhesive and substrate. This is exactly what has been observed in practice [275, 276]. However, it should be recalled that the measured adhesive failure energies required for the range of crack growth rates normally encountered are much higher than the values of the thermodynamic work of adhesion shown in Table 2.2 [277, 278] This is because, under an applied load, mechanical strain-energy is available to assist environmental cracking or debonding and this is reflected in inelastic energy dissipative processes, e.g. plastic flow, occurring in regions of the adhesive around the crack tip. The values of W_A and W_{AL} do not allow for such processes.

Interface	Work of adhesion mJ.m.$^{-2}$ Inert medium W_A	In liquid medium,	W_{AL}	Evidence of interfacial de-bonding after immersion of unstressed joints.	Ref. No.
Epoxy adhesive-ferric oxide (mild steel)	291	Ethanol	22	No	275
		Formamide	-166	Yes	275
		Water	-255	Yes	275
Epoxy adhesive-aluminium oxide	232	Water	-137	Yes	279
Epoxy adhesive-silica	178	Water	- 57	Yes	279
Epoxy adhesive-carbon fibre reinforced plastic	88-90	Water	22-44	No	280
Vinylidene chloride - methacrlate co-polymer-polypropylene	88	Water	37	No	281
		Sodium n-octyl sulphate (3.5% wt soln)	1.4	No	281
		Sodium n-dodecyl sulphate (o.5% wt soln)	-0.9	Yes	281
		Sodium n-hexadecyl sulphate (0.05% wt soln)	-0.8	Yes	281

Table 2.2 Values of W_A and W_{AL} for various interfaces and environments.

In those instances where W_{AL} is not negative but $W_A > W_{AL} \geq 0$ then the input of additional work is a necessary requisite for joint failure. However, as might be expected, the measured adhesive failure energy for interfacial crack growth is now reduced by the presence of the liquid[277, 282, 283] Gent and Schultz [283] measured the failure energy of a cross-linked styrenebutadiene rubber adhering to a polyethylene-terephthalate substrate and conducted experiments in air and in an alcohol-water series of liquids. They found that the failure energy was reduced from the latter experiments and that the reduction factor was in good agreement with that predicted from simple thermodynamic considerations, similar to those described above.

Finally, it should be noted that the thermodynamics as stated in Equation 16 to 19 take no account of interfacial adhesion forces arising from primary bonds or mechanical interlocking. Further, they provide no information on the expected service-life of joints upon being stressed in hostile environments. For this data the thermodynamic analysis needs to be combined with either a stress biased activated rate theory, as developed by Zhurkov and co-workers [284, 285] and used in joint fracture studies by Levi et al [286] or a continuum fracture-mechanics approach [287, 288].

2.10.2.3. Stability of the substrate

Obviously, environmental attack on the substrate material may well cause a loss in joint strength but, if "gross" effects are considered,

then this is not usually a major mechanism of environmental failure. For example, corrosion of the surface of a metallic substrate is often a post-failure phenomenon, occurring after the displacement of adhesive on the metal oxide by water [275] Only in special circumstances, for example with clad aluminium-alloys or in salt-water environments, is gross corrosion of the substrate an important failure mechanism.

The potential problem with clad aluminium-alloy is of particular interest and has been studied in detail by Riel [289] With clad aluminium-alloys the electrode potential of the cladding is generally higher than that of the base alloy. This choice is deliberate in that the clad material is selected to be anodic with respect to the base alloy so that, in a corrosive environment, the cladding will be consumed, thus protecting the base alloy. This mechanism is very effective in protecting the structure from surface corrosion, such as pitting, since pitting of clad alloy is less likely to occur due to the nature of the alloy and where pits do form and penetrate the clad surface its anodic nature will cause the pit to grow laterally once the base alloy is reached, rather than penetrating into the base alloys as is seen with unclad alloy. However, while this mechanism of corrosion protection inhibition may be effective for exposed aluminium-alloy structures, if one considers the mechanisms whereby clad aluminium-alloy achieves its corrosion resistance then the clad layer may be actually undesirable in the context of adhesive bonding. A galvanic cell may be established between cladding and base alloy with the progressive destruction of the interfacial regions.

In the United States aerospace industry the current trend is away from adhesive bonding to clad aluminium-alloys [269, 290, 291]. However, where unclad alloys are bonded and used in areas exposed to corrosive environments any non-bonded exterior surface must be protected by appropriate means in order to limit surface corrosion. With regard to more subtle changes induced in the nature of the surface of the substrate by an active environment, then Noland [292] has reported that the oxide produced on aluminium-alloys by a chromic-sulphuric acid etch, a common pre-treatment technique in the aerospace industry, is unstable in the presence of moisture. He has postulated that the oxide changes to a weaker, gelatinous type which is hydrated and is termed "gelatinous-boehmite" His evidence for the change in oxide structure comes from X-ray photoelectron spectroscopy analysis of the oxide surface before and after ageing and a change in binding energy is observed for the aluminium 2p-peak position, indicating a change in oxide structure. Noland also examined epoxy-aluminium-alloy joints after exposure to hot, humid conditions and reported that, although from a visual inspection apparent interfacial failure had occurred, in fact the locus of failure was in the mechanically-weak gelatinous-boehmite oxide layer. Recent work [293] using electron diffraction and scanning transmission electron microscopy has essentially confirmed the conclusions of this earlier study. The original oxide formed by the pre-treatment was found to be largely amorphous but, upon exposure to moisture, became hydrated and possessed a crystalline, pseudo-boehmite (i.e. a material containing somewhat more water than perfectly-crystallized boehmite) structure.

This hydrated oxide could be readily distinguished by its distinctive morphology which consisted of irregular-shaped platelets, which the author dubbed a "cornflake structure". This structure was, however, only loosely bound to the underlying oxide and thus represented a weak boundary layer,but one which was actually formed in situ in the joint.

However, the reason why certain pre-treatments coupled with specific grades of aluminium-alloy result in adhesive joints possessing vastly different resistances to enviromental attack by water has yet to be resolved in detail. Sun et al [294] have employed Auger spectroscopy to characterize acid etched aluminium alloys and have suggested that it is the accumulation of certain elements, such as copper and magnesium at the oxide-metal interface or in the oxide layer which are detrimental to oxide stability and joint durability. Kinloch and Smart [295] using X-ray photoelectron spectroscopy, have also recently identified a correlation between high magnesium content in the oxide layer and poor joint durability. These conclusions are qualitatively supported by observations from other sources [294]. For example, Minford [296] has reported extremely poor bond durability when bonding vapour-degreased 6061.T3 aluminium alloy while Smith and Martinsen [297] have reported that this alloy has a magnesium rich surface.

2.11. Kinetics of failure

Several workers [287, 275, 298, 304, 260, 266] have shown that the kinetics of the environmental failure mechanism may be governed by the rate of diffusion of water into the joint. Fortunately, water

up-take by cross-linked adhesives often behaves according to Fick's law and thus, from measuring the diffusion constant, using bulk adhesive film samples, the water concentration profile within the joint as a function of geometry, temperature and water activity may be predicted [287, 298, 303, 304] Comyn and co-workers [298, 305] and Althof [303, 304] have shown that these predictions are reasonably accurate, certainly around the periphery of the joint where the initial de-bonding occurs.

Comyn and co-workers [298, 299, 301, 302] have also demonstrated that a linear relationship often exists between loss of joint strength and total water content of the adhesive layer. Recently Gledhill et al [287] have undertaken quantitative predictions for the durability of unstressed butt joints consisting of mild-steel substrates bonded with a simple epoxide adhesive. First, from diffusion data for the adhesive, concentration profiles for water ingressing into the adhesive joint were calculated as a function of time and temperature. For this joint, environmental attack occurs by truly interfacial failure and, in the absence of an applied stress, the kinetics are governed solely by the rate of water diffusion. Second, therefore, by assigning a constant, critical water concentration for de-bonding, the interfacial environmental crack-length, a, as a function of the time spent in the water at a given temperature, was deduced. Third, this crack-length was combined with the independently measured values of $\mathcal{G}_{Ic}$ and E_a of the adhesive and used to predict the failure stress expected when the joint was subsequently removed from the environment and fractured. The predictions, over a wide range of times and temperatures, were in excellent agreement with the experimentally-determined values.

2.12. Effects of stress

The rate of loss of strength may be faster if a tensile or shear stress is present, albeit an externally applied stress or internal stresses induced by adhesive shrinkage (incurred during cure) or by adhesive swelling (due to water uptake) [224, 268, 269, 272, 278, 288, 290, 306,307] Such stresses render primary and secondary bonds more susceptible to environmental attack by lowering the free energy barrier that must be crossed if the bond is to change from an unbroken to a broken state, i.e., lower the activation energy for, and so increase the rate of bond rupture. Stress also probably increases the rate of diffusion of the ingressing medium. On the positive side, plasticization of the adhesive may diminish stresses by stress relaxation and crack blunting mechanisms. Indeed, crack-tip blunting may actually cause the apparent toughness of the adhesive to increase, and such an effect has been reported after short exposure times insufficient for significant interfacial attack [278, 308, 309]

2.13. Increasing joint durability

The deleterious effect of water on the joint strength and post-failure corrosion of the substrate could be avoided if the integrity of the interfacial regions could be maintained. Thus, either water must be prevented from reaching the interface in sufficient concentration to cause damage or the intrinsic stability of the interface must be increased.

2.13.1. Decreasing water permeation

All organic polymers are permeable to water and values of permeability coefficients and diffusion constants may be found in the literature (268, 298, 309) However, structural adhesives are usually based upon epoxy or phenolic polymers and these materials are already at the low end of the spectrum of such values. Thus, whilst there is undoubtedly room for improvement the other properties of any adhesive, such as wetting-adhesion chracteristics, processability, toughness, cost, etc., must be balanced against the need for low water permeability.

A second approach has been to use sealants (which are usually based upon organic polymers) to coat the edges of the exposed joint. However, while this will obviously slow down water penetration it is often not possible to apply a thick enough layer to be very effective and this approach has other disadvantages such as adding an extra operation and cost to the bonding process.

2.13.2. Substrate stability

Stability of the substrate surface to which the adhesive is attached is an obvious requirement for ensuring durable joints. This emphasizes the important role that the selection of pre-treatment technique, prior to adhesive bonding, assumes in ensuring adequate service-life of the bonded joint.

In the case of aluminium-alloys, workers (269, 310, 311) at the Boeing Commercial Airplane Company have recently developed a new surface pre-treatment method based upon phosphoric-acid anodizing.

This method results in improved joint durability, although the exact mechanism underlying this improvement has yet to be conclusively established. Noland [292] employed X-ray photoelectron spectroscopy and the results indicated that the oxide formed was more stable than that formed by a chromic-sulphuric acid-etch method to the presence of moisture. Also Bascom [272] has recently drawn attention to the thick, porous oxide structure [269, 312] produced by this pre-treatment. Penetration would result in a resin-metal oxide composite interface region that may contribute significantly to joint durability since failure through the oxide would involve plastic and viscoelastic deformation of the ligaments of the adhesive (or primer) (see Section 2.6.1.) Also, in such a process, mechanical interlocking may contribute significantly to the intrinsic adhesion [272, 312, 313] and thus invalidate the thermodynamic work of adhesion as a sole criteria for interface stability. Hence, it appears that in certain circumstances the oxide must possess both a resistance to attack by water and the "correct" microstructure for maximum joint durability. However, it is not, at present, possible to define in detail the exact surface chemical and physical parameters which are important for producing an oxide layer which will impart good environmental resistance to an adhesive joint.

2.14 Aims of programme

The project objectives are

1. To investigate the performance of adhesive bonds to aluminium with specific reference to the conditions under which structural joints must perform in a motor vehicle.

2. To evaluate the performance and suitability of existing surface treatments for aluminium, and to suggest alternatives where appropriate.

3. To assess methods for testing bond durability in both natural and service environments and recommend the most suitable techniques.

CHAPTER 3 EXPERIMENTAL

3.1. Materials

3.1.1. Aluminium alloys

BA 2117 and 5251 alloys containing respectively copper and magnesium as principal alloying elements, were used throughout this project. These materials, the specification details of which are provided in Table 3.1, were obtained in the "half-hard" form.

	2117	5251
	%	%
Cu	2.2 - 3.0	0.04 max.
Mg	0.2 - 0.5	1.8 - 2.4
Mn	0.2 max.	0.5 max.
Si	0.8 max.	0.5 max.
Fe	0.7 max.	0.5 max.
Cr	0.1 max.	0.3 max.
Zn	0.25 max.	0.05 max.
Ni		0.05 max.

Table 3.1

In the preparation of the metal-polyamide peel specimens described in Section 3.3.2., 0.2 mm thick pure aluminium foil was used.

3.1.2. Adhesives

3.1.2.1. Structure and curing mechanisms of epoxides

The high strength and versatility of epoxide and modified epoxide adhesives has resulted in rapidly increasing deployment in recent years. The development of these materials dates back to 1934 when Schlack prepared a resin derived from epichlorohydrin and bisphenol A, which could be cured by amines, acids or mercaptans.

Serious development of epoxides as adhesives was initiated in the late 1940's by Ciba-Geigy and Shell, and to-day a vast range of materials is commercially available. A particularly notable development has been the introduction of "toughened" epoxides, in which the precipitation of a rubber particulate phase during the curing process inhibits crack growth and enhances impact performance.

Bisphenol A and epichlorohydrin react to produce diglycidyl ethers as shown in Fig. 3.1.

The diglycidyl ether of bisphenol A (DGEBA) is a crystalline solid when n approaches zero. Commercially available blends of various diglycidyl ethers for which the average value of n is approximately 0.2 are suitable for adhesive manufacture.

There are two basic classes of curing agent available. The first class includes aliphatic primary and secondary amines, aromatic amines and various di- or polyfunctional carboxylic acids and their anhydrides. These agents cure by hydrogen addition to the epoxide group as shown in Fig. 3.2.

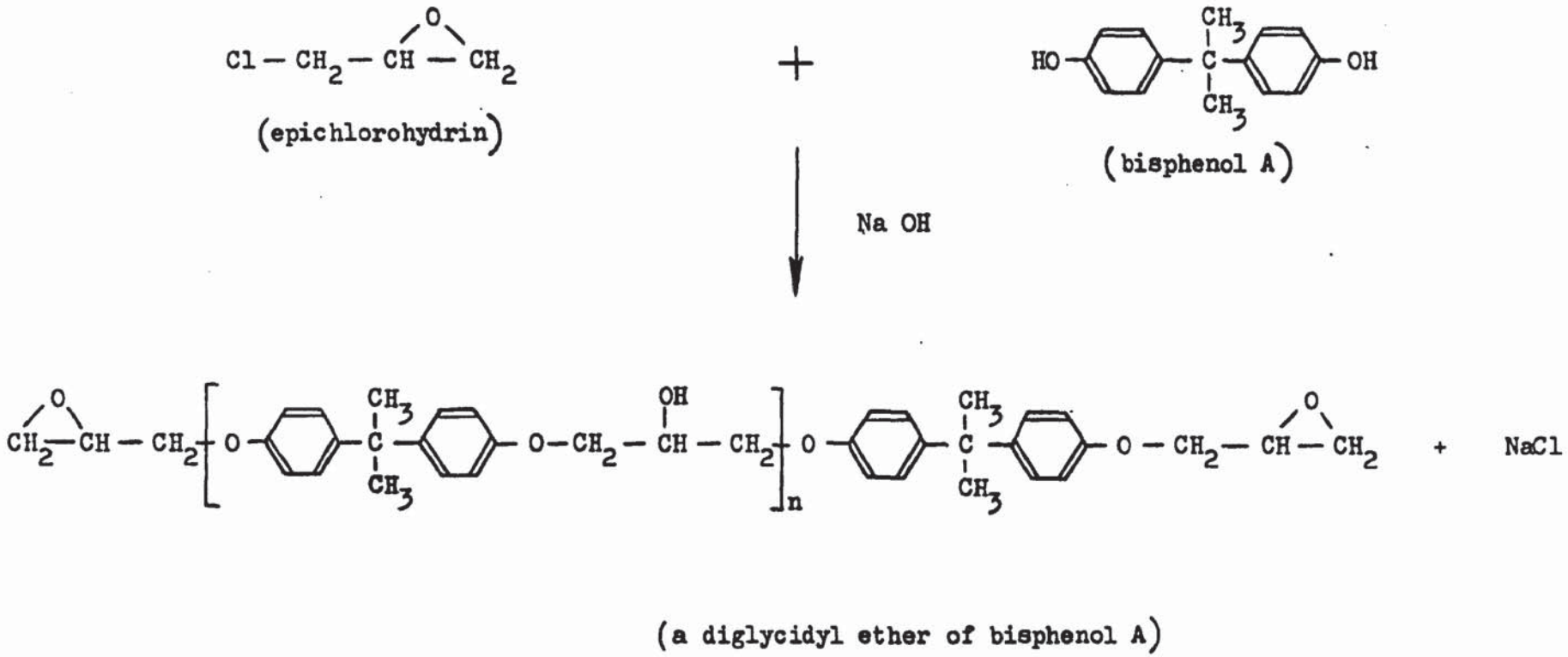

Fig. 3.1 The preparation of epoxide resins

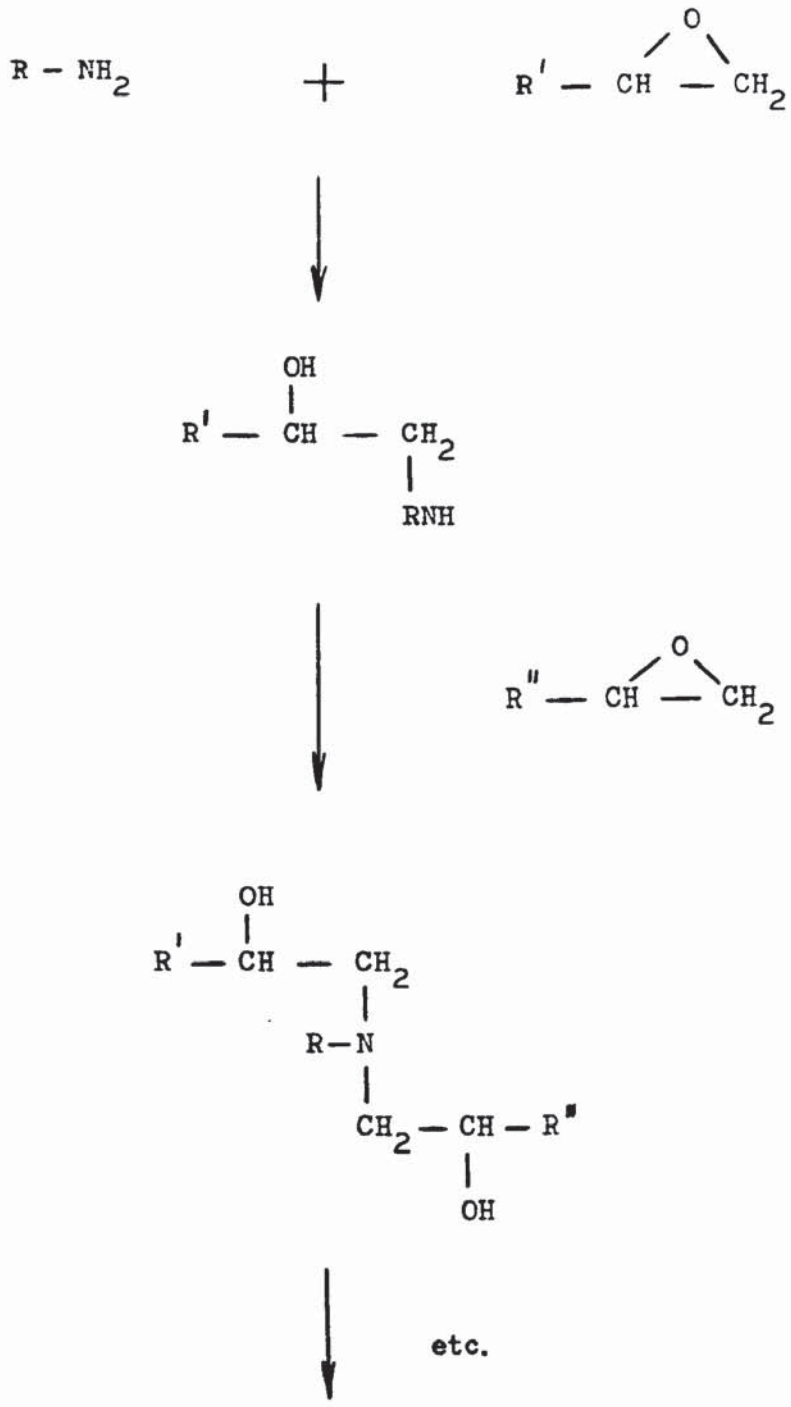

Fig. 3.2 Curing mechanisms (by primary amine)

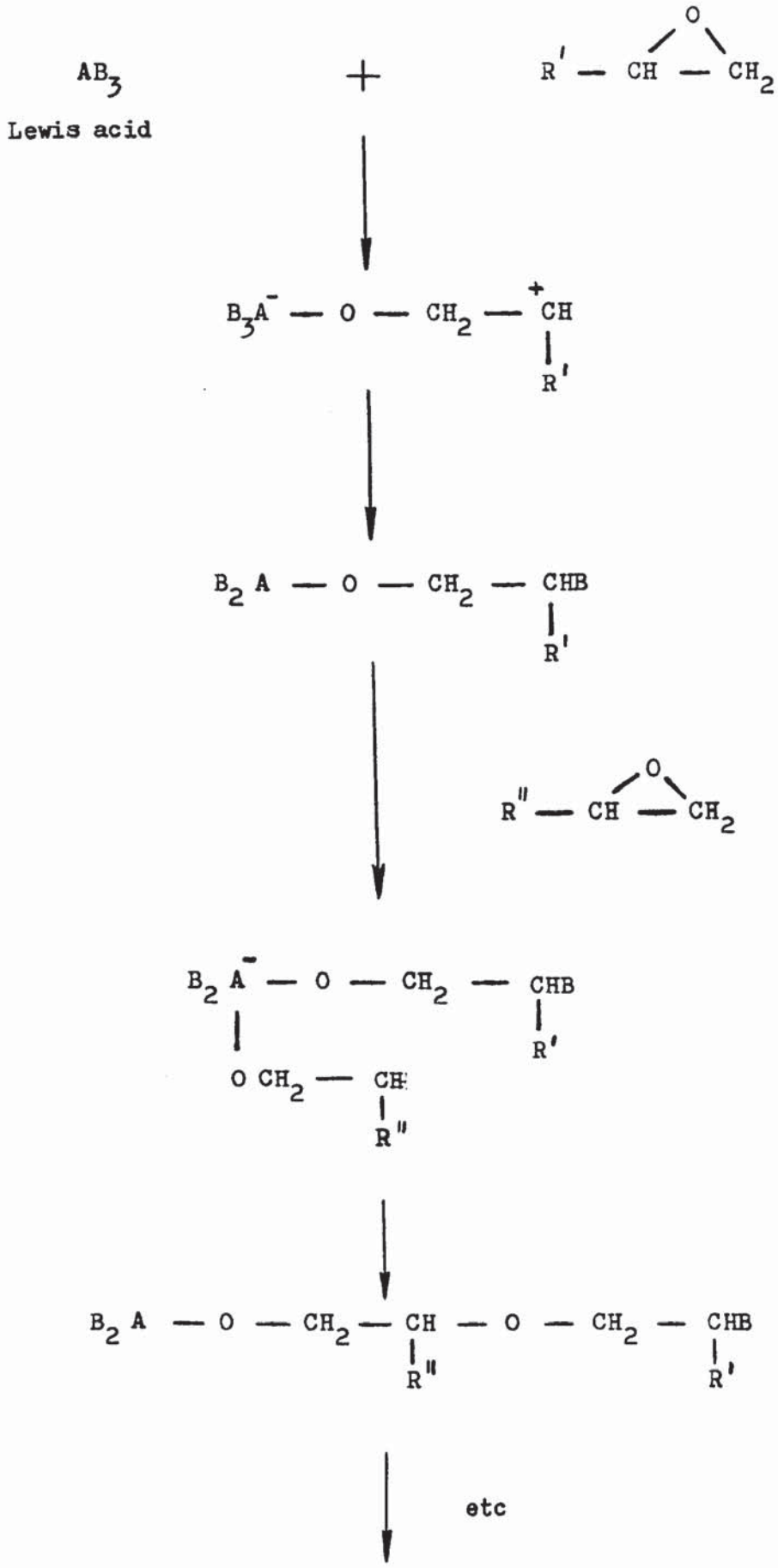

Fig. 3.3. Curing mechanisms (by Lewis acid)

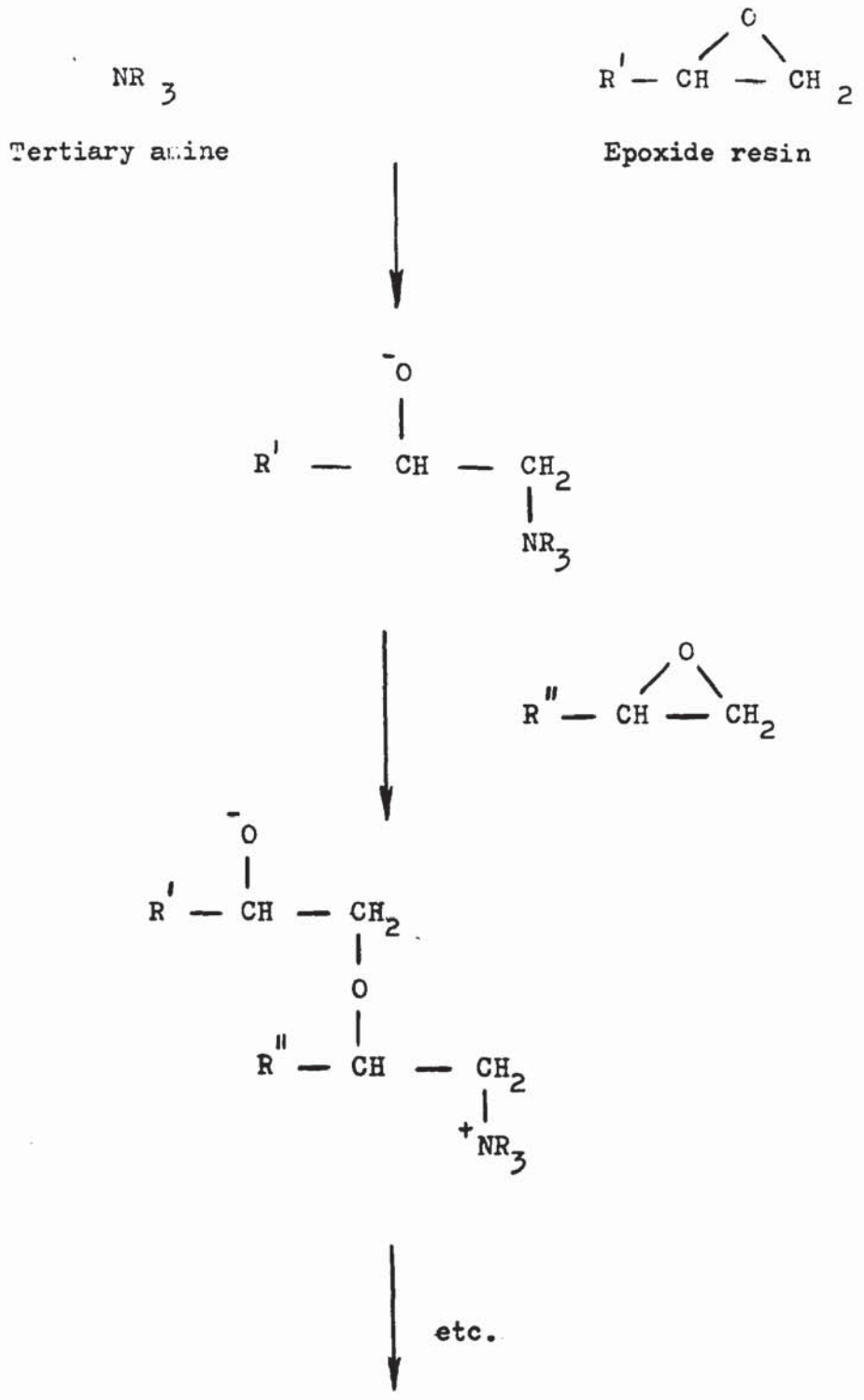

Fig. 3.4 Curing mechanism (by tertiary amine)

tautomerisation of dicyandiamide

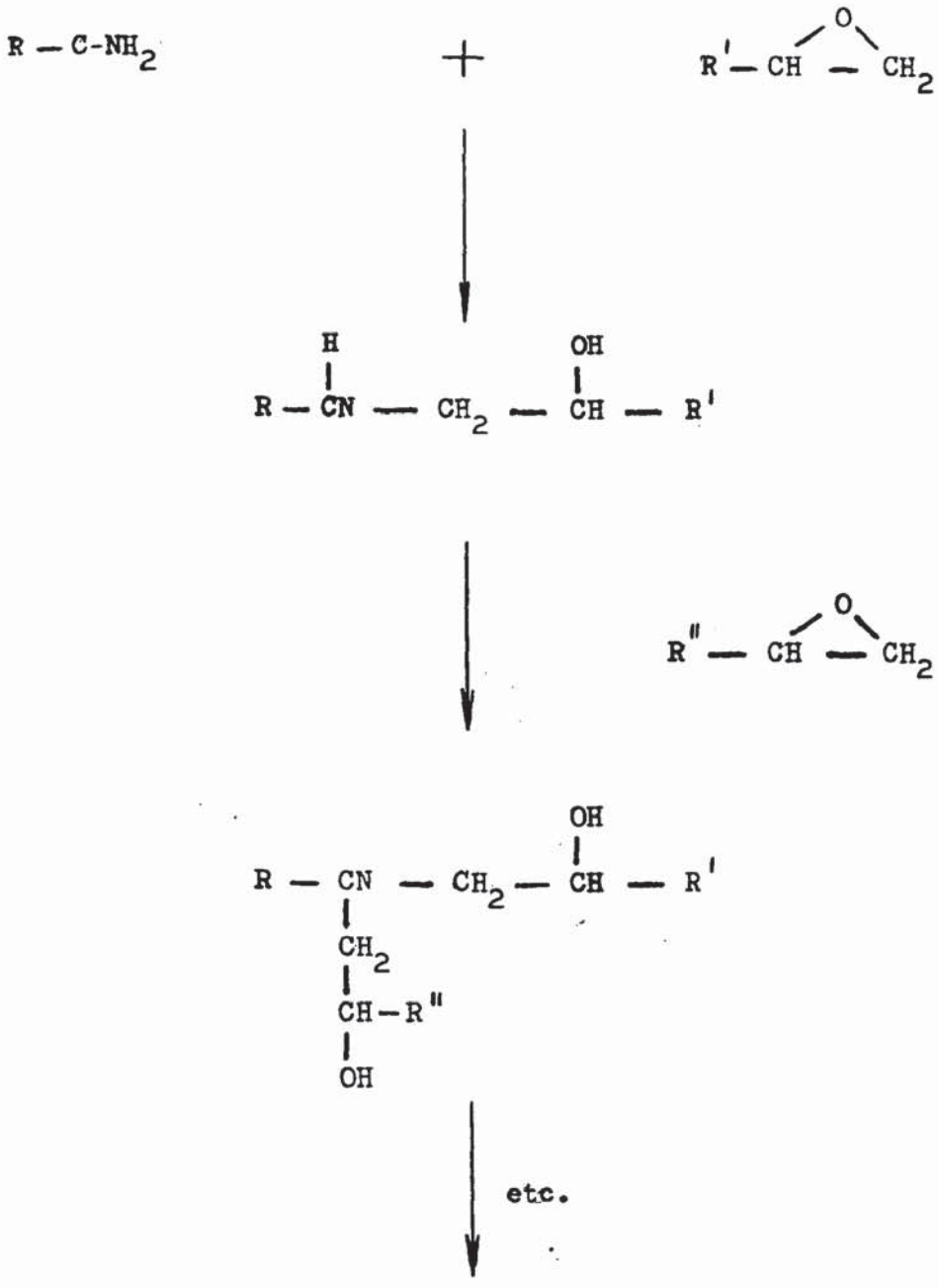

Fig. 3.5 Curing mechanism of WP9

The other class of curing agents are those compounds which catalyse the homopolymerisation of epoxides. Such catalysts include organic and inorganic acids and bases. Two examples of this type of reaction, both of which proceed via ionic mechanisms, are shown in Figs. 3.3 and 3.4.

3.1.2.2 Adhesives Used.

Three examples of proprietary epoxy adhesives have been used during the course of this work. All are single component systems requiring elevated temperature curing conditions. 10% by weight additions of 250 - 300 μm ballotini glass spheres were incorporated into the adhesive to provide control of bond line thickness. This technique has become standard practice as a result of earlier investigations by Wood[314] which had demonstrated a surprising lack of sensitivity of bond strength to ballotini concentration. Since test joints were assembled using only very low clamping pressures, lower levels of ballotini, say of the order of 1%, would have probably been equally effective in controlling the bond line. Adequate dispersion of low concentrations may involve an increased risk of air entrapment however and a 10% addition appeared a reasonable compromise. The adhesives employed were:-

(a) EC2214, supplied by 3M Co. Ltd. This aluminium-filled material was described only as a modified epoxy. No further information could be obtained but the adhesive is known to be a non-toughened type. The justification for its use in this project is largely historical, since much data concerning its performance had already been generated.

(b) ESP 105, manufactured by Permabond Ltd. This amine cured material is said to be based on a modified diglycidyl ether of bisphenol A, toughened with a carboxy-terminated butadiene rubber. It contains approximately 45% by weight aluminium powder. Such additions, frequently encountered in proprietary formulations, are said to increase modulus, improve thermal conductivity and reduce the difference between the coefficient of thermal expansion of the adhesive and that of the adherend.

(c) WP 9, an early experimental adhesive prepared by Dunlop Technology Division. It is an unfilled toughened epoxide also based on a diglycidyl ether of bisphenol A. The toughening phase is a carboxy-terminated butadiene-acrylonitrile rubber.

The curing agent used, dicyandiamide, is almost insoluble in the epoxy resin at temperatures below 120°C. At higher temperatures the dicyandiamide tautomerises to a more soluble configuration, the amine groups of which then react with the epoxide.

Curing mechanism is shown in Fig. 3.5.

3.2 Pretreatments

3.2.1 Apparatus

To facilitate the uniform and efficient processing of test coupons jigs were designed and constructed for use with small scale treatment tanks. The principle is shown in Fig. 3.6. The assembly is constructed entirely of aluminium alloy, the conical tipped alloy bolts providing both mechanical security and electrical contact when necessary. Several jigs of this type, each of which accomodates 24 coupons, were assembled. Tank dimensions and materials varied but all were compatible with the jigs.

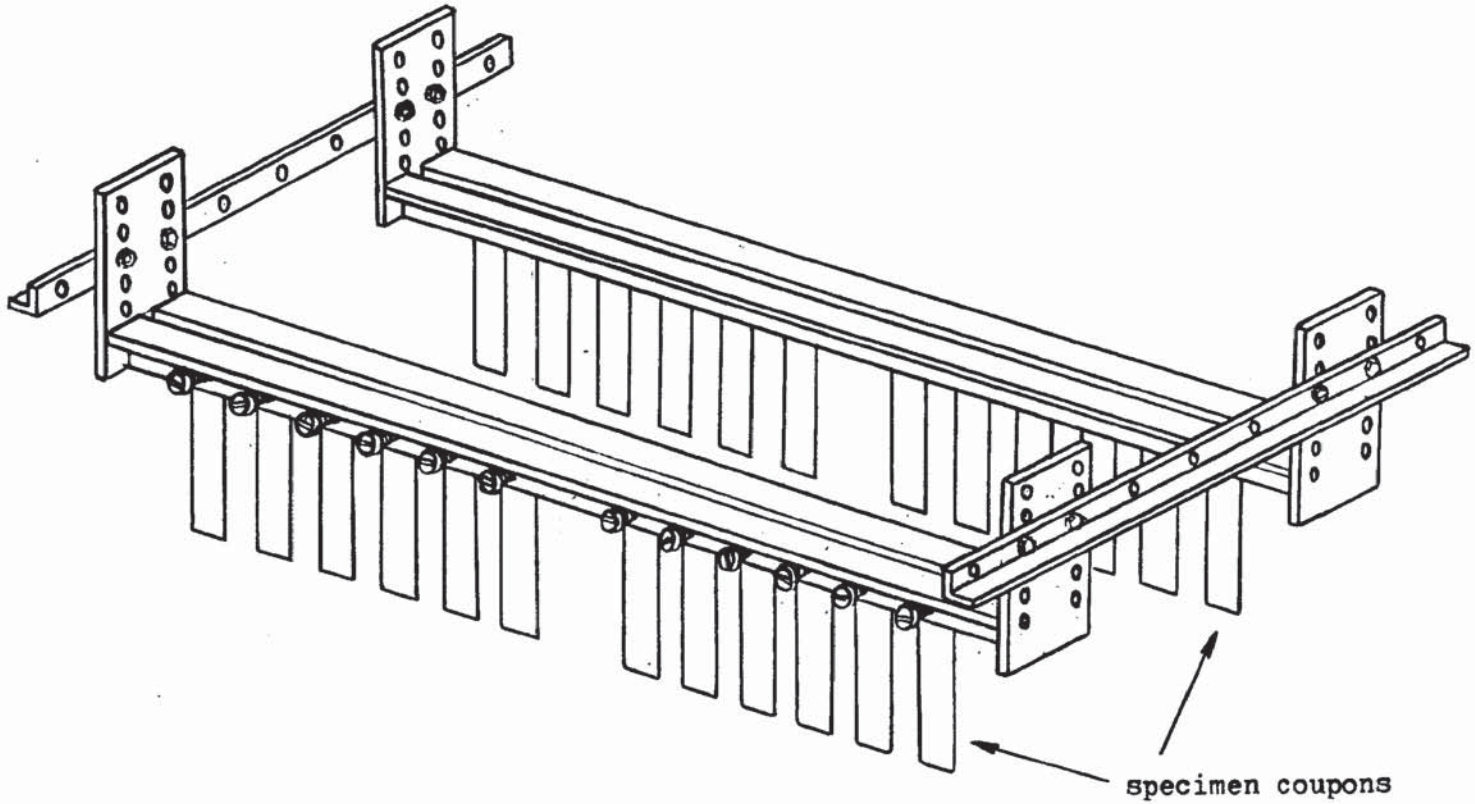

Fig. 3.6 Pretreatment jig.

Tap water rinse tanks were constructed of high density polyethylene with stainless steel jet tubes.

The stainless steel alkaline cleaner tank featured a submerged pump for agitation, and temperature control by contact thermometer and silica-sheathed heater. A similar arrangement was used for the FPL etch solution, except that the tank walls were completely lead lined and the pump shaft/impeller assembly was in titanium rather than stainless steel.

The proprietary deoxidiser solution used was operated at room temperature without agitation in a high density polyethylene tank.

Direct current phosphoric acid anodising e.g. to Boeing Aircraft Corporation BAC 5555 specification, was effected using a high density polyethylene tank fitted with stainless steel cathodes and air agitation. Polyethylene croffles were floated on the surface to reduce evaporative losses and the formation of acid mist.

A 5amp stabilised power supply provided a d.c. potential adjustable over the range 0 - 30 volts. All d.c. sulphuric acid and a.c. phosphoric acid anodising was carried out using a 2 litre beaker equipped with carbon electrode and a thermostirrer for heating and agitation purposes. Specimen coupons were clipped to the perimeter of a disc-shaped electrode arrangement which provided if desired simultaneous location of the specimens at a predetermined depth, and electrical contact to the voltage source.

A.C. sulphuric acid anodising was carried out using a cylindrical lead sheet cathode lining the beaker wall and electrical contact to the specimens was made before immersion, and broken after removal from the solution.

3.2.2 Processes

The most widely employed surface treatment procedures are listed below. Other processes investigated are described in the appropriate results section.

3.2.2.1 Degreasing

Initial cleaning to remove gross contamination was done using either trichloroethylene vapour or by rinsing in methyl ethyl ketone.

3.2.2.2 Alkaline cleaning

A proprietary non-etching solution of Oakite NST (10% by volume) operated at 50°C with continuous agitation was employed. An immersion period of 5 minutes was followed by a running tap water rinse also of 5 minutes duration. The above procedures invariably resulted in water break free surfaces and were included in all pre-treatment sequences.

3.2.2.3 Deoxidising

An acid solution of ICI's "Deoxidiser No.1." was operated at room temperature to remove pre-existing oxide. The recommended 3 minute immersion was followed by a 10 minute running tap water rinse. The principal constituents disclosed by ICI and subsequently confirmed qualitatively by analysis are listed in Table 3.2. The working strength solution contains 25g deoxidiser and 25ml concentrated sulphuric acid per litre.

Constituent	Concentration
Aluminium phosphate	< 10%
Fluorides (Ca, NH_4^+)	~ 10%
Potassium dichromate	balance

Table 3.2 Principal Constituents of I.C.I's Deoxidiser No.1

(working strength solution contains 25g + 25 ml. H_2SO_4 per litre).

3.2.2.4 F.P.L. etch (optimised)

This chromic-sulphuric acid solution, conforming to that specified by the U.S. Forest Products Laboratory for adhesive bonding applications differs from the UK's Defence Standard 03-2/1 Method O primarily in the chromium donor used. The former also contains small additions of dissolved copper and aluminium which are said to artificially "age" the solution and improve the consistency of the process. The sodium dichromate level was chosen to yield the same concentration of hexavalent chromium as that found in the chromic acid solution specified in Defence Standard 03-2/1 Method O. Compositional details are shown in Table 3.3. Specimens were treated for 10 minutes @ 65°C. with continuous agitation, then rinsed for 10 minutes in running tap water, followed by a brief rinse in deionised water.

Solution composition:-	
Sodium dichromate	$75g.l^{-1}$
conc. H_2SO_4	$150ml.l^{-1}$
Al	$1.5g.l^{-1}$
Cu	400 ppm

Table 3.3 Optimised F.P.L. etchant

3.2.2.5 Phosphoric acid anodising to BAC 5555

Details of solution composition and process conditions are given in Table 3.4. The anodising stage was always preceded by cleaning and "deoxdising" sequences, and followed by tap water and deionised water rinses. When dry, anodised surfaces may be observed through polarising filter at glancing angle to check for film continuity and freedom from gross contamination.

Solution composition	12% by weight H_3PO_4 in deionised water.
Solution temperature	20 - 25°C.
Voltage	10v. D.C.
Time	20 minutes.

Table 3.4. Phosphoric acid anodising conditions

3.2.2.6 Chromic acid anodising to Defence Standard 151 type 2

Specimens were prepared using commercial facilities because of a lack of suitable power supply. The anodising stage, carried out in 5% chromium trioxide solution at 40°C., conformed to the required voltage programme, i.e. gradual increase from 0 to 40 volts during first 10 minutes, maintained at 40 volts for 20 minutes, slowly increased to 50 volts during the next 5 minutes and maintained at 50 volts for a further 5 minutes. This stage was preceded by the usual cleaning cycles and followed by prolonged rinsing in running tap water, followed by a final rinses in deionised water.

3.3 Test joints

Three types of specimen with which the durability of adhesive bonds could be assessed were examined during the course of the project. They are the single lap shear joint, a polyamide—aluminium foil peel specimen, and a crack propagation wedge specimen developed by Boeing. The peel and wedge techniques, which were rejected in favour of the single lap joint, will be briefly described.

3.3.1 Boeing Wedge Test

This simplified crack propagation technique, described by Marceau et al [315], is claimed to provide qualitative indications of expected bond durability in hours, rather than weeks or months.
Specimen configuration is shown in Fig. 3.7. The wedge is inserted into one end of the bonded assembly and the crack tip located with the aid of a travelling microscope. The position of the crack tip is monitored after periods of exposure to hostile environments e.g. 100% RH @ 50° or 60°C. Interpretation of the results requires that an acceptance criterion be established based on a correlation between wedge test data and experience of bond failures in service.
Wedge specimens were prepared using 2117 and 5251 alloys, bonded with EC 2214 adhesive, and exposed to 100% RH conditions at 60°C.
Bonds to surfaces which had been only degreased generally failed completely within a few hours. Crack propagation rates for specimens the surface of which had been chromic acid etched or phosphoric acid anodised were low, but were invariably associated with yielding of the adherends and the subsequent loss of stress at the crack tip.

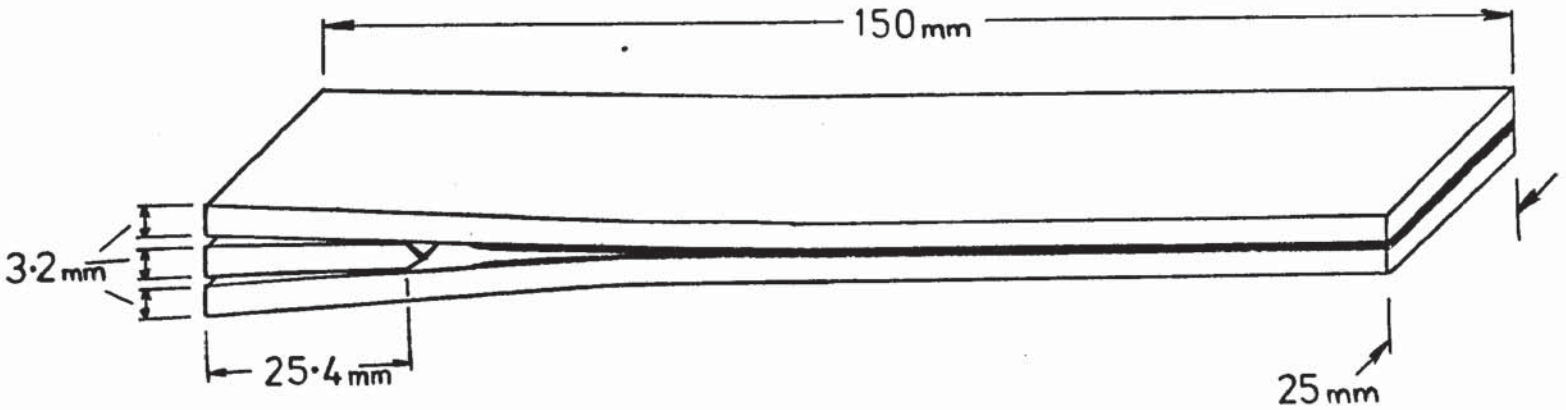

Fig 3.7 Boeing Wedge Test Specimen

Very thick or laminated adherends, or a change of alloy, did solve this problem, but the wedge test was abandoned at this stage for the following main reasons:-

(1) Alloys of interest cannot be used in the recommended specimen configuration.

(2) Acceptance criteria depend on real environment data and this is non-existent.

(3) Lack of quantitative information useful to the design engineer.

3.3.2 Modified peel test

Brockmann[316] has advocated a thin foil 180° peel test for adhesion measurement, claiming that failure always occurs within 200 Å of the metal surface. To overcome the problem of long diffusion paths and the necessarily prolonged periods of environmental exposure he has used a modified peel specimen prepared by bonding aluminium foil to 3 mm thick Nylon 66. This concept was examined, trying a range of adhesives in order to obtain the highest initial peel strength. Unfortunately, in the case of the most relevant types, the single-component elevated-temperature curing adhesives, severe distortion of the poylamide occurred, resulting in low and erratic failure loads. Some two-part room temperature cured epoxy adhesives were found to be more effective, providing reasonable peel strengths and a more uniform peeling action. These preliminary findings were not encouraging and further investigations were not pursued.

3.3.3 Single lap shear joint

3.3.3.1 Assembly considerations

The advantages of the single lap shear joint include the simplicity of its fabrication, the relative ease with which it can be stressed during environmental exposure and the engineering significance of the data produced. As indicated in Chapter 2, the failure mechanisms are complex, and therefore the control of certain variables when assembling these joints for test purposes is imperative. Existing assembly practice resulted in unacceptably high coefficients of variation in shear strength of ~ 20% within groups of 5 specimens. Inconsistent bond geometry was thought to be primarily responsible and a completely new type of assembly jig, as shown in Fig.3.8 was designed.

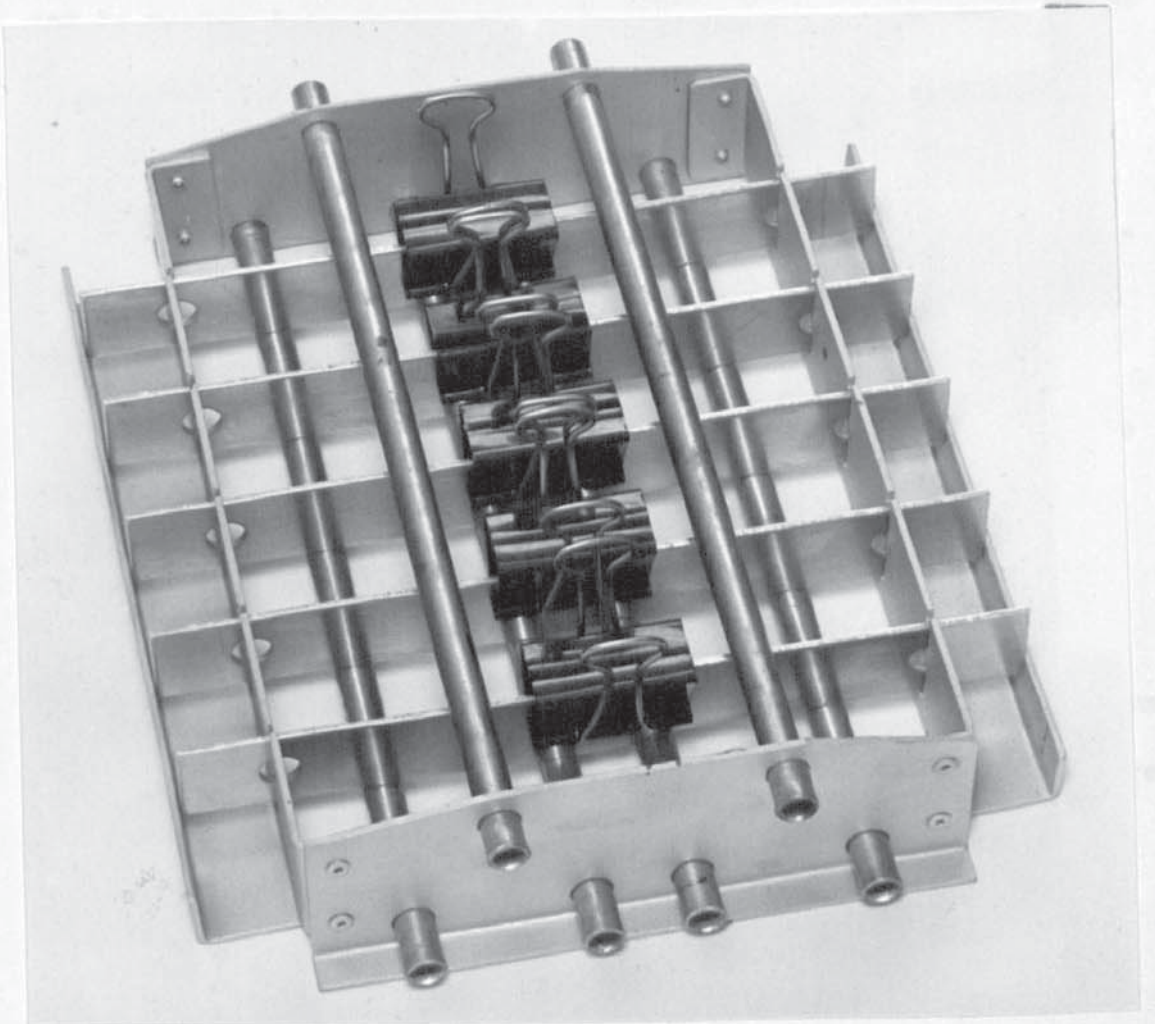

Fig. 3.8 Assembly jig, type I.

An additional consideration was control over curing profile, and the jig was designed to provide a heating rate at the bond line which closely resembles that of a vehicle body during the first paint stoving cycle. The standard curing cycle used for single lap shear joints is shown in Fig. 3.9.

The removal of fillet-forming excess adhesive prior to cure aids reproducibility. The retention of fillets at the ends of the overlap was found to increase mean strengths by approximately 13% and 42% in the case of ESP 105 and EC 2214 adhesives respectively. Clearly large coefficients of variation in strength may be measured in groups drawn from mixed populations, and the fillet-free configuration is potentially the more controllable. An additional advantage associated with the removal of adhesive fillets is reduced diffusion paths during environmental exposure.

During the course of this project assembly and test procedures have been refined. Increased geometrical accuracy is now attainable using punched specimen coupons and a derivative of the original assembly jig, the type II shown in Fig. 3.10.

A new perforated lap shear configuration was devised to further accelerate the degradation of adhesive bonds. The dimensions of these coupons are given in Fig. 3.11. The thickness is 1.63 mm unless specified otherwise. When assembled the bond area measures 20 mm wide x 10 mm overlap.

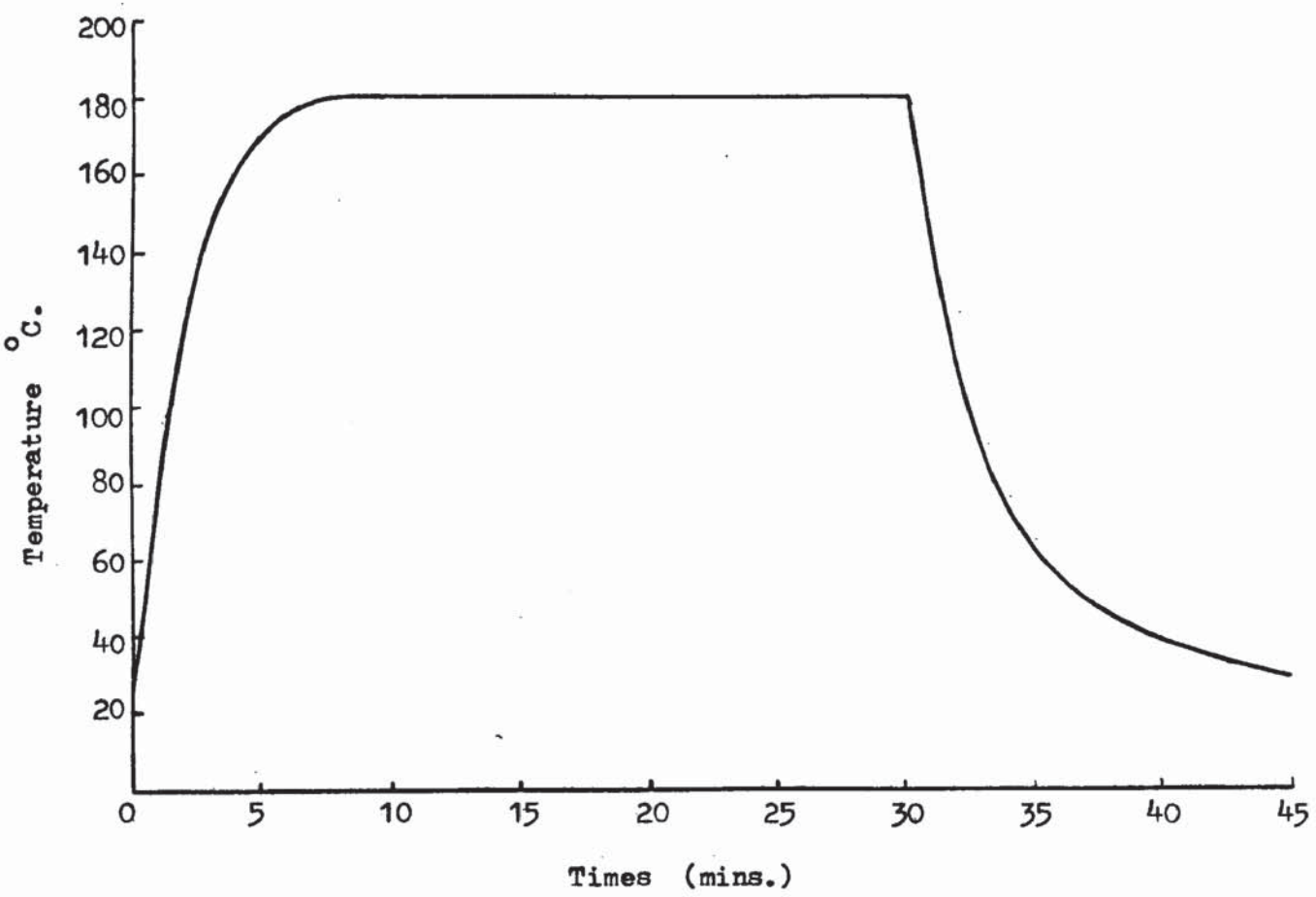

Fig 3.9 Standard lap shear cure profile, measured at the bond line.
(Type 1 assembly jig, ambient temp. 25°C. oven pre-heated to 180°C).

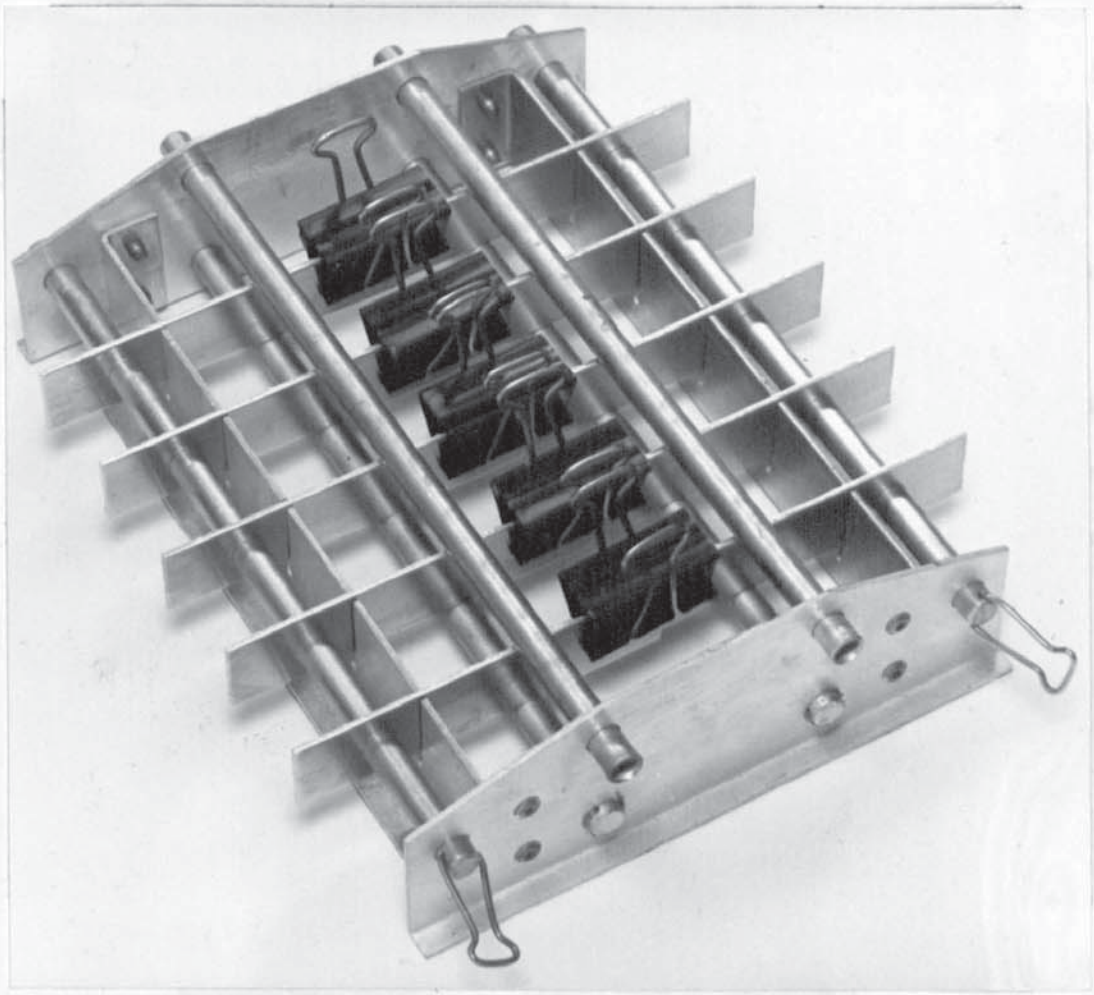

Fig. 3.10 Assembly jig, type II

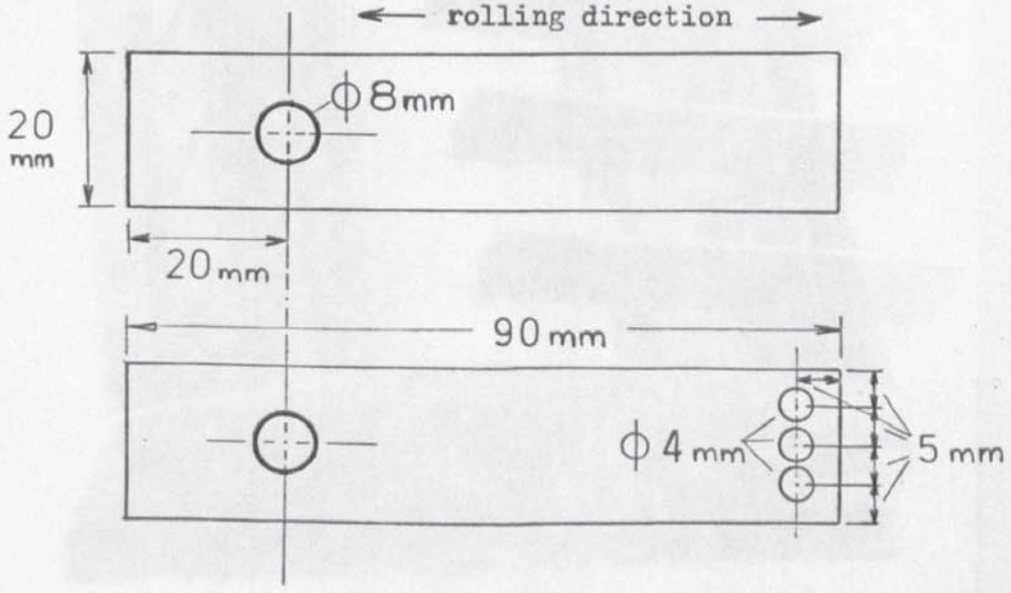

Fig. 3.11 Coupon dimensions

3.3.3.2 Assembly procedure

Standard i.e. non-perforated lap shear joints may be prepared using either type of assembly jig, depending on the method by which the coupons have been cut. The greatest geometrical accuracy will be attained using coupons which have been cut, with a location hole, using a press tool.

After application of a slight excess of adhesive five coupons are positioned in the jig slots as shown in Fig. 3.12, and located either by contact with the end-stop (type I) or by the engagement of a locating rod (type II).

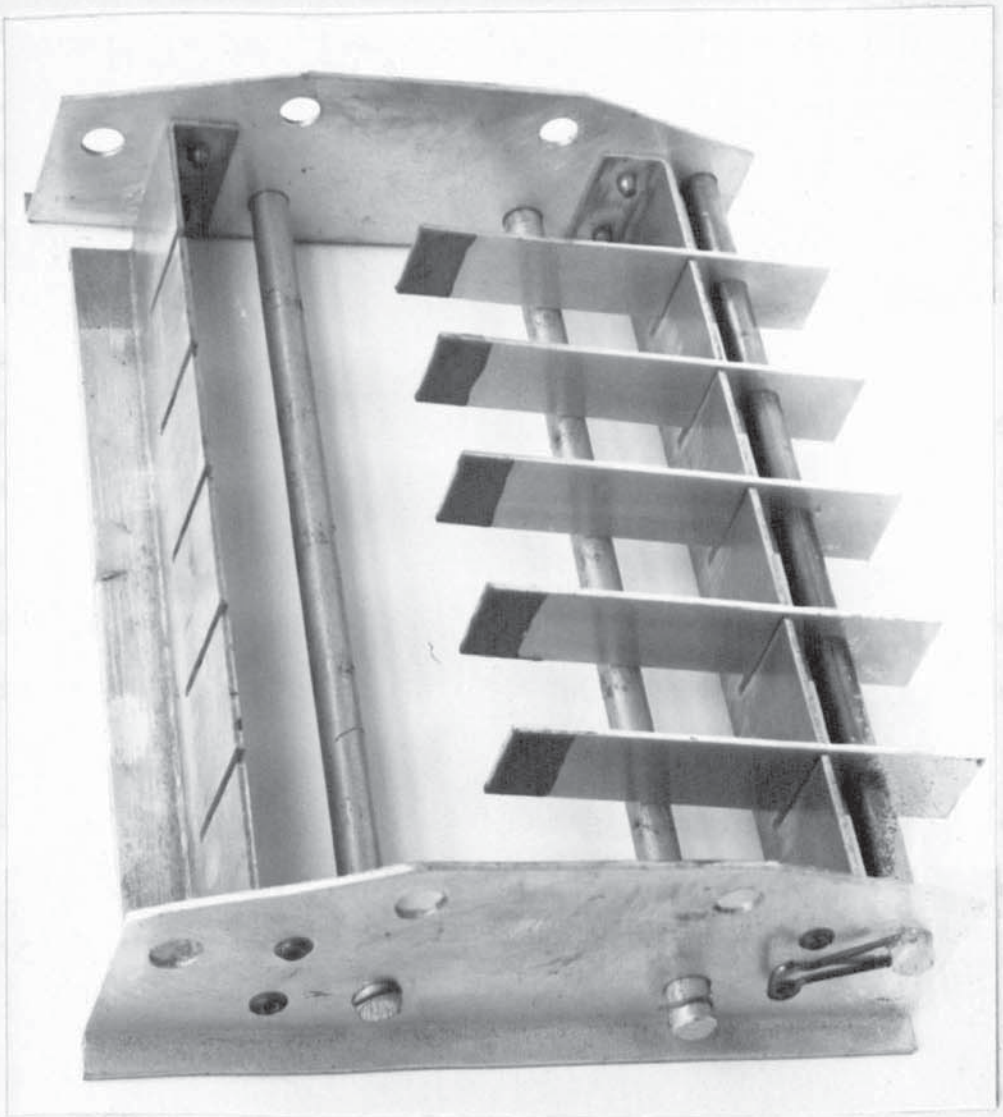

Fig. 3.12 Assembly procedure

A further five coupons are similarly positioned in the jig and the joints successively closed. Light finger pressure is exerted to reduce the bond line thickness to the ballotini-controlled value and maintained for a few seconds until all traces of exuded adhesive can be removed with the aid of a modified spatula. The joint is finally secured using a foldback clip.

(The joint should be closed by a single action and not re-opened unless indications of joint starvation are apparent. Ideally these adhesives should be applied to one surface and in bead form if the risk of air entrapment is to be minimised. The technique described above has been found to be effective however and bond line porosity attributable to joint preparation has been encountered extremely rarely). To ensure the maintenance of joint alignment during handling and subsequent cure the upper rods are installed. In the case of type I jigs a final check is made to ensure that the specimens are in contact with the end-stops. The bonds may now be cured, after which they are allowed to cool before removal from the jig.

This general procedure also applies to the preparation of perforated lap shear joints, except that the use of pressed coupons and type II jig is almost essential. After the adhesive has been cured the joints are perforated using the drilling jig, shown in Fig. 3.13., which was designed to ensure the necessary positional accuracy of the holes through the bond area. Lack of accuracy here will result in inconsistent diffusion-related effects during environmental exposure and the possibility of adherend failure along the plane of the holes during testing.

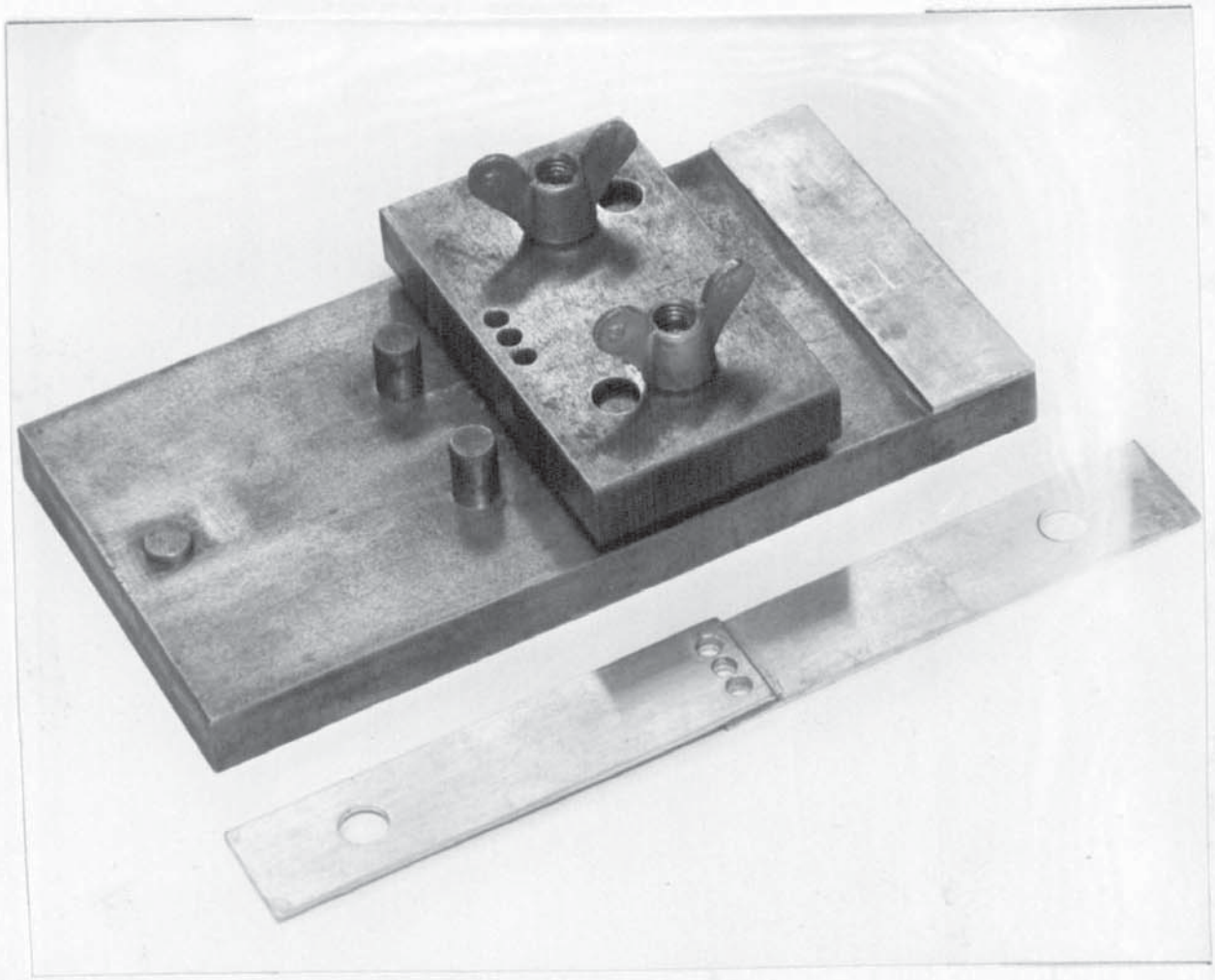

Fig. 3.13 Drilling jig for perforated specimens

Great care must be exercised during the drilling operation. A sharp, clean, lubricant-free 4 mm drill bit, rotating at high speed and advanced at a low feed rate is recommended. Localised overheating of the bond line, and the generation of internal burrs and subsequent bond line stresses must be avoided.

3.4 Environmental exposure

3.4.1 Salt-spray

Specimens were exposed unstressed to conditions established within a salt-spray cabinet supplied with a 5% neutral solution of sodium chloride. Operating temperature was initially a constant 35°C. but was raised during the course of this project to a constant 43°C. The temperature change followed claims made by British Hovercraft Corporation that this modest increase provided a useful degree of further acceleration. The results summarised in Table 3.5 confirm this view.

Table 3.5 The effects of salt-spray operating temperature on strength retention (%) of EC 2214 bonds to BA 2117 alloy.

Pretreatment	1 months exposure		6 months exposure	
	35°C.	43°C.	35°C.	43°C.
Optimised F.P.L. etch	100	81	93	24
Phosphoric acid anodise (BAC 5555)	99	88	100	69

3.4.2 Miscellaneous environments

Some test work, particularly that described in Section 4.2., involved exposure of relatively small numbers of specimens to a variety of environments, and this was conveniently accomplished using sealed Kilner storage jars at room or elevated temperatures.

3.5. Mechanical testing

Lap shear specimens were tested to destruction at room temperature using a Lloyds T22K tensile test machine equipped with 20kN Grade A load cell.

Crosshead speed was set to 2mm . min^{-1} and the residual strength of specimens which had been subjected to environmental exposure was determined without delay to avoid drying-out effects. Load to failure was recorded with an X-Y plotter and the mean failure stress for each specimen calculated. Results are plotted graphically and show the best fit curve through the sample means.

3.6 Measurement of absorption of water vapour

Two techniques were considered. The first was based on the use of an indicator described by Brockmann which was found to be unsuitable for use in tests of short duration.

The second method is quantitative and yields values for diffusion coeffi:cient and equilibrium water uptake.

3.6.1 Water sensitive indicator

Brockmann et al [317] have reported the use of 5, 8, dihydroxy - 1, 4, naphthoquinone to indicate the presence of water in bonded joints. Small additions(0.2% by weight) of the indicator were made to Ciba Geigy's AW106/HV953 cold curing epoxide.

Water absorption is said to result in the violet colour changing to orange, although it is also stated that diffusing oxygen produces a colour change to brown. To help establish the usefulness of this technique an attempt was made to correlate colour with water concentration. Thin films of the above adhesive containing the recommended concentration of reagent were cast and cured at room temperature. Weighed sections were immersed in deionised water at 60°C. Although saturation was achieved in less than 4 days, the colour change after 6 weeks immersion was minimal.

This slow response was confirmed by additional tests using metal-metal and glass-glass bonded joints exposed to 100% R.H. and salt-spray environments.

As a consequence of these disappointing findings no further investigations were undertaken.

3.6.2 Microbalance

Films of adhesive, about 250μm thick, and weighing approximately 40 mg were cast and taken to the Department of Chemistry, Leicester Polytechnic, where a sensitive microbalance had been developed for the measurement of sorption characteristics.

The instrument consists of a beam from which the adhesive specimen is suspended in the selected environment, in this case water vapour at 43°C. As the specimen absorbs water, the beam torque is balanced by a servo coil energised by amplified bridge current, derived from shuttered photo cells to detect beam displacement.

A meter, calibrated in units of weight, has five ranges reading from 25μg to 100mg f.s.d. By this means the increase in mass of the specimen as it absorbs water is monitored. The thin film of adhesive may be considered to be semi-infinite i.e. one in which edge diffusion can be neglected, and diffusion restricted to a direction, say x, which is perpendicular to the plane of the film. Thus, the appropriate form of Fick's second law is

$$\frac{\partial c}{\partial t} = D\left(\frac{\partial^2 c}{\partial^2 x}\right)$$

For a semi-infinite film in an infinite bath, the solution to Fick's second law is

$$\frac{M_t}{M_\infty} = 1 - \frac{8}{\pi^2}\sum_{n=0}^{\infty}\frac{1}{(2n+1)^2}\exp\left(\frac{-D(2n+1)^2\pi^2 t}{l^2}\right)$$

where M_t = mass of diffusant absorbed in time t

M_∞ = mass of diffusant absorbed at equilibrium

l = film thickness

n = integer over which the series is summed.

At short times this equation simplifies to:-

$$\frac{M_t}{M_\infty} = \frac{4}{l}\left(\frac{Dt}{\pi}\right)^{\frac{1}{2}}$$

The microbalance data can therefore be plotted as fractional uptake, Mt/M_∞ against $t^{\frac{1}{2}}$ If diffusion is Fickian the absorption curve is initially linear up to $Mt/M_\infty \sim 0.6$ and D may be obtained from the gradient of the linear region of the curve.

3.7 Examination of surfaces

3.7.1 Optical microscopy

Olympus BHB binocular microscope equipped with PM 10-M photomicrographic system and Nomarski differential interference phase contrast attachment.

3.7.2 Surface analysis

3.7.2.1 E.P.M.A.

International Scientific Instruments Model 60 scanning electron microscope, equipped with energy dispersive electron probe microanalysis.

3.7.2.2. E.S.C.A.

ESCALAB Mk1 X-ray photoelectron spectrometer using A1 K_α X-radiation and an AG 2 argon ion gun for depth profiling.

3.8. Measurement of current density

A one litre beaker, flat graphite cathode, 5251 alloy test anode, and appropriate electrolyte constituted the test cell. Agitation and heating requirments were provided by a thermostirrer unit. The anode was connected via a heat-sinked high wattage series resistor to a 5 amp. 0 - 30 volt stabilised d.c. power supply. The p.d.'s across the cell and the series resistor were monitored continuously using a twin channel recorder. By this means plots of current v time for a range of applied voltages, temperatures and electrolyte concentrations were obtained.

4.1. Evaluation of established pretreatments for aluminium

The three major pretreatment processes approved for bonding applications in the aerospace industry, i.e. chromic acid anodising, phosphoric acid anodising and the FPL etch, were evaluated using BA 2117 aluminium alloy and EC 2214 adhesive. Three simpler proprietary treatments, were included for comparison. These processes, all of which were preceded by vapour degreasing and non-etching alkaline cleaning stages, were carried out by Pyrene Ltd., on supplied specimen coupons. Two of the processes are Pyrene conversion treatments. The third treatment, Accomet C, is an Albright & Wilson product, described as a pretreatment process for aluminium, steel and galvanised steel prior to the application of stoving paints. Method of application was by dipping into a diluted solution, draining and oven drying at 120°C. The principal constituents of these solutions are given below:-

Process	Type	Principal constituents
Pyrene Bonderite 714	Rinse	Cr^{6+}, NO_3^-, F^-
Pyrene Bonderite 1415	Non-rinse	Cr^{6+}, Cr^{3+}, $(PO_4)^{3-}$, H_3PO_4, SiO_2
Accomet C	Non-rinse	Cr^{6+}, Cr^{3+}, SiO_2

Bonded lap shear specimens prepared using these pretreatment processes were suspended unstressed in a salt spray cabinet operated at 35°C. Groups of five joints were withdrawn for testing to destruction after periods of exposure of up to 1 year. The results are tabulated and expressed graphically in Tables/Figs. 4.1.1 to 4.1.6 and summarised in terms of percent strength retention in Table 4.1.7.

The results show that it is possible to achieve, with a simple conversion treatment, high initial bond strengths. Bonderite 1415 for example yielded a value identical to that obtained using the well established chromic acid anodise process. These treatments differ considerably however in terms of the maintenance of bond strength during environmental exposure. The most striking observation to be made is the failure of the conversion treatments to provide a joint life of one year under these conditions.

With the exception of chromic acid anodised material generalised adherend corrosion progressed with increasing severity during the test, and visible incidence of bond line corrosion was apparent after only 1 month in the case of Bonderite 1415 and 3 months for Bonderite 714. After the onset of bond line corrosion the durability data show a more rapid decline in mean shear strength and an increase in scatter, often rendering the calculation of standard deviation meaningless.

Results for Accomet C show that a high level of bond strength was maintained for at least six months, after which severe bond line corrosion developed and no specimens survived 1 year.

The superiority of the three established adhesive bonding surface treatments has been clearly confirmed. No indications of bond line corrosion were detected when any of these specimens were tested, although only chromic acid anodising had improved the general corrosion resistance of this alloy under salt spray conditions.

No significant difference in performance is observed between C.A.A. and optimised F.P.L. etch when initial strengths and residual

strengths after exposure for 1 year are considered. The initial strength of bonds to phosphoric acid anodised (BAC 5555) surfaces is lower than those to F.P.L. etched and chromic acid anodised material; the differences are significant at the 5% and 0.2% levels respectively. The results shown in Table 4.1.7 indicate however, the superior durability of bonds to phosphoric acid anodised surfaces. Even in absolute terms the residual strength of bonds to P.A.A. surfaces after an exposure period of 1 year is significantly higher than that to chromic acid anodised material.

Table 4.1.1. Durability of adhesive bonds to Bonderite 714 treated surfaces (2117 alloy, 2214 adhesive, salt spray @ 35°C).

EXPOSURE	FAILURE STRESS (MPa)	MEAN & STD. DEV. (MPa)	OBSERVATIONS
0	11.4	14.9 ±2.2	Apparent interfacial failure
	14.4		" " "
	15.8		" " "
	15.9		" " "
	17.1		" " "
4 days	10.9	12.4 ±1.0	" " "
	12.3		" " "
	12.5		" " "
	12.5		" " "
	13.7		" " "
1 week	11.6	12.8 ±0.9	" " "
	12.3		" " "
	12.8		" " "
	13.6		" " "
	13.8		" " "
4 weeks	8.0	10.0 ±1.4	" " "
	9.3		" " "
	10.5		" " "
	10.6		" " "
	11.5		" " "
3 months	0.6	5.9 ±3.7	Severe bond line corrosion
	3.5		Apparent interfacial failure
	7.7		" " "
	8.2		" " "
	9.5		" " "
6 months	0	5.8 ±5.5	Severe bond line corrosion
	0		" " " "
	8.3		Apparent interfacial failure
	9.0		" " "
	11.9		" " "
1 year	0	1.6	Severe bond line corrosion
	0		" " " "
	0		" " " "
	3.2		Apparent interfacial failure
	4.9		" " "

Table 4.1.2. Durability of adhesive bonds to Bonderite 1415 treated surfaces (2117alloy, 2214 adhesive, salt-spray @ 35°C).

EXPOSURE	FAILURE STRESS (MPa)	MEAN & STD. DEV. (MPa)	OBSERVATIONS
0	19.1 19.2 19.9 20.9 22.0	20.2 ±1.2	Apparent interfacial failure " " " " " " " " " " " "
2 days	15.8 19.1 19.4 20.1 20.4	19.0 ±1.9	" " " " " " " " " " " " " " "
1 week	16.1 16.2 17.0 18.4 19.9	17.5 ±1.6	" " " " " " " " " " " " " " "
4 weeks	11.4 16.1 16.9 17.0 18.3	15.9 ±2.7	Corrosion at bond edges Apparent interfacial failure " " " " " " " " "
3 months	9.8 10.7 12.9 13.7 14.6	12.4 ±2.0	Severe bond line corrosion " " " " Corrosion at bond edges " " " " " " " "
6 months	0 0 0.7 0.7 5.4	2.3	Severe bond line corrosion " " " " " " " " " " " " " " " "
1 year		0	No survivors

Table 4.1.3. Durability of adhesive bonds to Accomet C treated surfaces (2117 alloy, 2214 adhesive, salt-spray @ 35°C).

EXPOSURE	FAILURE STRESS (MPa)	MEAN & STD. DEV. (MPa)	OBSERVATIONS
0	15.0	16.9 ±2.4	Apparent interfacial failure
	15.3		" " "
	16.1		" " "
	17.2		" " "
	20.9		" " "
3 days	13.4	16.7 ±1.9	" " "
	16.9		" " "
	17.4		" " "
	17.6		" " "
	18.3		" " "
1 week	13.9	16.2 ±1.9	" " "
	15.2		" " "
	15.7		" " "
	17.7		" " "
	18.5		" " "
4 weeks	13.3	16.0 ±2.2	" " "
	15.0		" " "
	15.3		" " "
	17.8		" " "
	18.7		" " "
3 months	13.2	13.5 ±3.6	" " "
	15.4		" " "
	15.5		" " "
	16.1		" " "
	7.4		Severe bond line corrosion
6 months	12.1	14.0 ±1.8	Apparent interfacial failure
	12.6		" " "
	13.7		" " "
	15.3		" " "
	16.4		" " "
1 year		0	No survivors, severe bond line corrosion.

Table 4.1.4. Durability of adhesive bonds to optimised F.P.L. etched surfaces (2117 alloy, 2214 adhesive, salt-spray @ 35°C).

EXPOSURE	FAILURE STRESS (MPa)	MEAN & STD. DEV. (MPa)	OBSERVATIONS
0	17.0	19.0 ±1.7	Apparent interfacial failure
	18.2		" " "
	18.9		" " "
	19.2		" " "
	21.6		" " "
2 weeks	19.5	20.5 ±1.0	" " "
	20.1		" " "
	20.2		" " "
	20.4		" " "
	22.2		" " "
4 weeks	16.8	19.3 ±1.5	" " "
	18.9		" " "
	19.9		" " "
	20.2		" " "
	20.6		" " "
3 months	17.4	18.4 ±0.6	" " "
	18.3		" " "
	18.4		" " "
	18.7		" " "
	19.0		" " "
6 months	17.3	18.0 ±0.5	" " "
	17.9		" " "
	18.3		" " "
	18.4		" " "
1 year	14.4	15.9 ±1.4	" " "
	15.3		" " "
	15.8		" " "
	15.9		" " "
	18.3		" " "

Table 4.1.5. Durability of adhesive bonds to chromic acid anodised surfaces (2117 alloy, 2214 adhesive, salt-spray @ 35°C).

EXPOSURE	FAILURE STRESS (MPa)	MEAN & STD. DEV. (MPa)	OBSERVATIONS
0	19.3	20.2 ±0.9	Apparent interfacial failure
	19.5		" " "
	20.2		" " "
	20.4		" " "
	21.7		" " "
1 week	19.3	20.2 ±0.6	" " "
	20.1		" " "
	20.1		" " "
	20.6		" " "
	21.0		" " "
1 month	17.4	19.6 ±1.7	" " "
	18.6		" " "
	19.5		" " "
	20.9		" " "
	21.4		" " "
3 months	15.7	16.6 ±0.9	" " "
	16.0		" " "
	16.8		" " "
	16.9		" " "
	17.9		" " "
6 months	14.7	15.2 ±0.5	" " "
	14.8		" " "
	14.9		" " "
	15.4		" " "
	16.0		" " "
1 year	12.9	14.6 ±1.6	" " "
	14.8		" " "
	16.1		" " "

Table 4.1.6. Durability of adhesive bonds to phosphoric acid anodised (BAC 5555) surfaces (2117 alloy, 2214 adhesive, salt-spray @ 35°C).

EXPOSURE	FAILURE STRESS (MPa)	MEAN & STD. DEV. (MPa)	OBSERVATIONS
0	15.0	16.4 ±1.2	Apparent interfacial failure
	15.4		" " "
	16.5		" " "
	17.1		" " "
	17.8		" " "
1 month	13.3	16.2 ±2.1	" " "
	15.1		" " "
	16.9		" " "
	17.5		" " "
	18.4		" " "
3 months	15.0	16.7 ±1.6	" " "
	15.3		" " "
	16.8		" " "
	17.5		" " "
	19.1		" " "
6 months	15.4	16.5 ±0.9	" " "
	15.6		" " "
	16.8		" " "
	17.1		" " "
	17.4		" " "
1 year	15.0	16.7 ±1.3	" " "
	16.1		" " "
	16.5		" " "
	17.1		" " "
	18.6		" " "

Pretreatment	Initial Strength MPa	% Strength retention					
		0	1 week	4 weeks	3 months	6 months	1 year
Bonderite 714	14.9 ±2.2	100	86	67	40	39	11
Bonderite 1415	20.2 ±1.2	100	87	79	61	11	0
Accomet C	16.9 ±2.4	100	96	95	80	83	0
Opt. F.P.L.	19.0 ±1.7	100	2 weeks 108	102	97	95	84
C.A.A. (Def 151)	20.2 ±0.9	100	100	97	82	75	72
P.A.A. (BAC 5555)	16.4 ±1.2	100	-	99	102	101	102

Table 4.1.7 Comparison of pretreatments (BA 2117 alloy, EC 2214 adhesive, salt spray @ 35°C.)

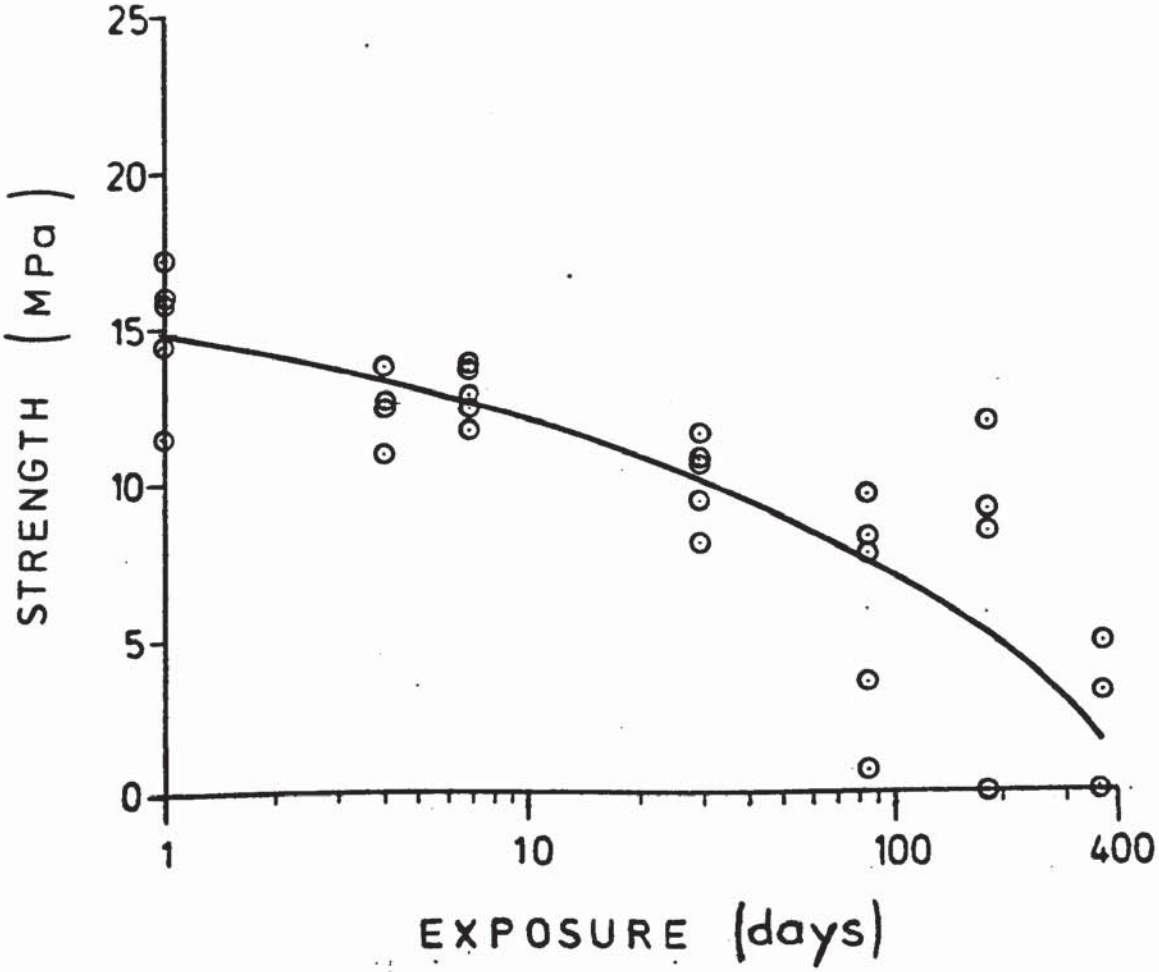

Fig. 4.1.1. Durability of adhesive bonds to Bonderite 714 treated surfaces (2117 alloy, 2214 adhesive, salt-spray @ 35°C).

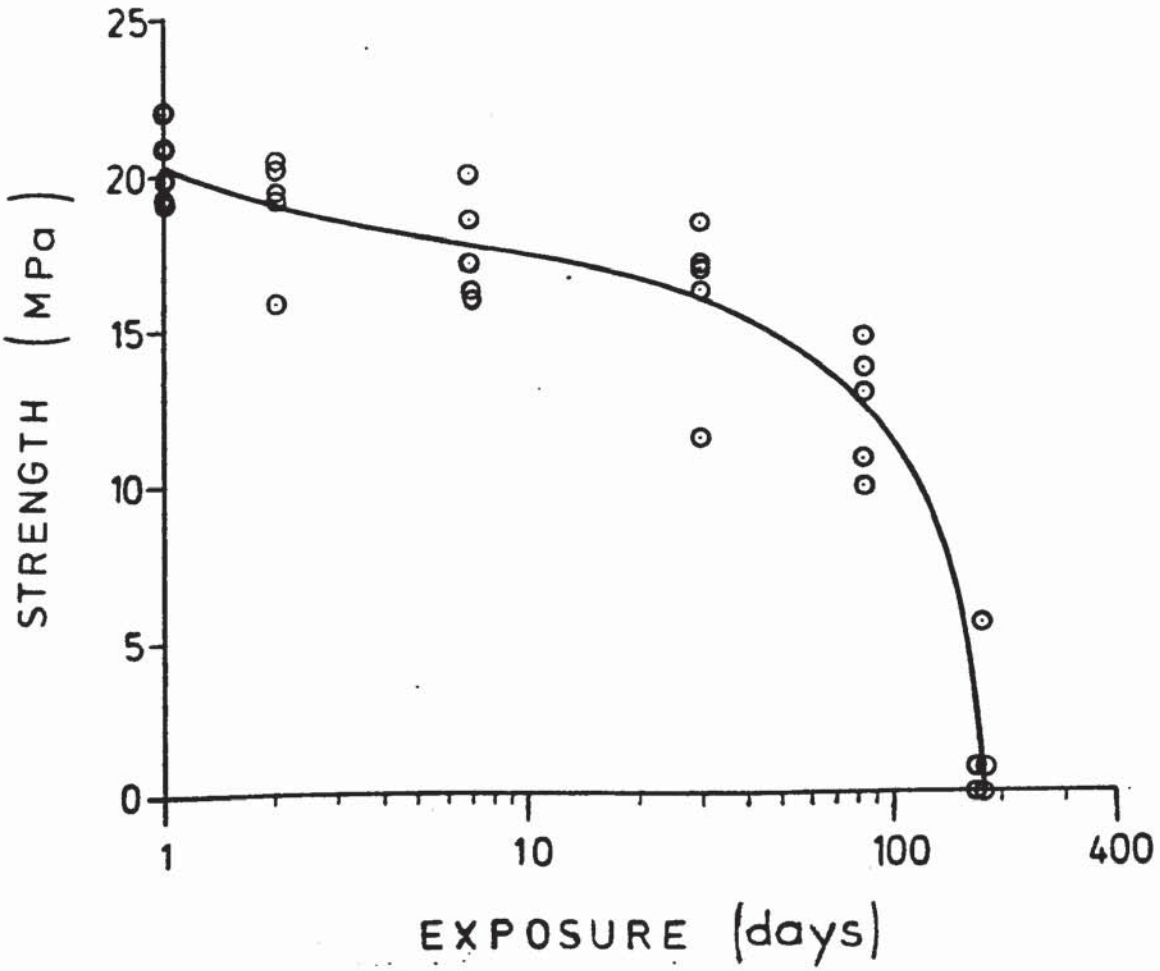

Fig. 4.1.2. Durability of adhesive bonds to Bonderite 1415 treated surfaces (2117 alloy, 2214 adhesive, salt-spray @ 35°C).

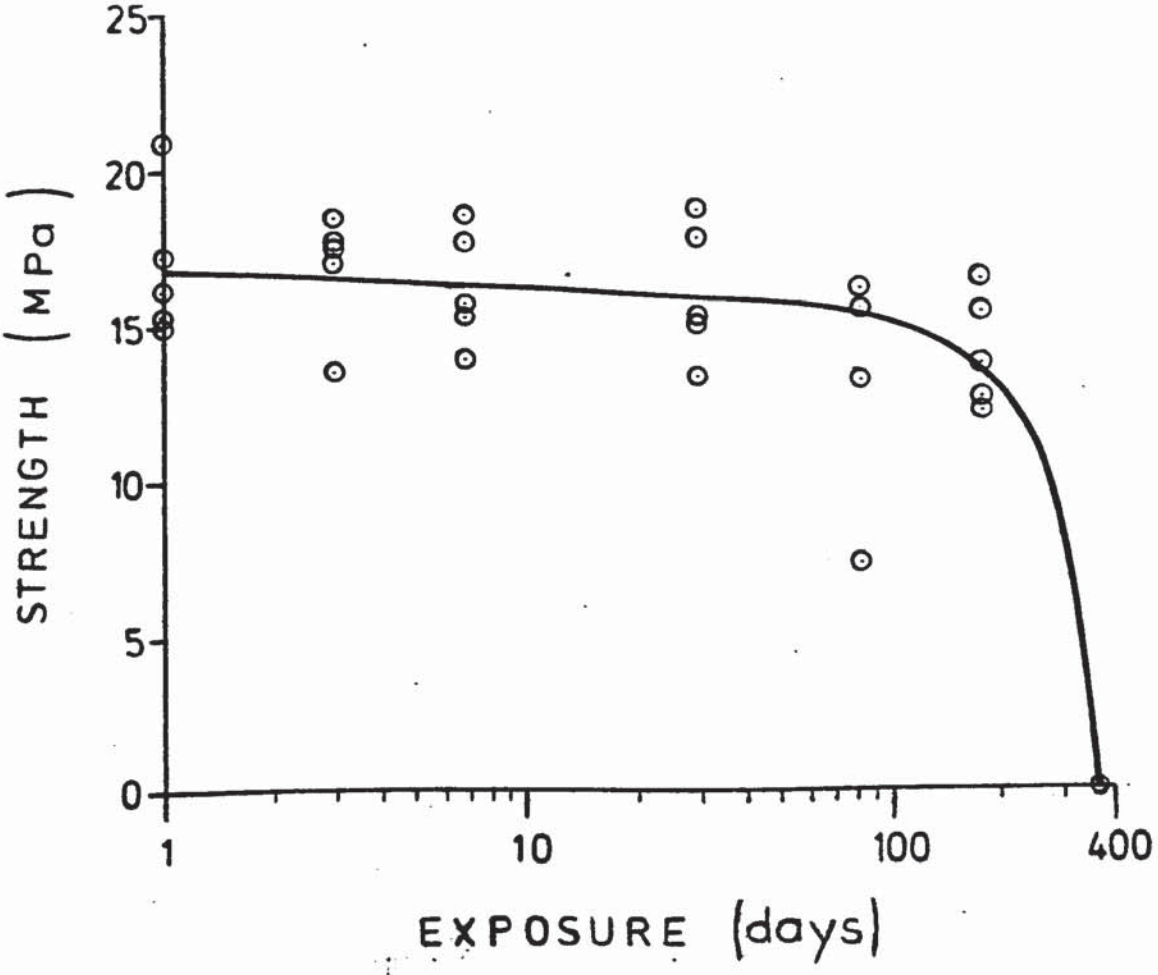

Fig. 4.1.3. Durability of adhesive bonds to Accomet C treated surfaces (2117 alloy, 2214 adhesive, salt-spray @ 35°C).

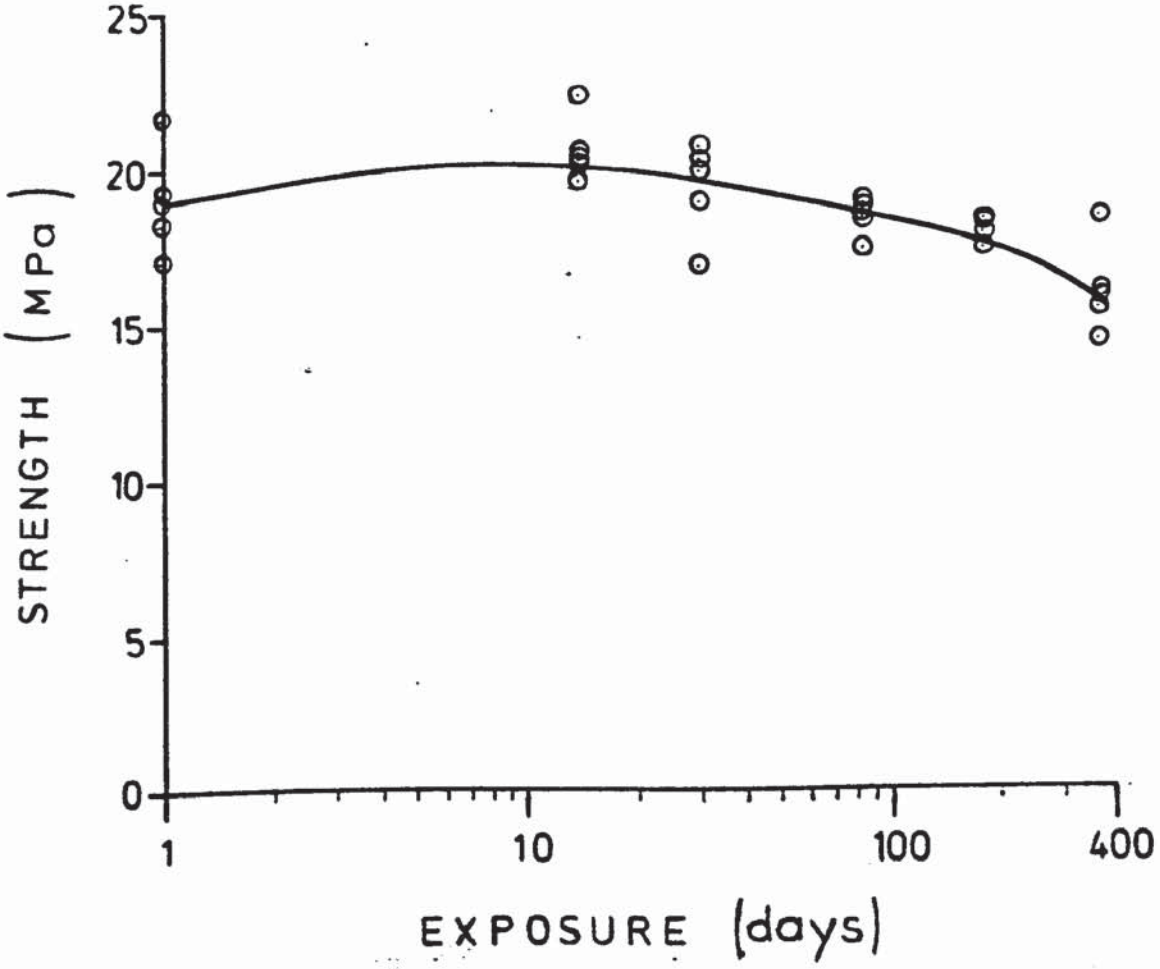

Fig. 4.1.4. Durability of adhesive bonds to optimised F.P.L. etched surfaces (2117 alloy, 2214 adhesive, salt-spray @ 35°C).

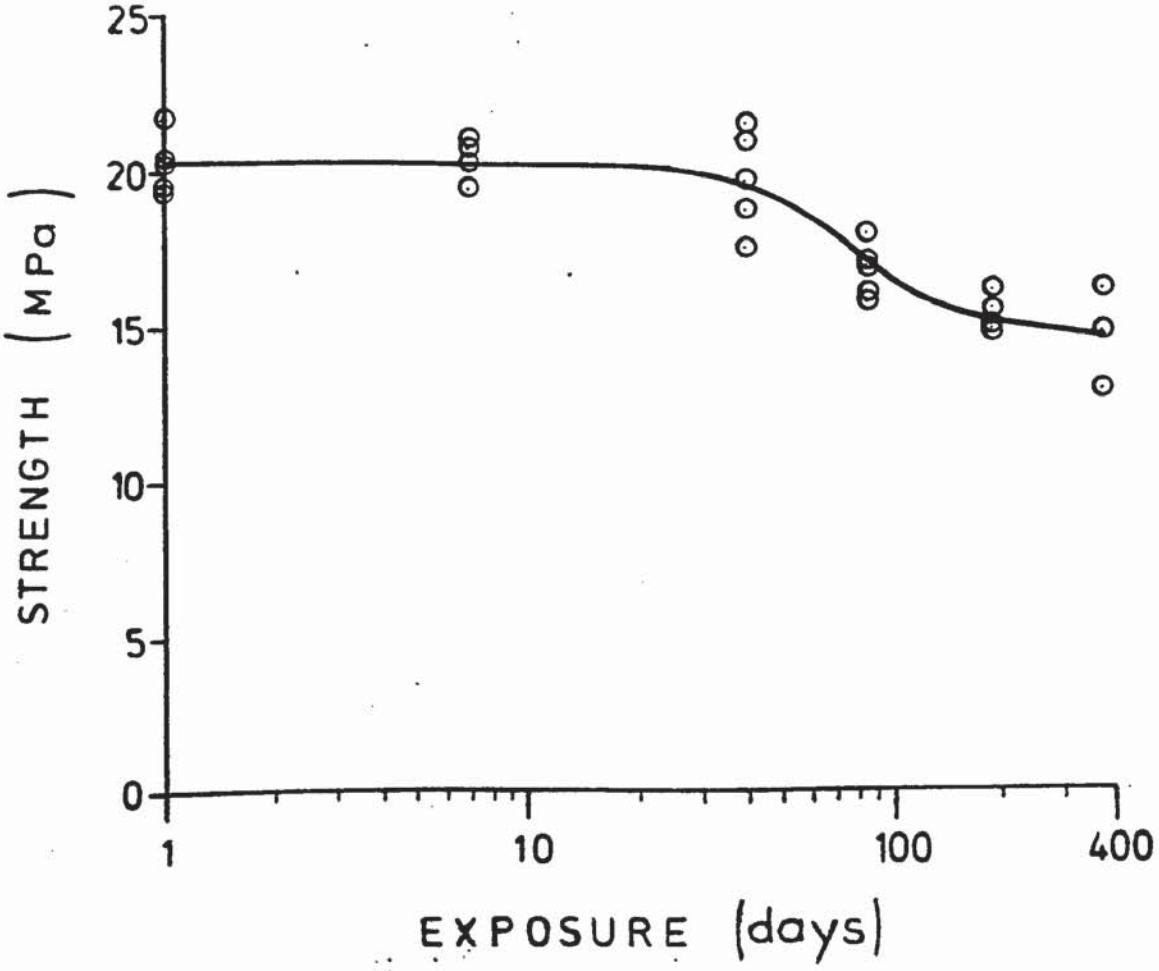

Fig. 4.1.5. Durability of adhesive bonds to chromic acid anodised surfaces (2117 alloy, 2214 adhesive, salt-spray @ 35°C).

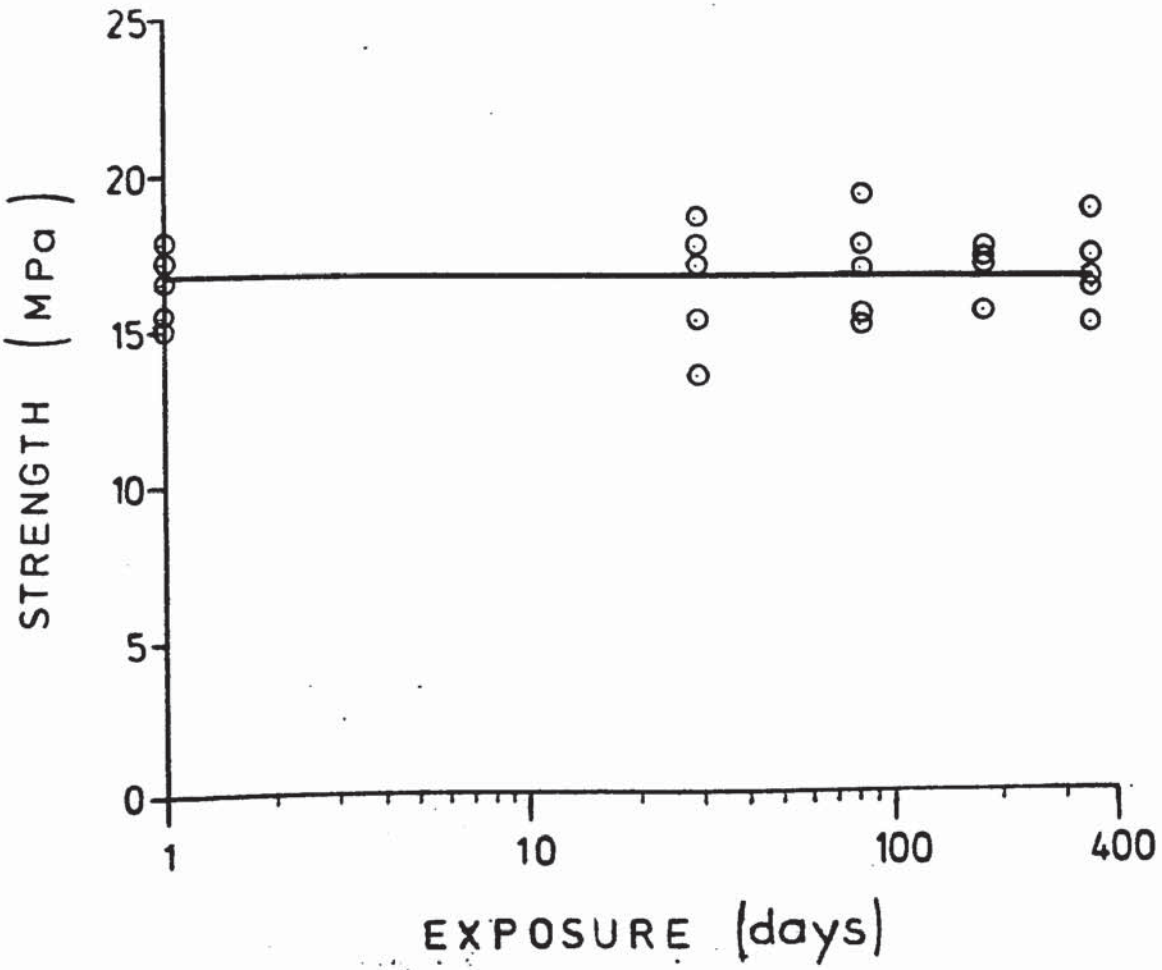

Fig. 4.1.6. Durability of adhesive bonds to phosphoric acid anodised (BAC 5555) surfaces (2117 alloy, 2214 adhesive, salt-spray @ 35°C).

4.2. Effect of environment on adhesive bond durability

The previous experiment considered bond durability as a function of pretreatment for a given alloy, adhesive and environment. Bonded vehicle components however, must tolerate exposure to a wide range of environments, some of the most important of which have been included in this experiment. The BA 2117 alloy used was pretreated to Boeing's BAC 5555 specification, i.e. vapour degreased, alkaline cleaned, F.P.L. etched then phosphoric acid anodised for 20 minutes. Single lap shear joints were bonded using EC 2114 adhesive, and type I jigs.

Unfortunately, some coupons were erroneously guillotined at 90° to the rolling direction, and although this was not expected to have a significant effect on the results, an additional set of control specimens was prepared.

Groups of specimens were stored in sealed Kilner jars containing the test liquids, in which the bonded areas were totally submerged. Most were placed in an air circulating oven maintained at 60°C. Exposure to petrol was undertaken at room temperature in the interests of safety. The test liquids selected were:-

1. Petrol @ 20°C.
2. Engine oil @ 60°C.
3. Detergent ("Zip Wax") 10% by volume in water, @ 60°C.
4. River water @ 60°C.
5. Bovine excrement, 50% by volume slurry in water, @ 60°C.
6. Sodium chloride solution, 5%, @ 60°C.
7. Antifreeze, 50% by volume in water, @ 60°C.
8. Deionised water @ 60°C.
9. Urine, human, undiluted, @ 60°C.

In addition, groups of specimens were stored in Kilner jars at 60°C. and room temperature as "atmosphere" controls. Detailed results are shown in Table 4.2.1 to 4.2.12 and Figs. 4.2.1 to 4.2.12. They are more readily compared by reference to Table 4.2.13 and Fig. 4.2.13. Differences between specimens of varying orientation are very small and not statistically significant. Examination by optical microscopy of the fracture surfaces of unexposed specimens revealed a locus of failure apparently at, or close to, the interface.

Similar observations were made when control specimens and those exposed to petrol and oil for one year were tested. All were found to retain high levels of strength. Indeed an increase in strength, significant at the 2% level, was developed in bonds stored in petrol or air at room temperature.

Atmospheric storage at 60°C. resulted in a loss of strength. In contrast, specimens stored in aqueous environments lost considerable strength, and exhibited obvious cohesive failure. Interestingly, the sodium chloride solution was the least aggressive of the aqueous environments used. Urine was exceptional in that it produced the only examples of visible bond line corrosion. The effect was detectable after the first test interval of only 7 weeks. An increasing incidence of bond line corrosion followed accompanied by a catastrophic loss of strength.

Table 4.2.1. Strength of adhesive bonds exposed to laboratory ambient conditions (2117 alloy, phosphoric acid anodised, 2214 adhesive).

EXPOSURE	FAILURE STRESS (MPa)	MEAN & STD. DEV. (MPa)	OBSERVATIONS
0	17.2	18.6 ±0.9	Apparent interfacial failure
	18.4		" " "
	18.8		" " "
	19.1		" " "
	19.6		" " "
7 weeks	19.0	20.1 ±0.8	" " "
	19.8		" " "
	20.0		" " "
	20.7		" " "
	20.9		" " "
18 weeks	19.4	22.0 ±1.5	" " "
	21.3		" " "
	21.5		" " "
	23.8		" " "
	24.0		" " "
52 weeks	20.2	21.2 ±0.9	" " "
	20.5		" " "
	21.3		" " "
	21.4		" " "
	22.3		" " "

Table 4.2.2. Strength of adhesive bonds exposed to atmosphere at 60°C. (2117 alloy, phosphoric acid anodised, 2214 adhesive).

EXPOSURE	FAILURE STRESS (MPa)	MEAN & STD. DEV. (MPa)	OBSERVATIONS
0	17.2	18.6 ±0.9	Apparent interfacial failure
	18.4		"
	18.8		"
	19.1		"
	19.6		"
7 weeks	14.7	17.5 ±2.6	"
	16.8		"
	17.0		"
	17.1		"
	21.8		"
18 weeks	17.0	18.2 ±0.7	"
	18.1		"
	18.1		"
	18.6		"
	19.2		"
52 weeks	14.3	15.2 ±0.7	"
	14.7		"
	15.6		"
	15.7		"
	16.0		"

Table 4.2.3 Strength of adhesive bonds exposed to atmosphere at 60°C. (2117 alloy, phosphoric acid anodised, 2214 adhesive). (Specimen coupons cut perpendicular to rolling direction).

EXPOSURE	FAILURE STRESS (MPa)	MEAN & STD. DEV. (MPa)	OBSERVATIONS
0	15.9	19.0 ±1.9	Apparent interfacial failure
	18.6		" " "
	19.6		" " "
	20.5		" " "
	20.5		" " "
7 weeks	16.5	17.8 ±1.2	" " "
	17.1		" " "
	17.9		" " "
	18.1		" " "
	19.5		" " "
18 weeks	16.1	18.4 1.6	" " "
	17.5		" " "
	19.1		" " "
	19.5		" " "
	20.0		" " "
52 weeks	14.0	15.9 ±1.4	" " "
	14.9		" " "
	16.4		" " "
	17.0		" " "
	17.2		" " "

Table 4.2.4. Strength of adhesive bonds immersed in petrol at room temperature (2117 alloy, phosphoric acid anodised, 2214 adhesive).

EXPOSURE	FAILURE STRESS (MPa)	MEAN & STD. DEV. (MPa)	OBSERVATIONS
0	17.2	18.6 ±0.9	Apparent interfacial failure
	18.4		" " "
	18.8		" " "
	19.1		" " "
	19.6		" " "
7 weeks	18.3	20.5 ±1.9	" " "
	19.4		" " "
	19.9		" " "
	22.1		" " "
	22.9		" " "
18 weeks	21.6	22.8 ±1.1	" " "
	21.7		" " "
	22.6		" " "
	23.4		" " "
	25.0		" " "
52 weeks	19.0	20.4 ±1.0	" " "
	19.8		" " "
	20.7		" " "
	21.3		" " "
	21.4		" " "

Table 4.2.5. Strength of adhesive bonds immersed in engine oil at 60°C. (2117 alloy, phosphoric acid anodised, 2214 adhesive).

EXPOSURE	FAILURE STRESS (MPa)	MEAN & STD. DEV. (MPa)	OBSERVATIONS
0	17.2	18.6 ±0.9	Apparent interfacial failure
	18.4		" " "
	18.8		" " "
	19.1		" " "
	19.6		" " "
7 weeks	15.9	17.2 ±0.8	" " "
	17.3		" " "
	17.4		" " "
	17.5		" " "
	17.9		" " "
18 weeks	15.5	17.7 ±1.0	" " "
	17.7		" " "
	18.4		" " "
	18.4		" " "
	18.6		" " "
52 weeks	15.1	16.9 ±1.7	" " "
	15.1		" " "
	17.5		" " "
	18.2		" " "
	18.7		" " "

Table 4.2.6. Strength of adhesive bonds immersed in detergent solution at 60°C. (2117 alloy, phosphoric acid anodised, 2214 adhesive).

EXPOSURE	FAILURE STRESS (MPa)	MEAN & STD. DEV. (MPa)	OBSERVATIONS
0	17.2	18.6 ±0.9	Apparent interfacial failure
	18.4		" " "
	18.8		" " "
	19.1		" " "
	19.6		" " "
7 weeks	12.5	13.4 ±0.8	Cohesive failure
	12.8		" "
	13.6		" "
	14.0		" "
	14.3		" "
18 weeks	6.7	7.6 ±0.5	" "
	7.5		" "
	7.6		" "
	7.8		" "
	8.5		" "
52 weeks	5.4	6.0 ±0.4	" "
	6.1		" "
	6.2		" "
	6.3		" "

Table 4.2.7. Strength of adhesive bonds immersed in river water at 60°C. (2117 alloy, phosphoric acid anodised, 2214 adhesive).

EXPOSURE	FAILURE STRESS (MPa)	MEAN & STD. DEV. (MPa)	OBSERVATIONS
0	17.2	18.6 ±0.9	Apparent interfacial failure
	18.4		" " "
	18.8		" " "
	19.1		" " "
	19.6		" " "
7 weeks	12.4	13.3 ±0.7	Cohesive failure
	12.8		" "
	13.4		" "
	13.9		" "
	14.2		" "
18 weeks	8.7	9.8 ±0.6	" "
	9.4		" "
	10.0		" "
	10.2		" "
	10.5		" "
52 weeks	4.7	6.7 ±1.6	" "
	5.6		" "
	7.0		" "
	7.8		" "
	8.6		" "

Table 4.2.8. Strength of adhesive bonds immersed in 50% by vol. slurry of bovine excrement in water at 60°C. (2117 alloy, phosphoric acid anodised, 2214 adhesive).

EXPOSURE	FAILURE STRESS (MPa)	MEAN & STD. DEV. (MPa)	OBSERVATIONS
0	17.2	18.6 ± 0.9	Apparent interfacial failure
	18.4		" " "
	18.8		" " "
	19.1		" " "
	19.6		" " "
7 weeks	12.6	13.3 ± 0.6	Cohesive failure
	13.0		" "
	13.2		" "
	13.3		" "
	14.2		" "
18 weeks	10.6	11.0 ± 0.3	" "
	10.7		" "
	11.1		" "
	11.1		" "
	11.3		" "
52 weeks	5.6	5.9 ± 0.5	" "
	5.6		" "
	5.6		" "
	5.8		" "
	6.8		" "

Table 4.2.9. Strength of adhesive bonds immersed in 5% sodium chloride solution at 60°C.
(2117 alloy, phosphoric acid anodised, 2214 adhesive).

EXPOSURE	FAILURE STRESS (MPa)	MEAN & STD. DEV. (MPa)	OBSERVATIONS
0	15.9	19.0 ±1.9	Apparent interfacial failure
	18.6		" " "
	19.6		" " "
	20.5		" " "
	20.5		" " "
7 weeks	14.1	14.5 ±0.5	Cohesive failure
	14.1		" "
	14.3		" "
	15.1		" "
	15.1		" "
18 weeks	12.7	13.4 ±0.4	" "
	13.0		" "
	13.6		" "
	13.7		" "
	14.1		" "
52 weeks	12.0	12.4 ±0.3	" "
	12.4		" "
	12.5		" "
	12.6		" "
	12.8		" "

Table 4.2.10 Strength of adhesive bonds immersed in 50% by vol. antifreeze solution @ 60°C. (2117 alloy, phosphoric acid anodised, 2214 adhesive).

EXPOSURE	FAILURE STRESS (MPa)	MEAN & STD. DEV. (MPa)	OBSERVATIONS
0	15.9	19.0 ±1.9	Apparent interfacial failure
	18.6		" " "
	19.6		" " "
	20.5		" " "
	20.5		" " "
7 weeks	13.7	14.8 ±0.9	Cohesive failure
	14.5		" "
	14.7		" "
	15.1		" "
	16.1		" "
18 weeks	9.4	10.5 ±0.6	" "
	10.3		" "
	10.8		" "
	11.0		" "
	11.1		" "
52 weeks	9.2	11.5 ±1.5	" "
	10.8		" "
	11.7		" "
	12.4		" "
	13.2		" "

Table 4.2.11 Strength of adhesive bonds immersed in de-ionised water @ 60°C. (2117 alloy, phosphoric acid anodised, 2214 adhesive).

EXPOSURE	FAILURE STRESS (MPa)	MEAN & STD. DEV. (MPa)	OBSERVATIONS
0	15.9	19.0 ±1.9	Apparent interfacial failure
	18.6		" " "
	19.6		" " "
	20.5		" " "
	20.5		" " "
9 weeks	11.8	13.8 ±1.5	Cohesive failure
	12.8		" "
	14.2		" "
	15.0		" "
	15.6		" "
18 weeks	9.1	10.6 ±0.8	" "
	10.4		" "
	10.5		" "
	10.9		" "
	12.0		" "
55 weeks	5.7	6.8 ±0.7	" "
	6.3		" "
	7.0		" "
	7.5		" "
	7.7		" "

Table 4.2.12. Strength of adhesive bonds immersed in human urine @ 60°C.
(2117 alloy, phosphoric acid anodised, 2214 adhesive).

EXPOSURE	FAILURE STRESS (MPa)	MEAN & STD. DEV. (MPa)	OBSERVATIONS
0	15.9	19.0 ±1.9	Apparent interfacial failure
	18.6		" " "
	19.6		" " "
	20.5		" " "
	20.5		" " "
7 weeks	0	8.7 ±6.1	Severe bond line corrosion
	5.0		" " " "
	11.2		Cohesive failure
	13.3		" "
	14.2		" "
18 weeks	0	3.1	Severe bond line corrosion
	0		" " " "
	1.1		" " " "
	3.1		" " " "
	11.1		Cohesive failure
55 weeks	0	1.6	Severe bond line corrosion
	0		" " " "
	0		" " " "
	1.0		" " " "
	6.9		" " " "

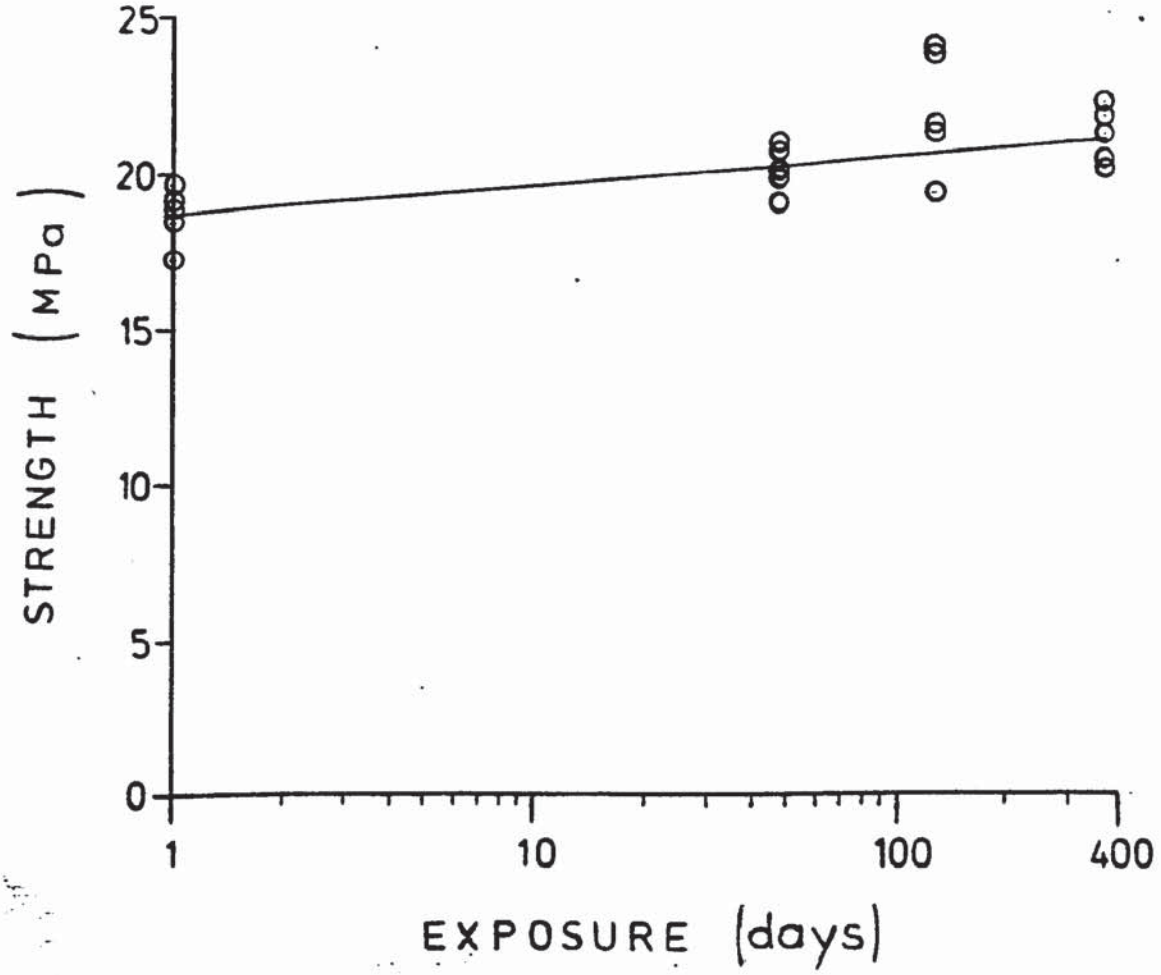

Fig. 4.2.1. Strength of adhesive bonds exposed to laboratory ambient conditions (2117 alloy, phosphoric acid anodised, 2214 adhesive).

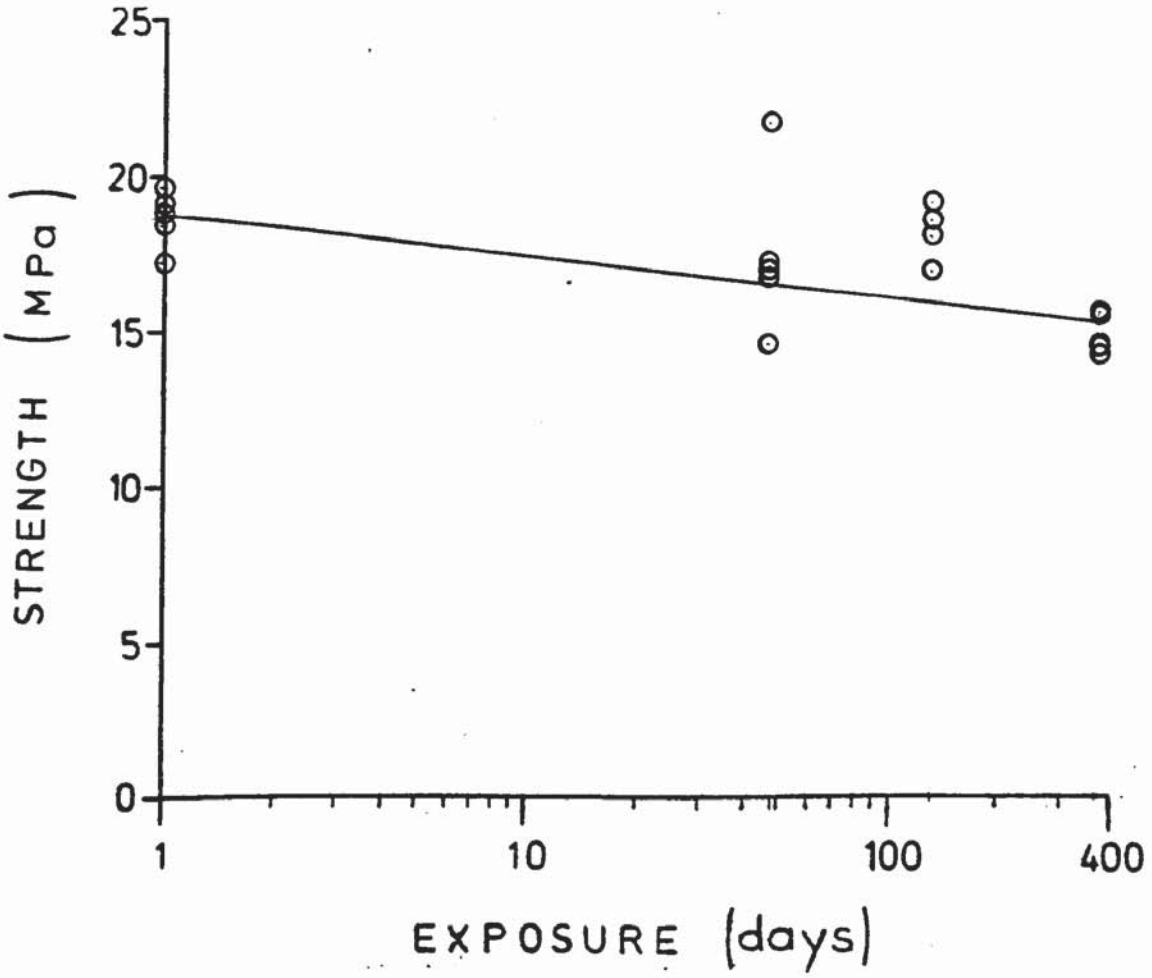

Fig. 4.2.2. Strength of adhesive bonds exposed to atmosphere at 60°C (2117 alloy, phosphoric acid anodised, 2214 adhesive).

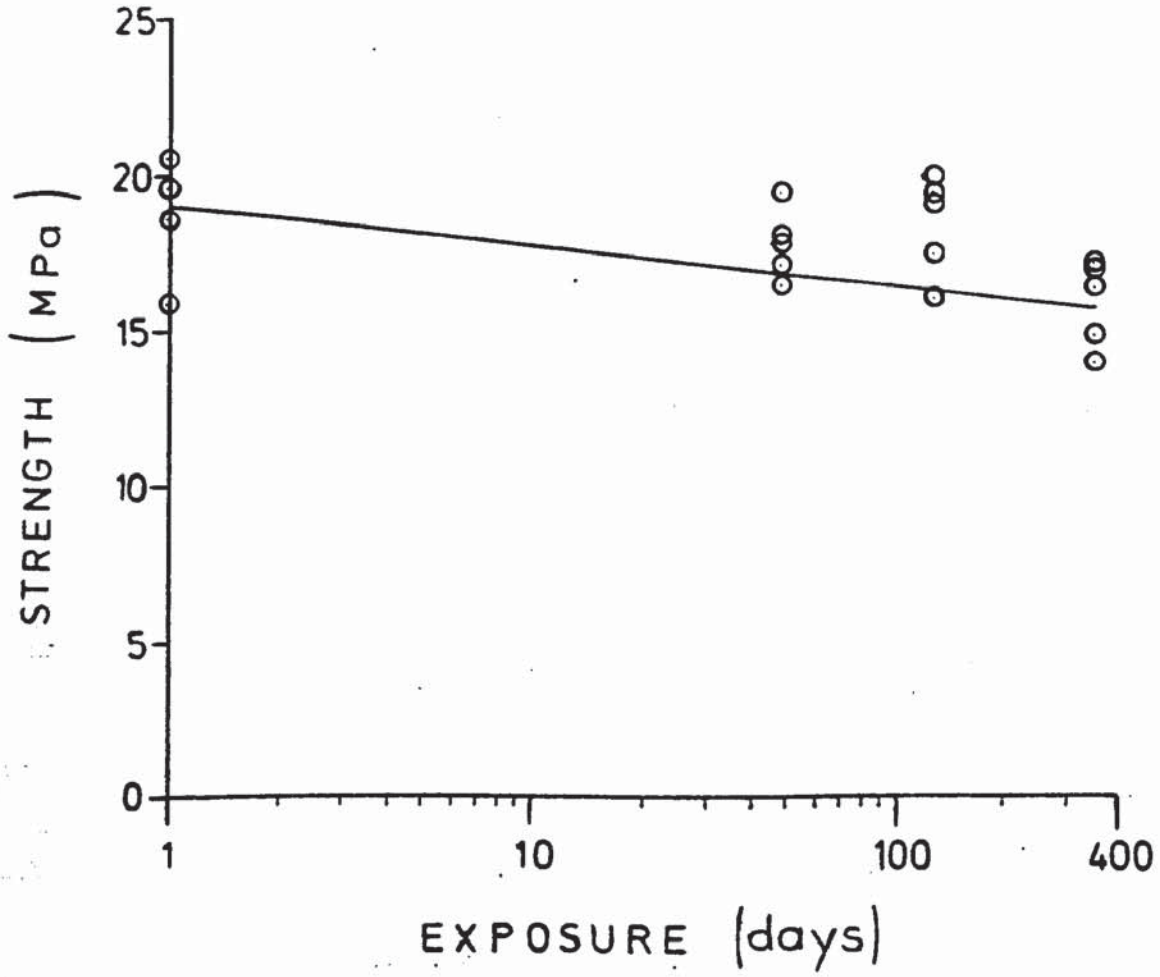

Fig. 4.2.3. Strength of adhesive bonds exposed to atmosphere at 60°C. (2117 alloy, phosphoric acid anodised, 2114 adhesive). (Specimen coupons cut perpendicular to rolling direction).

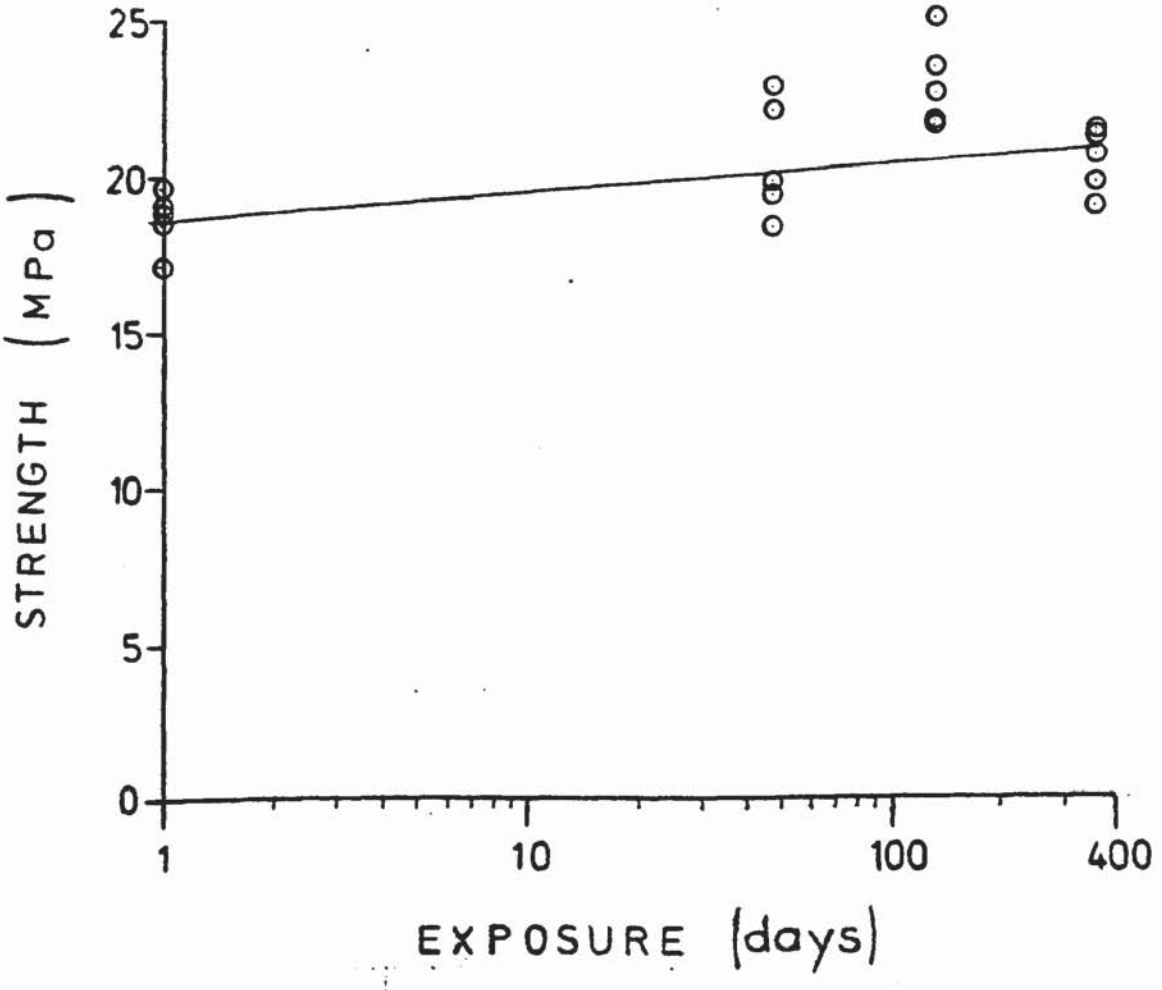

Fig. 4.2.4. Strength of adhesive bonds immersed in petrol at room temperature (2117 alloy, phosphoric acid anodised, 2214 adhesive).

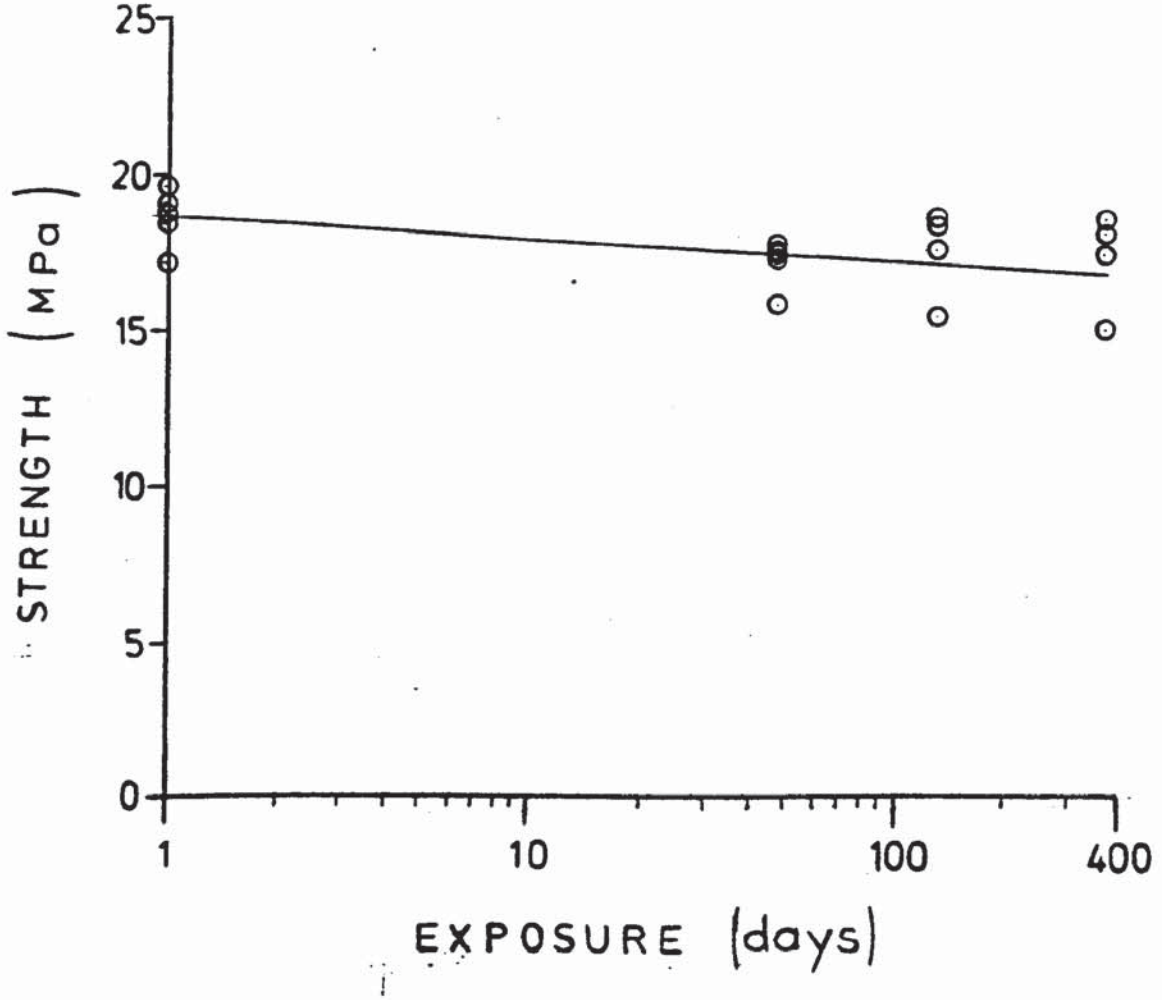

Fig. 4.2.5. Strength of adhesive bonds immersed in engine oil at 60°C. (2117 alloy, phosphoric acid anodised, 2214 adhesive).

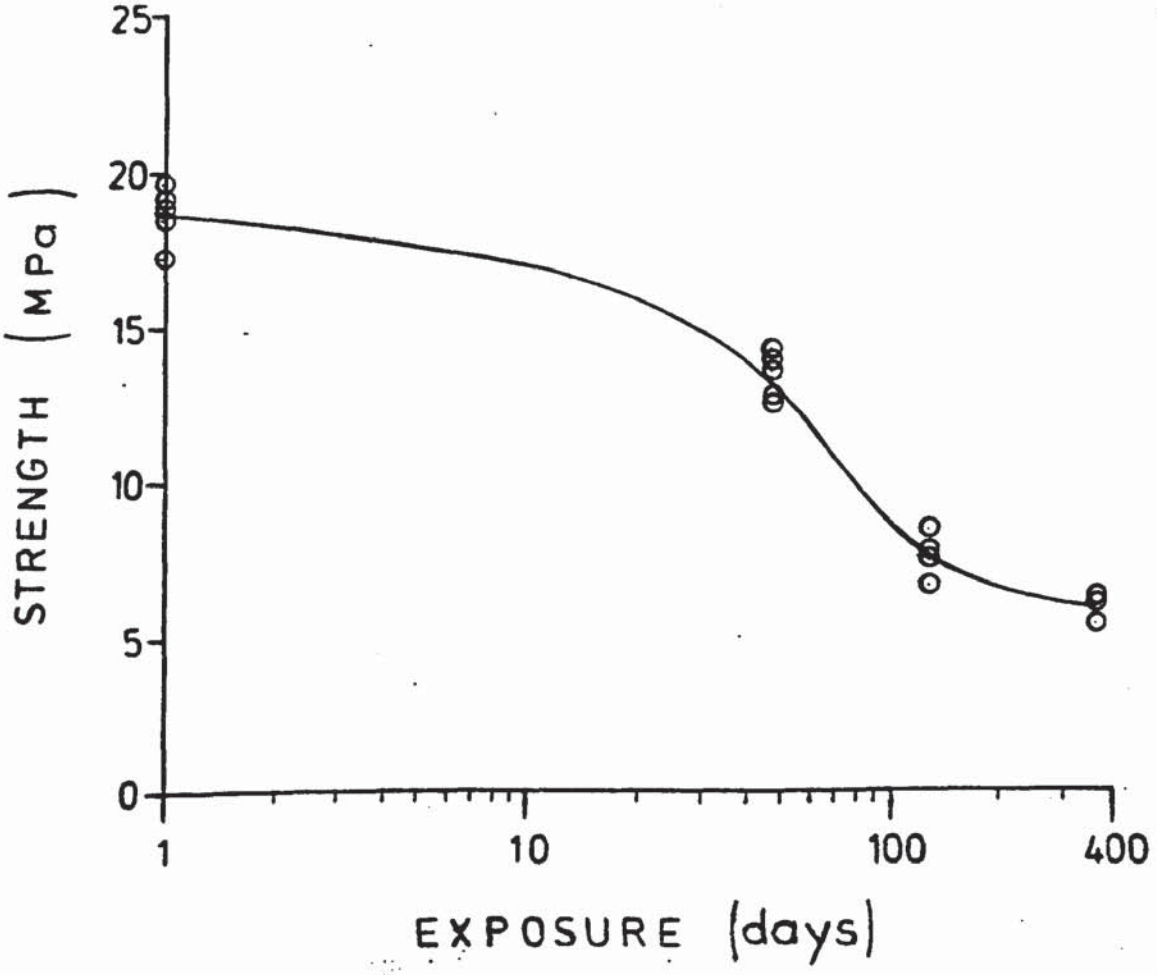

Fig. 4.2.6. Strength of adhesive bonds immersed in detergent solution at 60°C. (2117 alloy, phosphoric acid anodised, 2214 adhesive).

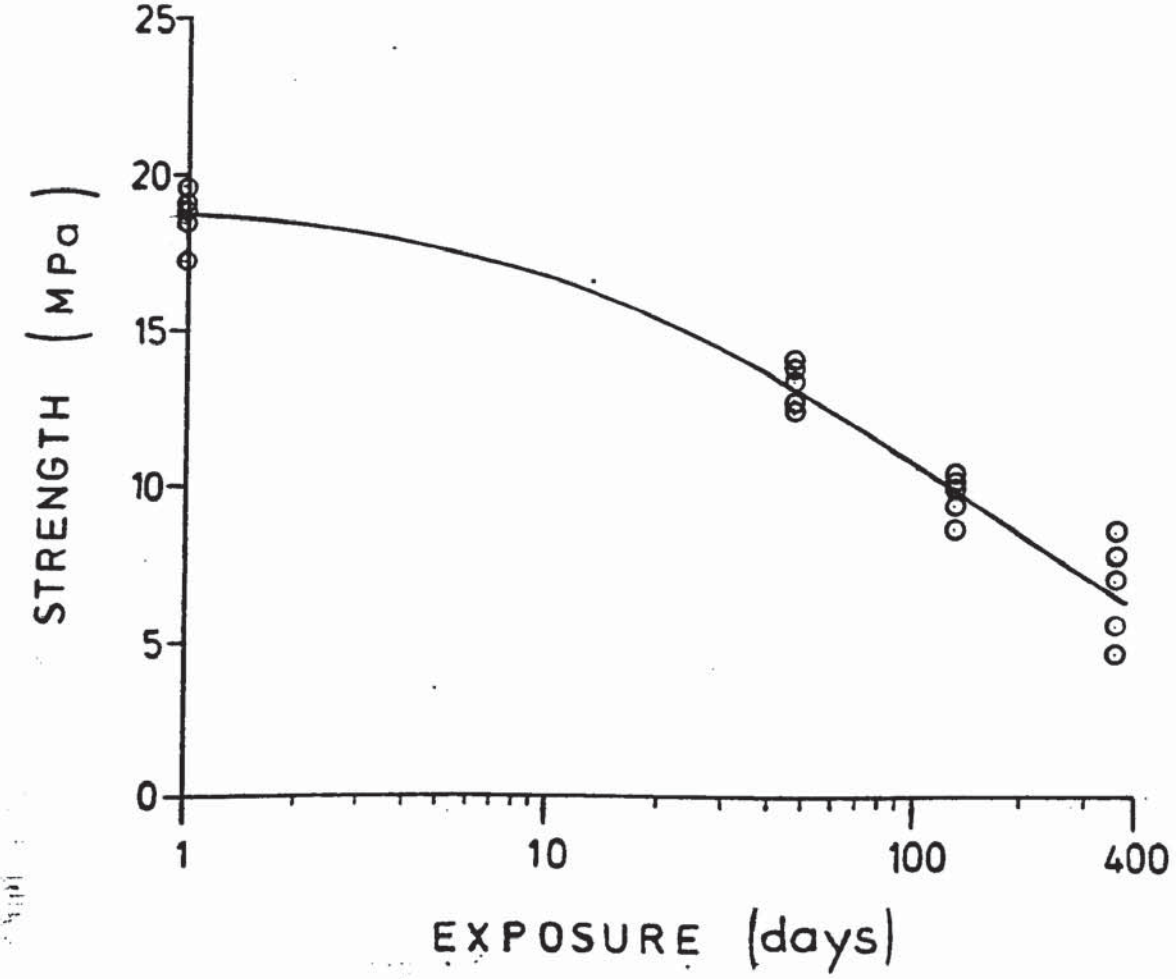

Fig. 4.2.7. Strength of adhesive bonds immersed in river water at 60°C. (2117 alloy, phosphoric acid anodised, 2214 adhesive).

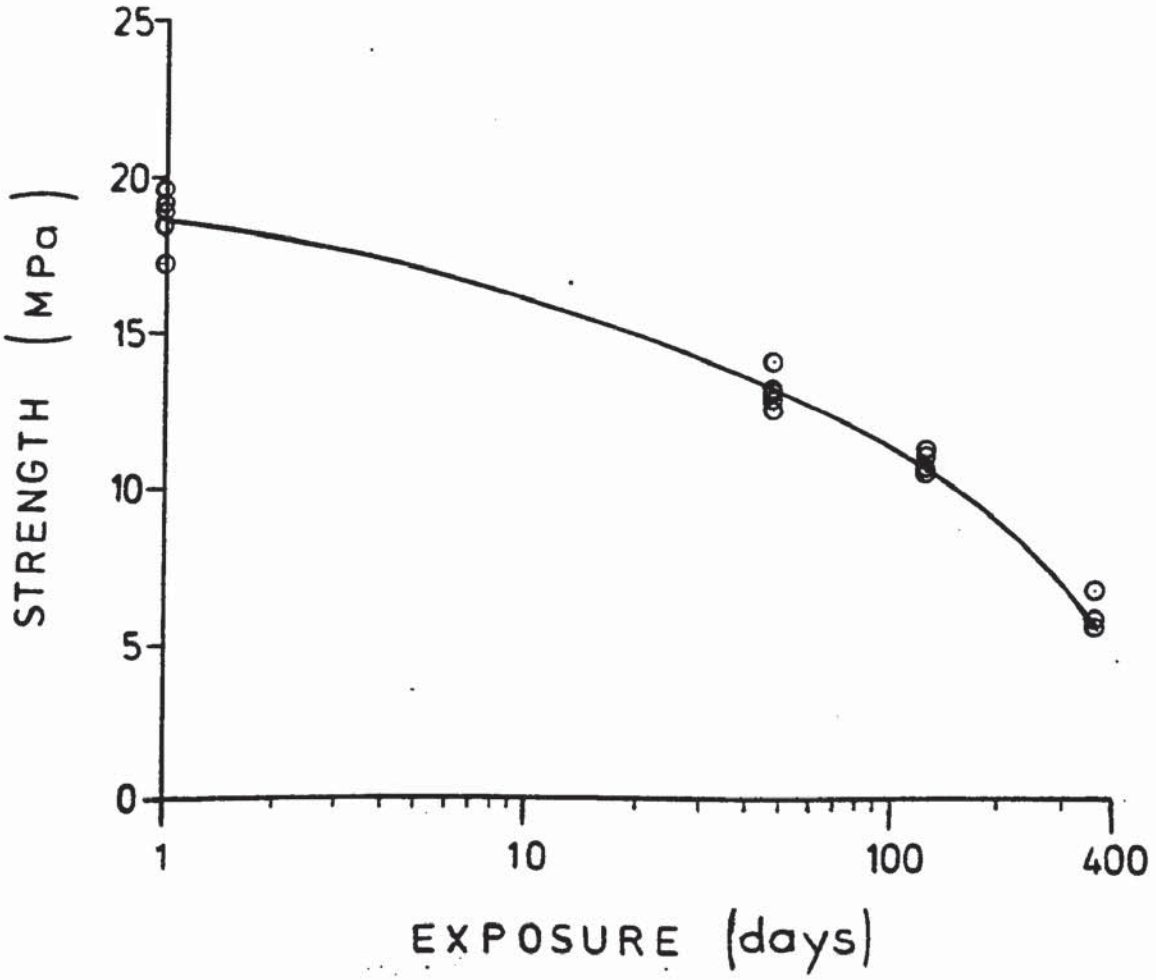

Fig. 4.2.8. Strength of adhesive bonds immersed in 50% by vol. slurry of bovine excrement in water at 60°C. (2117 alloy, phosphoric acid anodised, 2214 adhesive).

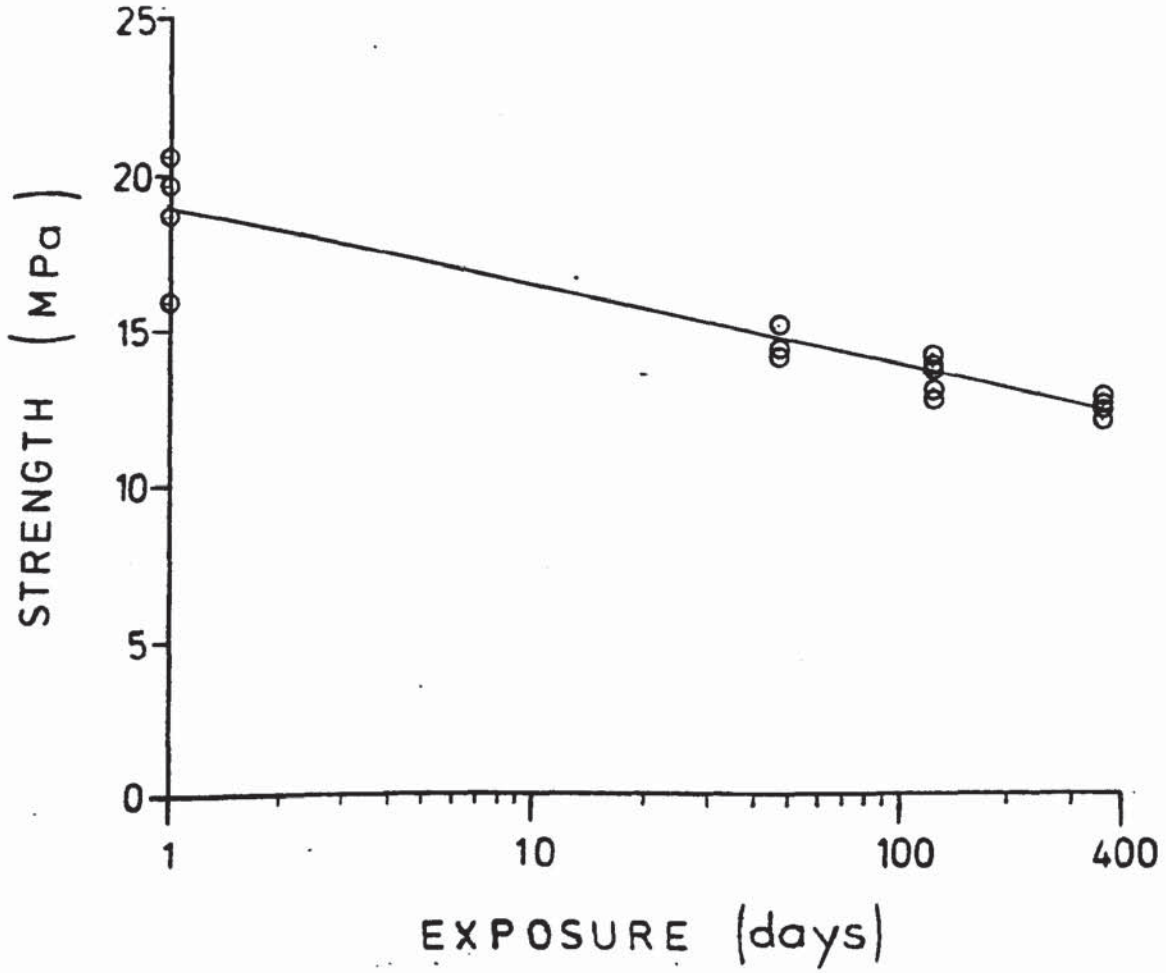

Fig. 4.2.9. Strength of adhesive bonds immersed in 5% sodium chloride solution at 60°C. (2117 alloy, phosphoric acid anodised, 2214 adhesive).

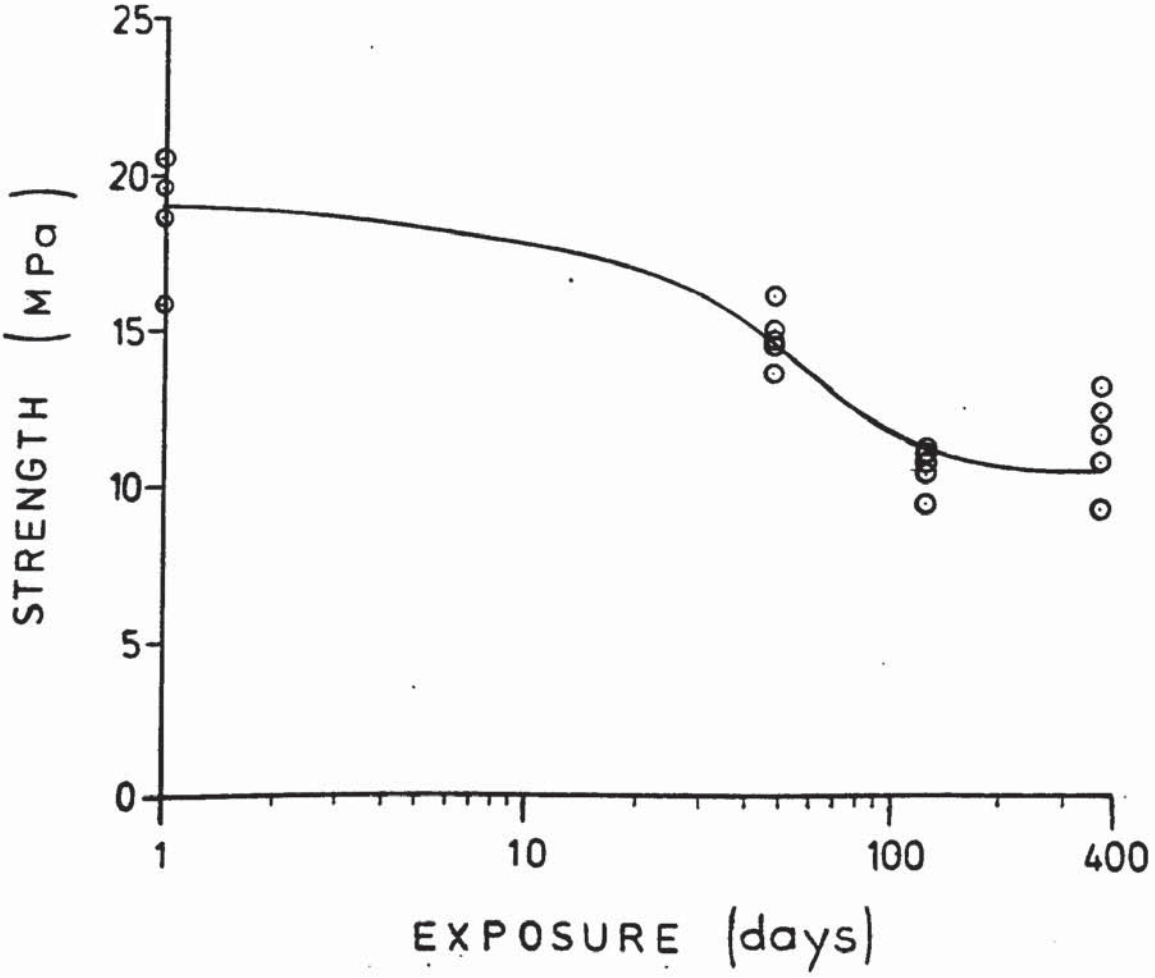

Fig. 4.2.10. Strength of adhesive bonds immersed in 50% by vol. antifreeze solution @ 60°C. (2117 alloy, phosphoric acid anodised, 2214 adhesive).

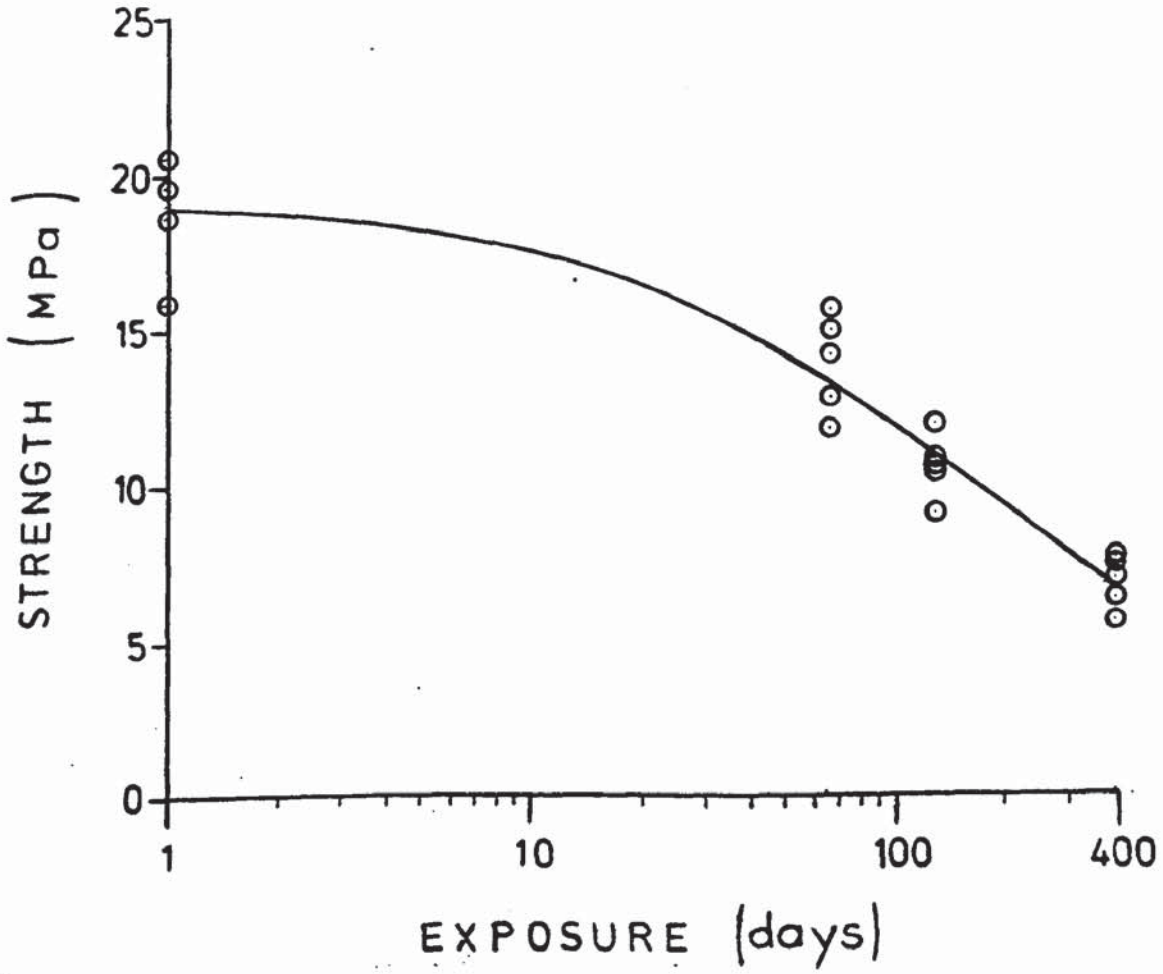

Fig. 4.2.11. Strength of adhesive bonds immersed in de-ionised water @ 60°C.
(2117 alloy, phosphoric acid anodised, 2214 adhesive).

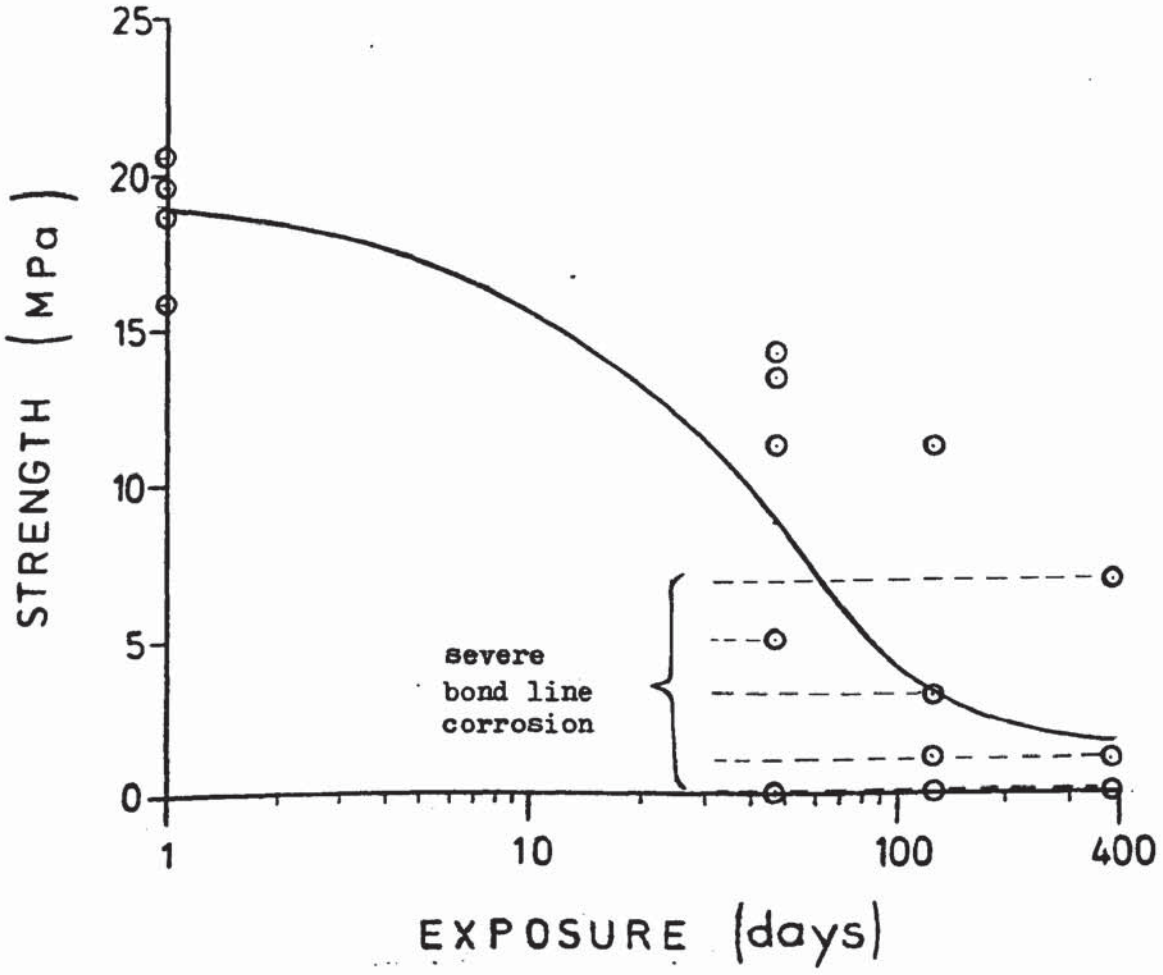

Fig. 4.2.12. Strength of adhesive bonds immersed in human urine @ 60°C.
(2117 alloy, phosphoric acid anodised, 2214 adhesive).

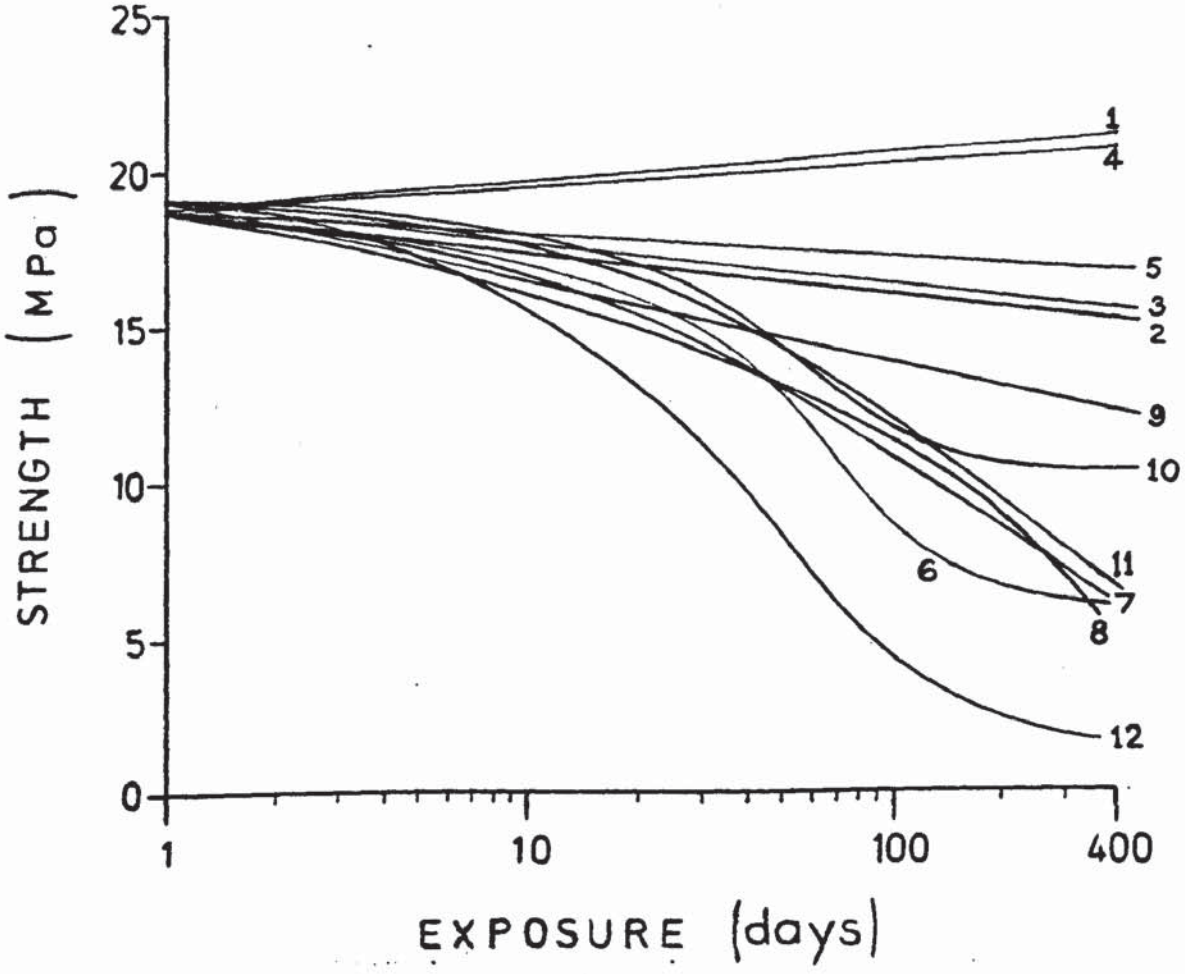

Fig. 4.2.13. Effect of environment on bond durability (2117 alloy, phosphoric acid anodised, (BAC 5555) 2214 adhesive.

orientation w.r.t. roll direction

Key:

1.	Atmosphere @ 20°C.	(∥)
2.	Atmosphere @ 60°C.	(∥)
3.	Atmosphere @ 60°C.	(⊥)
4.	Petrol @ 20°C.	(∥)
5.	Engine oil @ 60°C.	(∥)
6.	Detergent solution @ 60°C.	(∥)
7.	River water @ 60°C.	(∥)
8.	Bovine excrement @ 60°C.	(∥)
9.	5% Sodium Chloride @ 60°C.	(⊥)
10.	Antifreeze solution @ 60°C.	(⊥)
11.	De-ionised water @ 60°C.	(⊥)
12.	Urine @ 60°C.	(⊥)

Environment (orientation)		Strength retention		Failure mode
		% initial value	% control value	
Atmosphere @ 20°C.	(‖)	114	100	Apparently interfacial
Atmosphere @ 60°C.	(‖)	82	100	Apparently interfacial
Atmosphere @ 60°C.	(⊥)	84	100	Apparently interfacial
Petrol @ 20°C.	(‖)	110	96	Apparently interfacial
Engine oil @ 60°C.	(‖)	91	111	Apparently interfacial
Detergent solution @ 60°C.	(‖)	32	39	Cohesive
River water @ 60°C.	(‖)	36	44	Cohesive
Bovine excrement @ 60°C.	(‖)	32	39	Cohesive
5% Sodium Chloride @ 60°C.	(⊥)	65	78	Cohesive
Antifreeze solution @ 60°C.	(⊥)	61	72	Cohesive
De-ionised water @ 60°C.	(⊥)	36	44	Cohesive
Urine @ 60°C.	(⊥)	8	10	Severe bond line corrosion

Table 4.2.13 Effect of environment on bond durability (2117 alloy, phosphoric acid anodised (BAC 5555), 2214 adhesive). Approximately 1 year exposure.

4.3 Effect of reducing phosphoric acid anodising time

Exclusive of solvent degreasing and final drying stages, typical process times for the established bonding pretreatments are 30 minutes for the F.P.L. etch, 60 minutes for phosphoric acid anodising to BAC 5555, and 80 minutes for chromic acid anodising to Def. Std. 151.

These times are considered to be unacceptably long for volume production applications. An experiment was therefore undertaken to establish the influence of reducing the 20 minutes anodising time specified by Boeing. Coupons of BA 2117 alloy were cleaned and F.P.L. etched prior to anodising for times of $\frac{1}{2}$, 1, 2, 5, 10 and 20 minutes. They were bonded using EC 2114 adhesive. Unfortunately the assembly of zero anodising time i.e. F.P.L. etched coupons was overlooked. This was remedied later, but an additional set of 2 minute anodised specimens was prepared for control purposes.

Durability was assessed by testing to destruction groups of specimens withdrawn from a salt-spray cabinet operated at 43°C.

The effects on joints strength of exposure to salt-spray conditions as a function of anodising time are shown in Table 4.3.1 to 4.3.8 and Figs. 4.3.1. to 4.3.8.

Anodising times of 10 and 20 minutes yielded the highest initial bond strengths and, more importantly, much better durability. The difference in strengths retained by the 10 and 20 minute anodised specimens after exposure to salt-spray conditions for 1 year is not statistically significant. Two of the 10 minute anodised specimens exhibited severe bond line corrosion however, one after 6 months and the other after 12 months exposure.

The initial strengths of bonds to surfaces anodised for ½, 1, 2 and 5 minutes were very similar, ranging from 18.2 to 18.6 MPa. The two sets of 2 minute anodised results are in very close agreement, even during environmental exposure. The general trends are seen in Fig. 4.3.8. Durability deteriorates with decreasing anodising time. The poorest levels of performance are associated with anodising times of ½, 1 and 2 minutes, the results for which were substantially inferior to those obtained by bonding to the non-anodised FPL etched surface. In the case of F.P.L. etched, and the ½, 1, 2 and 5 minute anodised material, examination of the fracture surfaces of unexposed specimens revealed the existence of thin films of adhesive over much of the surface, as shown in Figs. 4.3.17a to 4.3.20a. In contrast much less adhesive was evident on the corresponding surfaces of 10 and 20 minute anodised specimens as seen in Figs. 4.3.21a and 4.3.22a. During exposure to salt-spray conditions the fracture surfaces of the 1, 2 and 5 minute anodised specimens exhibited a clearly visible "border" effect, the front of which had advanced in 3 months approximately 3mm. from the edge of the bond area, as shown in Figs. 4.3.12 to 4.3.14.

Optical microscopy detected little adhesive on perimeter surfaces, but the central region was very similar in appearance to the fracture surface seen in the corresponding unexposed specimen. Figs. 4.3.19b and 4.3.20b each show areas representative of these two distinct regions. Such distinct perimeter regions were not evident in the case of the 10 and 20 minute anodised specimens. Figs. 4.3.10b and 4.3.17b show the fracture surfaces of F.P.L. etched specimens which had been exposed for 8 weeks.

Failure mode was unmistakably cohesive, occurring close to the interface and leaving a thin, almost continuous film of adhesive on the substrate.

The concentrations of phosphorus in the anodic films were determined semi-quantitatively by electron probe microanalysis, using a low accelerating voltage (5kV). Phosphorus and aluminium peaks were compared and the relative concentrations in wt% deduced. Phosphorus was detected on surfaces which had been anodised for 2 minutes or more. The results are plotted in Fig. 4.3.9.

Table 4.3.1. Durability of bonds to FPL etched surfaces (zero anodising time, 2117 alloy, 2214 adhesive, salt-spray @ 43°C).

EXPOSURE	FAILURE STRESS (MPa)	MEAN & STD. DEV. (MPa)	OBSERVATIONS
0	18.4	19.1 ±0.3	Cohesive fail. near interface
	19.1		" " "
	19.1		" " "
	19.4		" " "
	19.4		" " "
3 days	17.1	17.6 ±0.3	" " "
	17.6		" " "
	17.7		" " "
	17.8		" " "
	18.0		" " "
7 days	17.1	17.5 ±0.3	" " "
	17.4		" " "
	17.6		" " "
	17.8		" " "
	17.9		" " "
20 days	16.7	17.6 ±0.4	" " "
	17.7		" " "
	17.7		" " "
	17.7		" " "
	18.0		" " "
4 weeks	17.2	17.6 ±0.2	" " "
	17.6		" " "
	17.6		" " "
	17.7		" " "
	17.8		" " "
8 weeks	17.0	17.3 ±0.3	" " "
	17.0		" " "
	17.5		" " "
	17.5		" " "
	17.6		" " "
24 weeks	0	7.2	Severe bond line corrosion
	2.5		" " " "
	5.5		" " " "
	13.1		Bond line corrosion
	15.1		" " "

Table 4.3.2. Durability of bonds to phosphoric acid anodised surfaces (30 seconds anodising time, 2117 alloy, 2214 adhesive, salt-spray @ 43°C).

EXPOSURE	FAILURE STRESS (MPa)	MEAN & STD. DEV. (MPa)	OBSERVATIONS
0	17.5	18.2 ±0.8	Apparent interfacial failure
	17.7		" " "
	17.9		" " "
	18.5		" " "
	19.6		" " "
3 days	13.8	15.5 ±1.6	" " "
	14.1		" " "
	15.8		" " "
	16.7		" " "
	17.3		" " "
11 days	15.1	15.8 ±0.7	" " "
	15.4		" " "
	15.4		" " "
	16.2		" " "
	16.8		" " "
19 days	13.9	14.4 ±0.5	" " "
	14.1		" " "
	14.4		" " "
	14.6		" " "
	15.2		" " "
4 weeks	12.7	13.7 ±0.8	" " "
	13.1		" " "
	13.6		" " "
	14.5		" " "
	14.6		" " "
12 weeks	12.0	2.8	" " "
	2.1		Bond line corrosion
	0		" " "
	0		" " "
	0		" " "

Table 4.3.3. Durability of bonds to phosphoric acid anodised surfaces (1 min. anodising time, 2117 alloy, 2214 adhesive, salt-spray @ 43°C).

EXPOSURE	FAILURE STRESS (MPa)	MEAN & STD. DEV. (MPa)	OBSERVATIONS
0	18.0 18.2 18.4 18.5 18.9	18.4 ±0.3	Apparent interfacial failure " " " " " " " " " " " "
3 days	14.6 15.5 16.0 16.3 17.0	15.9 ±0.9	" " " " " " " " " " " " " " "
11 days	14.7 16.0 16.4 16.5 16.5	16.0 ±0.7	" " " " " " " " " " " " " " "
19 days	14.1 14.4 14.7 15.4 15.5	14.8 ±0.7	" " " " " " " " " " " " " " "
4 weeks	13.2 13.9 14.4 14.4 16.0	14.4 ±1.1	" " " " " " " " " " " " " " "
12 weeks	10.9 11.3 12.2 0 0	6.9 ±6.3	" " " " " " " " " Severe bond line corrosion " " " "
24 weeks		0	" " " " (all failed on handling)

Table 4.3.4. Durability of bonds to phosphoric acid anodised surfaces (2 min. anodising time, 2117 alloy, 2214 adhesive, salt-spray @ 43°C).

EXPOSURE	FAILURE STRESS (MPa)	MEAN & STD. DEV. (MPa)	OBSERVATIONS
0	16.8	18.5 ± 1.3	Apparent interfacial failure
	18.0		"
	18.3		"
	19.8		"
	19.8		"
3 days	15.7	16.2 ± 0.8	"
	15.8		"
	15.8		"
	16.2		"
	17.7		"
11 days	14.2	15.2 ± 0.9	"
	14.5		"
	15.4		"
	15.5		"
	16.6		"
19 days	14.4	14.5 ± 0.2	"
	14.4		"
	14.5		"
	14.5		"
	14.9		"
4 weeks	13.1	14.3 ± 0.7	"
	14.2		"
	14.3		"
	14.6		"
	15.1		"
12 weeks	8.5	9.8 ± 1.0	"
	9.2		"
	9.6		"
	10.8		"
	10.9		"
24 weeks	2.4		Severe bond line corrosion
	0		"
	0		"
	0		"
	0		"

Table 4.3.5. Durability of bonds to phosphoric acid anodised surfaces (repeat of 2 mins. anodising time, 2117 alloy, 2214 adhesive, salt-spray @ 43°C).

EXPOSURE	FAILURE STRESS (MPa)	MEAN & STD. DEV. (MPa)	OBSERVATIONS
0	18.2	18.6 ± 0.3	Apparent interfacial failure
	18.3		" " "
	18.6		" " "
	18.7		" " "
	19.1		" " "
3 days	15.8	16.2 ± 0.3	" " "
	16.0		" " "
	16.1		" " "
	16.5		" " "
	16.6		" " "
7 days	14.5	15.0 ± 0.3	" " "
	15.0		" " "
	15.0		" " "
	15.1		" " "
	15.6		" " "
20 days	13.3	14.5 ± 0.3	Starved joint result ignored
	14.0		Apparent interfacial failure
	14.3		" " "
	14.7		" " "
	14.9		" " "
4 weeks	13.0	13.9 ± 0.5	" " "
	13.7		" " "
	14.0		" " "
	14.0		" " "
	14.5		" " "
8 weeks	13.0	13.5 ± 0.3	" " "
	13.2		" " "
	13.7		" " "
	13.7		" " "
	13.7		" " "
24 weeks	0	3.6	Severe bond line corrosion
	0		" " " "
	2.0		" " " "
	4.6		" " " "
	11.4		" " " "

Table 4.3.6. Durability of bonds to phosphoric acid anodised surfaces (5 min. anodising time, 2117 alloy, 2214 adhesive, salt-spray @ 43°C).

EXPOSURE	FAILURE STRESS (MPa)	MEAN & STD. DEV. (MPa)	OBSERVATIONS
	17.3		Apparent interfacial failure
	17.8		" " "
0	18.0	18.3	" " "
	18.8	±1.0	" " "
	19.7		" " "
	18.5		" " "
	18.5		" " "
3 days	19.0	19.1	" " "
	19.5	±0.6	" " "
	19.8		" " "
	15.5		" " "
	16.1		" " "
11 days	16.3	16.8	" " "
	17.1	±1.3	" " "
	19.0		" " "
	14.8		" " "
	14.8		" " "
19 days	15.0	15.2	" " "
	15.7	±0.5	" " "
	16.0		" " "
	14.1		" " "
	15.3		" " "
4 weeks	16.0	15.6	" " "
	16.1	±0.9	" " "
	16.3		" " "
	12.0		" " "
	12.2		" " "
12 weeks	13.6	13.3	" " "
	14.2	±1.2	" " "
	14.5		" " "
	15.3		" " "
	13.8		" " "
24 weeks	6.3	8.3	Severe bond line corrosion
	6.1	±6.3	" " " "
	0		" " " "
	0		" " " "
48 weeks	0		" " " "
	6.1		" " " "
	12.1		Apparent interfacial failure
	13.4		" " "

Table 4.3.7. Durability of bonds to phosphoric acid anodised surfaces (10 min. anodising time, 2117 alloy, 2214 adhesive, salt-spray @ 43°C).

EXPOSURE	FAILURE STRESS (MPa)	MEAN & STD. DEV. (MPa)	OBSERVATIONS
0	19.1	20.8 ±1.8	Apparent interfacial failure.
	19.8		" " "
	19.8		" " "
	21.0		" " "
	23.3		" " "
3 days	18.6	20.0 ±0.8	" " "
	20.1		" " "
	20.3		" " "
	20.5		" " "
	20.7		" " "
11 days	18.4	19.4 ±0.9	" " "
	18.7		" " "
	19.4		" " "
	19.8		" " "
	20.7		" " "
19 days	17.1	17.8 ±0.6	" " "
	17.5		" " "
	17.7		" " "
	18.4		" " "
	18.4		" " "
4 weeks	19.5	20.6 ±0.8	" " "
	20.1		" " "
	20.7		" " "
	21.3		" " "
	21.4		" " "
12 weeks	15.0	15.6 ±0.4	" " "
	15.6		" " "
	15.7		" " "
	15.8		" " "
	15.9		" " "
24 weeks	15.7	14.2 ±4.4	" " "
	15.9		" " "
	16.4		" " "
	16.8		" " "
	6.3		Severe bond line corrosion
48 weeks	3.4	11.1 ±4.4	" " " "
	11.5		Cohesive failure
	12.7		" "
	13.2		" "
	14.6		" "

Table 4.3.8. Durability of bonds to phosphoric acid anodised surfaces (20 min. anodising time, 2117 alloy, 2214 adhesive, salt-spray @ 43°C.

EXPOSURE	FAILURE STRESS (MPa)	MEAN & STD. DEV. (MPa)	OBSERVATIONS
0	20.4	21.1 ±1.0	Apparent interfacial failure
	20.4		" " "
	20.6		" " "
	21.9		" " "
	22.5		" " "
3 days	17.5	19.2 ±1.5	" " "
	18.0		" " "
	19.1		" " "
	20.4		" " "
	20.9		" " "
11 days	17.2	18.3 ±0.9	" " "
	17.3		" " "
	18.8		" " "
	19.0		" " "
	19.0		" " "
19 days	16.0	16.9 ±0.9	" " "
	16.2		" " "
	16.8		" " "
	17.8		" " "
	17.9		" " "
4 weeks	17.5	18.7 ±0.9	" " "
	18.0		" " "
	19.0		" " "
	19.1		" " "
	19.7		" " "
12 weeks	14.6	15.9 ±1.0	" " "
	15.3		" " "
	16.2		" " "
	16.3		" " "
	17.1		" " "
24 weeks	14.1	14.8 ±0.4	" " "
	14.7		" " "
	14.8		" " "
	15.0		" " "
	15.2		" " "
48 weeks	12.4	13.6 ±1.2	Cohesive failure
	12.9		" "
	13.5		" "
	13.7		" "
	15.4		" "

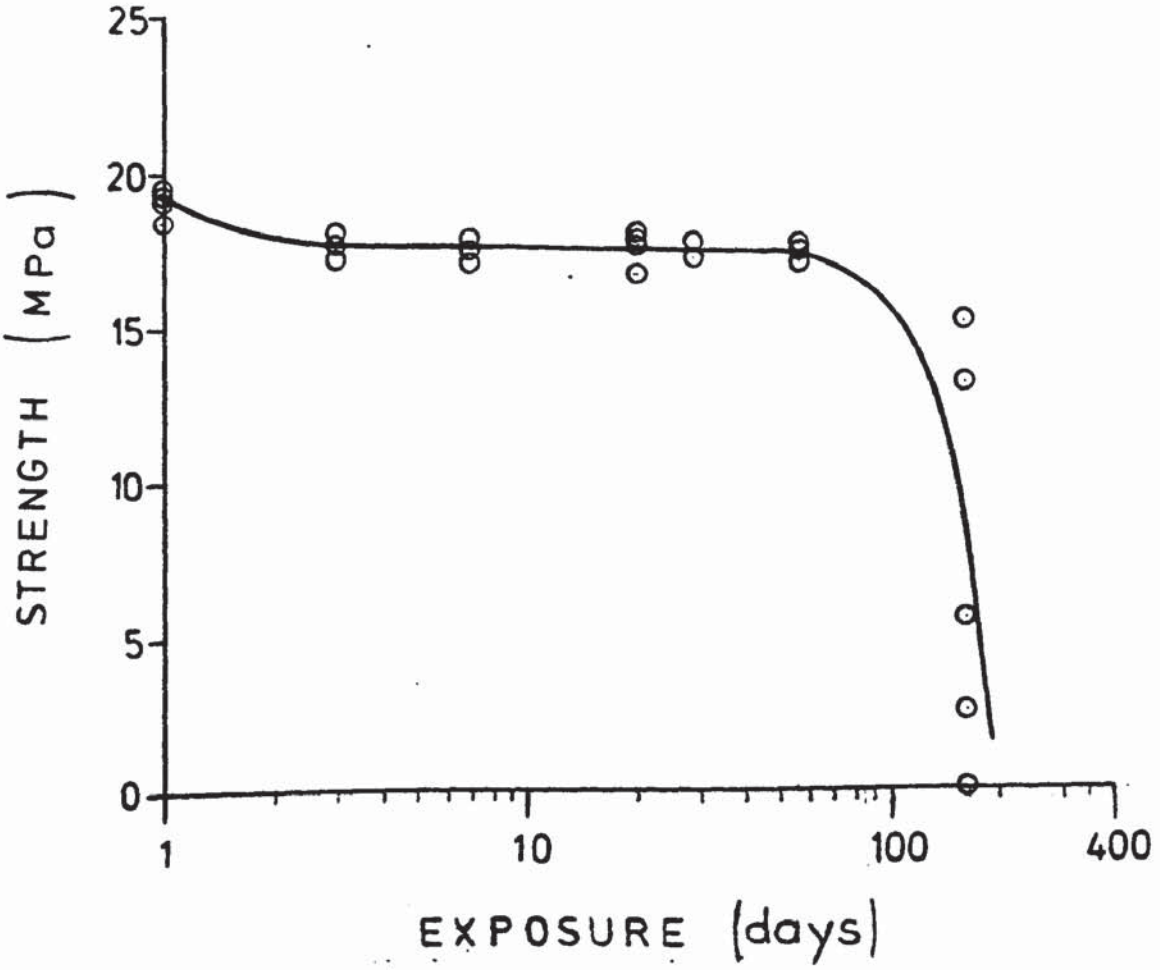

Fig. 4.3.1. Durability of bonds to FPL etched surfaces (zero anodising time, 2117 alloy, 2214 adhesive, salt-spray @ 43°C).

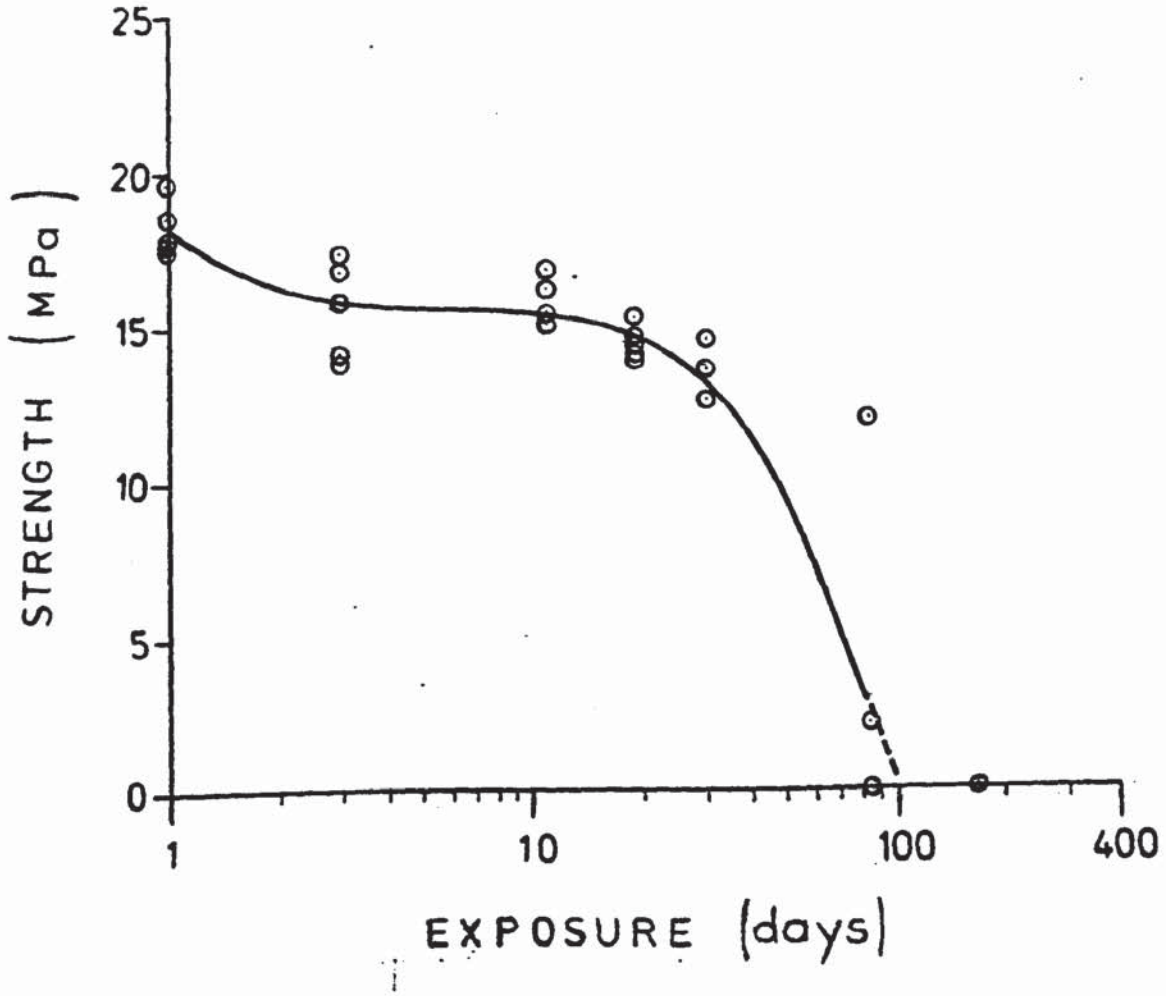

Fig. 4.3.2. Durability of bonds to phosphoric acid anodised surfaces (30 seconds anodising time, 2117 alloy, 2214 adhesive, salt-spray @ 43°C).

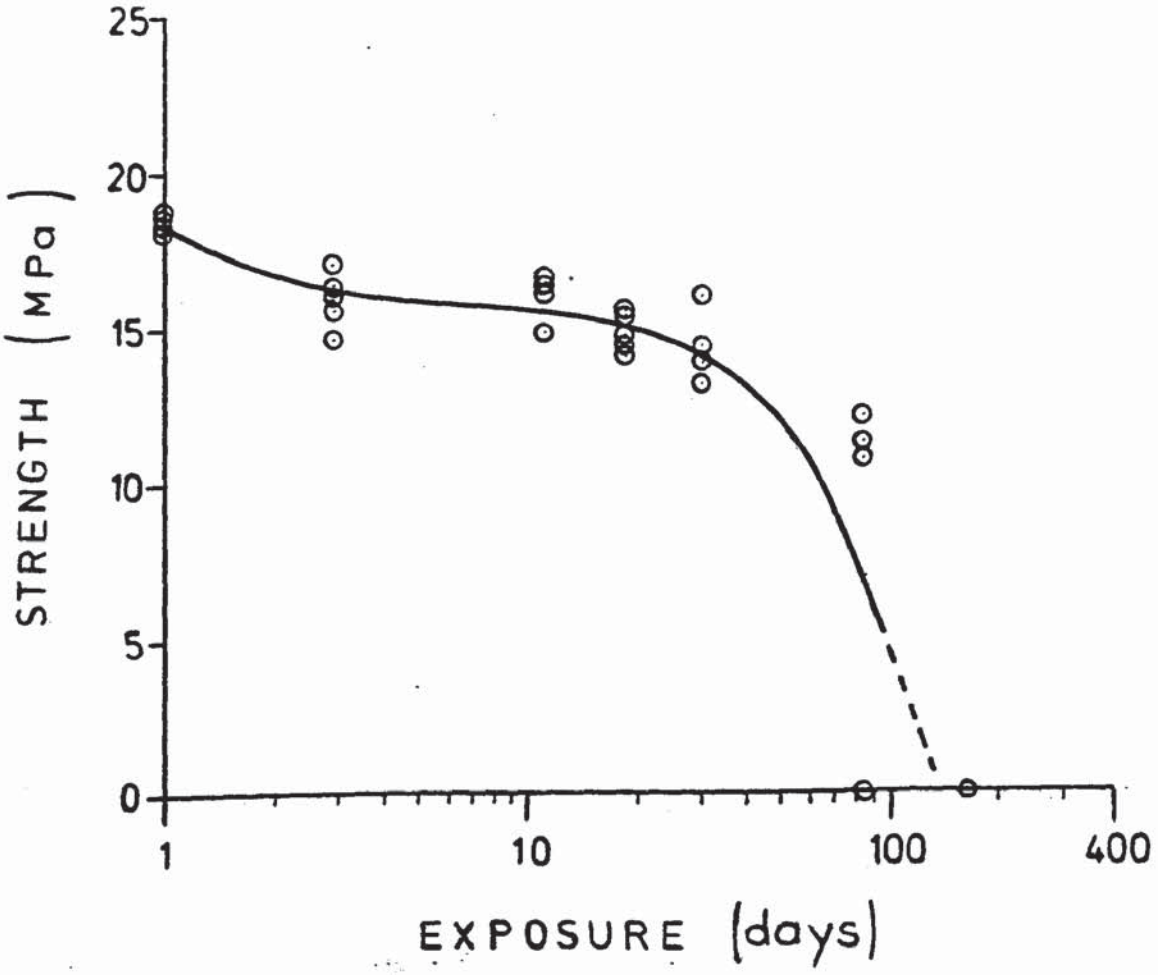

Fig. 4.3.3. Durability of bonds to phosphoric acid anodised surfaces (1 min. anodising time, 2117 alloy, 2214 adhesive, salt-spray @ 43°C).

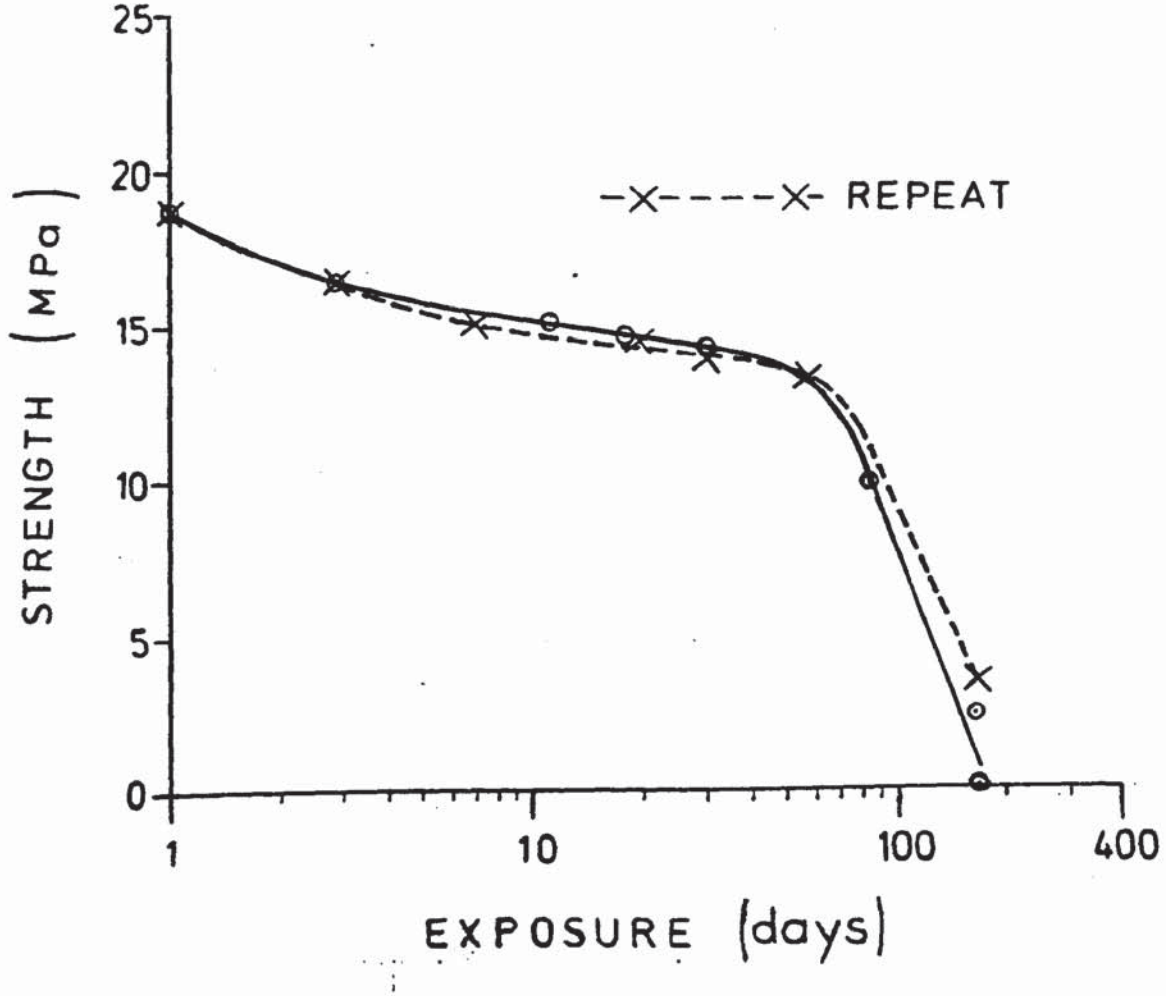

Fig. 4.3.4. Durability of bonds to phosphoric acid anodised surfaces (2 mins. anodising time, 2117 alloy, 2214 adhesive, salt-spray @ 43°C).

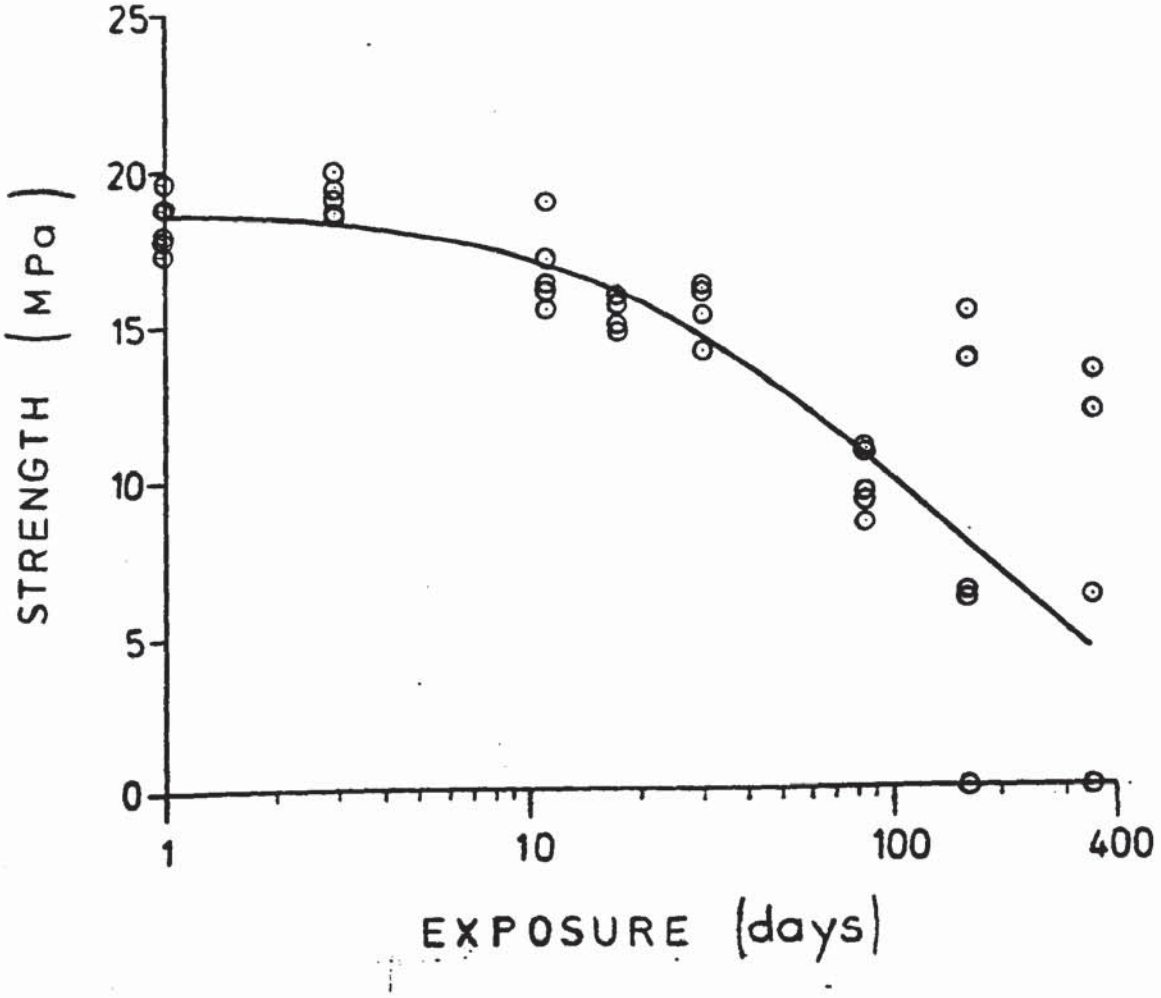

Fig. 4.3.5. Durability of bonds to phosphoric acid anodised surfaces (5 min. anodising time, 2117 alloy, 2214 adhesive, salt-spray @ 43°C).

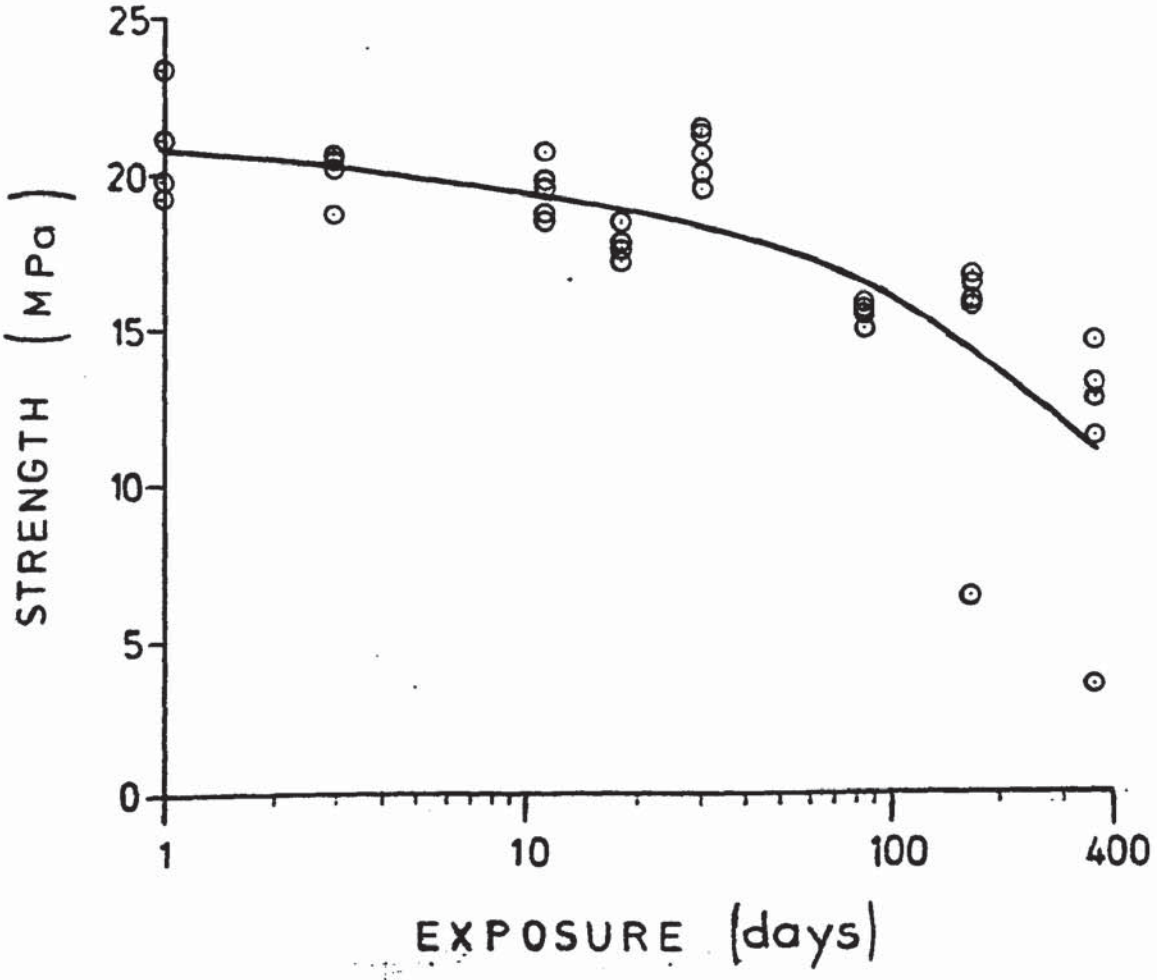

Fig. 4.3.6. Durability of bonds to phosphoric acid anodised surfaces (10 min. anodising time, 2117 alloy, 2214 adhesive, salt-spray @ 43°C).

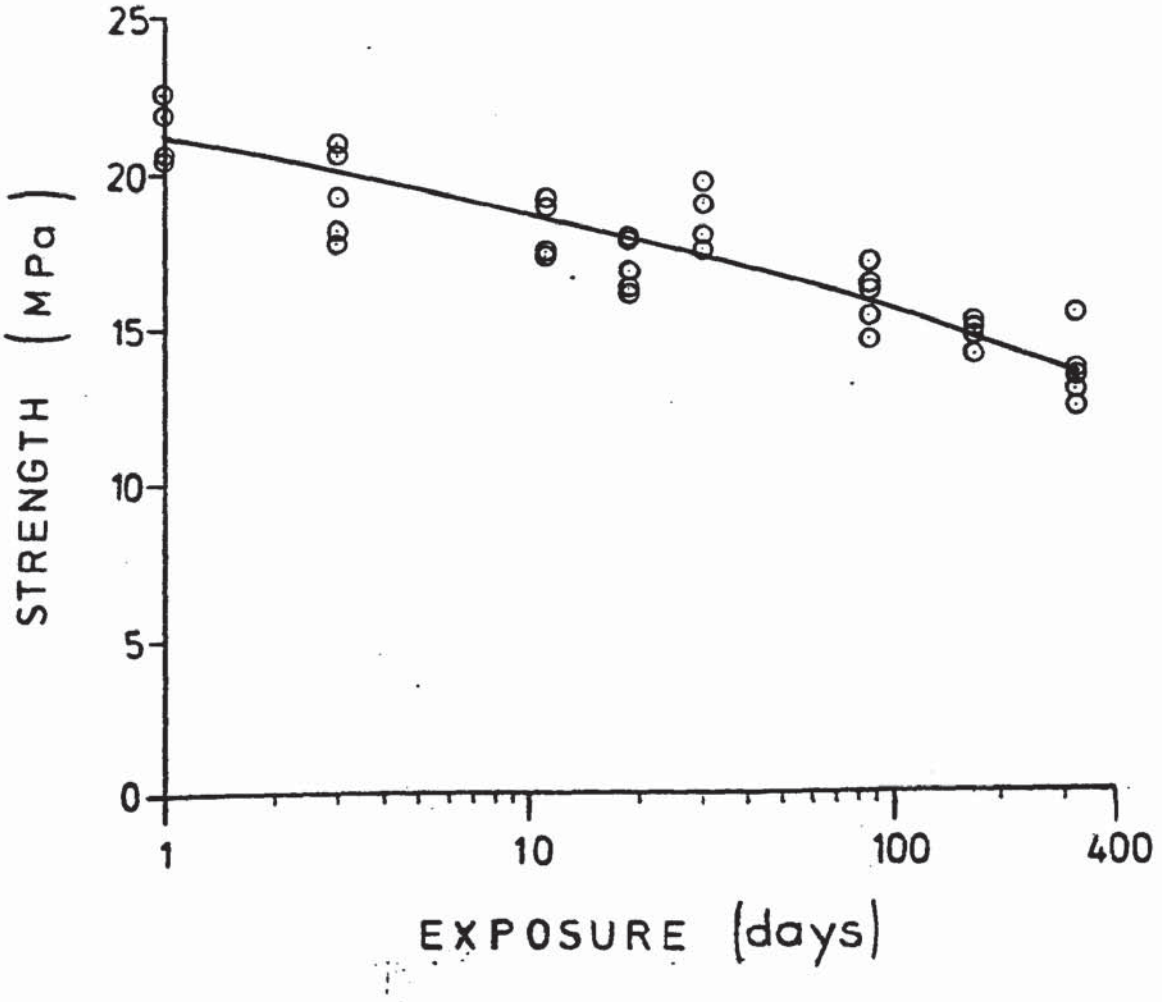

Fig. 4.3.7. Durability of bonds to phosphoric acid anodised surfaces (20 min. anodising time, 2117 alloy, 2214 adhesive, salt-spray @ 43°C).

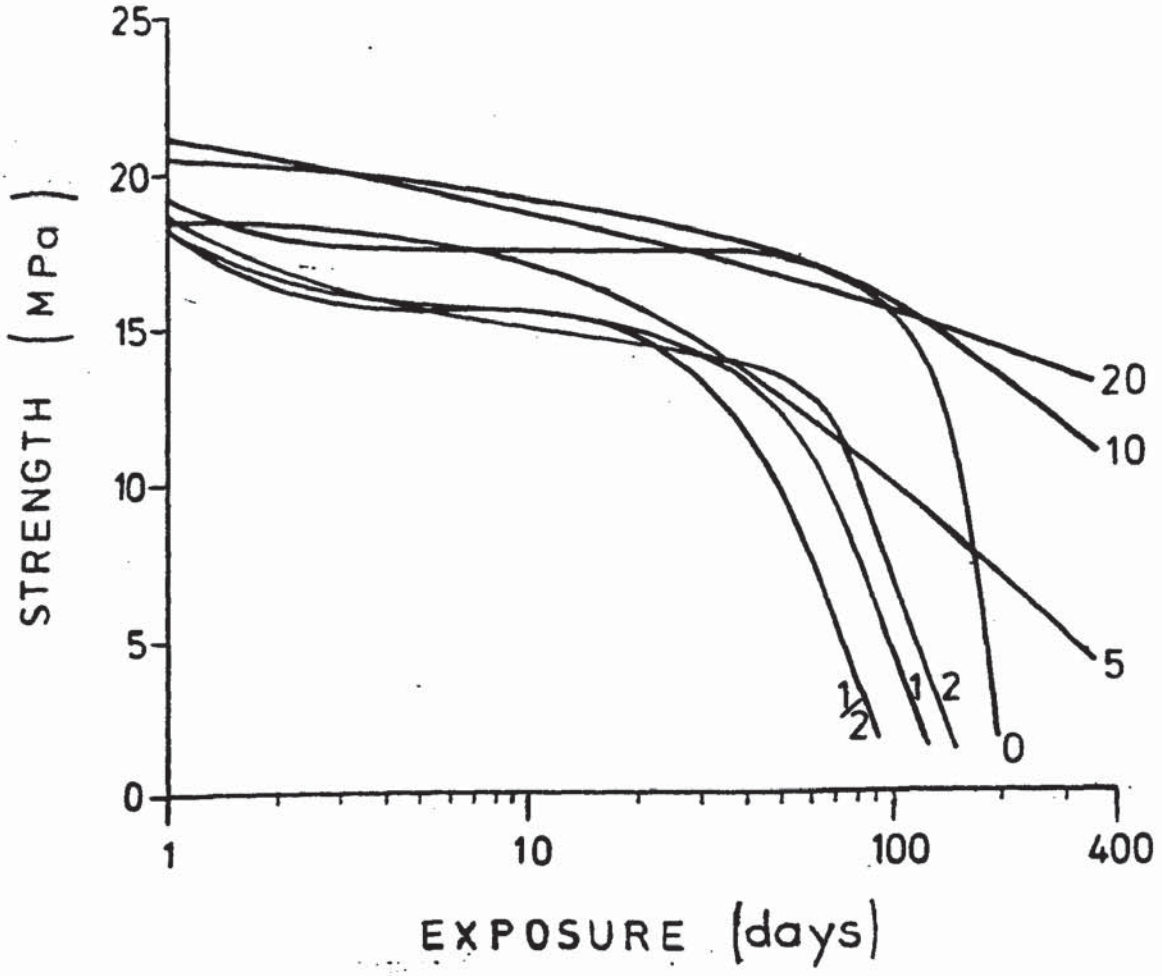

Fig. 4.3.8. Durability of bonds to 2117 alloy as a function of anodising time, (mins)

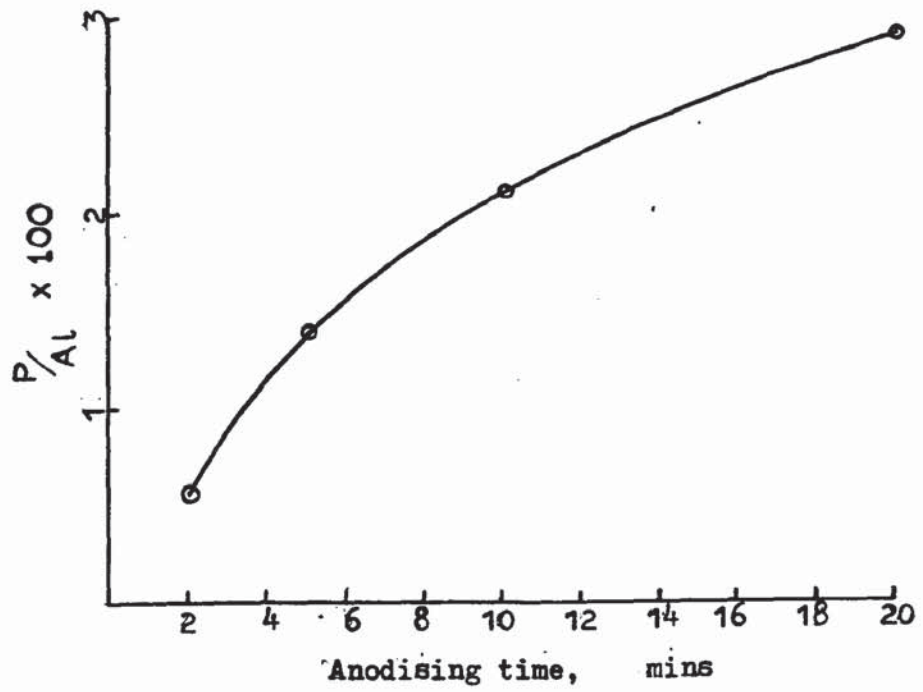

Fig. 4.3.9 Variation of phosphorus concentration with anodising time.

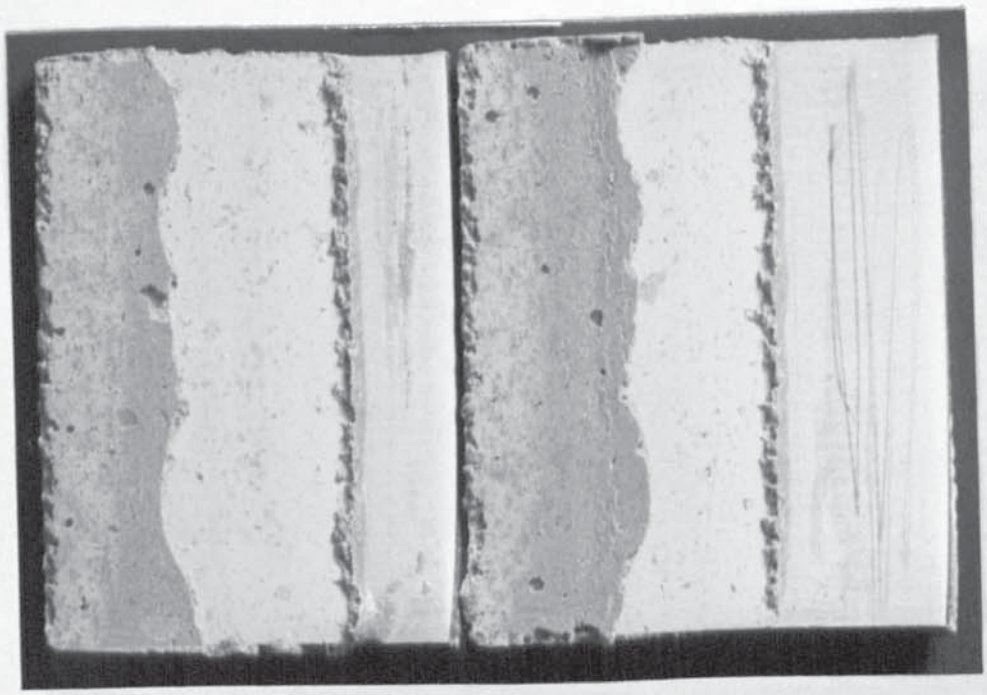

(a) Unexposed

Fig. 4.3.10. Optimised FPL etch, 10 minutes @ 65°C.
(BA 2117 alloy, EC 2214 adhesive)

(b) 8 wk. exposure S/S @ 43°C.

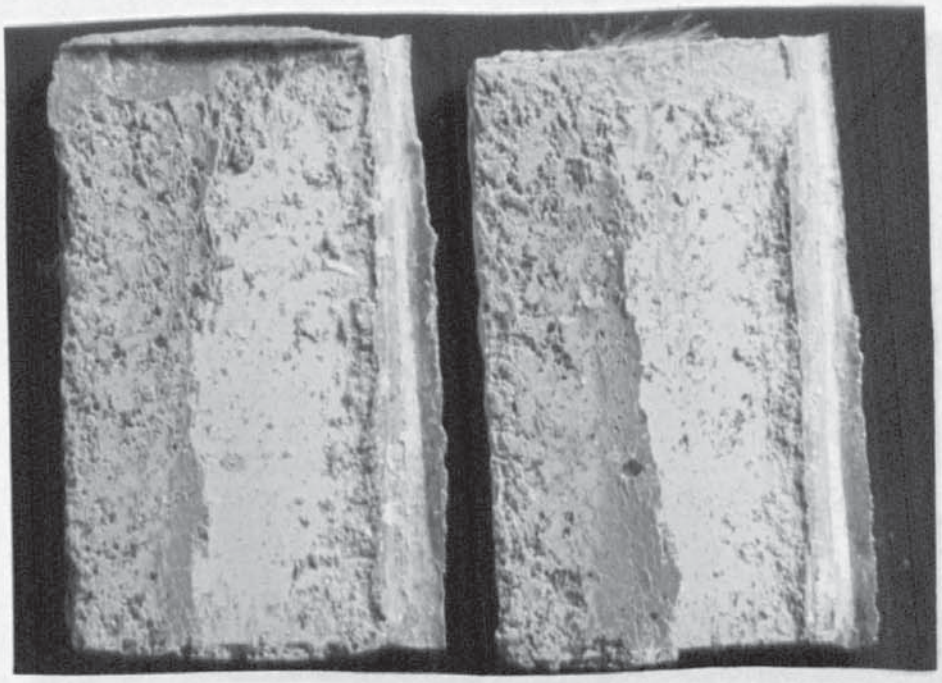

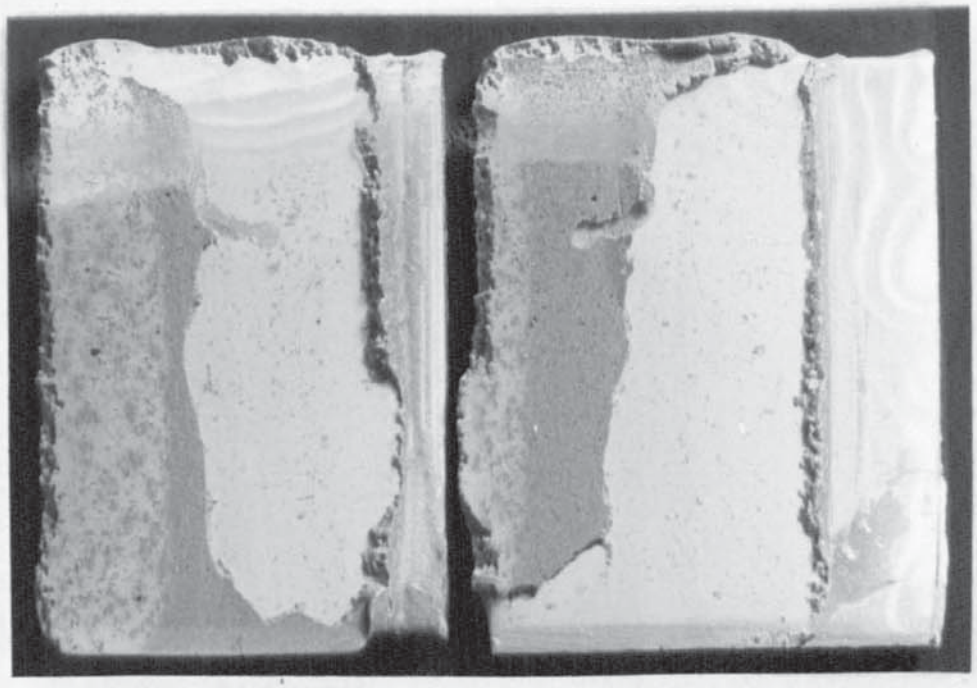

(a) Unexposed

Fig. 4.3.11. Phosphoric acid anodised, 30 seconds.
(BA 2117 alloy, EC 2214 adhesive)

(b) 12 wk. exposure S/S @ 43°C.

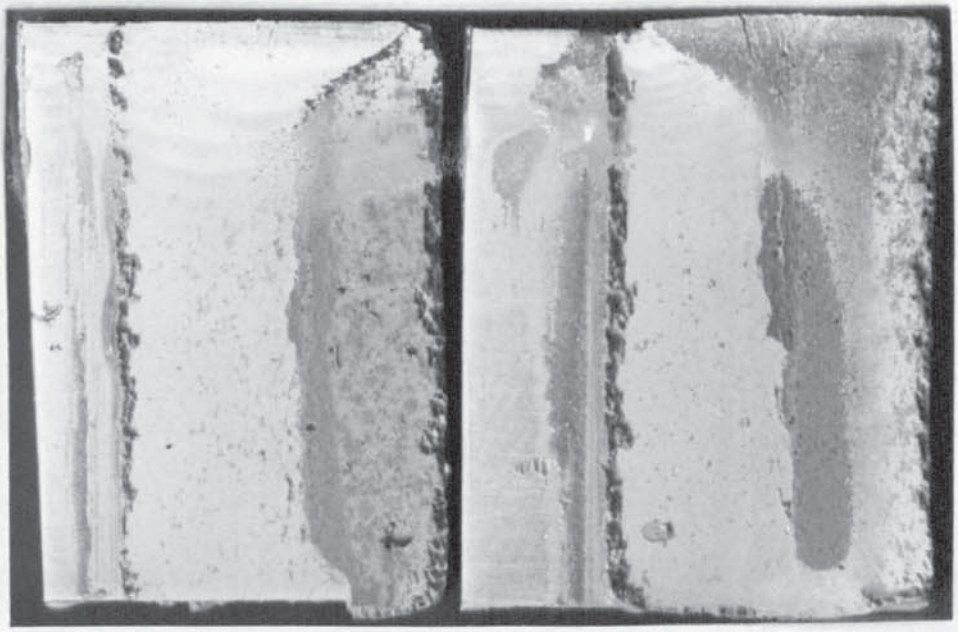

(a) Unexposed

Fig. 4.3.12. Phosphoric acid anodised, 1 minute. (BA 2117 alloy, EC 2214 adhesive)

(b) 12 wk. exposure S/S @ 43°C.

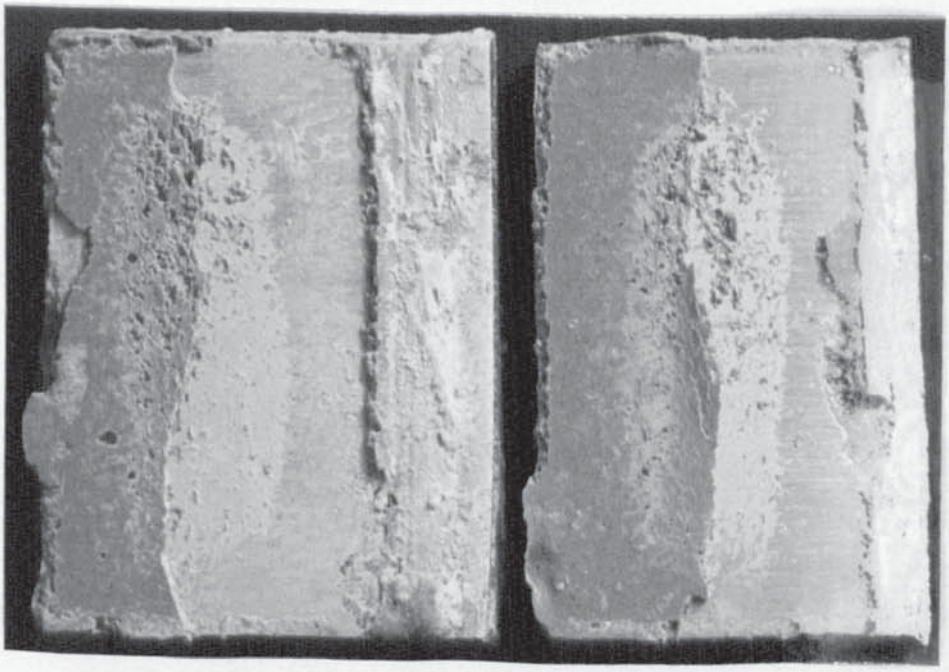

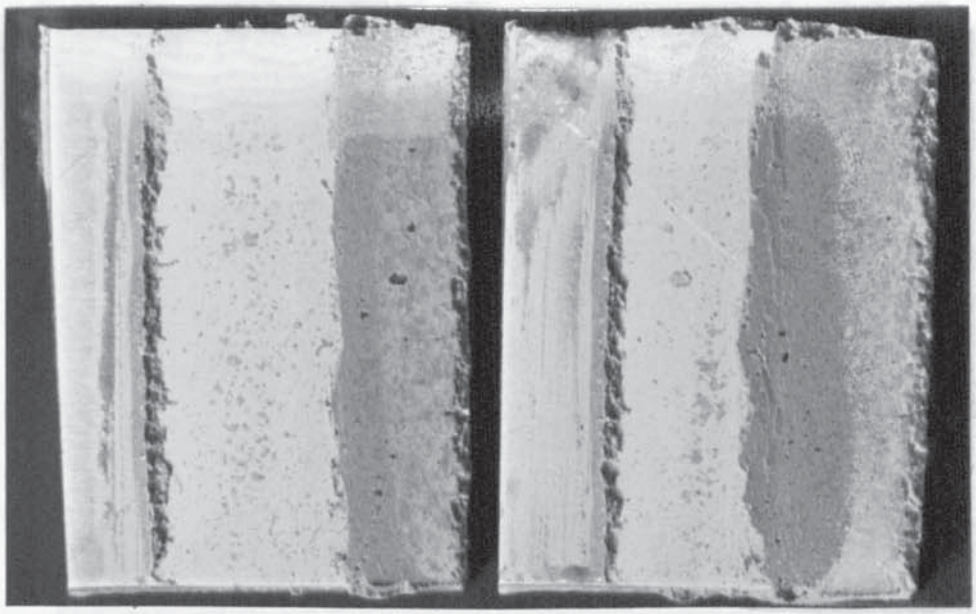

(a) Unexposed

Fig. 4.3.13. Phosphoric acid anodised, 2 minutes. (BA 2117 alloy, EC 2214 adhesive)

(b) 12 wk. exposure S/S @ 43°C.

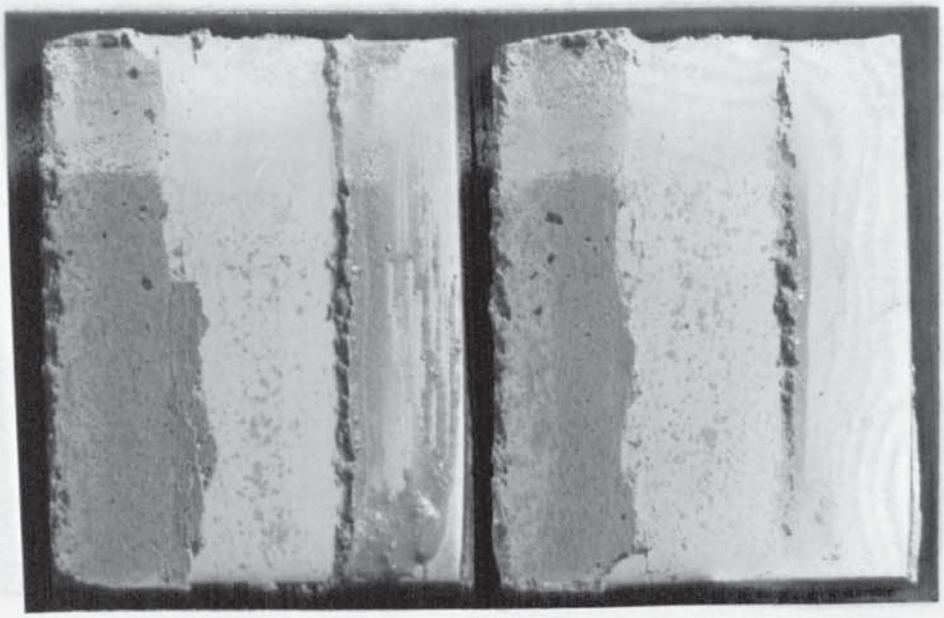

(a) Unexposed

Fig. 4.3.14. Phosphoric acid anodised, 5 minutes. (BA 2117 alloy, EC 2214 adhesive)

(b) 12 wk. exposure S/S @ 43°C.

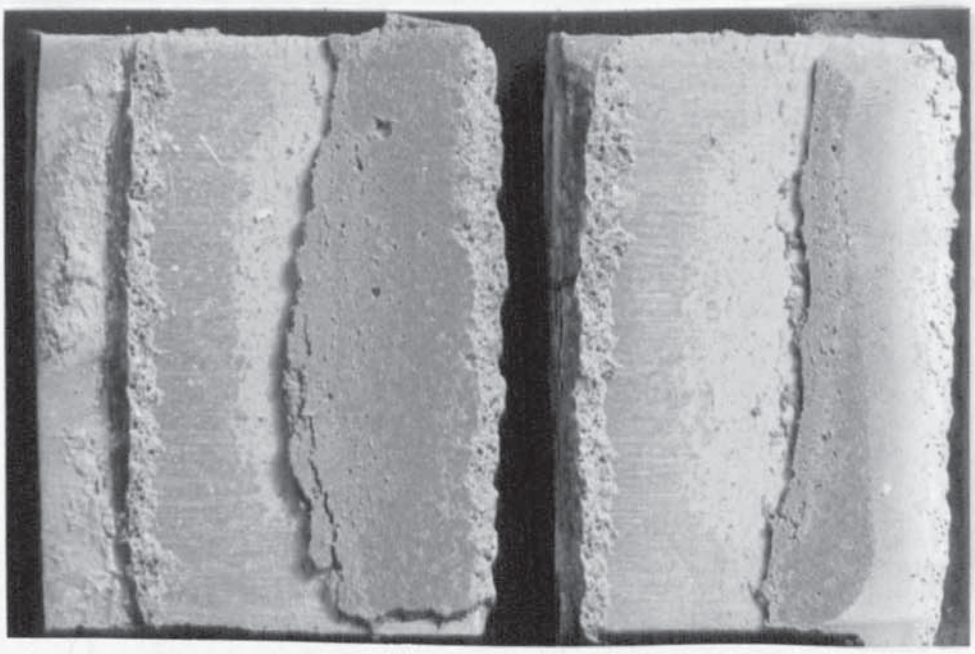

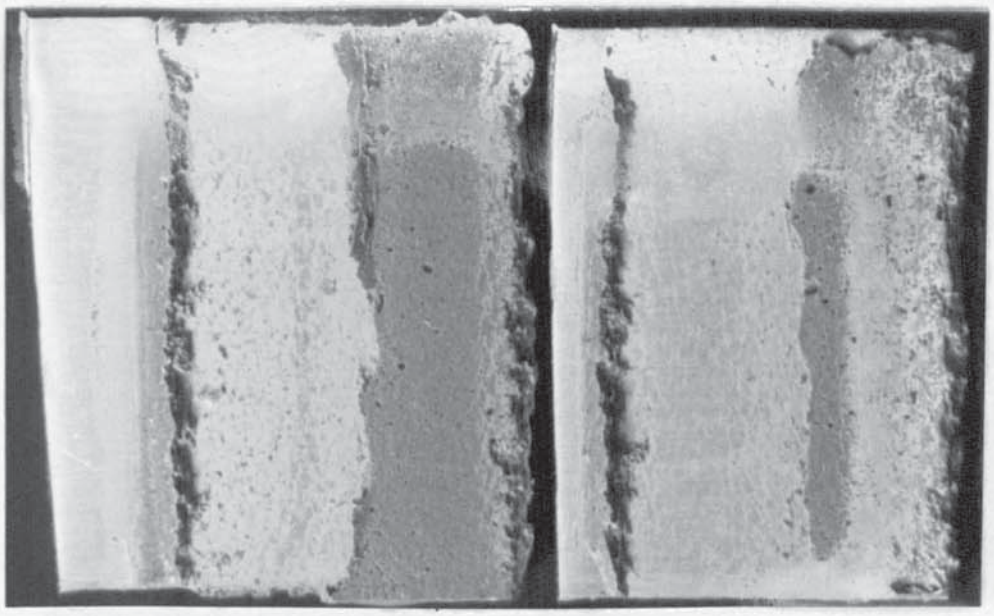

(a) Unexposed

Fig. 4.3.15. Phosphoric acid anodised, 10 minutes. (BA 2117 alloy, EC 2214 adhesive)

(b) 12 wk. exposure S/S @ 43°C.

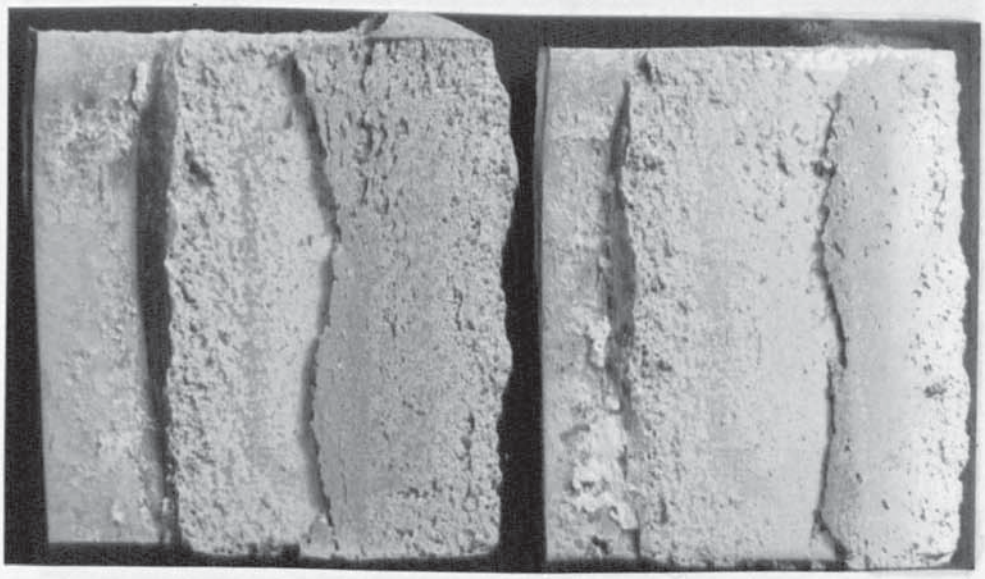

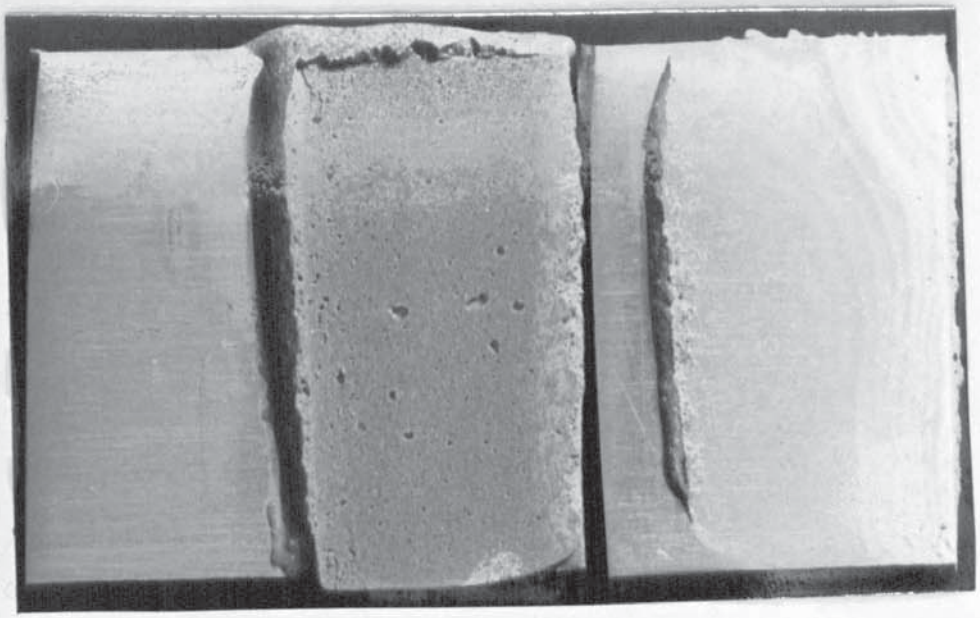

(a) Unexposed

Fig. 4.3.16. Phosphoric acid anodised, 20 minutes. (BA 2117 alloy, EC 2214 adhesive)

(b) 12 wk. exposure S/S @ 43°C.

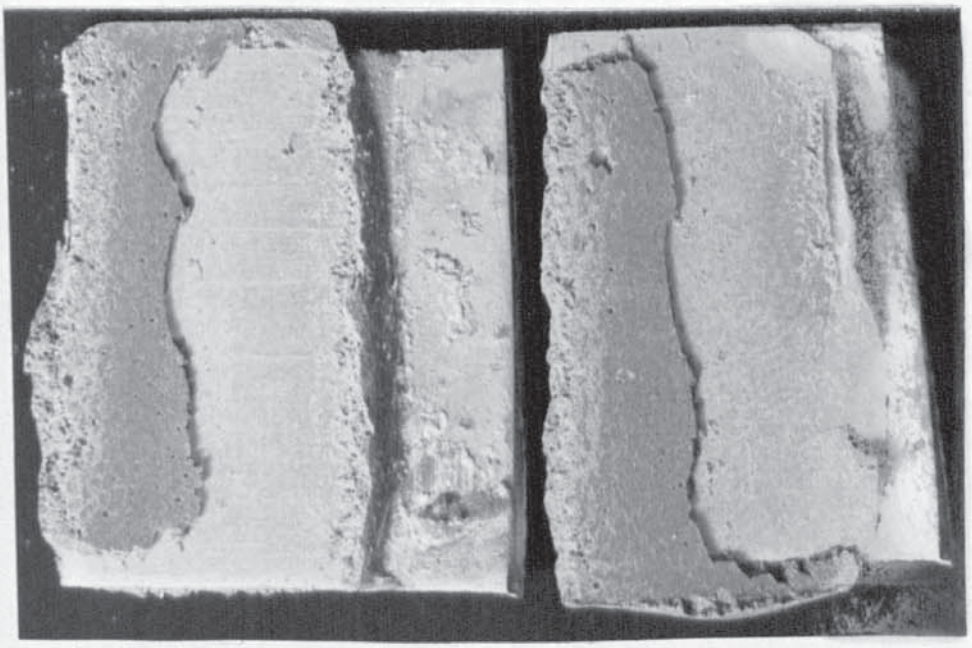

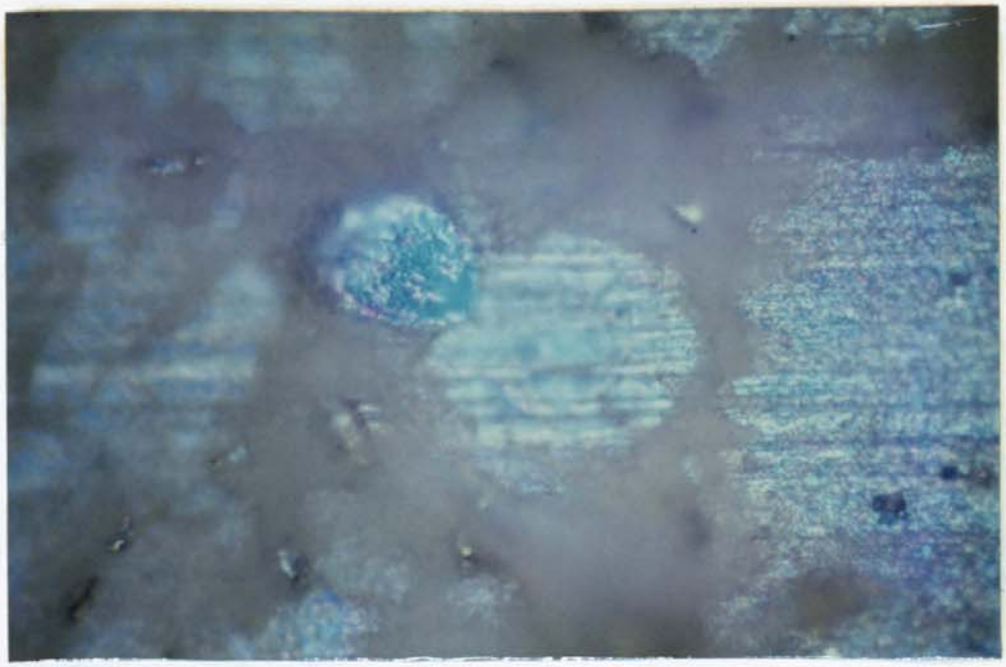

(a) Unexposed

1μm

Fig. 4.3.17. Optimised FPL etch, 10 minutes @ 65°C.
(BA 2117 alloy, EC 2214 adhesive)

(b) 8 wk. exposure S/S @ 43°C.

1μm

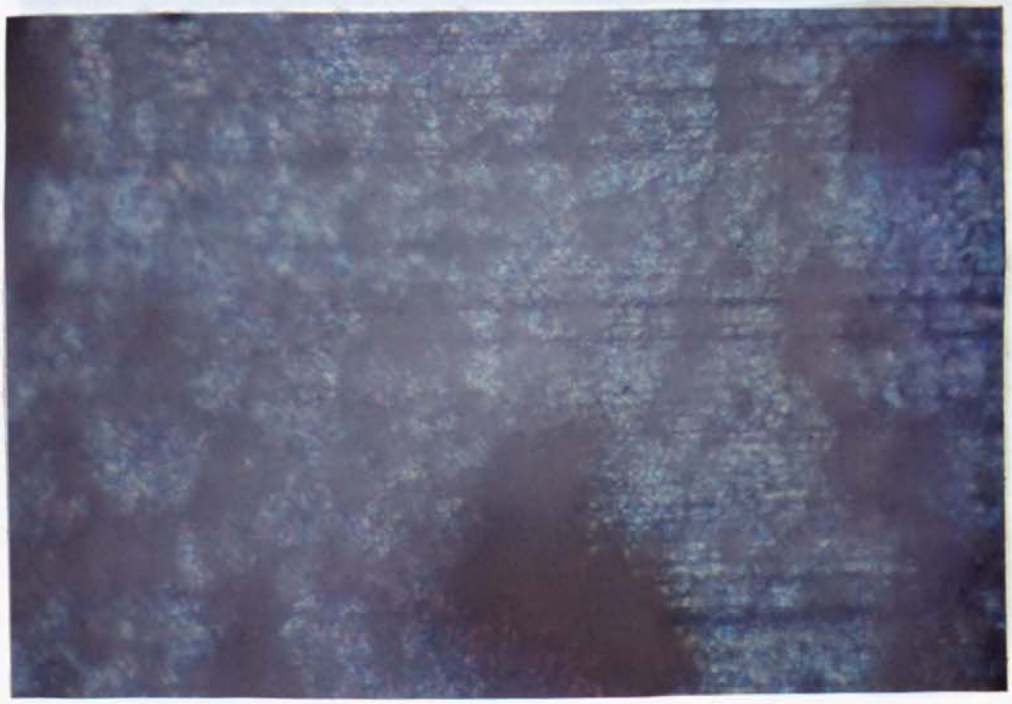

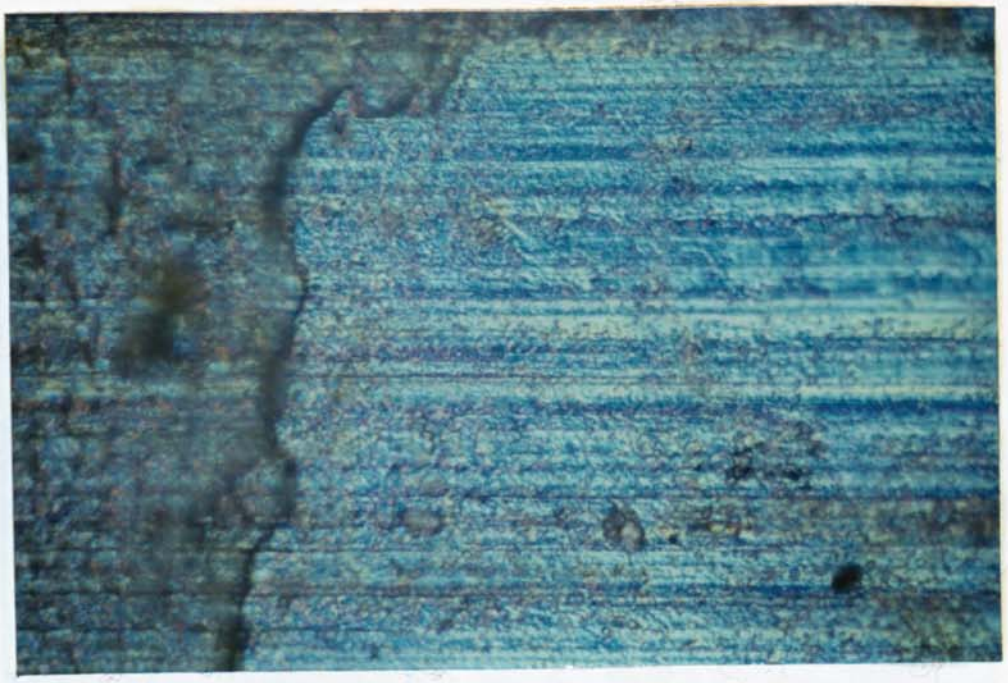

(a) Unexposed

1μm

Fig. 4.3.18. Phosphoric acid anodised, 30 seconds. (BA 2117 alloy, EC 2214 adhesive)

(b) 12 wk. exposure S/S @ 43°C.

1μm

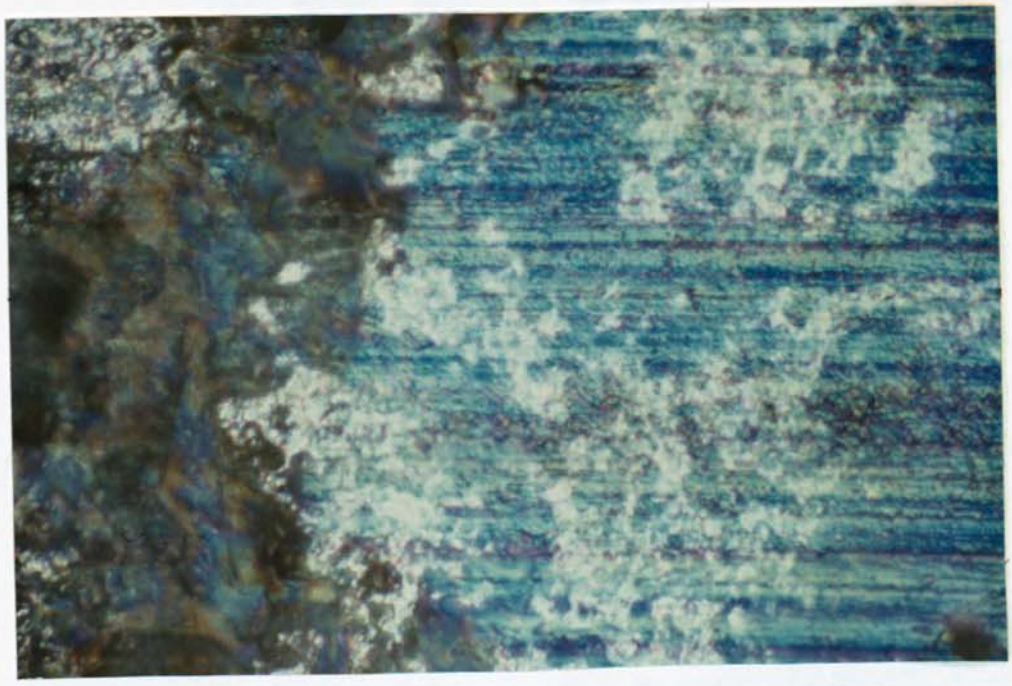

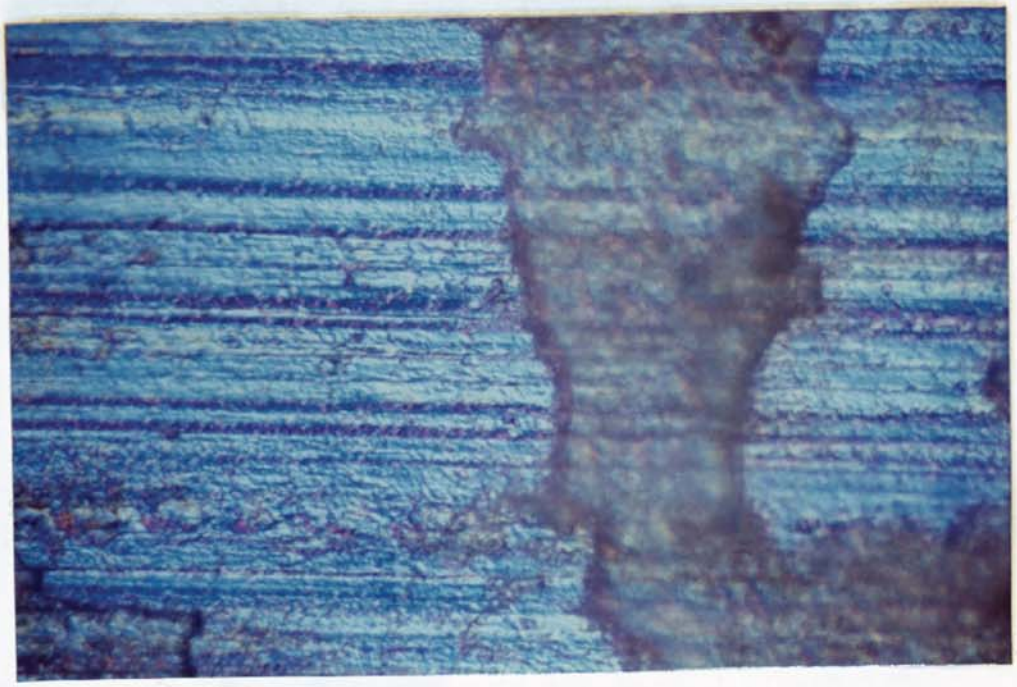

(a) Unexposed

1 μm

Fig. 4.3.19. Phosphoric acid anodised, 2 minutes. (BA 2117 alloy, EC 2214 adhesive)

1 μm

(b) 12 wk. exposure S/S @ 43°C.

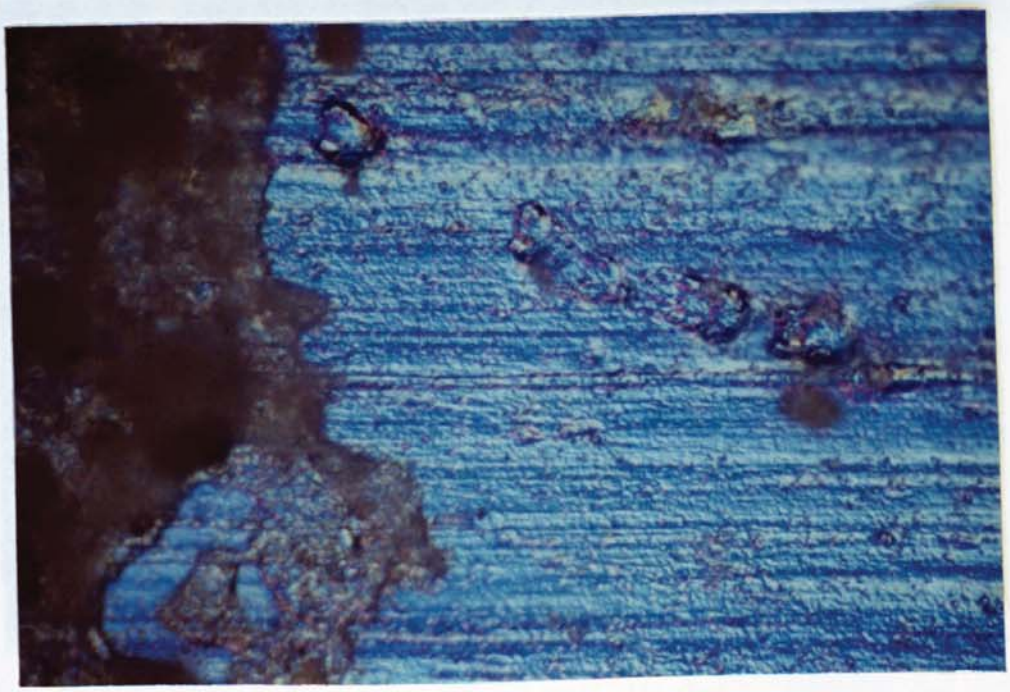

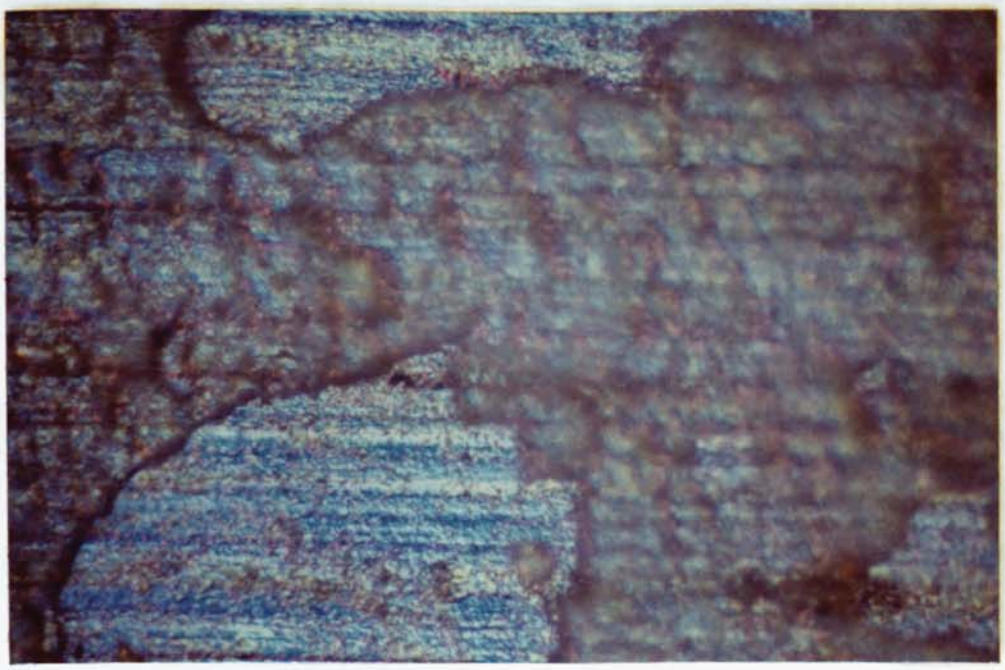

(a) Unexposed

1 μm

Fig. 4.3.20. Phosphoric acid anodised, 5 minutes. (BA 2117 alloy, EC 2214 adhesive)

1 μm

(b) 12 wk. exposure S/S @ 43°C.

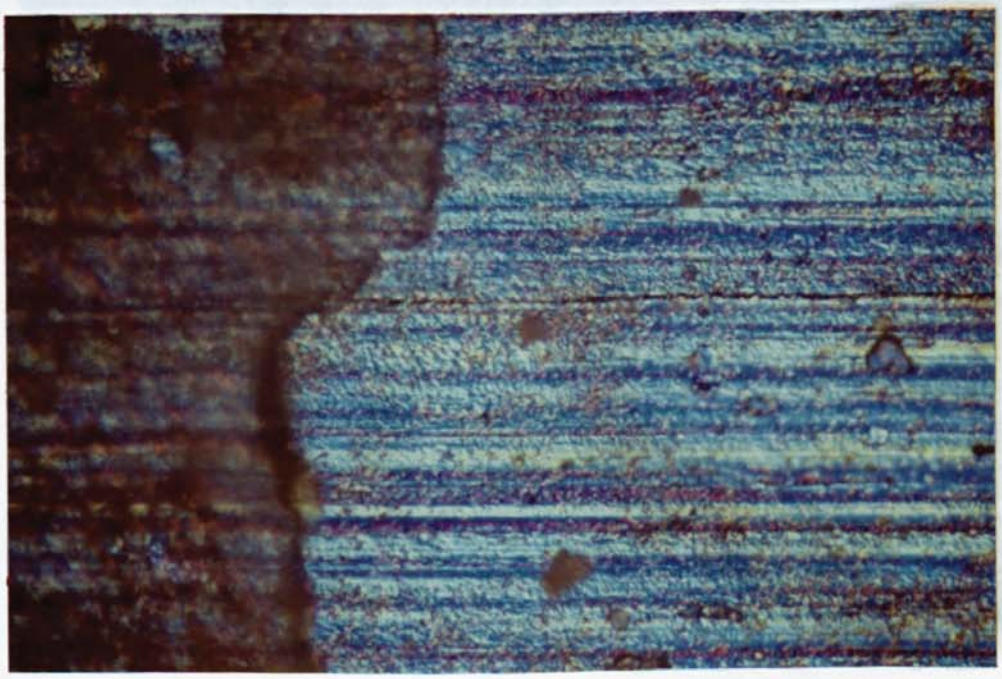

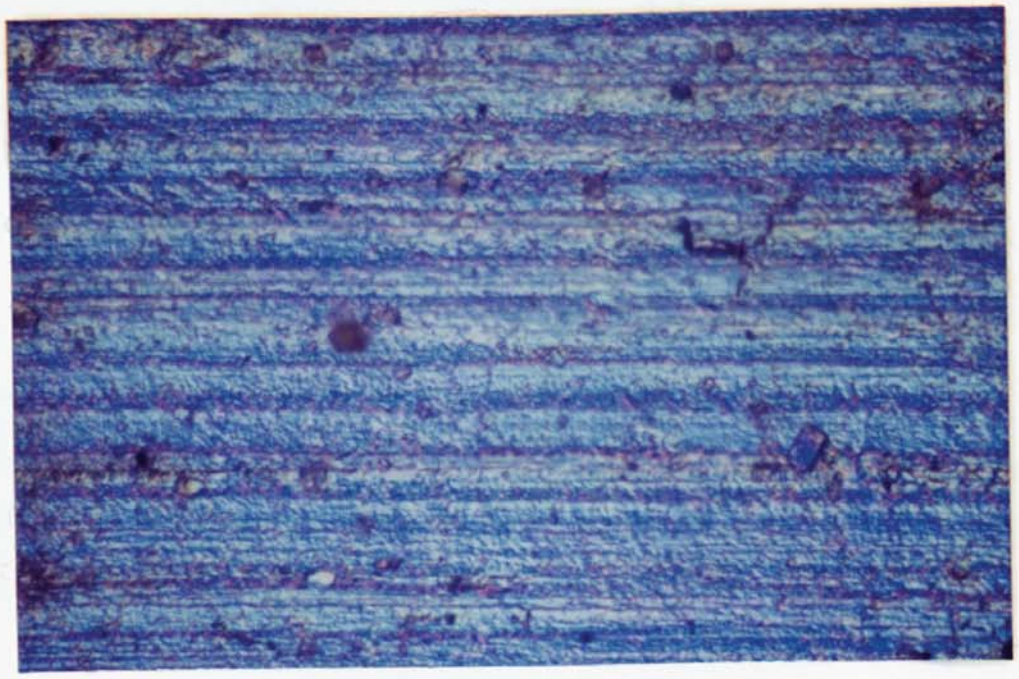

(a) Unexposed

1 μm

Fig. 4.3.21. Phosphoric acid anodised, 10 minutes (BA 2117 alloy, EC 2214 adhesive)

1 μm

(b) 12 wk. exposure S/S @ 43°C.

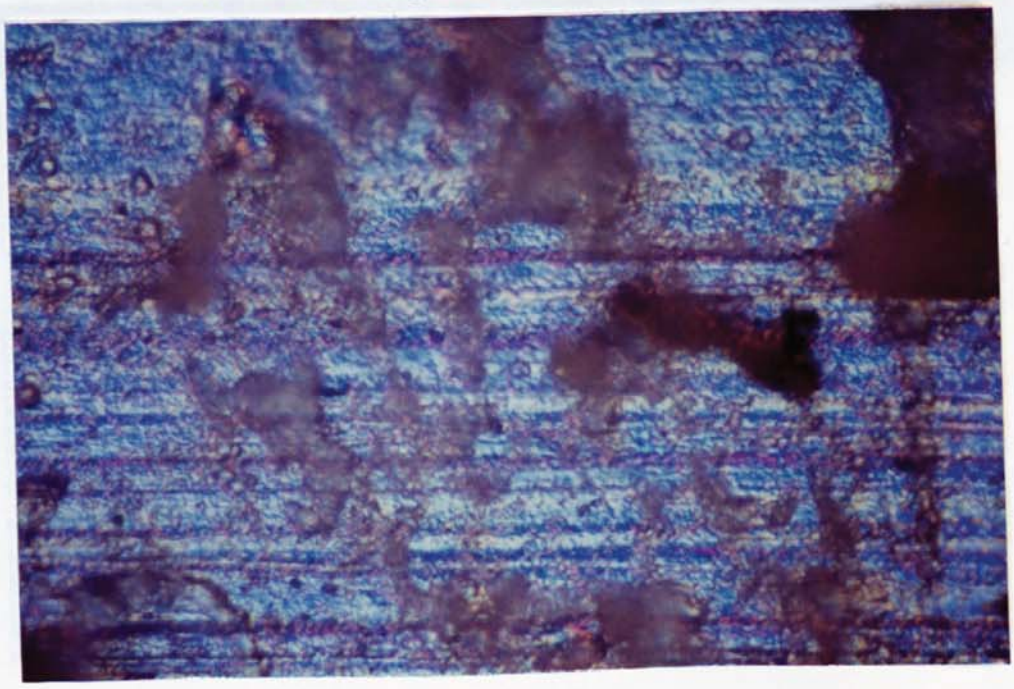

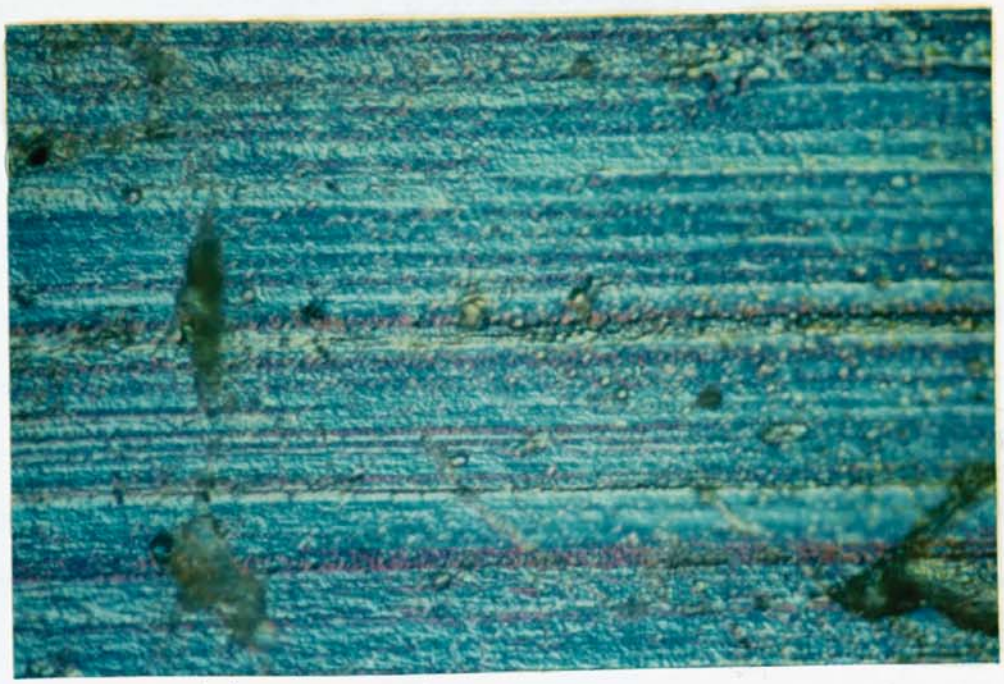

(a) Unexposed

1μm

Fig. 4.3.22. Phosphoric acid anodised, 20 minutes. (BA 2117 alloy, EC 2214 adhesive)

1μm

(b) 12 wk. Exposure S/S @ 43°C.

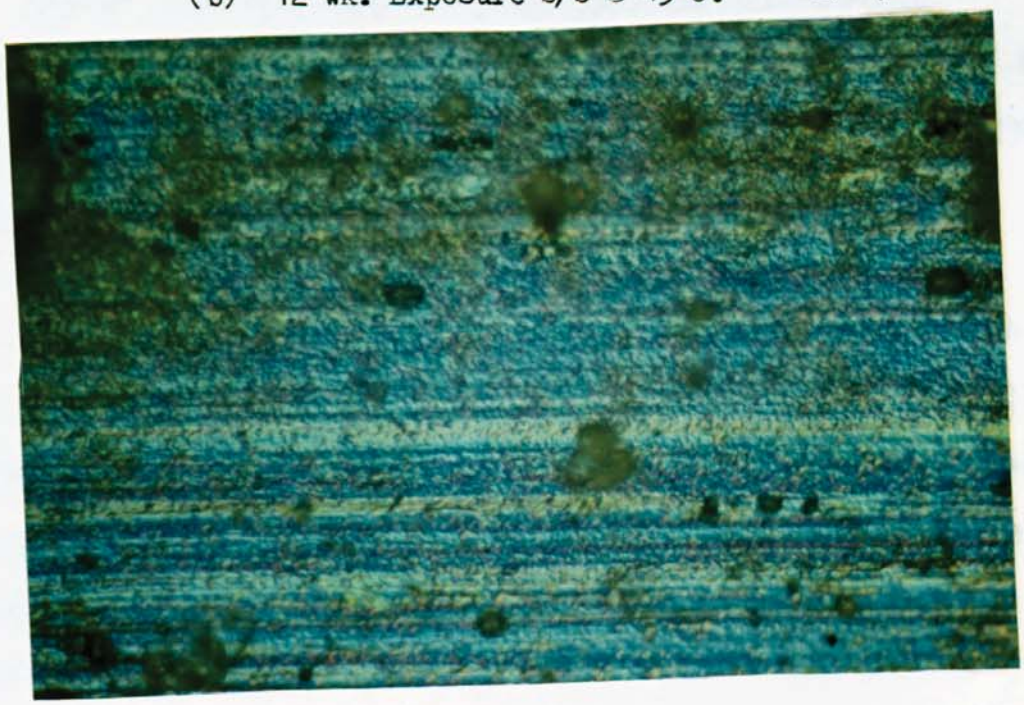

4.4 Durability of adhesive bonds to 5251 alloy

The evaluation of adhesive bonds to 1.2mm thick 5251 alloy was carried out using ESP 105 adhesive, a rubber toughened material which had exhibited superior performance under impact conditions [319]. Such types are therefore considered to be more likely candidates for future vehicle applications. Later, a sample of Dunlop Technology's rubber toughened WP 9 was obtained and included in the trial.

Three rapid electrolytic processes were compared to the three control treatments, A, B and C, described below. Since previous experiments had indicated the necessity for prolonged environmental exposure in order to discriminate between the higher performance pretreatments, immersion of additional control specimens in de-ionised water at 60°C. was included in an attempt to accelerate degradation mechanisms.

The pretreatments used were as follows:-

A. Vapour degrease, alkaline clean, deoxidise.

B. Vapour degrease, alkaline clean, optimised FPL etch, BAC 5555.

C. Vapour degrease, alkaline clean, deoxidise, BAC 5555.

D. Vapour degrease, alkaline clean, deoxidise, anodise for 1 minute in 10% by weight orthophosphoric acid solution at 20°C. and 10v AC.

E. As in D, but 2 minute anodise.

F. Vapour degrease, alkaline clean, deoxidise, anodise for 10 seconds in 10% by weight sulphuric acid at 90°C. and 4v AC.

Pretreatments D and E were based on processes learned in a discussion with Pennwalt Chemical Ltd. Pretreatment F is based on Alcan's hot AC sulphuric acid process used on coil lines.

The results are detailed in Table 4.4.1 to 4.4.10, and plotted graphically in Figs. 4.4.1 to 4.4.12.

The most striking feature of this data is the apparent relative lack of sensitivity to pretreatment. The simple acid clean (A) and the Boeing phosphoric acid anodise (B) treatments were intended to provide reference curves against which experimental pretreatments could be assessed. The comparisons made in Fig. 4.4.11 show that the durabilities produced by A, B and C treatments are virtually indistinguishable, when tested by exposure to de-ionised water. All exhibited very high levels of strength retention in this environment. Exposure to salt-spray conditions resulted in greater strength losses in all three systems and better discrimination between A and B, for which strength retention levels at 1 year were 56% and 74% respectively. Bonds prepared for evaluating pretreatments D, E and F were exposed only to salt-spray conditions, and the results are detailed in Tables 4.4.7 to 4.4.10 and plotted in Figs. 4.4.6 to 4.4.10. The results for all bonding systems tested in this environment are compared in Fig. 4.4.12. The initial strengths of specimens produced using ESP 105 and pretreatments C, D, E and F are virtually identical. Differences in retained strength were detected, the AC sulphuric acid anodised specimens tending to be more durable than those involving AC phosphoric acid anodising. The differences were significant at the 1% level for the 1 minute process, and very nearly significant at the 2% level for the 2 minute AC phosphoric acid treatment. Specimens produced using Dunlop's WP 9 adhesive and AC sulphuric acid anodised substrate retained the same fractional strength as similar bonds using ESP 105, but in absolute terms were considerably stronger.

Examination of coupons produced when initial strengths were determined revealed the existence of adhesive on all fracture surfaces, as shown in Figs. 4.4.13 to 4.4.18. In the case of the simple deoxidising treatment, A, the adhesive did not appear to be evenly distributed, and areas of what appeared to be substrate were clearly visible. To a lesser extent similar observations applied to the A.C. sulphuric acid anodise/WP 9 adhesive system. During the course of environmental exposure the loci of failure for most of the systems continued to be primarily cohesive but close to the interface.

Those joints produced using the simple deoxidising treatment differed in that a bond edge effect similar to that previously observed and described in Section 4.3., slowly developed during the period of test.

Table 4.4.1. Durability of 5251/pre-treatment A/ESP 105 bonds in salt-spray at 43°C.

EXPOSURE	FAILURE STRESS (MPa)	MEAN & STD. DEV. (MPa)	OBSERVATIONS
0	18.6 18.7 18.8 19.6	18.9 ±0.4	Cohesive fail. near interface " " "
2 weeks	15.0 15.1 15.1 15.1 16.0	15.3 ±0.4	" " " " "
4 weeks	15.0 15.5 15.5 15.6 16.1	15.5 ±0.3	" " " " "
9 weeks	13.8 14.7 14.8 15.3 15.4	14.8 ±0.5	Apparent interfacial failure at bond edges " " "
20 weeks	10.5 11.6 12.6 13.1 13.8	12.3 ±1.3	" " " " "
33 weeks	8.6 11.5 11.7 12.5 12.5	11.4 ±1.6	" " " " "
54 weeks	8.0 10.4 11.0 11.1 12.3	10.6 ±1.6	" " " " "

Table 4.4.2. Durability of 5251/pre-treatment A/ESP 105 bonds in de-ionised water @ 60°C.

EXPOSURE	FAILURE STRESS (MPa)	MEAN & STD. DEV. (MPa)	OBSERVATIONS
0	18.6	18.9 ±0.4	Cohesive fail. near interface
	18.7		" " "
	18.8		" " "
	19.6		" " "
2 weeks	17.1	17.9 ±0.5	" " "
	17.5		" " "
	18.0		" " "
	18.2		" " "
	18.5		" " "
4 weeks	18.8	17.8 ±0.6	" " "
	17.4		" " "
	17.4		" " "
	15.6		Starved joint } results
	15.6		Adherend failed } ignored
9 weeks	17.0	17.4 ±0.3	Cohesive fail. near interface
	17.3		" " "
	17.4		" " "
	17.6		" " "
	17.9		" " "
20 weeks	15.6	17.3 ±1.0	" " "
	17.4		" " "
	17.5		" " "
	17.5		" " "
	18.4		" " "
33 weeks	17.0	17.3 ±0.5	" " "
	17.0		" " "
	17.2		" " "
	17.3		" " "
	18.2		" " "
54 weeks	16.6	17.3 ±0.5	" " "
	17.0		" " "
	17.3		" " "
	17.4		" " "
	18.1		" " "

Table 4.4.3. Durability of 5251/pre-treatment B/ESP 105 bonds in salt-spray @ 43°C.

EXPOSURE	FAILURE STRESS (MPa)	MEAN & STD. DEV. (MPa)	OBSERVATIONS
	23.7		Excess fillet, result ignored
	23.7		" " " "
0	19.6	20.1	Cohesive fail. near interface
	20.0	±0.4	" " "
	20.7		" " "
	16.8		" " "
2 weeks	17.1	18.2	" " "
	18.1	±1.5	" " "
	18.3		" " "
	20.7		" " "
	19.0		Excess fillet, result ignored
	18.3		" " " "
4 weeks	17.1	17.6	Cohesive fail. near interface
	17.8	±0.3	" " "
	18.0		" " "
	15.9		" " "
9 weeks	16.5	16.9	" " "
	16.6	±0.8	" " "
	17.0		" " "
	18.5		" " "
	15.2		" " "
	16.1		" " "
20 weeks	16.3	16.5	" " "
	16.7	±1.0	" " "
	18.0		" " "
	14.1		" " "
33 weeks	14.5	15.0	" " "
	14.8	±0.8	" " "
	15.8		" " "
	15.3		" " "
	13.4		" " "
	14.6		" " "
54 weeks	15.1	14.8	" " "
	15.2	±0.8	" " "
	15.5		" " "

Table 4.4.4. Durability of 5251/pre-treatment B/ESP 105 bonds in de-ionised water at 60°C.

EXPOSURE	FAILURE STRESS (MPa)	MEAN & STD. DEV. (MPa)	OBSERVATIONS
0	19.6	20.1 ±0.4	Cohesive fail. near interface
	20.0		" " "
	20.7		" " "
	23.7		Excess fillet, result ignored
	23.7		" " " "
2 weeks	17.5	18.7 ±1.4	Cohesive fail. near interface
	17.7		" " "
	18.5		" " "
	18.7		" " "
	21.1		" " "
4 weeks	17.1	17.7 ±0.4	" " "
	18.0		" " "
	18.1		" " "
	21.2		Excess fillet, result ignored
	21.7		" " " "
9 weeks	17.1	17.6 ±0.4	Cohesive fail. near interface
	17.4		" " "
	17.5		" " "
	18.2		" " "
20 weeks	16.7	18.8 ±2.0	" " "
	17.8		" " "
	18.0		" " "
	19.8		" " "
	21.7		" " "
33 weeks	16.9	17.4 ±0.6	" " "
	17.0		" " "
	17.2		" " "
	17.5		" " "
	18.4		" " "
54 weeks	17.5	17.8 ±0.4	" " "
	17.8		" " "
	18.2		" " "

Table 4.4.5. Durability of 5251/pre-treatment C/ESP 105 bonds in salt-spray @ 43°C.

EXPOSURE	FAILURE STRESS (MPa)	MEAN & STD. DEV. (MPa)	OBSERVATIONS
0	20.7	21.1 ± 0.3	Cohesive fail. near interface
	20.8		" " "
	21.2		" " "
	21.4		" " "
	21.5		" " "
2 weeks	16.4	16.9 ± 0.6	" " "
	16.4		" " "
	16.7		" " "
	16.8		" " "
	17.9		" " "
4 weeks	17.2	17.4 ± 0.2	" " "
	17.2		" " "
	17.3		" " "
	17.5		" " "
	17.6		" " "
9 weeks	14.5	16.5 ± 0.4	" " "
	15.8		" " "
	16.5		" " "
	16.6		" " "
	16.7		" " "
20 weeks	14.2	15.3 ± 0.8	" " "
	15.0		" " "
	15.2		" " "
	16.0		" " "
	16.3		" " "
33 weeks	13.8	14.8 ± 0.7	" " "
	14.2		" " "
	15.1		" " "
	15.2		" " "
	15.5		" " "
54 weeks	13.8	14.6 ± 0.7	" " "
	14.2		" " "
	14.4		" " "
	15.2		" " "
	15.4		" " "

Table 4.4.6. Durability of 5251/pre-treatment C/ESP 105 bonds in de-ionised water @ 60°C.

EXPOSURE	FAILURE STRESS (MPa)	MEAN & STD. DEV. (MPa)	OBSERVATIONS
0	20.7	21.1 ±0.3	Cohesive fail. near interface
	20.8		" " "
	21.2		" " "
	21.4		" " "
	21.5		" " "
2 weeks	16.9	17.7 ±0.5	" " "
	17.6		" " "
	17.9		" " "
	18.1		" " "
	18.2		" " "
4 weeks	18.0	18.1 ±0.2	" " "
	18.0		" " "
	18.0		" " "
	18.1		" " "
	18.5		" " "
9 weeks	17.1	17.8 ±0.5	" " "
	17.5		" " "
	18.0		" " "
	18.1		" " "
	18.3		" " "
20 weeks	17.0	17.2 ±0.2	" " "
	17.0		" " "
	17.1		" " "
	17.4		" " "
	17.4		" " "
33 weeks	17.0	17.7 ±0.5	" " "
	17.3		" " "
	17.8		" " "
	17.9		" " "
	18.3		" " "
54 weeks	16.9	17.5 ±0.5	" " "
	17.4		" " "
	17.5		" " "
	17.9		" " "
	18.0		" " "

Table 4.4.7. Durability of 5251/pre-treatment D/ESP 105 bonds in salt-spray @ 43°C.

EXPOSURE	FAILURE STRESS (MPa)	MEAN & STD. DEV. (MPa)	OBSERVATIONS
0	20.4	20.9 ±0.4	Cohesive fail. near interface
	20.5		" " "
	21.1		" " "
	21.1		" " "
	21.5		" " "
3 weeks	16.9	17.4 ±0.4	" " "
	17.0		" " "
	17.2		" " "
	17.9		" " "
	18.0		" " "
4 weeks	16.6	17.4 ±0.5	" " "
	17.0		" " "
	17.3		" " "
	17.8		" " "
	18.0		" " "
8 weeks	16.5	16.9 ±0.2	" " "
	16.7		" " "
	16.9		" " "
	17.0		" " "
	17.3		" " "
14 weeks	13.1	14.9 ±1.2	" " "
	14.4		" " "
	15.3		" " "
	15.4		" " "
	16.3		" " "
27 weeks	11.9	13.2 ±1.3	" " "
	12.1		" " "
	13.0		" " "
	14.4		" " "
	14.8		" " "
48 weeks	11.9	12.5 ±0.7	" " "
	11.9		" " "
	12.5		" " "
	12.7		" " "
	13.5		" " "

Table 4.4.8. Durability of 5251/pre-treatment E/ESP 105 bonds in salt-spray @ 43°C.

EXPOSURE	FAILURE STRESS (MPa)	MEAN & STD. DEV. (MPa)	OBSERVATIONS
0	20.3	21.0 ± 0.6	Cohesive fail. near interface
	20.5		" " "
	20.7		" " "
	21.1		" " "
	22.3		" " "
3 weeks	16.1	17.6 ± 0.7	" " "
	17.4		" " "
	17.9		" " "
	18.0		" " "
	18.4		" " "
4 weeks	17.4	17.9 ± 0.4	" " "
	17.5		" " "
	18.0		" " "
	18.1		" " "
	18.6		" " "
8 weeks	16.0	16.9 ± 0.5	" " "
	16.6		" " "
	17.2		" " "
	17.3		" " "
	17.4		" " "
14 weeks	13.0	15.1 ± 1.3	" " "
	15.1		" " "
	15.4		" " "
	16.0		" " "
	16.1		" " "
27 weeks	10.9	13.1 ± 1.5	" " "
	12.8		" " "
	13.6		" " "
	13.6		" " "
	14.8		" " "
48 weeks	12.0	13.2 ± 0.9	" " "
	12.9		" " "
	13.5		" " "
	13.6		" " "
	14.2		" " "

Table 4.4.9. Durability of 5251/pre-treatment F/ESP 105 bonds in salt-spray at 43°C.

EXPOSURE	FAILURE STRESS (MPa)	MEAN & STD. DEV. (MPa)	OBSERVATIONS
0	20.3	21.0 ± 0.5	Cohesive fail. near interface
	20.5		" " "
	21.0		" " "
	21.2		" " "
	21.8		" " "
2 weeks	17.9	18.4 ± 0.4	" " "
	18.1		" " "
	18.2		" " "
	18.9		" " "
	19.1		" " "
4 weeks	17.3	17.9 ± 0.3	" " "
	17.7		" " "
	18.0		" " "
	18.1		" " "
	18.3		" " "
8 weeks	18.0	18.4 ± 0.2	" " "
	18.2		" " "
	18.4		" " "
	18.5		" " "
	18.7		" " "
13 weeks	16.0	16.4 ± 0.4	" " "
	16.3		" " "
	16.3		" " "
	16.4		" " "
	17.1		" " "
26 weeks	14.3	15.6 ± 0.8	" " "
	15.5		" " "
	15.6		" " "
	16.2		" " "
	16.4		" " "
48 weeks	13.0	15.2 ±1.3	" " "
	15.4		" " "
	15.6		" " "
	15.9		" " "
	16.1		" " "

Table 4.4.10. Durability of 5251/pre-treatment F/WP9 bonds in salt-spray @ 43°C.

EXPOSURE	FAILURE STRESS (MPa)	MEAN & STD. DEV. (MPa)	OBSERVATIONS
0	28.0	28.5 ±0.3	Cohesive fail. near interface
	28.5		" " "
	28.5		" " "
	28.6		" " "
	29.0		" " "
2 weeks	26.6	26.9 ±0.2	" " "
	27.0		" " "
	27.0		" " "
	27.0		" " "
	27.1		" " "
4 weeks	24.2	25.0 ±0.5	" " "
	24.6		" " "
	25.5		" " "
	25.5		" " "
	22.4		Starved joint result ignored
8 weeks	21.5	25.2 ±0.6	" " " "
	24.3		Cohesive fail. near interface
	25.0		" " "
	25.6		" " "
	26.0		" " "
12 weeks	20.8	21.5 ±0.6	" " "
	21.2		" " "
	21.4		" " "
	22.1		" " "
	22.3		" " "
25 weeks	16.2	18.6 ±1.9	" " "
	17.9		" " "
	18.4		" " "
	19.6		" " "
	21.1		" " "
48 weeks	19.7	20.6 ±0.7	" " "
	20.4		" " "
	20.5		" " "
	20.9		" " "
	21.7		" " "

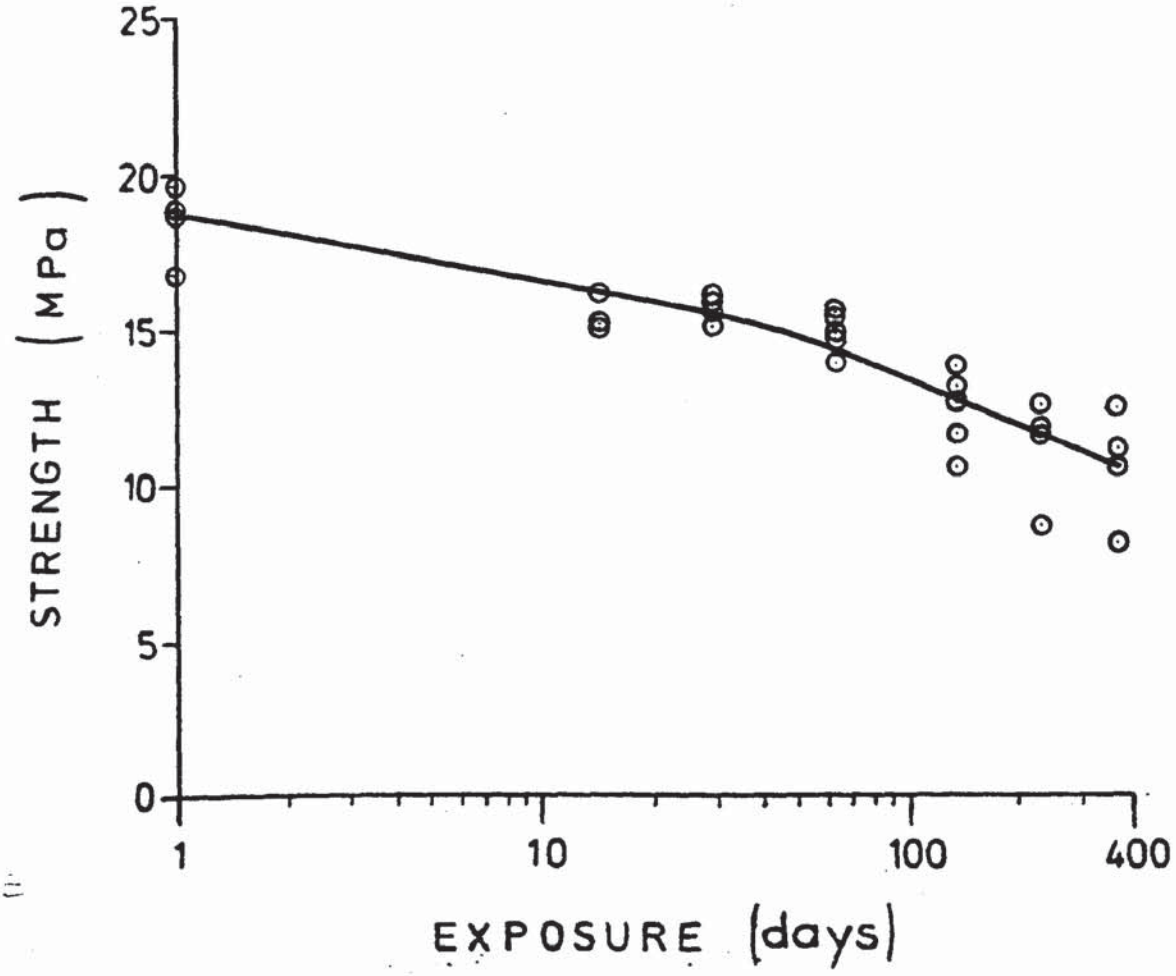

Fig. 4.4.1. Durability of 5251/pre-treatment A/ESP 105 bonds in salt-spray at 43°C.

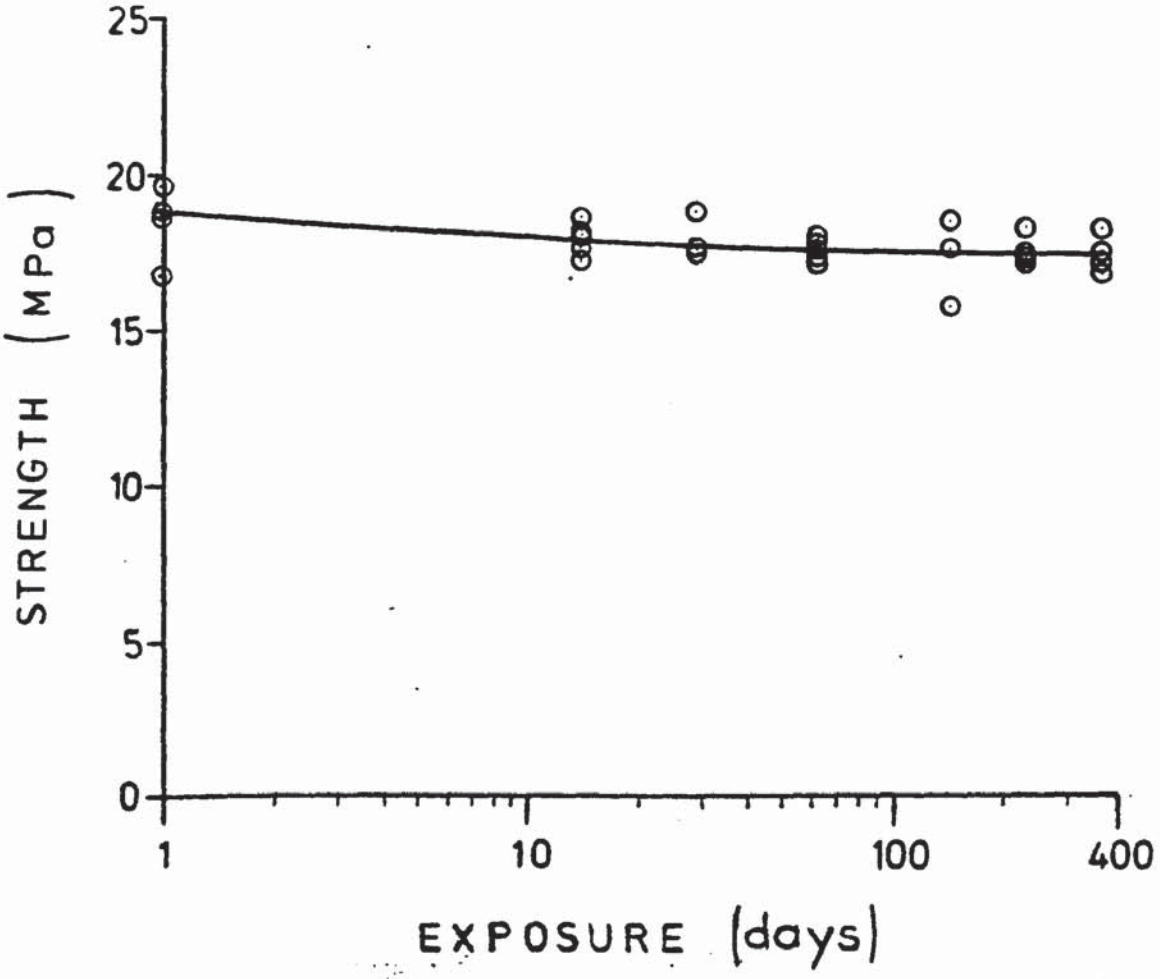

Fig. 4.4.2. Durability of 5251/pre-treatment A/ESP 105 bonds in de-ionised water @ 60°C.

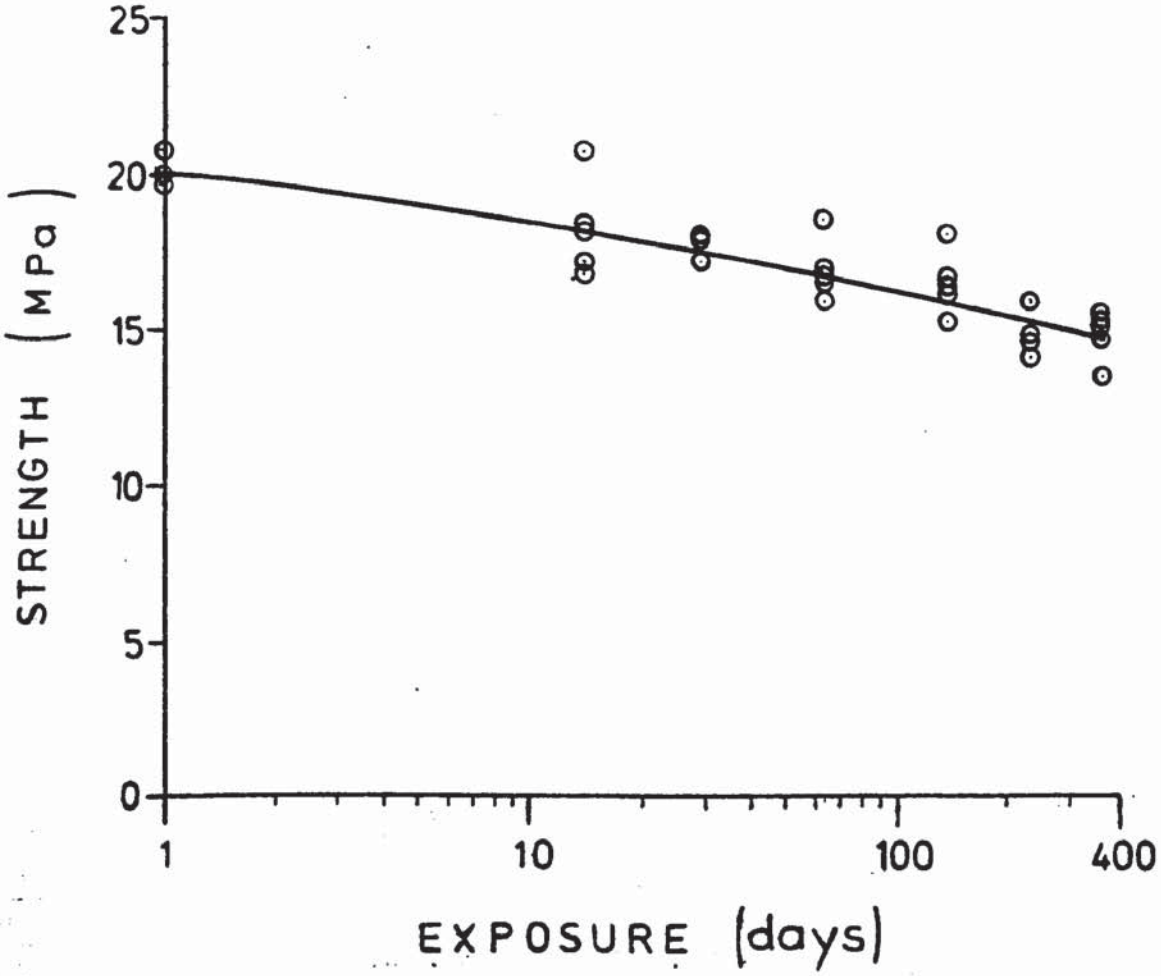

Fig. 4.4.3. Durability of 5251/pre-treatment B/ESP 105 bonds in salt-spray at 43°C.

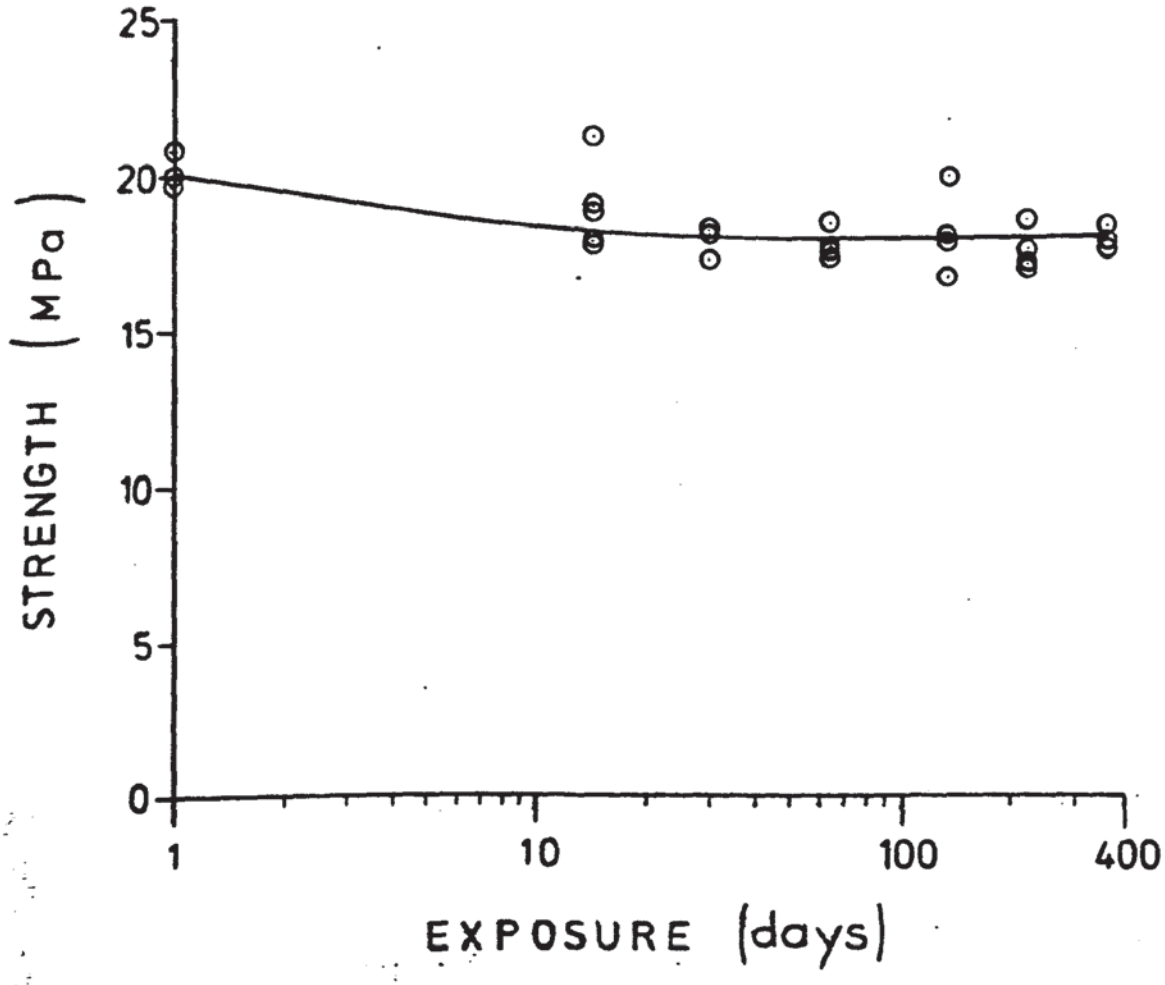

Fig. 4.4.4. Durability of 5251/pre-treatment B/ESP 105 bonds in de-ionised water @ 60°C.

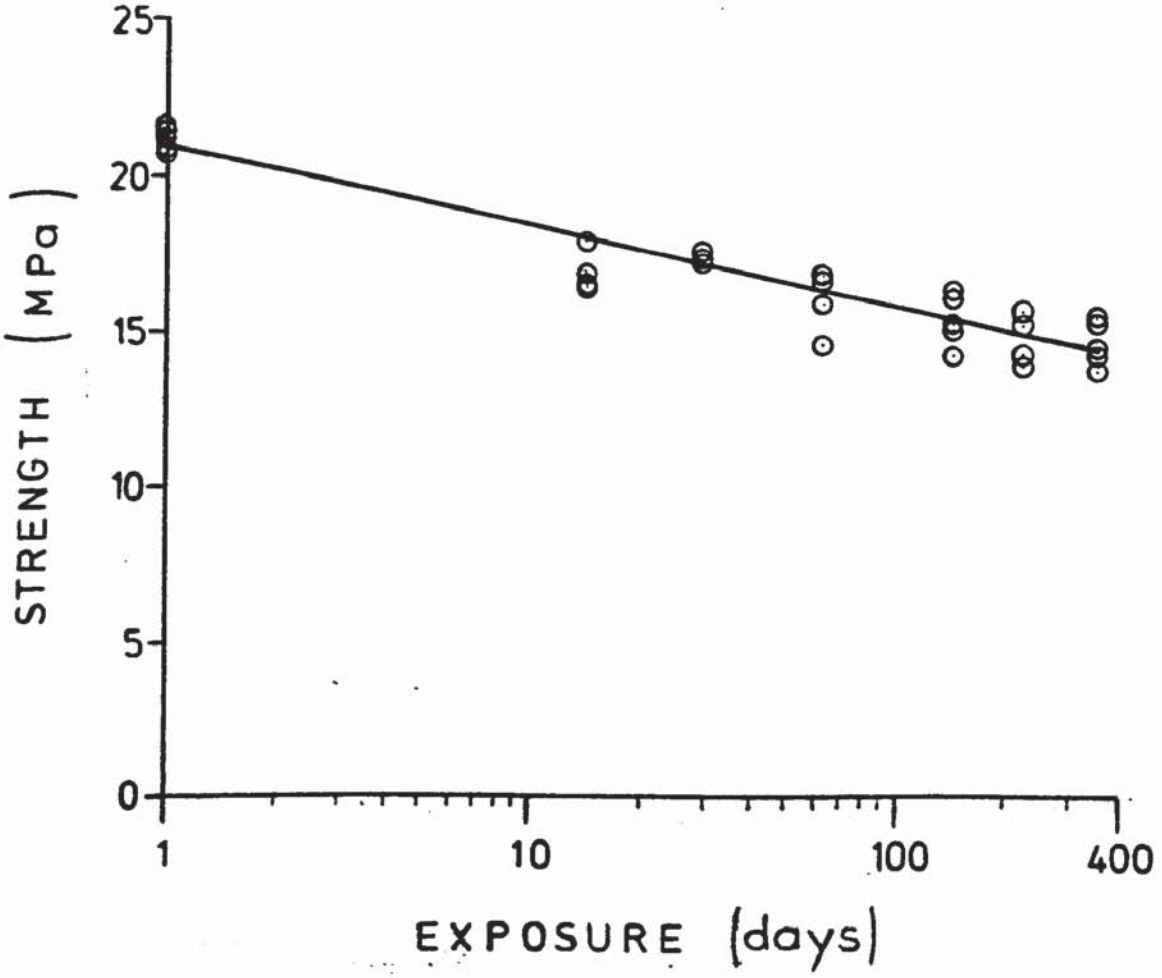

Fig. 4.4.5. Durability of 5251/pre-treatment C/ESP 105 bonds in salt-spray @ 43°C.

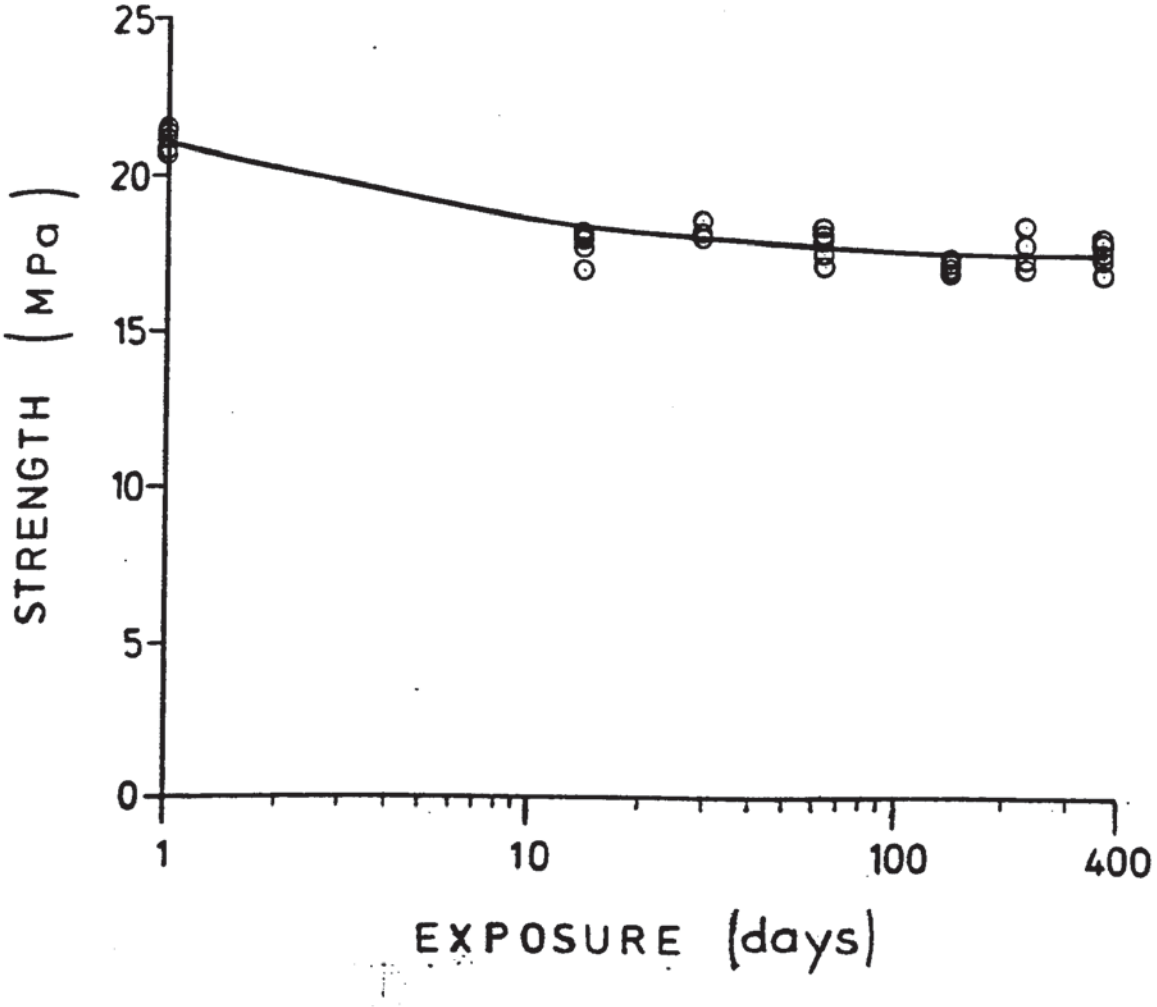

Fig. 4.4.6. Durability of 5251/pre-treatment C/ESP 105 bonds in de-ionised water @ 60°C.

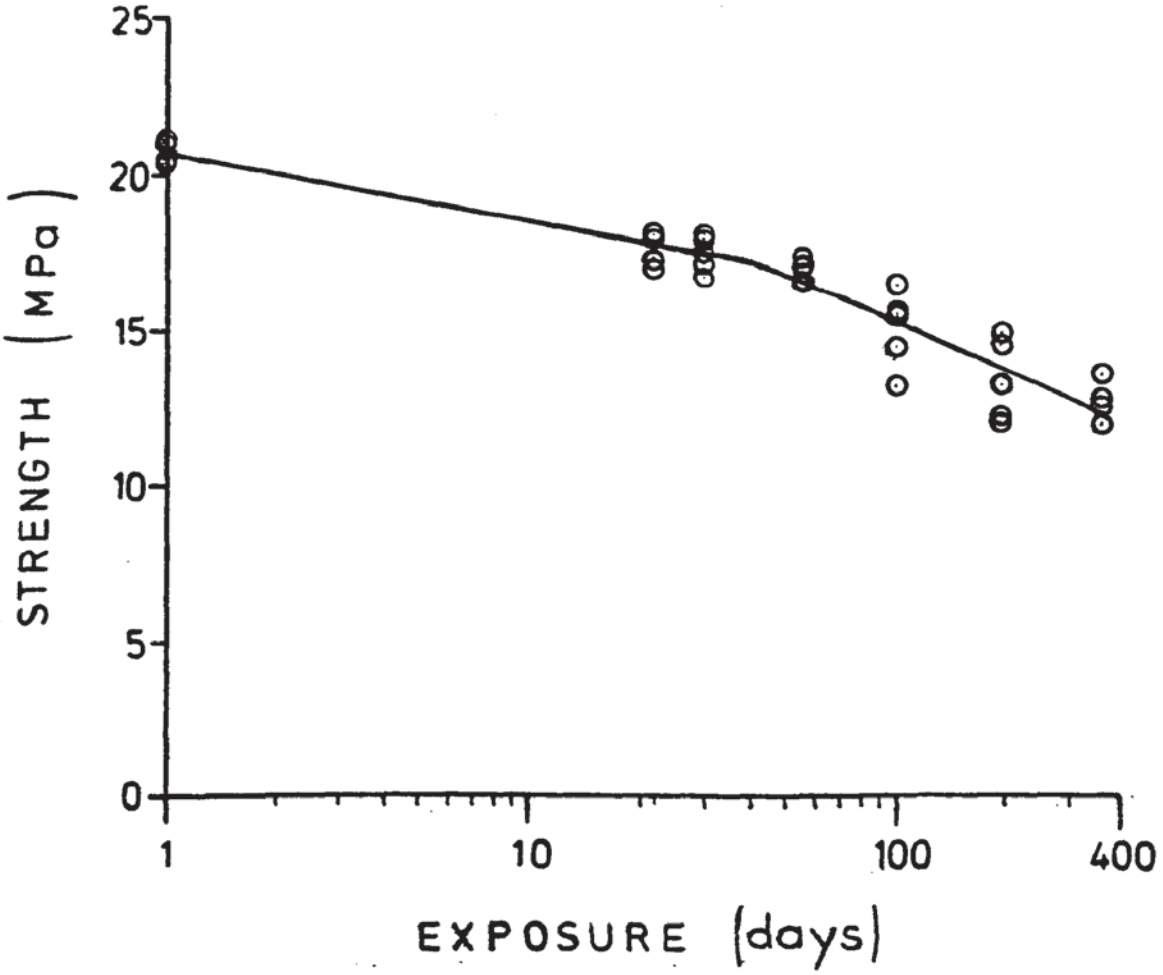

Fig. 4.4.7. Durability of 5251/pre-treatment D/ESP 105 bonds in salt-spray @ 43°C.

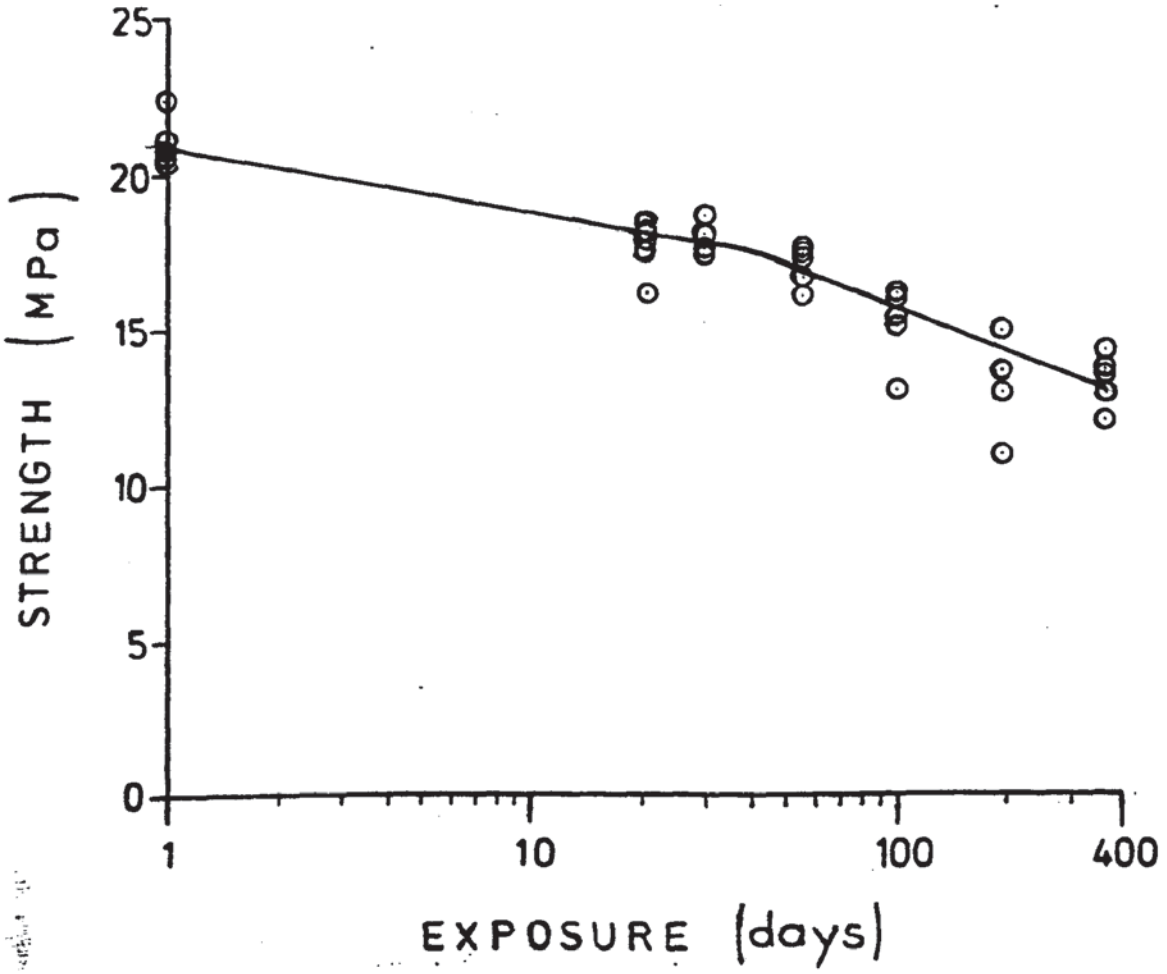

Fig. 4.4.8. Durability of 5251/pre-treatment E/ESP 105 bonds in salt-spray @ 43°C.

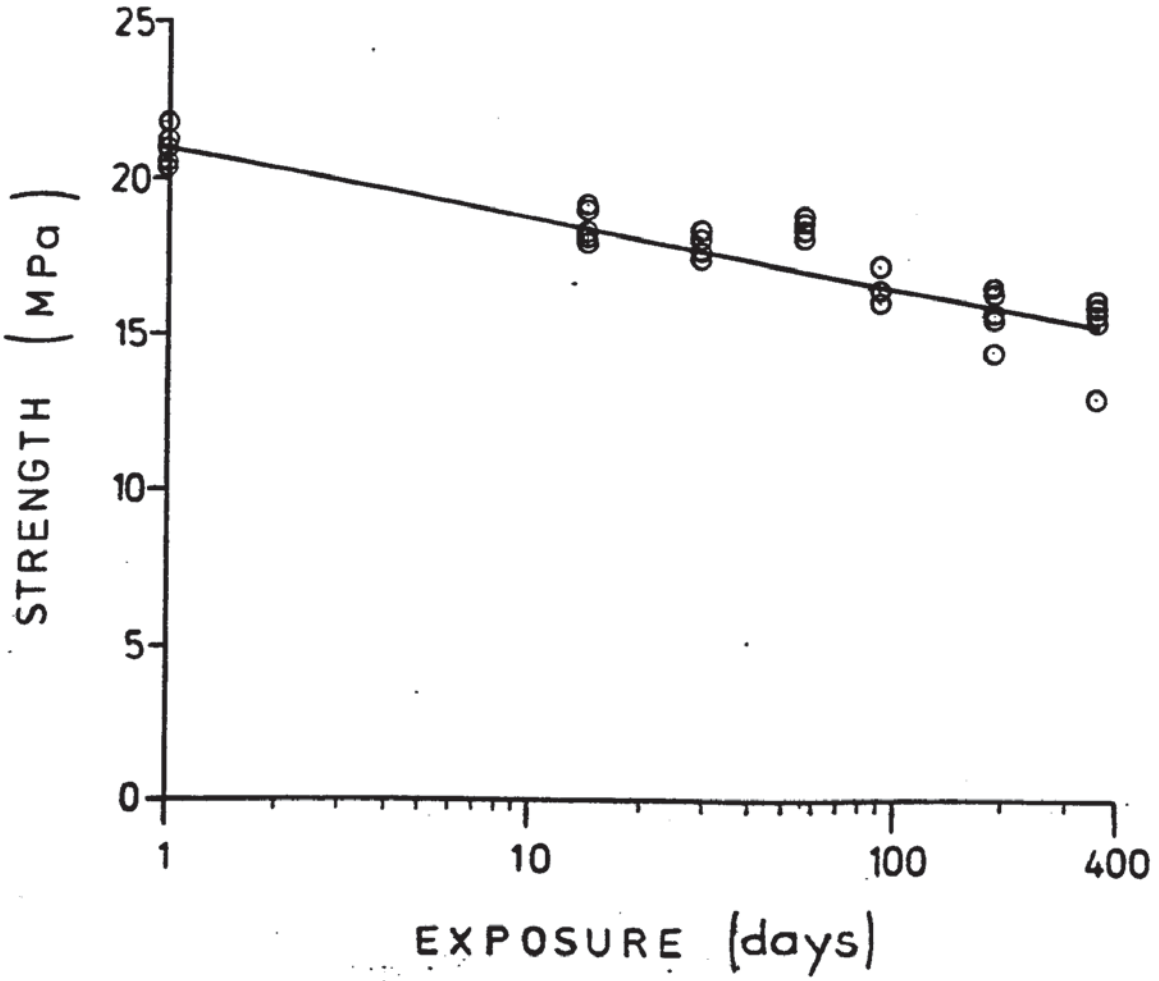

Fig. 4.4.9. Durability of 5251/pre-treatment F/ESP 105 bonds in salt-spray @ 43°C.

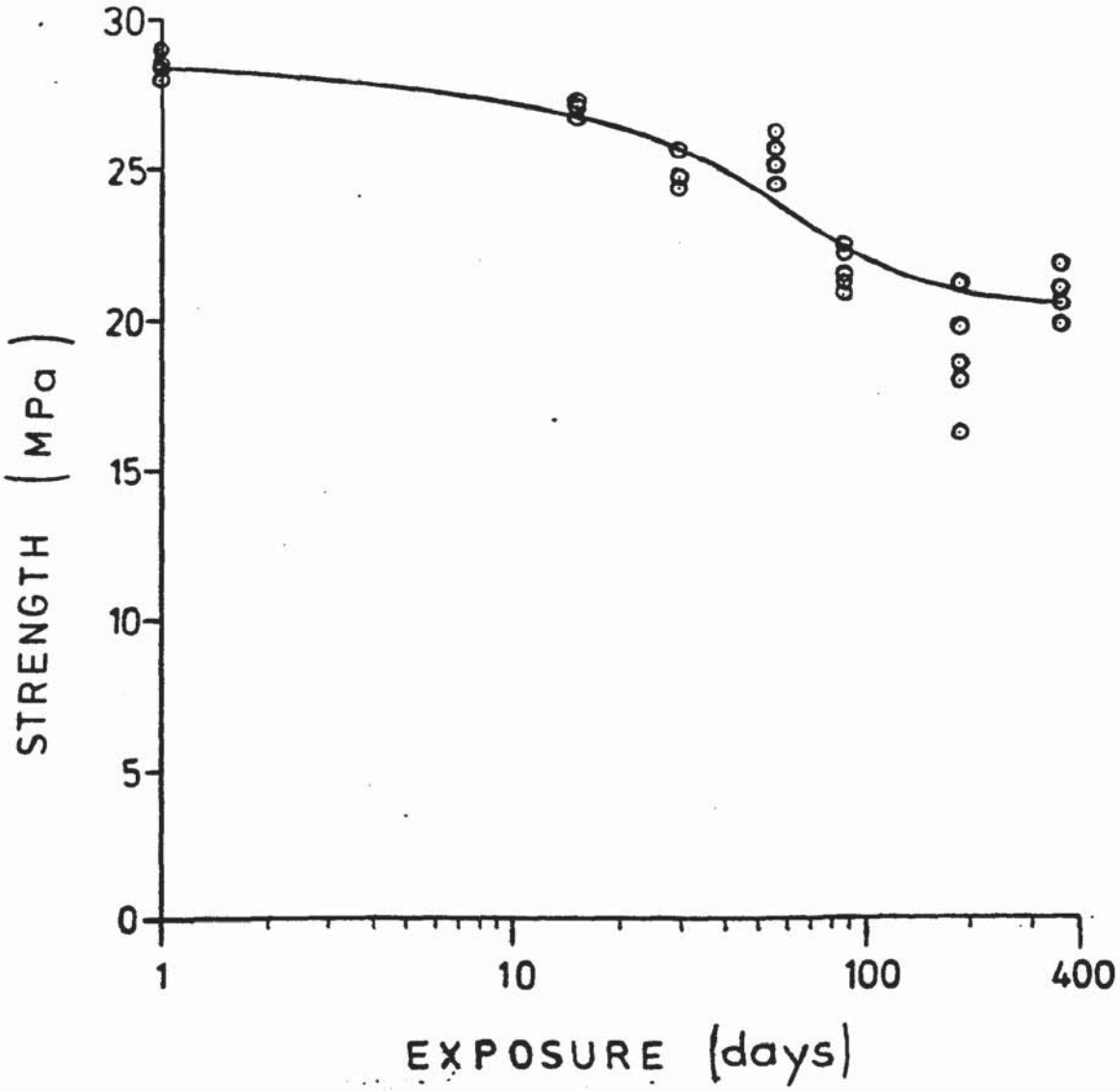

Fig. 4.4.10. Durability of 5251/pre-treatment F/WP9 bonds in salt-spray @ 43°C.

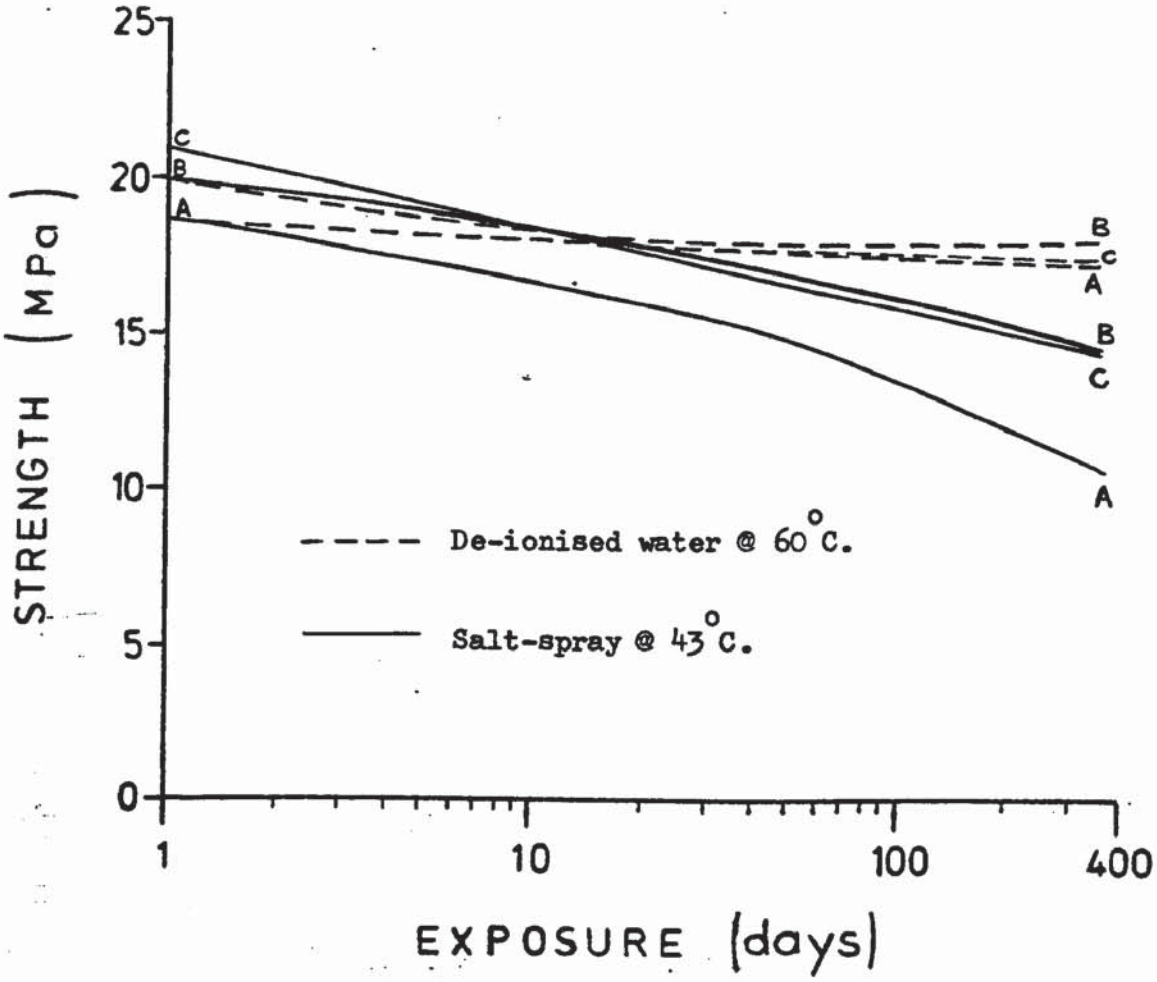

Fig. 4.4.11. Comparison control pre-treatments A.B. and C. in salt-spray and liquid water environments.

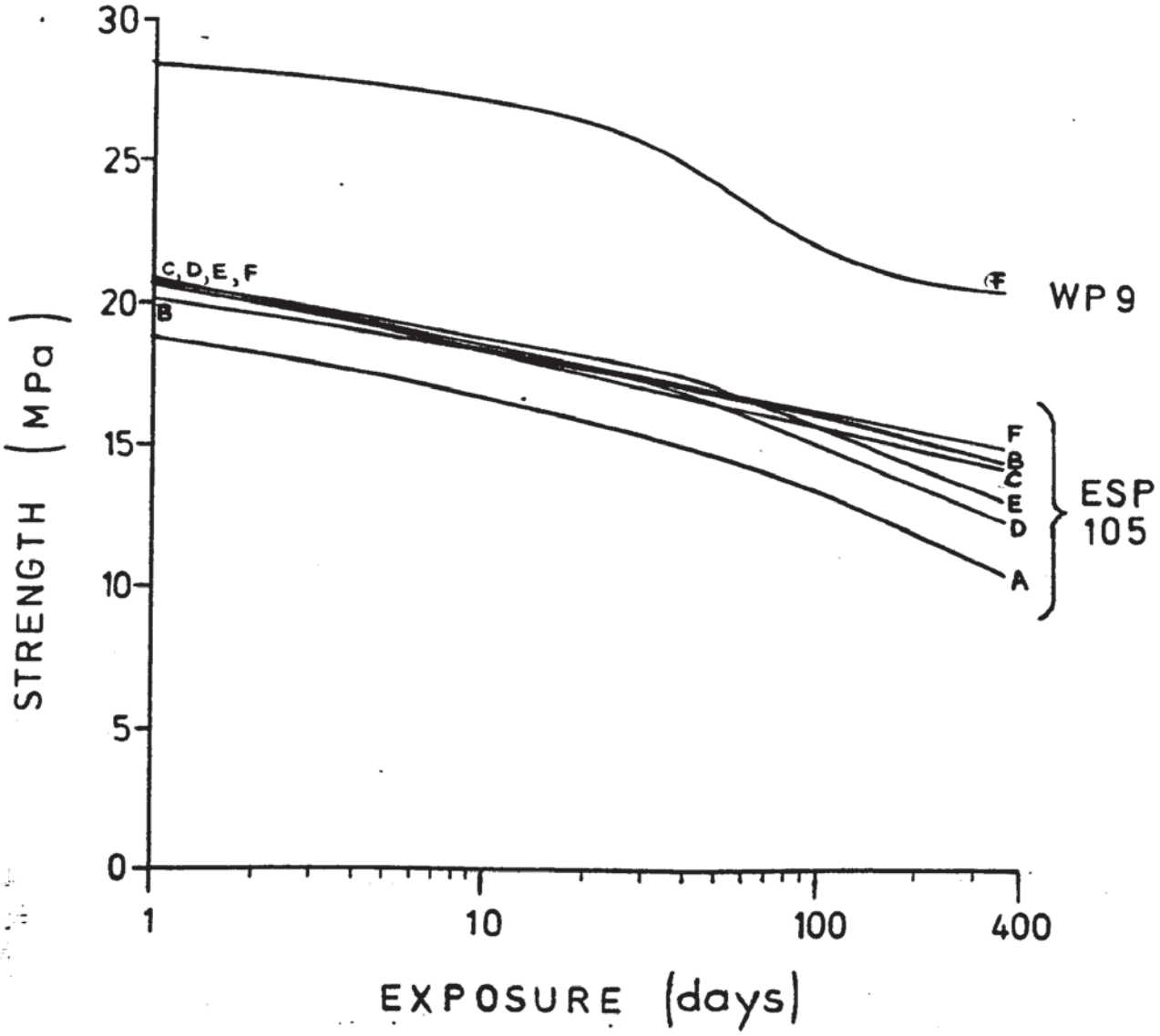

Fig. 4.4.12. Comparison of durability of pretreatments A to F in salt-spray @ 43°C.

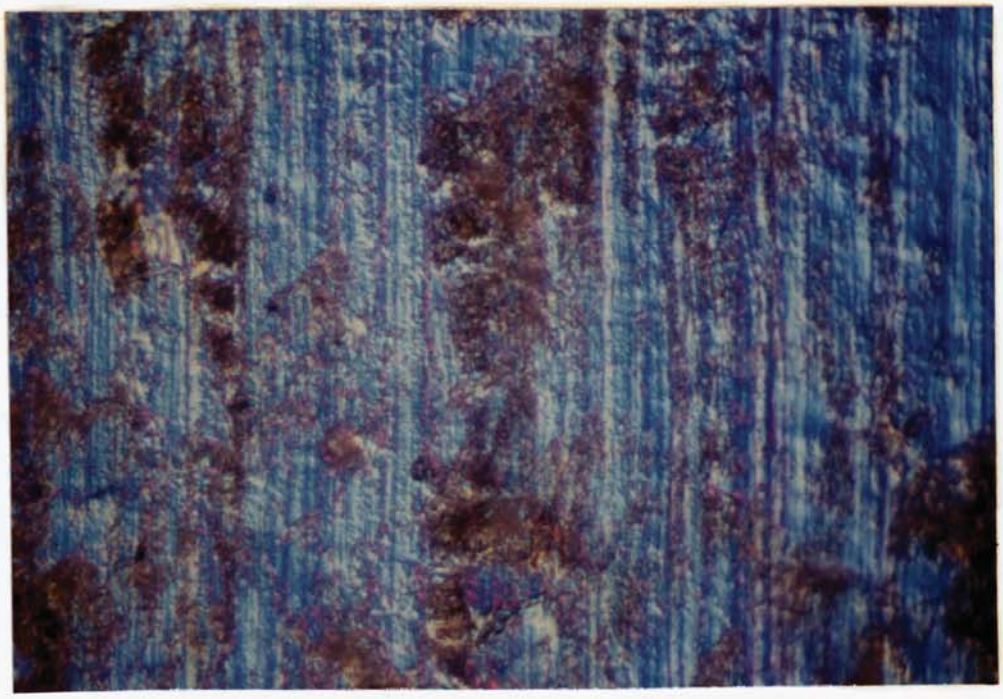

Fig. 4.4.13. Fracture surface of unexposed 5251/deoxidised/ ESP 105 adhesive bond.
(differential interference phase contrast)

1 µm

Fig. 4.4.14. Fracture surface of unexposed 5251/opt.FPL + 20 min PAA/ESP 105 adhesive bond
(differential interference phase contrast)

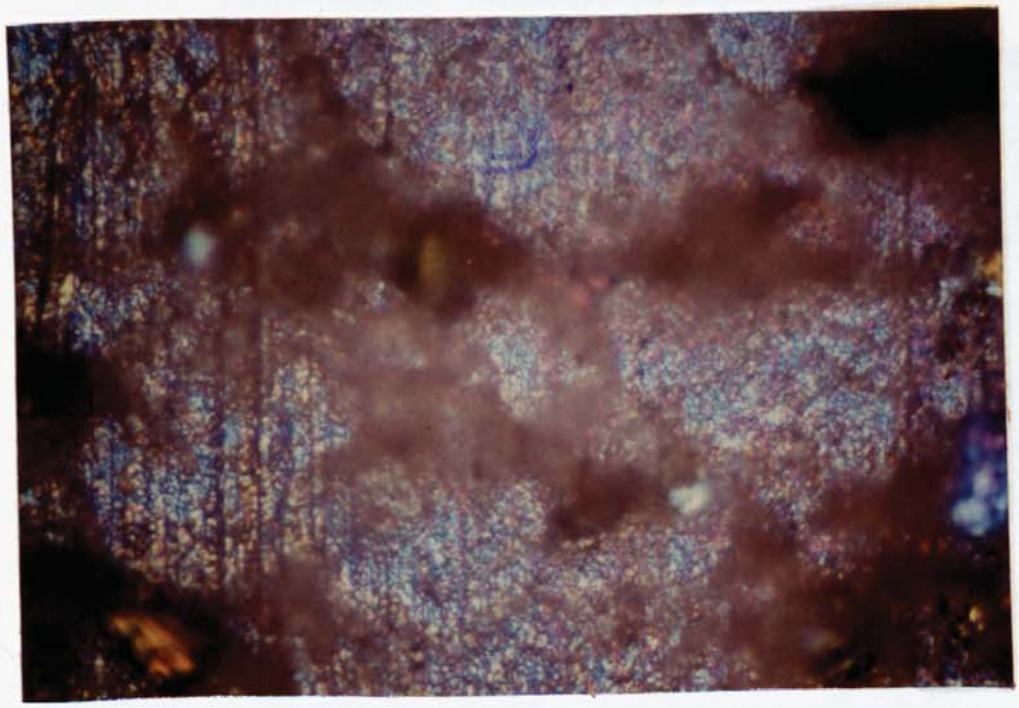

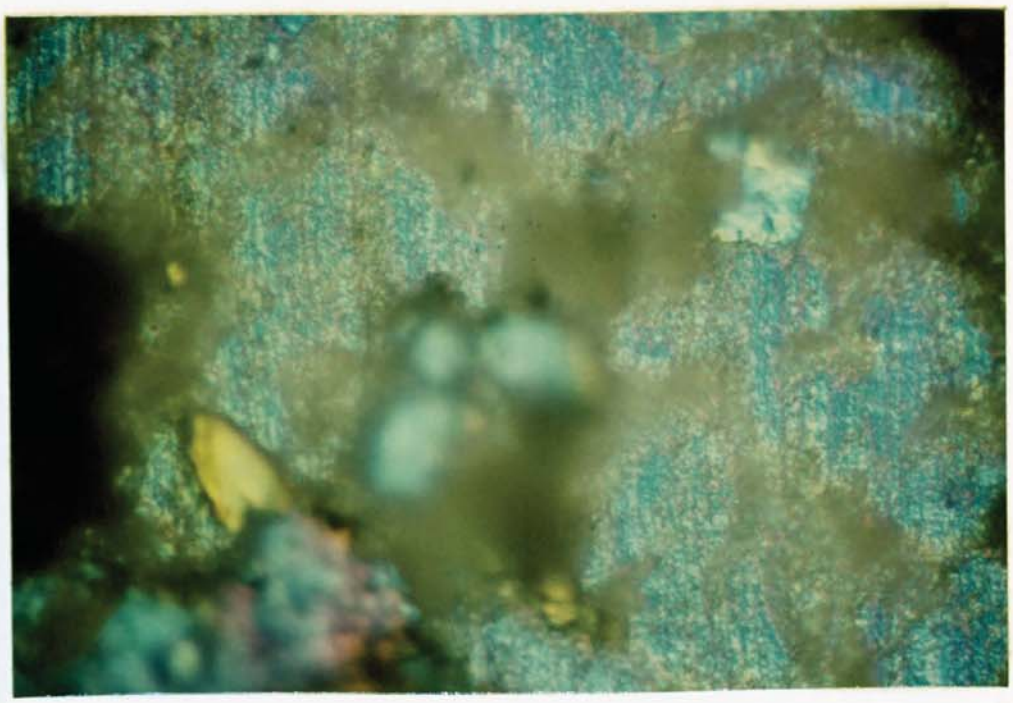

Fig. 4.4.15. Fracture surface of unexposed 5251/deox + 20 min DC PAA/ESP 105 adhesive bond.
(differential interference phase contrast)

1 µm

Fig. 4.4.16. Fracture surface of unexposed 5251/deox + 2 min AC PAA/ESP 105 adhesive bond.
(differential interference phase contrast)

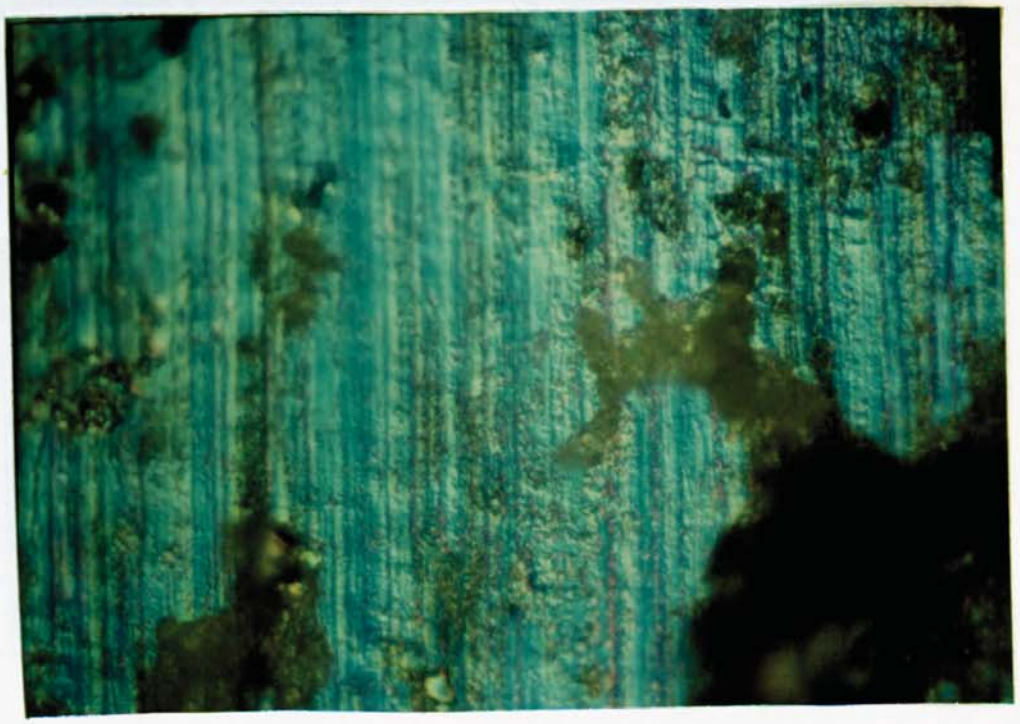

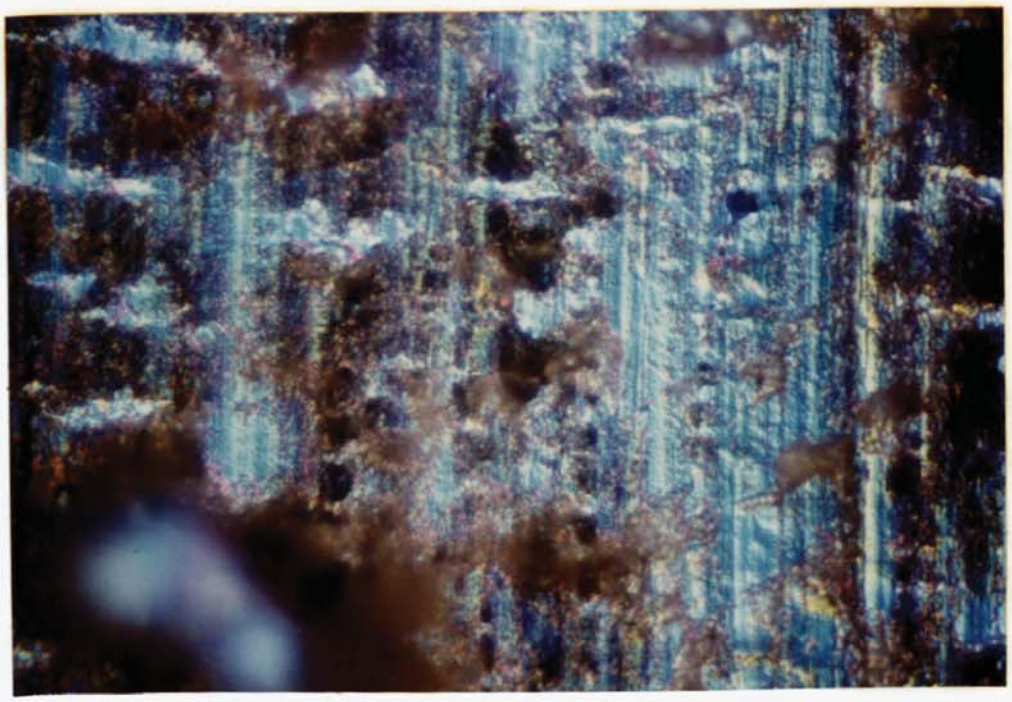

Fig. 4.4.17. Fracture surface of 5251/deox. + 10 sec. AC H_2SO_4 anodise/ESP 105 adhesive bond. (differential interference phase contrast)

1μm

Fig. 4.4.18. Fracture surface of 5251/deox. + 10 sec. AC H_2SO_4 anodise/WP 9 adhesive bond. (differential interference phase contast)

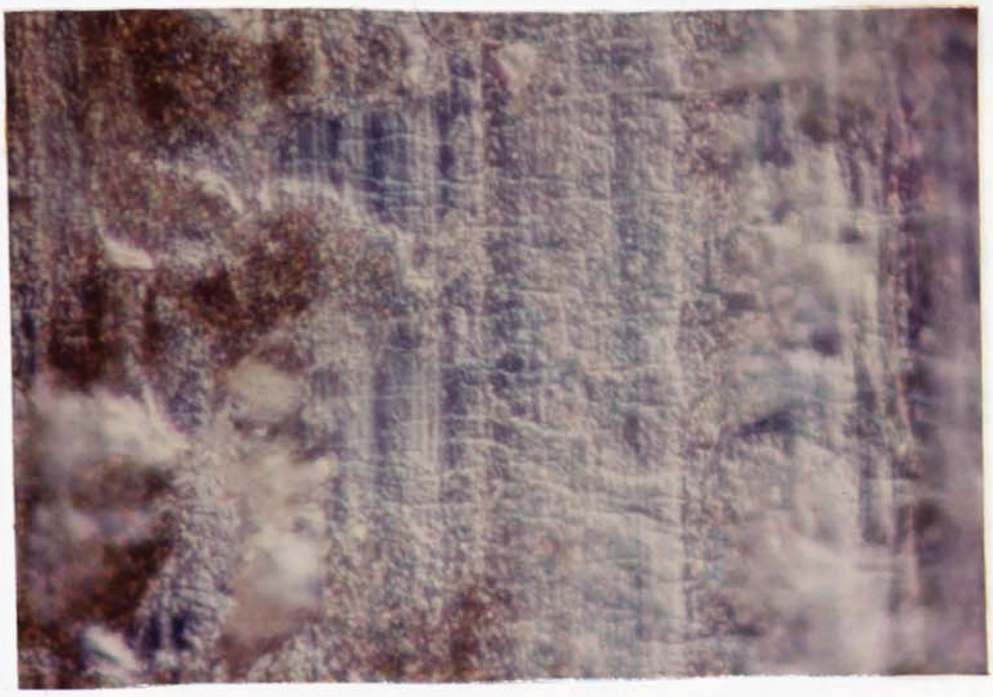

4.5 Modification of lap shear joint

The generation of the results previously obtained required undesirably long periods of environmental exposure. More severe, less realistic environments, whilst reducing test time, may promote failure modes which would not predominate under service conditions.

A major consideration was therefore the role of water diffusion and the influence of bond geometry on the rate of strength loss, whether adhesive or pretreatment dependent. The existing 20mm x 10mm bond area is considerably smaller than that generally employed elsewhere. (The traditional 1" wide x $\frac{1}{2}$" overlap shear joint continues to be widely used by both the manufacturers and consumers of structural adhesives). A simple reduction in bond overlap would reduce diffusion paths, but at the expense of initial strength and sensitivity. The stress distribution in the overlap of a single lap joint has been discussed in Chapter 2. The central region of the 10mm overlap joint used in this project is relatively unstressed, as suggested by an exercise carried out using photoelastic techniques. Some of the results are shown in Fig. 4.5.1.

The model joint used did not fail "instantaneously", and it was just possible to photograph the progress of bond failure during which the transfer of stress to the central regions can be clearly observed. The removal of material from the centre of metal-metal test joints in order to reduce diffusion paths was therefore considered.

The ideal rectangular aperture presents severe machining difficulties. The compromise solution, seen in Fig. 3.11., requires the drilling of three 4mm diameter holes across the width of the specimen on the centre line of the bond area.

Fig. 4.5.1 (a) 1.71 MPa

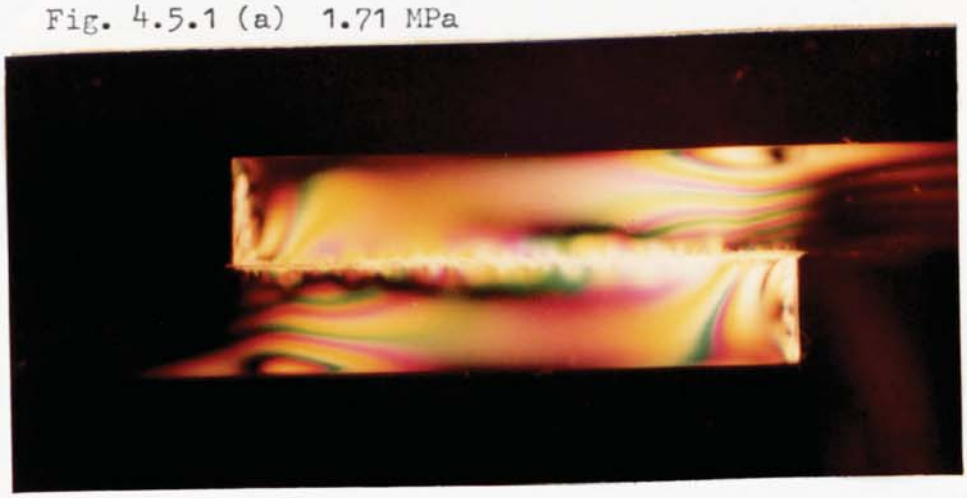

Fig. 4.5.1 (b) 2.13 MPa (peak stress, initiation of failure)

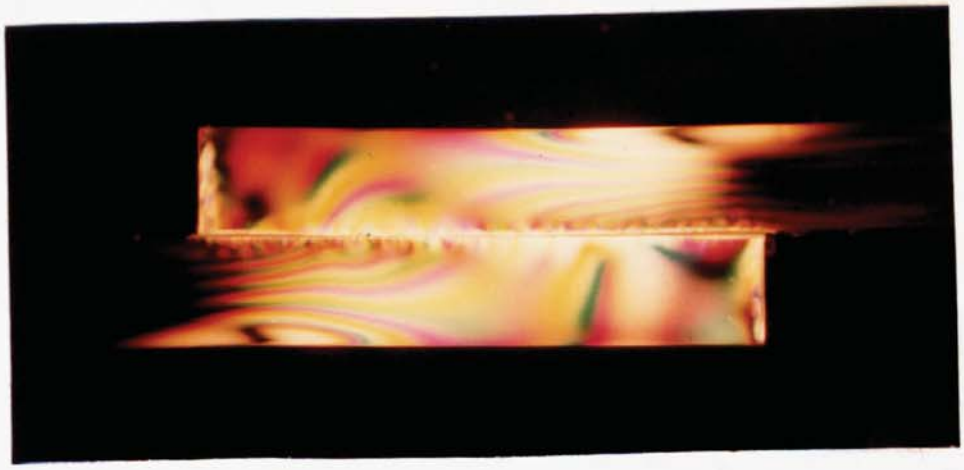

Fig. 4.5.1 (c) Failure in progress

Fig. 4.5.1. Stress distribution in lap joint.

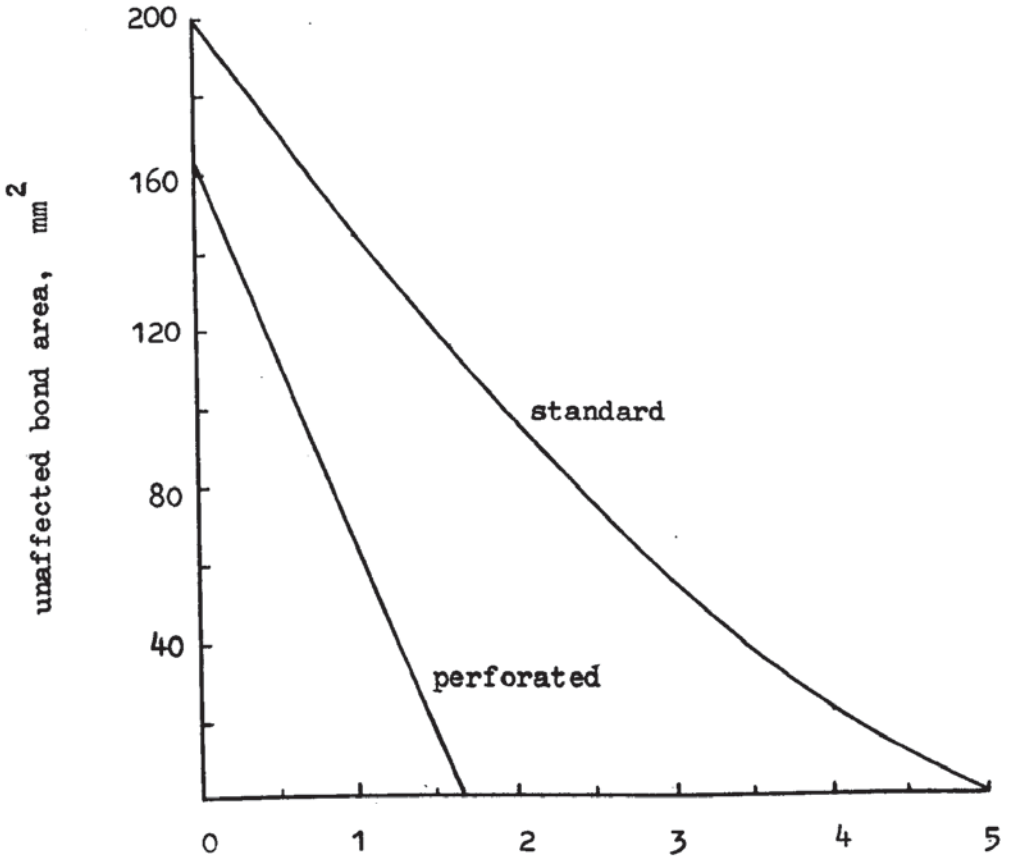

Fig. 4.5.2 Comparison of standard and perforated configurations.

The bond area is reduced from 200mm to 162mm, but the bond perimeter is increased from 60 to 98mm, i.e. the perimeter : area ratio has been doubled. The maximum diffusion path of 5mm is reduced effectively to 1.5mm. Fig. 4.5.2 compares the standard and perforated configurations in terms of the approximate area of bond remaining completely unaffected and the distance advanced by the diffusion front. In order to compare these configurations bonded joints based on BA 2117 alloy and EC 2214 adhesive were prepared. The following pretreatments were selected to provide a wide range of performances under salt-spray conditions.

1. Phosphoric acid anodising to BAC 5555 specification.
2. Optimised F.P.L. etch.
3. Optimised F.P.L. etch followed by a 2 minute anodise in phosphoric acid (as in Section 4.3).
4. Deoxidise, 3 minutes @ room temperature in proprietary I.C.I. solution.

In each case, specimens were randomised and half were perforated using a drilling jig which had been designed for this purpose and illustrated in Fig. 3.

The results of salt-spray exposure are given in Tables 4.5.1 to 4.5.8. In every case, no significant difference between the failure loads of perforated and standard specimens was observed. The mean stresses quoted for the perforated configuration have been calculated on the basis of the measured failure load and a nominal bond area of 200mm rather than the actual value of 162mm , facilitating the easier assessment of the effects of the holes on joint strength.

All perforated joints lost strength more rapidly than the standard form during environmental exposure.

Results for the phosphoric acid anodised specimens are compared in Fig. 4.5.5. All failures were cohesive,close to the interface, and after the 8 week exposure period the strength of perforated joints was reduced to 58% of the initial value, compared with 88% for the standard configuration. The standard specimens of all pretreatments exhibited cohesive failure close to the interface throughout the total exposure period. With the exception of those associated with the BAC 5555 pretreatment, however, bond line corrosion was encountered in all perforated joints. This was first detected after 4 weeks exposure and varied considerably in severity, giving rise to large coefficients of variation.

Whilst bond line corrosion effects prevented meaningful comparisons being made between these three particular treatments, a considerable acceleration in bond strength loss has been achieved without resorting to unrealistically severe environmental conditions.

Table 4.5.1. Durability of 2117/BAC 5555/2214 adhesive bonds in salt-spray @ 43°C. measured using standard lap shear joints.

EXPOSURE	FAILURE STRESS (MPa)	MEAN & STD. DEV. (MPa)	OBSERVATIONS
0	17.8	18.6 ±0.8	Cohesive fail. near interface
	18.1		" " " "
	18.2		" " " "
	19.4		" " " "
	19.4		" " " "
1 week	17.5	18.1 ±0.7	" " " "
	17.6		" " " "
	18.0		" " " "
	18.2		" " " "
	19.3		" " " "
2 weeks	17.0	17.9 ±0.9	" " " "
	17.1		" " " "
	18.1		" " " "
	18.4		" " " "
	19.1		" " " "
4 weeks	17.0	17.3 ±0.3	" " " "
	17.1		" " " "
	17.4		" " " "
	17.5		" " " "
	17.7		" " " "
6 weeks	16.4	16.9 ±0.4	" " " "
	16.7		" " " "
	16.8		" " " "
	17.1		" " " "
	17.5		" " " "
8 weeks	15.5	16.4 ±1.0	" " " "
	15.9		" " " "
	15.9		" " " "
	17.1		" " " "
	17.7		" " " "

Table 4.5.2. Durability of 2117/BAC 5555/2214 adhesive bonds in salt-spray @ 43°C. measured using perforated lap shear joints.

EXPOSURE	FAILURE STRESS (MPa)	MEAN & STD. DEV. (MPa)	OBSERVATIONS
0	17.0 17.8 17.8 18.2 19.7	18.1 ±1.0	Cohesive fail. near interface " " " " " " " " " " " " " " " "
1 week	15.5 16.1 16.2 16.6 17.0	16.3 ±0.6	" " " " " " " " " " " " " " " " " " " "
2 weeks	14.0 14.0 14.8 15.4 15.6	14.8 ±0.8	" " " " " " " " " " " " " " " " " " " "
4 weeks	12.9 12.9 13.4 13.4 14.5	13.4 ±0.7	" " " " " " " " " " " " " " " " " " " "
6 weeks	13.4 13.5 13.5 13.6 14.0	13.6 ±0.2	" " " " " " " " " " " " " " " " " " " "
8 weeks	9.6 10.2 10.2 10.5 11.9	10.5 ±0.9	" " " " " " " " " " " " " " " " " " " "

Table 4.5.3. Durability of 2117/FPL etched /2214 adhesive bonds in salt-spray @ 43°C. measured using standard lap shear joints.

EXPOSURE	FAILURE STRESS (MPa)	MEAN & STD. DEV. (MPa)	OBSERVATIONS
0	17.1	18.0 ±0.5	Cohesive fail. near interface
	18.1		" " " "
	18.2		" " " "
	18.3		" " " "
	18.4		" " " "
1 week	16.1	16.5 ±0.3	" " " "
	16.3		" " " "
	16.7		" " " "
	16.8		" " " "
	16.8		" " " "
2 weeks	15.1	16.7 ±1.2	" " " "
	16.2		" " " "
	16.8		" " " "
	17.0		" " " "
	18.2		" " " "
4 weeks	16.5	17.0 ±0.3	" " " "
	16.9		" " " "
	17.0		" " " "
	17.2		" " " "
	17.3		" " " "
6 weeks	16.0	16.3 ±0.3	" " " "
	16.2		" " " "
	16.3		" " " "
	16.6		" " " "
	16.7		" " " "
8 weeks	16.2	17.2 ±0.9	" " " "
	16.5		" " " "
	17.1		" " " "
	18.0		" " " "
	18.1		" " " "

Table 4.5.4. Durability of 2117/FPL etched/2214 adhesive bonds in salt-spray at 43°C., measured using perforated lap shear joints.

EXPOSURE	FAILURE STRESS (MPa)	MEAN & STD. DEV. (MPa)	OBSERVATIONS
0	17.8	18.2 ±0.4	Cohesive fail. near interface
	17.9		" " " "
	17.9		" " " "
	18.5		" " " "
	18.7		" " " "
1 week	15.5	16.0 ±0.4	" " " "
	15.8		" " " "
	15.9		" " " "
	16.0		" " " "
	16.5		" " " "
2 weeks	13.1	14.5 ±1.0	" " " "
	14.1		" " " "
	14.4		" " " "
	15.0		" " " "
	15.7		" " " "
4 weeks	5.3	11.2 ±3.4	Severe bond line corrosion
	11.9		Apparent interfacial failure
	12.3		" " "
	12.8		" " "
	13.8		" " "
6 weeks	2.9	4.4 ±1.5	Bond line corrosion
	3.2		" " "
	4.0		" " "
	5.2		" " "
	6.5		" " "
8 weeks	0	1.7 ±1.0	" " "
	1.9		" " "
	2.0		" " "
	2.0		" " "
	2.7		" " "

Table 4.5.5. Durability of 2117/2 min PAA/2214 adhesive bonds in salt spray at 43°C. measured using standard lap shear joints.

EXPOSURE	FAILURE STRESS (MPa)	MEAN & STD. DEV. (MPa)	OBSERVATIONS
0	16.8	17.4 ± 0.7	Cohesive fail. near interface
	17.0		" " " "
	17.1		" " " "
	17.6		" " " "
	18.6		" " " "
1 week	14.0	14.7 ± 0.5	" " " "
	14.3		" " " "
	15.0		" " " "
	15.0		" " " "
	15.2		" " " "
2 weeks	14.1	14.4 ± 0.4	" " " "
	14.1		" " " "
	14.2		" " " "
	14.5		" " " "
	15.1		" " " "
4 weeks	13.3	13.7 ± 0.3	" " " "
	13.5		" " " "
	13.5		" " " "
	14.0		" " " "
	14.0		" " " "
6 weeks	13.1	13.8 ± 0.4	" " " "
	13.7		" " " "
	13.9		" " " "
	14.0		" " " "
	14.1		" " " "
8 weeks	12.1	12.8 ± 1.1	" " " "
	12.1		" " " "
	12.2		" " " "
	12.7		" " " "
	14.7		" " " "

Table 4.5.6 Durability of 2117/2min PAA/2214 adhesive bonds in salt spray @ 43°C. measured using perforated lap shear joints.

EXPOSURE	FAILURE STRESS (MPa)	MEAN & STD. DEV. (MPa)	OBSERVATIONS
	15.6		Cohesive fail. near interface
	15.7		" " " "
0	17.3	16.8	" " " "
	17.5	±1.0	" " " "
	17.8		" " " "
	11.7		" " " "
	11.8		" " " "
1 week	11.9	12.3	" " " "
	13.0	±0.7	" " " "
	13.1		" " " "
	9.2		" " " "
	10.3		" " " "
2 weeks	11.0	11.0	" " " "
	12.0	±1.3	" " " "
	12.5		" " " "
	6.8		" " " "
	7.0		" " " "
4 weeks	10.5	7.2	" " " "
	10.9	±4.0	" " " "
	1.0		Severe bond line corrosion
	2.1		" " " "
	5.9		" " " "
6 weeks	8.2	6.3	" " " "
	5.0	±3.0	Apparent interfacial failure
	10.0		" " "
	0		Bond line corrosion
	3.5		" " "
	4.3		" " "
8 weeks	10.2	6	" " "
	11.9		" " "

Table 4.5.7. Durability of 2117/ICI deoxidiser No.1./2214 adhesive bonds in salt spray at 43°C. measured using standard lap shear joints.

EXPOSURE	FAILURE STRESS (MPa)	MEAN & STD. DEV. (MPa)	OBSERVATIONS
0	16.4 16.9 17.1 17.1 17.1	16.9 ±0.3	Cohesive fail. near interface " " " " " " " " " " " " " " " "
1 week	12.6 13.1 13.2 13.8 14.0	13.4 ±0.6	" " " " " " " " " " " " " " " " " " " "
2 week	12.4 14.0 14.7 14.7 15.5	14.3 ±1.2	" " " " " " " " " " " " " " " " " " " "
4 weeks	12.8 13.2 13.7 13.8 14.8	13.7 ±0.8	" " " " " " " " " " " " " " " " " " " "
6 weeks	11.2 11.4 12.5 12.6 12.9	12.1 ±0.8	" " " " " " " " " " " " " " " " " " " "
8 weeks	11.4 13.0 13.0 13.0 13.0	13.2 ±1.5	" " " " " " " " " " " " " " " " " " " "

Table 4.5.8. Durability of 2117/ICI deoxidiser No.1./2214 adhesive bonds in salt spray at 43°C. measured using perforated lap shear joints.

EXPOSURE	FAILURE STRESS (MPa)	MEAN & STD. DEV. (MPa)	OBSERVATIONS
0	15.5 17.4 17.5 18.2 18.3	17.4 ±1.1	Cohesive fail. near interface " " " " " " " " " " " "
1 week	11.7 12.0 12.6 13.3 13.6	12.6 ±0.8	" " " " " " " " " " " " " " " " " " " "
2 weeks	7.0 8.4 10.0 10.7 10.8	9.4 ±1.6	" " " " " " " " " " " " " " " " " " " "
4 weeks	1.7 4.1 6.7 10.0 10.7	6.6 ±3.8	Severe bond line corrosion " " " " " " " " " " " " Apparent interfacial failure
6 weeks	4.2 6.5 7.6 10.4 11.0	7.9 ±2.8	Bond line corrosion " " " " " " " " " " " "
8 weeks	0 0 0 1.0 1.1	0.4	" " " " " " " " " " " " " " "

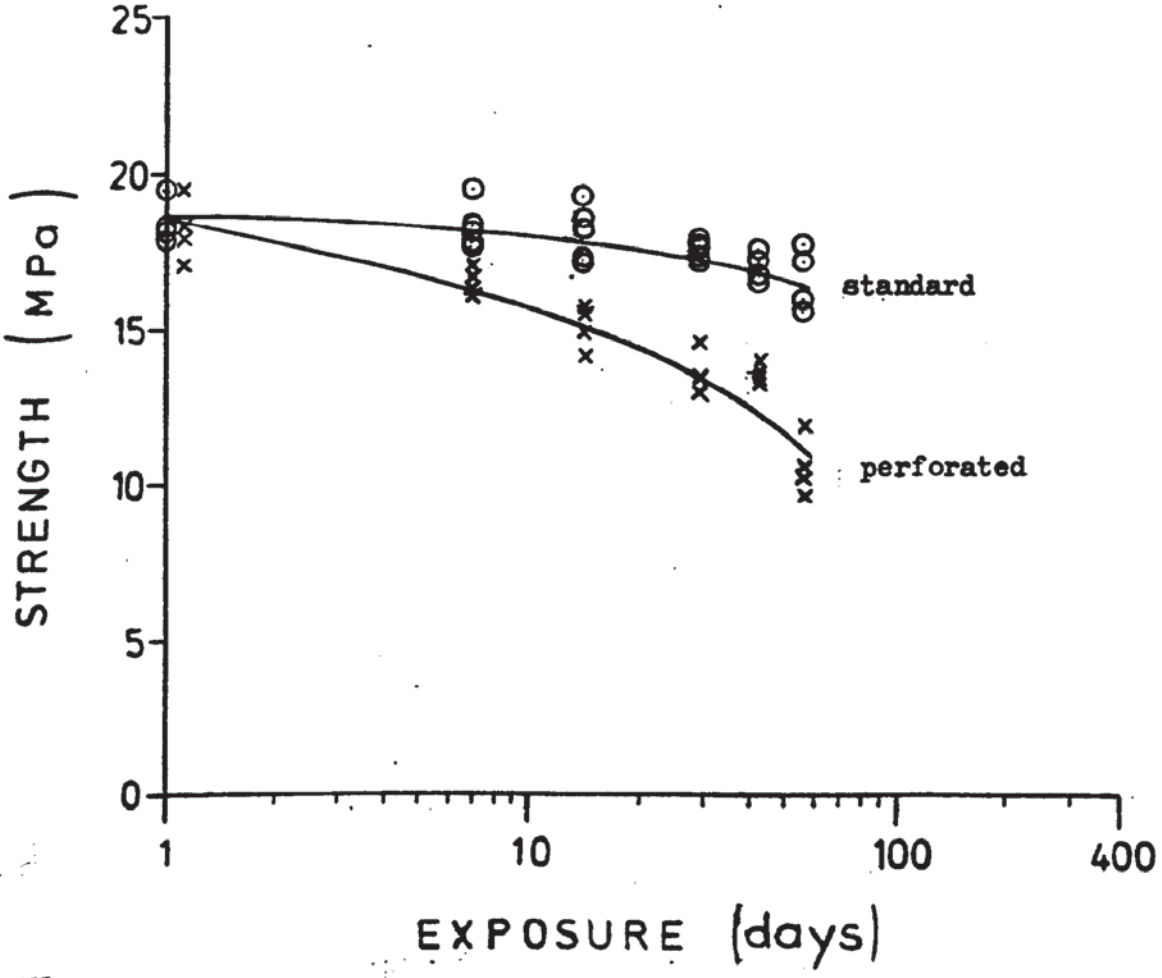

Fig. 4.5.3. Comparison of lap shear joint configurations for measurement of durability of 2117/BAC 5555/2214 adhesive bonds in salt-spray at 43°C.

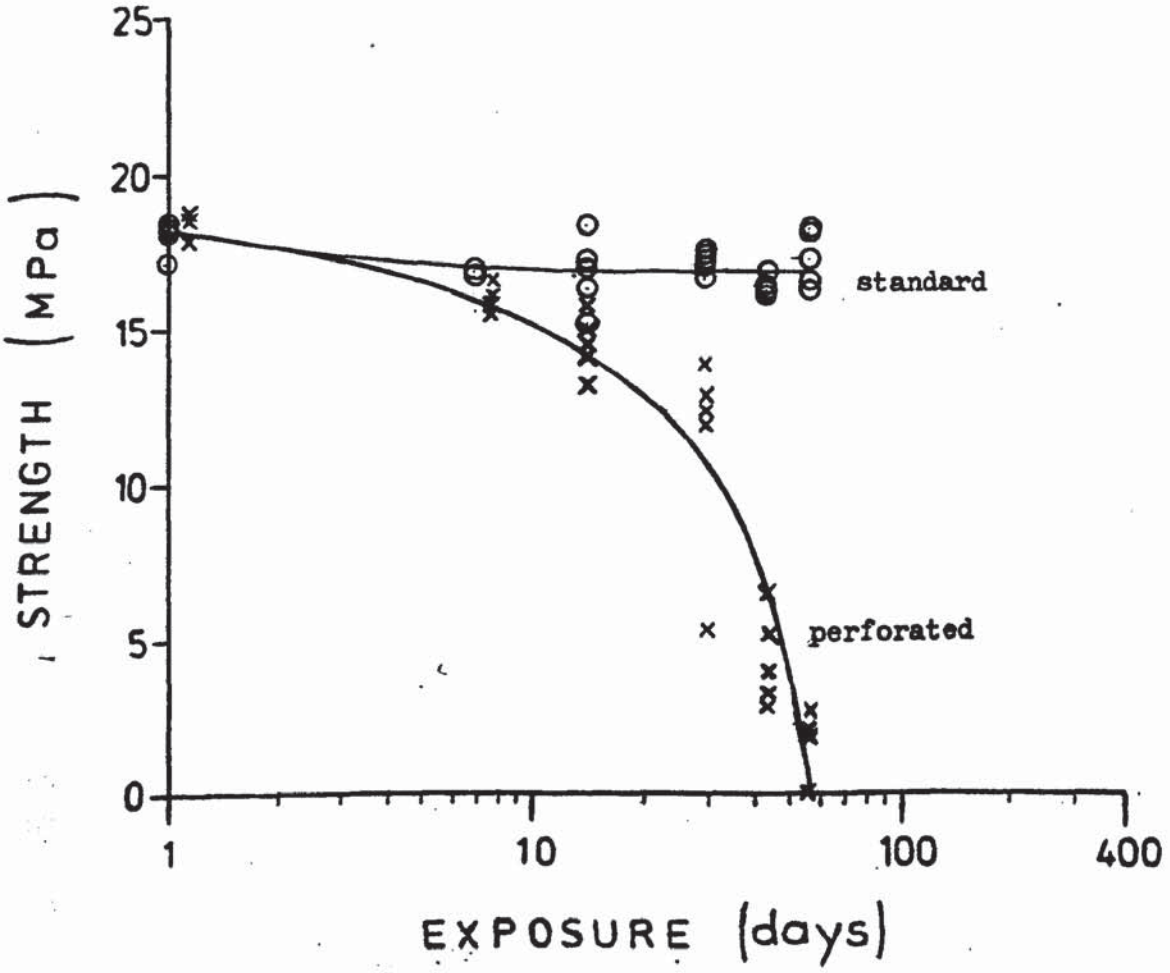

Fig. 4.5.4. Comparison of lap shear joint configurations for measurement of durability of 2117/FPL etched/2214 adhesive bonds in salt-spray at 43°C.

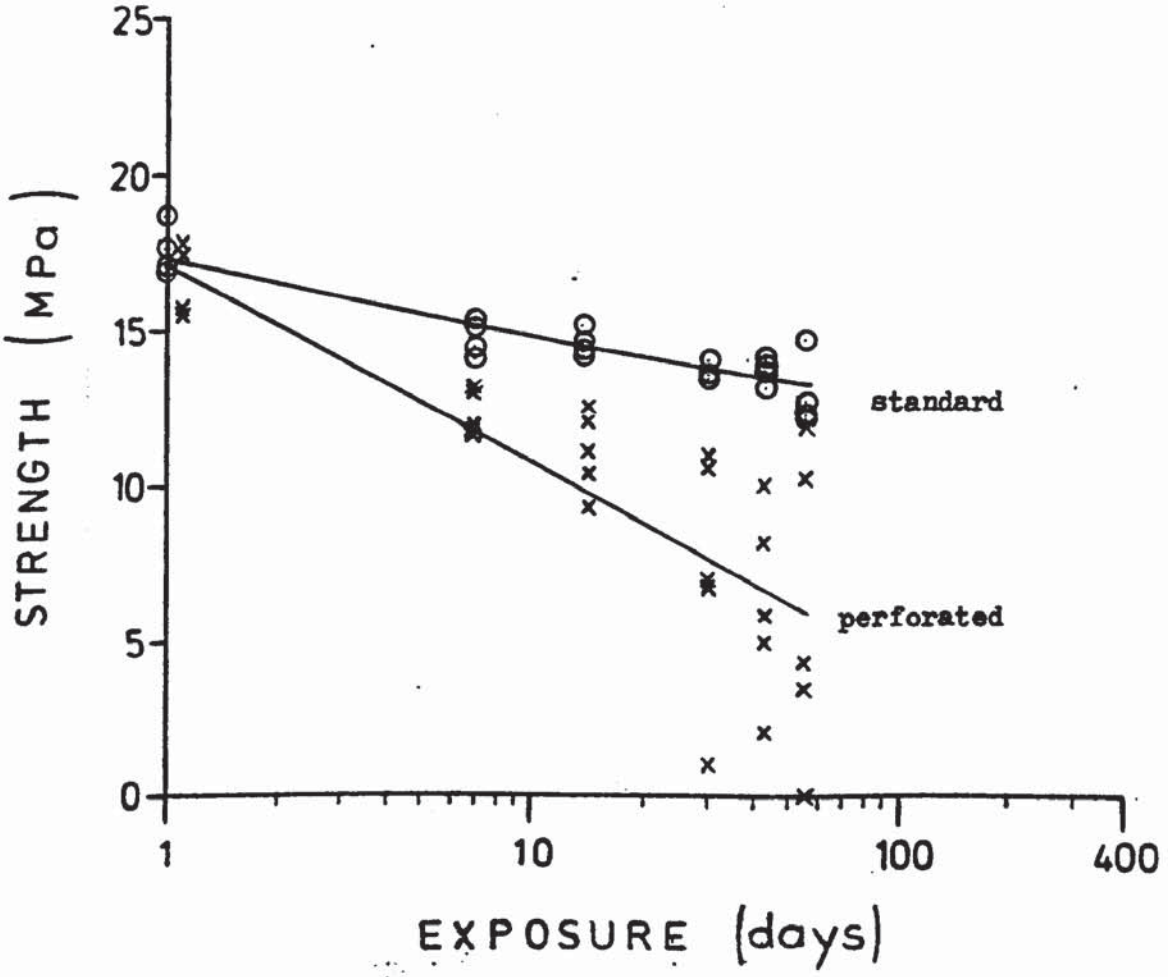

Fig. 4.5.5. Comparison of lap shear joint configurations for measurements of durability of 2117/2 min. PAA/2214 adhesive bonds in salt-spray at 43°C.

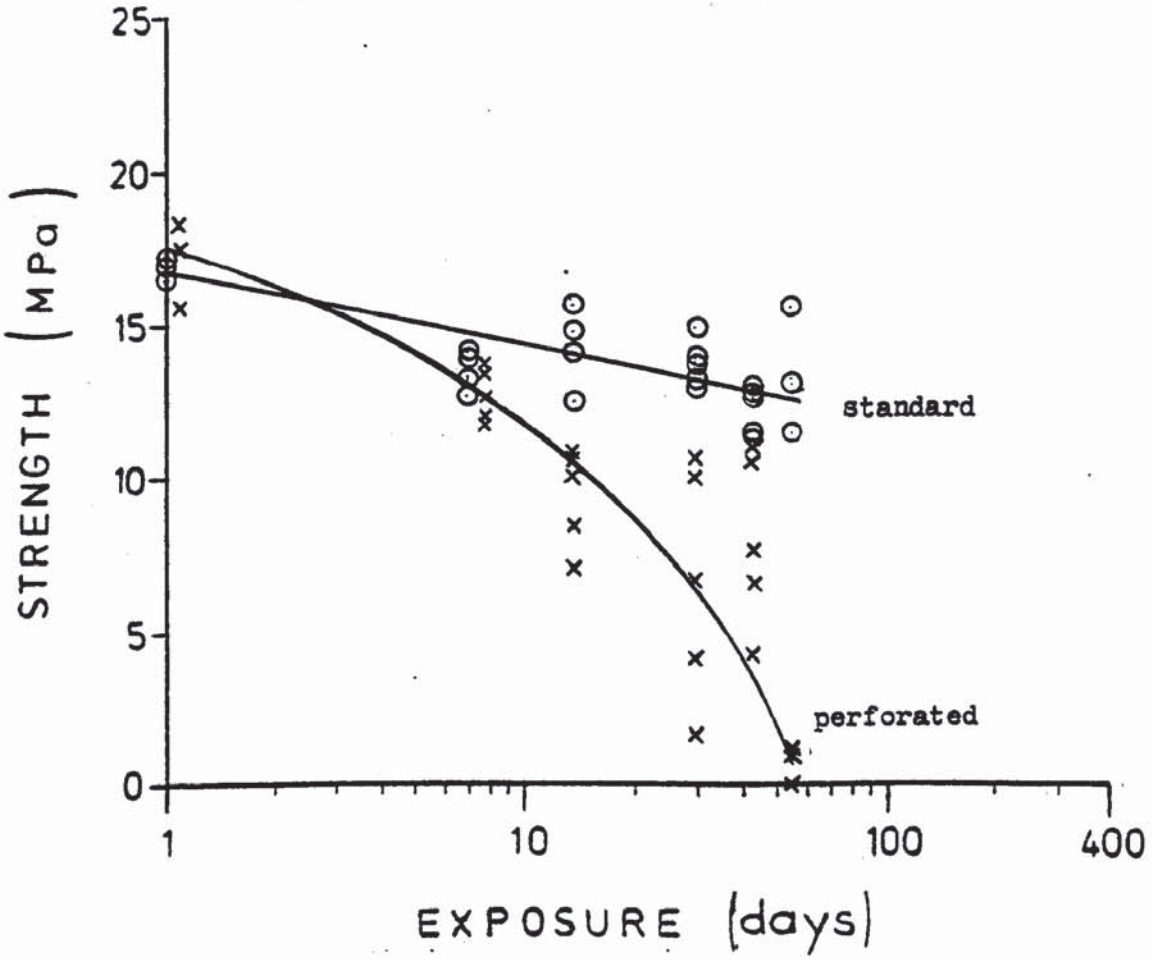

Fig. 4.5.6. Comparison of lap shear joint configurations for measurements of durability of 2117/ICI deoxidiser No.1./2214 adhesive bonds in salt-spray at 43°C.

4.6 Influence of alloy and adhesive types on bond durability

The results in previous sections have indicated the considerable extent to which bond durability is dependent on pretreatment (4.1) and environment (4.2). The combination of 5251 alloy and ESP 105 adhesive however showed little sensitivity to pretreatment, at least in the environment employed.

This experiment was designed to investigate, with the aid of perforated lap shear joints, the performance of different alloy/adhesive combinations. Specimen coupons of 2117 and 5251 alloys were alkaline cleaned, deoxidised (3minutes @ R.T. I.C.I. No.1), rinsed and dried, then bonded using EC 2214 and ESP 105 adhesives. Cured joints were perforated and installed in the salt-spray cabinet. One group of specimens were placed in a sealed Kilner jar containing a small quantity of water and the whole transferred to the salt-spray cabinet. These were to be tested with the last group of salt-spray specimens after 8 weeks exposure.

The results are shown in Tables 4.6.1 to 4.6.4 and Figs. 4.6.1 to 4.6.4. The initial strengths of ESP 105 bonds were slightly higher than those produced by EC 2214. The loci of failure of all unexposed specimens appeared cohesive, very close to the interface. The residual EC 2214 adhesive was seen as a thinner and more uniform film than that of ESP 105. During environmental exposure early signs of bond line corrosion appeared in 2117/2214 specimens. This was followed by rapid degradation as a consequence of which the humidity specimens were tested after only 31 days. No sign of bond line corrosion was observed in these joints, although very little adhesive was detectable on the fracture surface by optical microscopic means.

ESP 105 bonds to 2117 alloy exhibited much better strength retention, the failure mode remaining largely cohesive, although signs of bond line corrosion were detected in two specimens after 49 days exposure to salt-spray. Evidence of bond line corrosion was again absent in the joints exposed only to the high relative humidity.

Bonds to 5251 alloy yielded durability performances which were almost identical for the two adhesives, if expressed in terms of % strength retention. The high humidity results are in close agreement with the corresponding salt-spray data. In addition to durability measurements, absorption characteristics of the adhesives were determined. Estimates of diffusion coefficients and equilibrium water uptake for ballotini-containing films of adhesive exposed to water vapour at 43°C. were:-

EC 2214	Diffusion coefficient	1.3×10^{-13} m.sec.$^{-1}$
	Equilibrium water uptake	4.5%
ESP 105	Diffusion coefficient	9.5×10^{-14} m.sec.$^{-1}$
	Equilibrium water uptake	1.8%

The surface composition of each alloy was examined using X-ray photoelectron spectroscopy, and the results are shown in Tables 4.6.5. to 4.6.8.

Table 4.6.1. Durability of 2117/deoxidised/EC 2214 adhesive bonds (perforated lap shear joints).

EXPOSURE	FAILURE STRESS (MPa)	MEAN & STD. DEV. (MPa)	OBSERVATIONS
Salt spray	17.0		Cohesive fail. near interface
	17.2		" " " "
0	17.2	17.4	" " " "
	17.7	±0.3	" " " "
	17.7		" " " "
	11.9		" " " "
	12.2		" " " "
7 days	12.5	12.5	" " " "
	13.0	±0.5	" " " "
	13.0		" " " "
	6.0		Bond line corrosion
	8.5		" " "
14 days	10.7	9.8	Apparent interfacial failure
	11.0	±2.6	" " "
	12.6		" " "
	1.3		Bond line corrosion
	1.5		" " "
31 days	1.9	2.1	" " "
	2.7	±0.8	" " "
	3.2		" " "
49 days		0	No survivors
100% R.H. @ 43°C.	9.7		Apparent interfacial failure
	10.0		" " "
	10.3	10.5	" " "
31 days	10.5	±0.7	" " "
	11.9		" " "

Table 4.6.2. Durability of 2117/deoxidised/ESP 105 adhesive bonds. (perforated lap shear joints)

EXPOSURE	FAILURE STRESS (MPa)	MEAN & STD. DEV. (MPa)	OBSERVATIONS
Salt spray			
	17.0		Cohesive fail. near interface
	17.9		" " " "
0	18.0	18.0	" " " "
	18.3	±0.6	" " " "
	18.7		" " " "
	14.0		" " " "
	14.2		" " " "
7 days	14.5	14.5	" " " "
	14.6	±0.5	" " " "
	15.2		" " " "
	14.9		" " " "
	15.1		" " " "
14 days	15.8	15.6	" " " "
	15.8	±0.6	" " " "
	16.2		" " " "
	12.3		" " " "
	14.1		" " " "
31 days	14.7	14.3	" " " "
	15.2	±1.2	" " " "
	15.2		" " " "
	8.3		Bond line corrosion
	10.4		" " "
49 days	13.0	11.8	Cohesive fail. near interface
	13.6	±2.4	" " " "
	13.6		" " " "
100% R.H. @ 43°C.			
	11.0		" " " "
	13.5		" " " "
	13.5	13.2	" " " "
49 days	14.0	±1.3	" " " "
	14.0		" " " "

Table 4.6.3 Durability of 5251/de-oxidised/2214 adhesive bonds (perforated lap shear joints)

EXPOSURE	FAILURE STRESS (MPa)	MEAN & STD. DEV. (MPa)	OBSERVATIONS
Salt spray	16.3		Cohesive fail. near interface
	16.5		" " " "
0	17.1	17.0	" " " "
	18.2	±0.9	" " " "
	11.0		" " " "
	11.2		" " " "
7 days	13.8	14.0	" " " "
	15.4	±3.1	" " " "
	18.5		" " " "
	7.7		" " " "
	9.0		" " " "
14 days	12.8	11.4	" " " "
	13.8	±2.9	" " " "
	14.0		" " " "
	9.5		" " " "
	10.7		" " " "
31 days	11.0	11.0	" " " "
	11.4	±1.0	" " " "
	12.3		" " " "
	10.5		" " " "
	10.9		" " " "
49 days	12.5	11.9	" " " "
	12.5	±1.1	" " " "
	13.0		" " " "
100% R.H. @ 43°C.	10.8		" " " "
	11.5		" " " "
	11.6	11.7	" " " "
49 days	11.8	±0.7	" " " "
	12.6		" " " "

Table 4.6.4 Durability of 5251/deoxidised/ESP 105 adhesive bonds. (perforated lap shear joints)

EXPOSURE	FAILURE STRESS (MPa)	MEAN & STD. DEV. (MPa)	OBSERVATIONS
Salt spray	17.6		Cohesive fail. near interface
	18.0		" " " "
0	19.3	18.8	" " " "
	19.5	±0.9	" " " "
	19.5		" " " "
	9.6		" " " "
	13.0		" " " "
7 days	13.2	12.8	" " " "
	13.3	±1.9	" " " "
	14.7		" " " "
	5.6		Starved joint result ignored
	10.3		Cohesive fail. near interface
14 days	13.5		" " " "
	15.4	13.7	" " " "
	15.8	±2.5	" " " "
	10.6		" " " "
	13.5		" " " "
31 days	14.4	13.9	" " " "
	14.5	±2.1	" " " "
	16.2		" " " "
	12.1		" " " "
	13.3		" " " "
49 days	14.0	13.7	" " " "
	14.3	±1.0	" " " "
	14.6		" " " "
100% R.H. @ 43°C.	9.0		" " " "
	12.2		" " " "
	13.9	13.0	" " " "
49 days	14.8	±2.5	" " " "
	15.0		" " " "

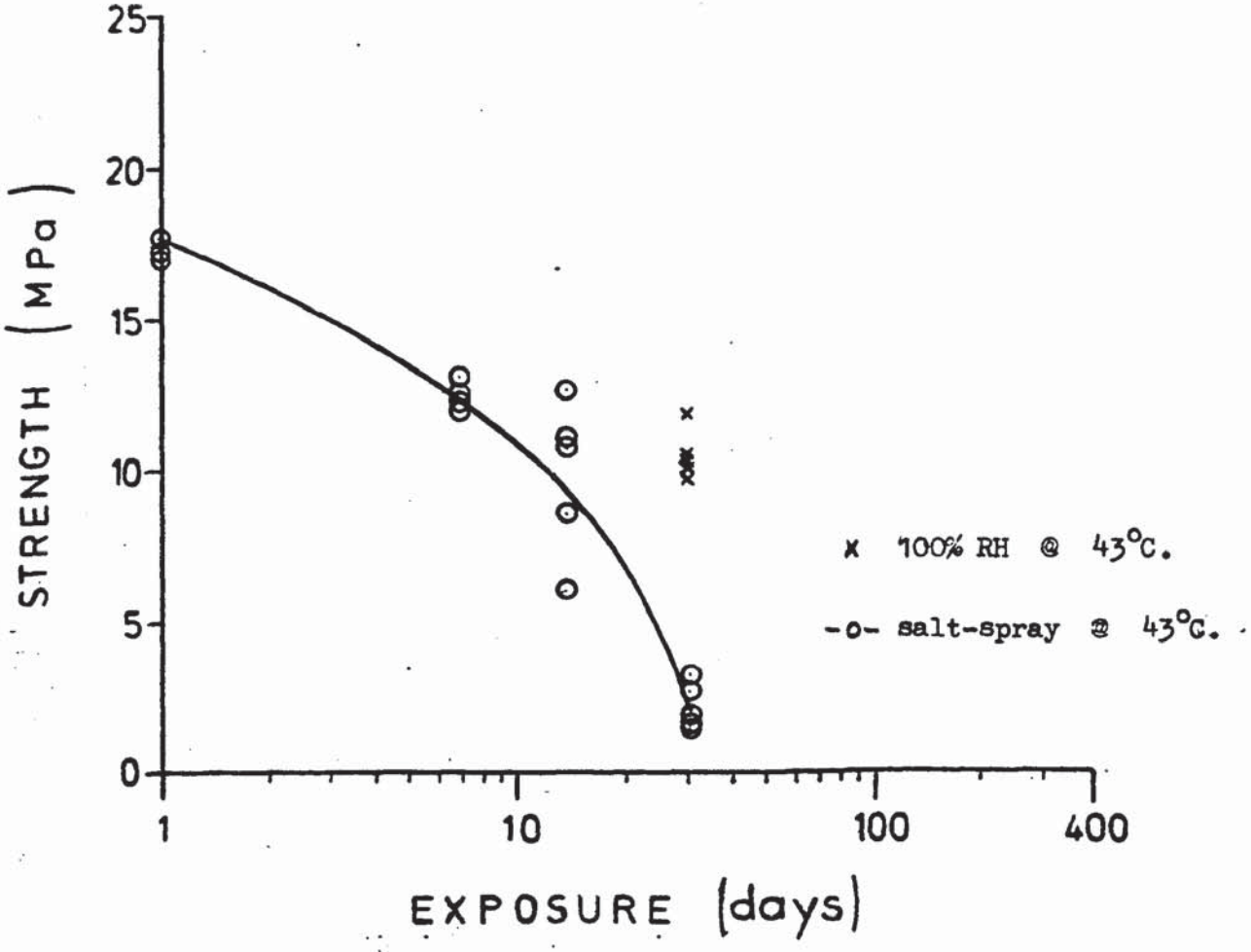

Fig. 4.6.1. Durability of 2117/deoxidised/2214 adhesive bonds in salt-spray @ 43°C.
(perforated lap shear joints)

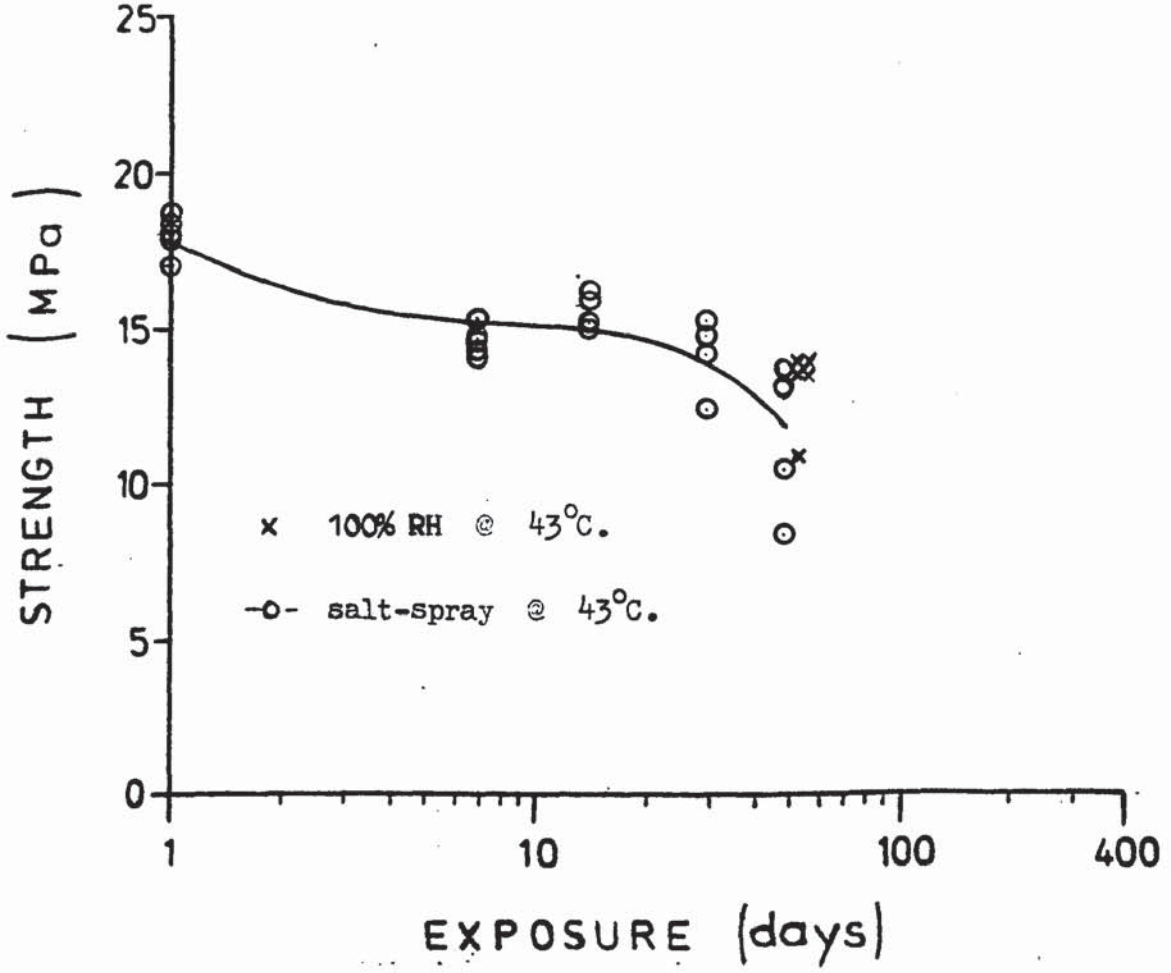

Fig. 4.6.2. Durability of 2117/deoxidised/ESP 105 adhesive bonds. (perforated lap shear joints)

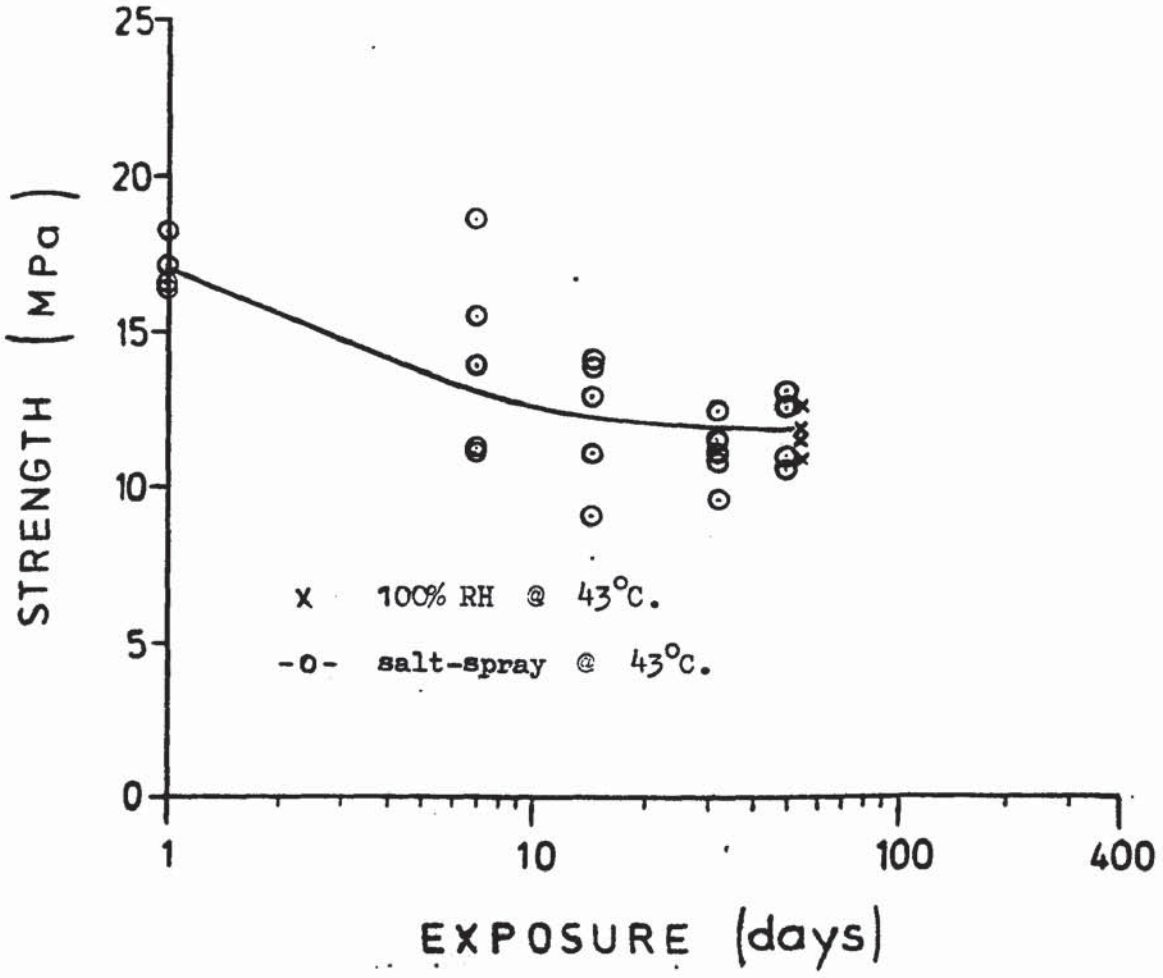

Fig. 4.6.3 Durability of 5251/de-oxidised/2214 adhesive bonds.
(perforated lap shear joints)

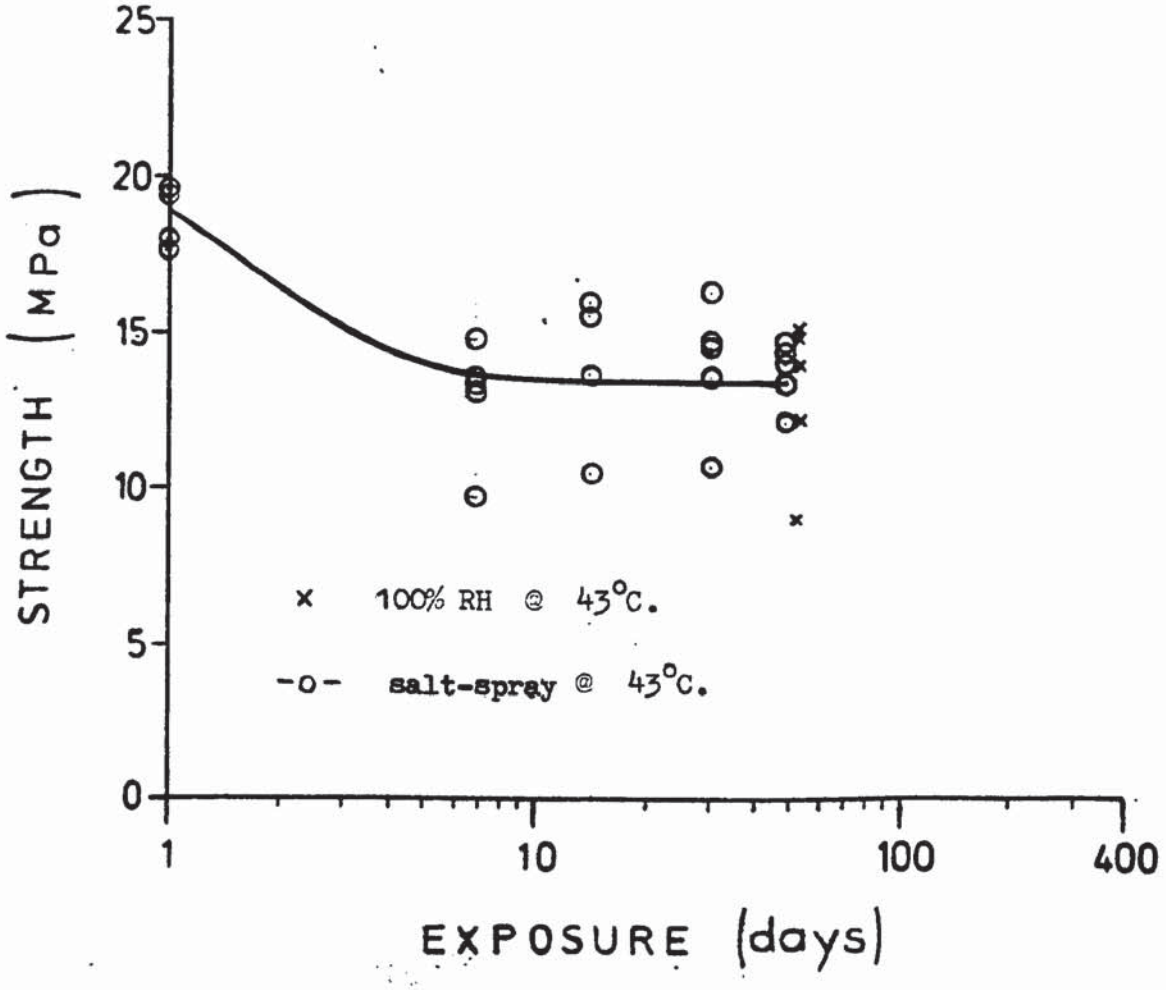

Fig. 4.6.4 Durability of 5251/deoxidised/ESP 105 adhesive bonds. (perforated lap shear joints)

2117 Alkaline cleaned surface

	Al 2p	AlO 2p	P 2p	C 1s	CO 1s	Mg Aug	O 1s	Cu 2p*
Corrected B.E.	71.8	74.5	134.1	285.0	289.6	306.1	531.6	933.7
Width	1.50	2.15	2.50	2.25	2.50	2.95	2.95	2.25
Intensity	305.1	1773.4	324.9	2211.9	296.6	1583.3	16666.7	1233.1
Molar ratio	.19	1.08	.09	1.00	.13	.09	2.85	.03
Mole fract.	.034071	.198053	.017209	.182790	.024512	.015577	.521722	.006065

2117 Alkaline cleaned, ion etched to depth ~6 Å

	Al 2p	AlO 2p	P 2p	C 1s	CO 1s	Mg Aug	O 1s	Cu 2p*
Corrected B.E.	71.5	74.7	-2.1	284.7	-2.1	306.8	531.5	934.4
Width	1.50	2.30	1.00	2.20	1.00	2.70	2.45	2.70
Intensity	406.8	2339.0	0.0	522.0	0.0	1784.7	17994.4	1464.4
Molar ratio	.17	1.00	0.00	.17	0.00	.07	2.16	.03
Mole fract.	.048440	.278528	0.000000	.046001	0.000000	.018723	.600627	.007681

Table 4.6.5. XPS analysis of alkaline cleaned 2117 alloy surface

2117 de-oxidised surface

	Al 2p	AlO 2p	S 2p	C 1s	CO 1s	Mg Aug	O 1s	F 1s	Cu 2p*	CuI 2p*
Corrected B.E.	72.5	74.7	168.9	285.0	288.5	306.2	531.7	686.7	933.7	935.3
Width	1.70	2.40	3.00	2.30	2.60	2.80	2.65	3.65	2.40	2.50
Intensity	403.4	1735.6	254.2	1949.2	440.7	1139.0	15271.2	1608.5	2888.1	2457.6
Molar ratio	.23	1.00	.05	.83	.19	.06	2.47	.17	.07	.06
Mole fract.	.045281	.194825	.009777	.161910	.036606	.011263	.480503	.033403	.014280	.012152

2117 de-oxidised, ion etched to depth ~6 Å

	Al 2p	AlO 2p	S 2p	C 1s	CO 1s	Mg Aug	O 1s	F 1s	Cu 2p*	CuI 2p*
Corrected B.E.	71.7	74.6	-1.8	284.7	-1.8	307.0	531.5	686.5	933.1	-1.8
Width	1.40	2.70	1.00	2.35	1.00	2.90	2.70	3.10	2.25	1.00
Intensity	403.4	2333.9	0.0	969.2	0.0	1228.8	16016.9	2574.6	8135.6	0.0
Molar ratio	.17	1.00	0.00	.31	0.00	.05	1.92	.20	.15	0.00
Mole fract.	.045391	.262619	0.000000	.080704	0.000000	.012181	.505187	.053595	.040323	0.000000

Table 4.6.6. XPS analysis of deoxidised 2117 alloy surface

5251 alkaline cleaned surface

	Al 2p	AlO 2p	C 1s	CO 1s	Mg Aug	O 1s	Cu 2p*
Corrected B.E.	71.9	74.5	285.0	288.8	306.7	532.1	933.6
Width	1.60	2.20	2.30	2.50	3.00	3.15	2.30
Intensity	207.9	1578.5	2144.1	339.0	864.4	18330.5	610.7
Molar ratio	.13	1.00	1.01	.16	.05	3.25	.02
Mole fract.	.023453	.178062	.178974	.028296	.008590	.579591	.003035

5251 alkaline cleaned, ion etched to depth ~6 Å

	Al 2p	AlO 2p	C 1s	CO 1s	Mg Aug	O 1s	Cu 2p*
Corrected B.E.	72.0	74.6	284.7		306.5	531.3	933.2
Width	1.60	2.15	2.40		2.75	2.80	2.60
Intensity	253.1	1773.4	1993.2	0.0	870.1	16452.0	852.0
Molar ratio	.14	1.00	.83	0.00	.04	2.60	.02
Mole fract.	.030765	.215558	.179280	0.000000	.009316	.560520	.004561

Table 4.6.7. XPS analysis of alkaline cleaned 5251 alloy surface

5251 de-oxidised surface

	Al 2p	AlO 2p	C 1s	CO 1s	Mg Aug	MgO Aug	O 1s	F 1s	Cu 2p*
Corrected B.E.	72.1	74.6	285.0	289.6	299.8	307.1	531.9	685.9	932.9
Width	1.60	2.25	2.00	2.50	1.20	3.06	2.95	3.02	2.00
Intensity	593.9	1352.7	2458.0	168.8	106.1	811.2	14242.6	1840.1	292.0
Molar ratio	.44	1.00	1.34	.09	.01	.05	2.95	.25	.01
Mole fract.	.071413	.162648	.218706	.015015	.001124	.008593	.480025	.040931	.001547

5251 de-oxidised surface, ion etched to depth ~ 6 Å

	Al 2p	AlO 2p	C 1s	CO 1s	Mg Aug	MgO Aug	O 1s	F 1s	Cu 2p*
Corrected B.E.	72.0	74.9	284.7	-8.3	300.2	307.2	531.6	686.4	932.7
Width	1.45	2.20	2.20	1.00	1.70	3.40	2.32	2.70	2.10
Intensity	654.0	1779.8	827.2	0.0	147.9	1060.0	13156.7	4101.3	470.4
Molar ratio	.37	1.00	.34	0.00	.01	.05	2.07	.43	.01
Mole fract.	.085825	.233581	.080336	0.000000	.001710	.012255	.483997	.099577	.002719

Table 4.6.8 XPS analysis of deoxidised 5251 alloy surface

4.7 Influence of phosphates on bond durability

The high durability of adhesive bonds to aluminium surfaces which have been anodised in phosphoric acid to Boeing's BAC 5555 specification is considered to be due, at least in part, to the presence of hydration-inhibiting phosphate ions incorporated in the oxide structure. The Boeing process, however, is time consuming and requires a relatively expensive electrolyte.

An experiment was therefore designed to determine the effect on bond durability of the absorption of phosphates from a second solution immediately after anodic oxide formation in a sulphuric acid electrolyte.

4.7.1 Specimen preparation and testing

To simplify interpretation of the results, bond line corrosion effects were minimised by choosing 5251 alloy and humid rather than salt-spray conditions. EC 2214 adhesive, possessing, for test purposes, the better sorption characteristics i.e. a higher equilibrium water uptake value, was used.

The pretreatment conditions employed in this preliminary investigation were based on the results of current density measurements taken using a 6 cm^2 test anode of freshly deoxidised 5251 alloy immersed in phosphoric acid and sulphuric acid solutions. The data have been re-plotted as current density as a function of applied D.C. voltage and electrolyte temperature for a range of acid concentrations. Some of the results are shown in Figs. 4.7.1 to 4.7.4.

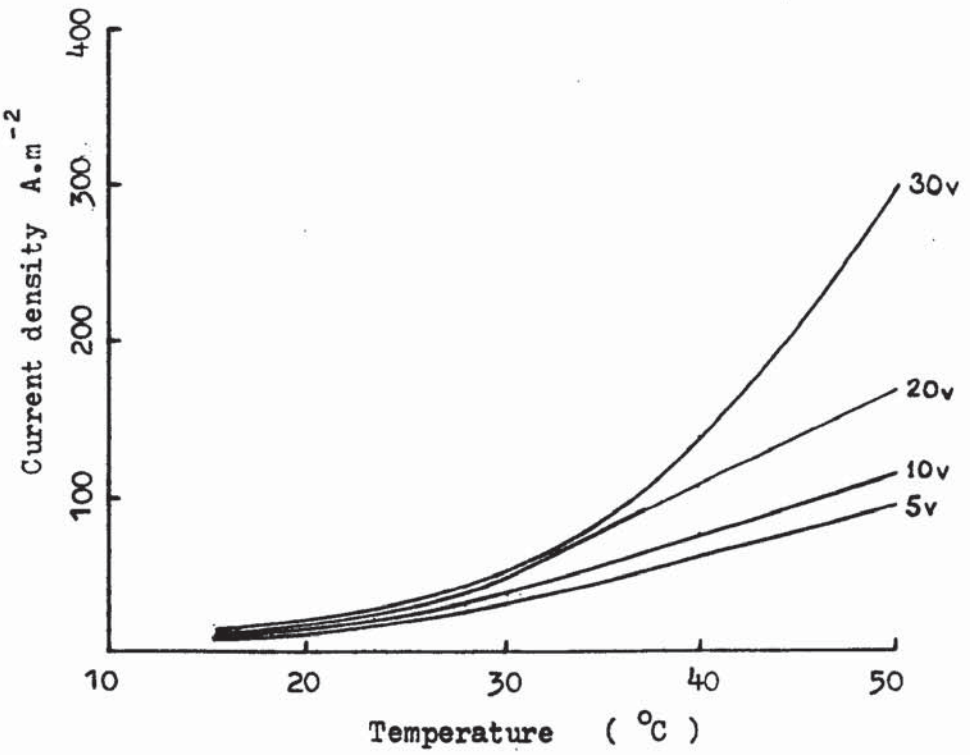

Fig. 4.7.1 Current density, voltage, temperature relationship for 5% by volume H_3PO_4

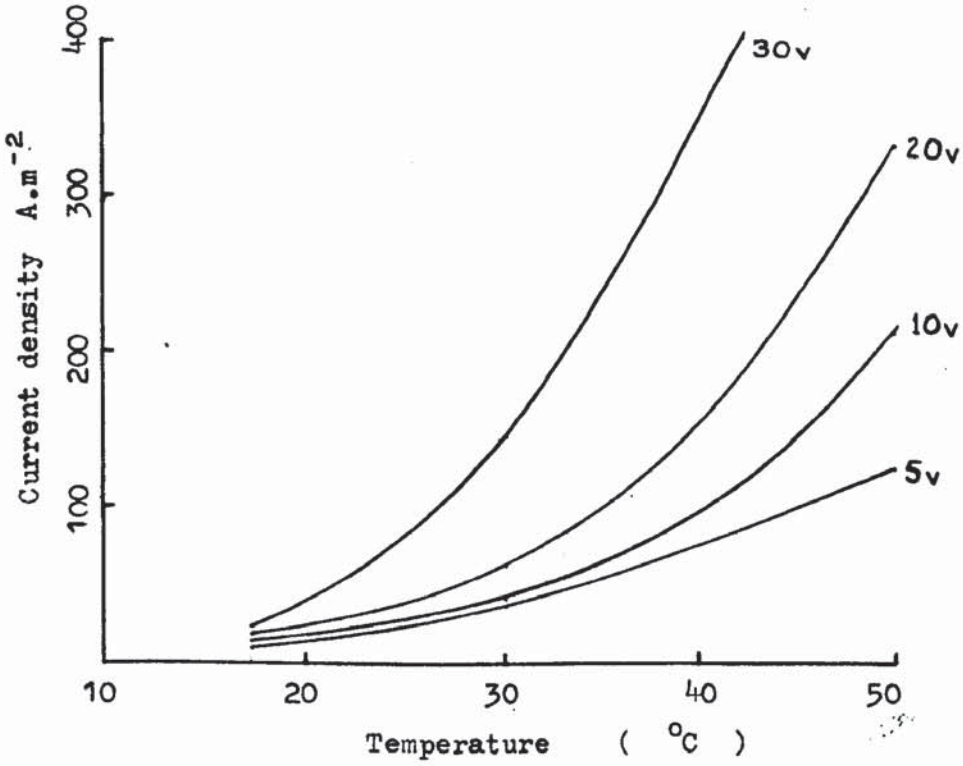

Fig. 4.7.2 Current density, voltage, temperature relationship for 12.5% by volume H_3PO_4

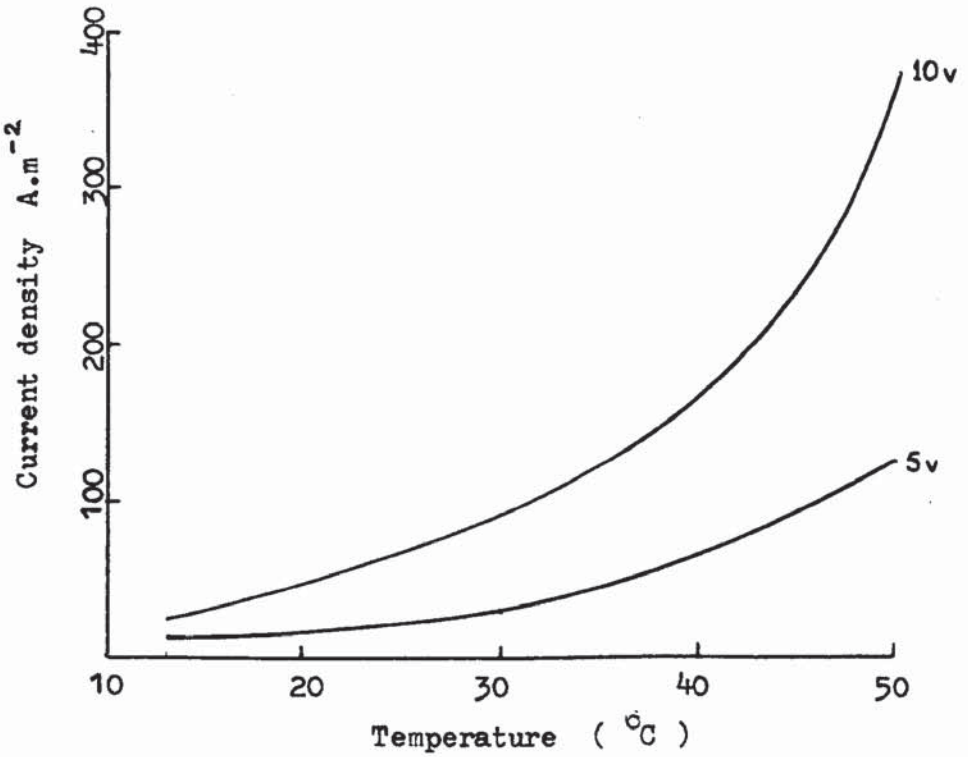

Fig. 4.7.3 Current density, voltage, temperature relationship for 5% by volume H_2SO_4

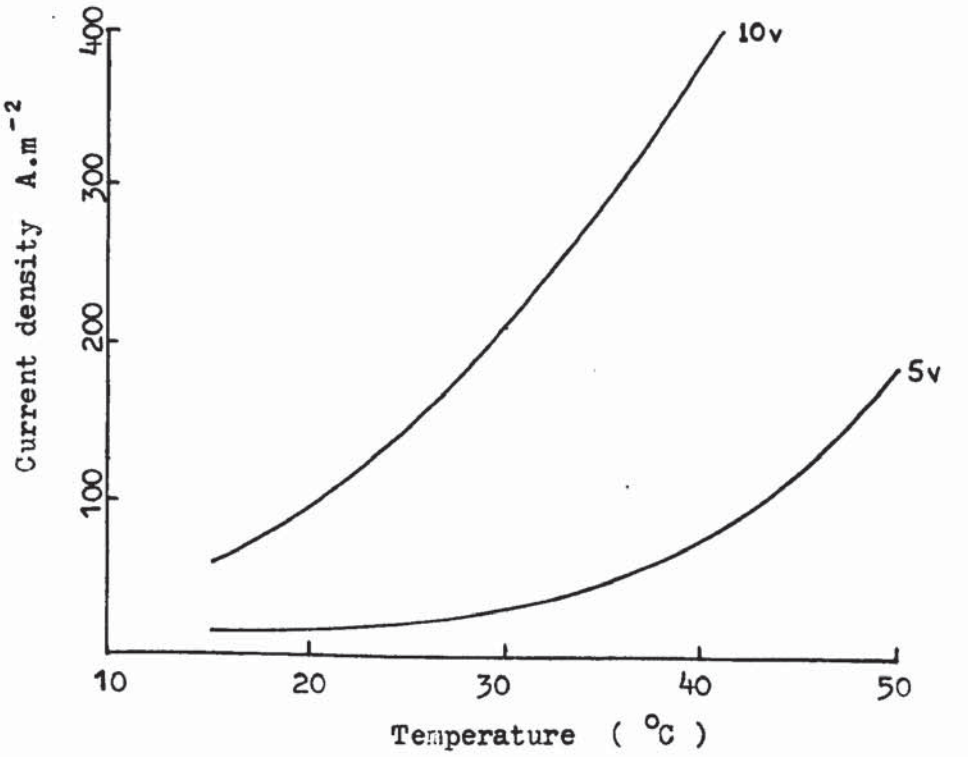

Fig. 4.7.4 Current density, voltage, temperature relationship for 12.5% by volume H_2SO_4

The anodising conditions chosen for the bond durability tests were:-

Electrolyte	:	12.5% by volume sulphuric acid solution
Operating temperature	:	35 °C.
Cell voltage	:	10 volts D.C.
Anodising time	:	2 minutes
Agitation	:	magnetic stirrer
Current density	:	280 $A.m^{-2}$

Specimen coupons of 5251 alloy were deoxidised, anodised, then rinsed in deionised water. The post-anodising treatments employed were either:-

Immersion for 2 minutes at room temperature in a 2% solution of di-sodium hydrogen phosphate, adjusted to pH 7.00 using ortho-phosphoric acid. A 1 minute rinse in running de-ionised water was followed by air drying at 50°C.

or,

Immersion for 10 seconds at room temperature in a 800 ppm. solution of tri-ethyl phosphate in di-ethyl ether, followed by air drying at room temperature. Standardless electron probe micro-analysis revealed the presence of phosphorus only in the surface treated in the aqueous phosphate solution. The relative amounts of aluminium, sulphur and phosphorus found are shown in Table 4.7.1

Element	SAA	SAA + aq. PO_4	SAA + T.E.P
Al	98.13 wt%	97.43 wt%	98.03 wt%
S	1.84 wt%	2.18 wt%	1.97 wt%
P	0.03 wt%	0.39 wt%	0 wt%

Table 4.7.1

The treated coupons were bonded without delay to produce single lap shear joints which, after curing, were converted to the perforated configuration.

Bond durability under 100% RH conditions at 43°C. was subsequently determined.

4.7.2 Results

Durability results are shown in Tables 4.7.1 to 4.7.3.

The lowest initial strength values were measured for those specimens which were treated in the aqueous phosphate solution after anodising. The difference in the initial strengths of the anodised controls and the triethyl phosphate treated anodised specimens is not statistically significant.

Exposure to the humid test atmosphere revealed differences in performance and failure mode. The anodised-only controls which had yielded the highest strengths initially exhibited the lowest strengths at the end of the eight week exposure period. Bonds to surfaces which had been anodised and immersed in the aqueous phosphate solution produced an almost identical value after exposure, and mixed failure modes were observed in both cases.

The bonds which incorporated treatment in tri-ethyl phosphate solution were found to be approx. 20% stronger than the controls after 8 weeks exposure, and this difference is significant at the 0.2% level. The fracture surfaces of the tri-ethyl phosphate treated joints consistently revealed a locus of failure within the adhesive and close to the interface.

Table 4.7.1. Durability of 5251/SAA/EC2214 adhesive bonds in 100% RH @ 43°C.
(perforated lap shear joints)

EXPOSURE	FAILURE STRESS (MPa)	MEAN & STD. DEV. (MPa)	OBSERVATIONS
0	16.7	17.3 ±0.9	Apparent interfacial failure
	16.6		"
	17.2		"
	18.6		"
2 weeks	10.6	10.2 ±0.6	"
	10.5		"
	9.8		"
	9.3		"
	10.5		"
4 weeks	10.9	10.4 ±0.3	Cohesive failure/cohesive failure near interface
	10.5		"
	10.1		"
	10.3		"
	10.4		"
8 weeks	9.0	8.7 ±0.6	Cohesive failure/apparent interfacial failure
	8.3		"
	8.2		"
	8.3		"
	9.5		"

Table 4.7.2 Durability of 5251/SAA + aq. PO_4 /EC 2214 adhesive bonds in 100% RH @ 43°C.
(perforated lap shear joints)

EXPOSURE	FAILURE STRESS (MPa)	MEAN & STD. DEV. (MPa)	OBSERVATIONS
0	14.7 16.2 15.6 14.4	15.2 ±0.8	Cohesive failure near interface/apparent interfacial failure. " "
2 weeks	9.3 11.0 10.7 6.6 9.6	9.4 ±1.7	Apparent interfacial failure. Cohesive failure/apparent interfacial failure. Apparent interfacial failure. Cohesive failure.
4 weeks	10.6 11.5 5.5 10.5 10.1	9.6 ±2.4	Cohesive failure/apparent interfacial failure. Apparent interfacial failure. Cohesive failure/apparent interfacial failure.
8 weeks	9.2 8.2 8.4 9.6 9.6	9.0 ±0.7	" " " " " " " " " " " " " " "

Table 4.7.3 Durability of 5251/SAA + triethyl phosphate/EC 2214 adhesive bonds in 100% RH @ 43°C. (perforated lap shear joints)

EXPOSURE	FAILURE STRESS (MPa)	MEAN & STD. DEV. (MPa)	OBSERVATIONS
0	17.0	16.8 ±0.6	Cohesive fail. near interface
	16.1		" " " "
	16.5		" " " "
	17.5		" " " "
2 weeks	10.5	10.5 ±1.1	" " " "
	10.3		" " " "
	10.3		" " " "
	12.3		" " " "
	9.3		" " " "
4 weeks	9.1	10.3 ±1.2	" " " "
	10.8		" " " "
	12.0		" " " "
	9.4		" " " "
	10.3		" " " "
8 weeks	10.5	10.5 ±0.1	" " " "
	10.5		" " " "
	10.5		" " " "
	10.6		" " " "
	10.4		" " " "

CHAPTER 5 DISCUSSION OF RESULTS

5.1 Measurement of lap shear strength

The advantages of the single lap joint for adhesive bond testing include simplicity of fabrication, the relative ease with which it can be stressed during environmental exposure, and the engineering significance of the data produced. The strength of this configuration is, however, influenced considerably by geometrical factors as discussed in sections 2.7 and 2.8 and in this project the control of important strength-related variables has received particular attention. Jigs have been designed which both facilitate the accurate assembly of bonded joints and ensure consistent curing conditions for the adhesive.

The effect of adhesive spew fillets at the ends of the joint overlap in reducing peak stresses and increasing observed bond strengths has been shown to depend considerably on the adhesive used. Accordingly, careful fillet control during assembly is now exercised, the ideal specimen exhibiting after cure the minimum possible excess adhesive outside the intended bond area.

A further precaution concerns the side of the coupon which is bonded. There is evidence that the response of an aluminium substrate to pretreatment may differ between the two sides of the sheet [318].

An additional consideration has been the standardisation of the specimen side used for bonding in terms of the pressing direction. The press tool obtained in the later stages of this project produces a minute chamfer on one side of the specimen coupon which could constitute an internal fillet in the plane of the bondline that may conceivably affect the results.

The consequence of such refinements to specimen preparation procedures introduced during the course of the project has been a progressive reduction in experimental variation. For example, a recent investigation involving perforated lap shear joints yielded the following data:-

Exposure	Strength (MPa) (sample size 3)	Coefficient of variation
0	20.45 ± 0.18	0.88%
2 weeks	16.37 ± 0.08	0.49%
5 weeks	15.37 ± 0.03	0.2%
8 weeks	14.32 ± 0.18	1.26%
15 weeks	14.48 ± 0.13	0.9%

Table 5.1 Coefficients of variation, perforated lap shear data.

Considering the most variable result (14.32 ± 0.18), though the sample size is small, a difference between means of only ~0.5 MPa would be significant at the 2% level indicating that these refinements in experimental technique offer much improved resolution, and permit a very useful reduction in specimen numbers, justifiable at least for initial screening purposes.

5.2 Bond durability testing

5.2.1 Introduction

The results in Chapter 4 emphasise the extent to which the durability of adhesive bonds vary, depending on alloy, pretreatment, adhesive and environment. Clearly it is sometimes possible to distinguish, in reasonably short times, the performances of

bonding systems using standard techniques. Some systems, however, may require extremely long periods of exposure before bond strength is significantly affected, as the results of Section 4.4 demonstrate.

The rate of strength change in an adhesively bonded joint may be considered to be primarily dependent on

(i) The rate of diffusion of environmental species into the bond line.

(ii) The effects of such absorption on the bulk properties of the adhesive eg. reductions in modulus and Tg.

(iii) The concentration of diffusant along the adhesive/substrate interface.

(iv) The rate at which such diffusant concentrations result in losses of interfacial adhesion.

The existence of non-uniform diffusant concentration, the lack of information concerning the kinetics of interfacial reactions, and the application of non-uniform stresses within the bond line when a single lap shear joint is tested, complicate interpretation of results. Nevertheless, it is clearly essential that for test purposes significant concentrations of diffusant should be established throughout the bond line as quickly as possible, particularly in view of the results for the magnesium-containing aluminium alloy and ESP 105 adhesive reported in Section 4.4. An understanding of the absorption characteristics of a bonded test specimen is therefore of fundamental importance in considering techniques for the evaluation of bond durability.

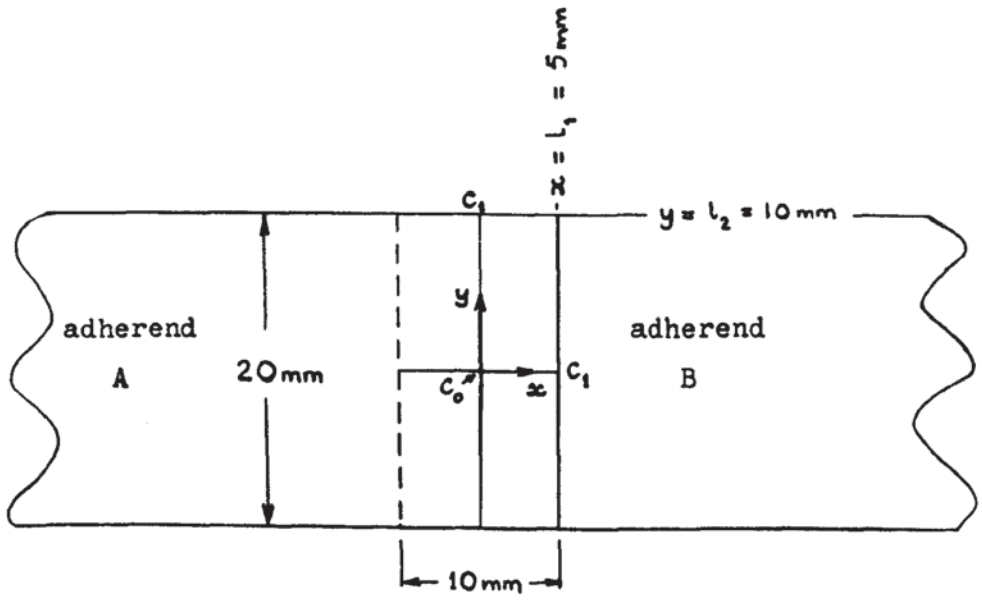

Fig 5.1. Co-ordinate system used for standard lap joint.

5.2.2 Theoretical analysis of water distribution in the lap shear joint

The bond line of a lap joint may be regarded as a normal section of an infinitely long prism which is formed at the intersection of two semi-infinite slabs at right angles. The solution to Fick's second law for sorption by a semi-infinite slab in an infinite bath is given by (319)

$$\frac{C - C_o}{C_1 - C_o} = 1 - \frac{4}{\pi} \sum_{n=0}^{\infty} \frac{(-1)^n}{2n+1} \exp\left(\frac{-D(2n+1)^2 \pi^2 t}{4l^2}\right) \frac{\cos(2n+1)\pi x}{2l}$$

where C = concentration at x at time t

C_o = initial concentration within the slab

C_1 = surface concentration

D = diffusion coefficient

$2l$ = thickness of the slab

The equation is applied separately to diffusion in the x and y directions, but because of joint symmetry it is only necessary to

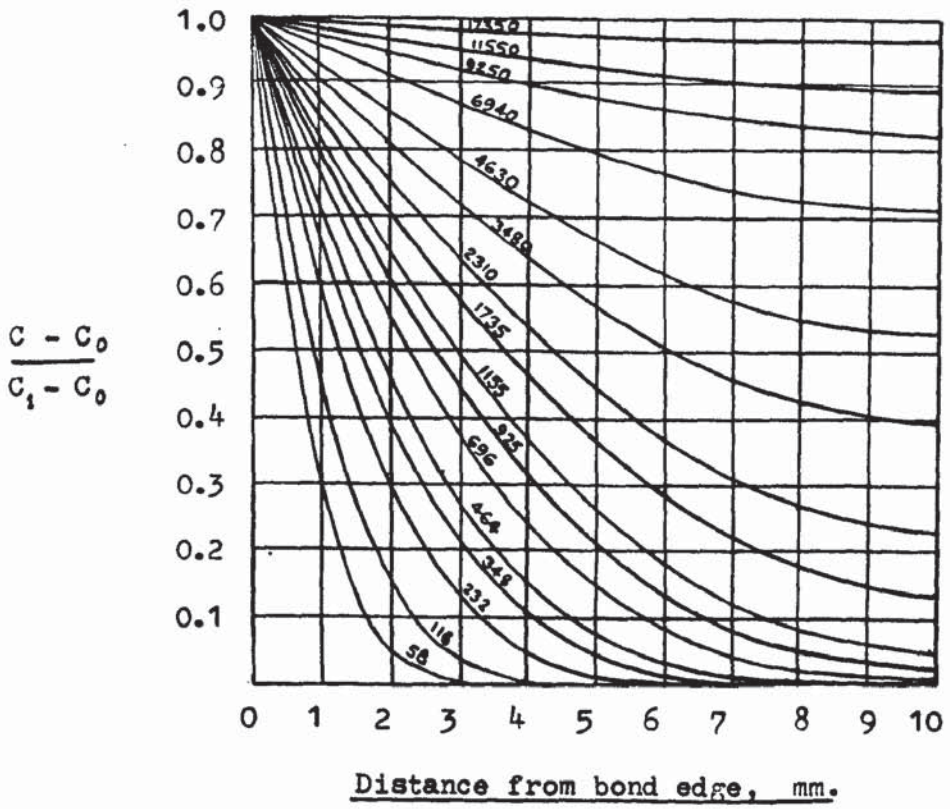

Fig 5.2. Concentration distributions, attributable to uniaxial diffusion, based on $D = 10^{-13}\ m^2\ s^{-1}$. Values of t are shown in days.

evaluate fractional water concentrations for one quarter of the bond area i.e. between the limits $0 \leqslant x \leqslant 5$ mm and $0 \leqslant y \leqslant 10$ mm as shown in Fig 5.1. The distributions in Fig 5.2 illustrate diffusant concentration as a function of distance from the bond edge assuming no pretreatment effects. They are based on a value for D of $10^{-13}\ m^2\ s^{-1}$ to approximate to the values which were obtained for EC 2214 and ESP 105 adhesives. The total concentration at any point within the bond line may be determined from the product of the concentrations relative to the x - and y - slabs, i.e.

If $C_x = f(x)$ for the x - slab

and $C_y = f(y)$ for the y - slab

$C_{xy} = f(x)\, f(y)$,

or

$$\left(1 - \frac{C_{xy}}{C_i}\right) = \left(1 - \frac{C_x}{C_i}\right) \cdot \left(1 - \frac{C_y}{C_i}\right)$$

The advantage of the perforated lap shear configuration is readily appreciated on inspection of the distribution curves shown in Fig. 5.2. Since the maximum diffusion path has been shortened from 5 mm to effectively 1.5 mm, the time required by the diffusion front to reach the remotest points within the adhesive layer is reduced by an order of magnitude. This is obviously the major factor contributing to the acceleration in bond strength loss reported in sections 4.5 to 4.7.

An additional advantage of the perforated joint configuration has since been identified in the context of a durability test which involves applied stress.

5.2.3. Stress-Humidity testing

The technique simply involves the exposure of stressed specimens to a humid environment at above-ambient temperatures.

In this case, the conditions are 100% relative humidity at a temperature which continuously cycles between 42°C. and 48°C.

An electronic programmer controls heating and cooling rates to

provide a peak-peak time of 30 minutes i.e. a 1 hour period. (These conditions comply with the requirements of BS 3900 Part F 2, a British Standard test for paints).

Groups of six lap shear joints are joined using 6 mm pop rivets and the resulting assemblies tensioned using calibrated springs in carrier tubes, constructional details of which are shown in Fig. 5.3. Previous unpublished work, using a range of surface treatments, ESP 105 adhesive, and standard lap shear joints stressed to 5 MPa, failed to discriminate between pretreatments or stress levels. All specimens lost some strength but survived the 12 month test period and when tested to destruction exhibited no significant strength differences which could be attributed to either the pretreatment employed or the presence of stress during exposure.

Recent work however has shown the perforated lap shear joint to be considerably more sensitive to these test conditions. This is probably the result of the removal of bonded material from the centre of the joint which would otherwise assume a load bearing function as the outer regions of the bond are progressively degraded. This mechanical factor, coupled with enhanced penetration by water vapour, very considerably reduces times to failure under sustained load, and is now very readily resolving surface and adhesive variables. The technique is also providing valuable information on the effects of stress itself.

The current experimental procedure requires only 21 specimens, which are assigned as follows:-

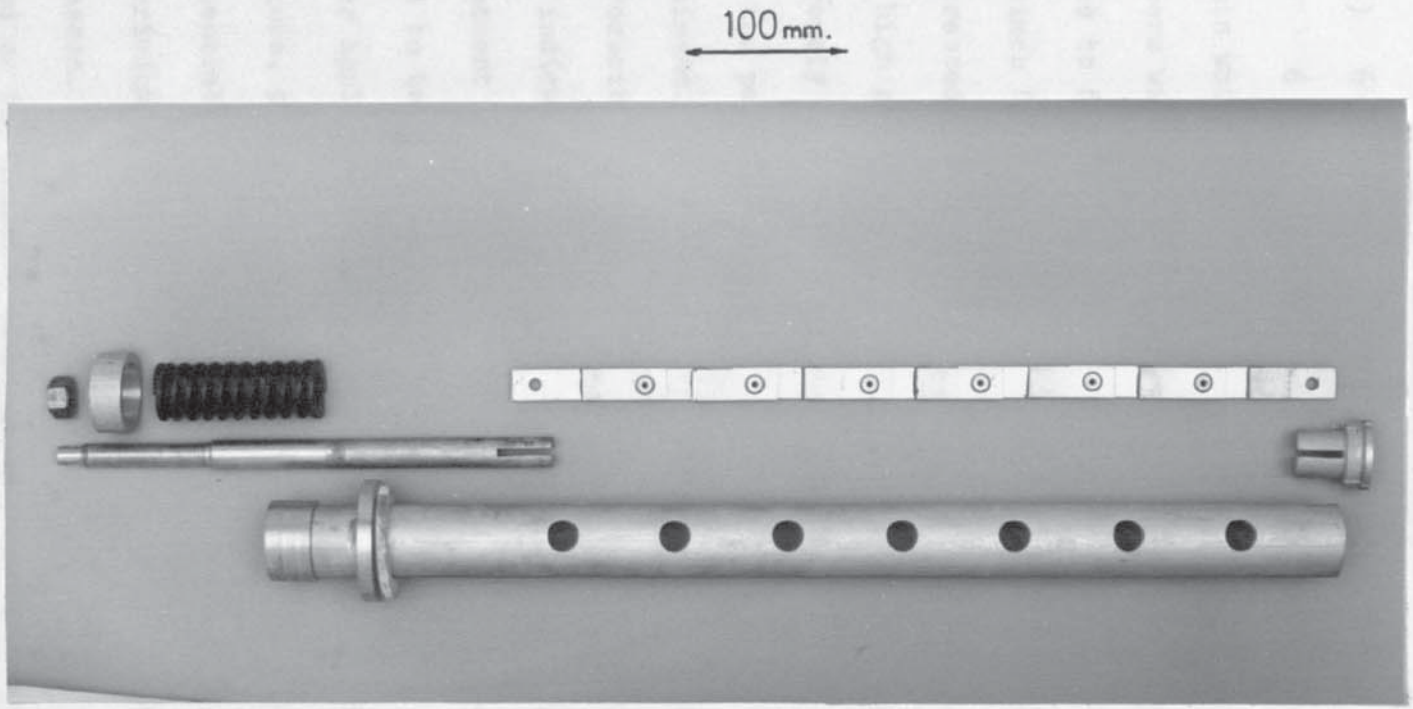

Fig. 5.3 Specimen carrier for stress-humidity testing (standard lap shear joints shown).

(i) 3 specimens tested for initial strength

(ii) 6 specimens stressed @ X MPa

(iii) 6 specimens stressed @ Y MPa

(iv) 6 specimens unstressed, as controls for (ii) and (iii)

Joints which fail under stress during exposure are replaced by spacers with the minimum of delay and the test is continued. Times to failure are recorded, and when the third stressed specimen fails the three surviving joints, together with three unstressed controls, are tested for residual strength.

The high geometrical accuracy of the lap shear joints used is extremely important in ensuring that the mean applied stresses, and the peel components, are uniform within a series of six specimens. This factor undoubtedly contributes to the reproducibility in failure times which has been observed.

The indications to date are that, given that an adequate surface treatment has been used, failures under high applied stresses tend to be cohesive i.e. adhesive-controlled. Failures under lower applied stresses tend to exhibit apparent interfacial failure, probably because of the greater interfacial water concentrations association with the longer exposure periods. Discrimination of pretreatments is thus favoured by low applied stresses. The stress level(s) chosen should therefore be based on the adhesive employed and the experimental objectives. For ESP 105 adhesive values of 2 MPa and 5 MPa have been found to be suitable.

Further useful reductions in test duration, can be achieved by using adhesives with higher values of diffusion coefficient. In the case of pretreatment investigations carried out under stressed conditions the adhesive used must however provide adequate cohesive strength when plasticised by water.

The evaluations of the effects of natural environments on adhesive bond durability has, in the past, often required a considerable number of years of exposure, using, typically, 1" x ½" lap joints.

Some alternative techniques are not suitable, e.g. the wedge test, which would be difficult to monitor and interpret, and in any case would be too fast to capture a reasonably representative environmental period.

The perforated lap shear joint, used in conjunction with a carefully selected adhesive, may however provide an ideal compromise for the study of adhesive bond degradation in hostile natural environments.

For comparable test results two internal standards should generally be incorporated into each experiment:-

1) A standard pretreatment, e.g. BAC 5555

2) A standard adhesive, prepared under controlled conditions by the experimenter. Such a material would be produced using simple, stable constituents to a standard formulation without unknown proprietary additives. This practice would help overcome the problems associated with the batch variables encountered in commercially supplied adhesives.

5.3 Evaluation of established adhesive bonding pretreatments

The strength and durability of adhesive bonds to aluminium have been shown to be influenced considerably by the type of alloy, the pretreatment employed, the adhesive used and the environment to which the joint is exposed. It is therefore not surprising that exact numerical comparisons with published values are very rarely valid, even if the test techniques used were similar. Nevertheless, the test data obtained in the course of this project, previously discussed in mechanical terms in the results section of Chapter 4, tend to confirm the claims made in the literature that specific chromic acid etching, chromic acid anodising and phosphoric acid anodising processes yield highly durable adhesive bonds.

5.3.1 Chromic-sulphuric acid etching

This long established process, two main versions of which are currently practised (Def. Std. 03/2-1 and the U.S. FPL etch) has been very extensively studied, primarily in terms of the influence of process parameters on subsequent bond performance. The form of oxide found on freshly-etched aluminium is the subject of some controversy. Bowen [320] considers it to be boehmite ($Al_2O_3.H_2O$) whereas McCarvill and Bell [321] consider the fresh oxide to be γAl_2O_3

There is evidence to suggest that the oxide layer mainly develops

during the rinse rather than the etching operation.

McCarvill and Bell [321] have studied the influence of rinse water composition, and rinse time and temperature, on bond strength and found the presence of soluble cations of ~0.8 Å radius e.g. Fe^{3+} and Cu^{2+} to be beneficial. He postulated that the small cations could occupy cationic vacancies in the defect spinel structure of the γAl_2O_3, resulting in a reduction in surface negative charge thus increasing attraction for electronegative species, such as the oxygen and nitrogen atoms existing in cured epoxy structures. Smith [322] has suggested that the improved bond strength and durability associated with a tap water rinse after FPL etching is due to the presence of carbonate ions which are claimed to inhibit hydration of the oxide film.

Efforts have been made to replace chromic acid etchants with chromium-free processes. Taking into account the observations of Weber [328] and Pattnaik [329] that elemental sulphur, but not chromium, is detectable on FPL etched aluminium surfaces, Russell [323] has developed semi-empirically an alternative solution containing sulphuric and nitric acids and sodium and ferric sulphates which is said to provide a bond performance comparable to that of the FPL etch. Further work has been done to eliminate nitric acid from the solution and the latest etchant contains only sulphuric acid and ferric sulphate. [330]

Bijlmer [324] has advocated a potentiostatic method involving the maintenance of a surface potential (- 100 to + 200 mV ref SCE)

during a 30 minute immersion in 25% by weight sulphuric acid solution @ 50°C. Again, the process is claimed to compare favourably with the FPL etch. These alternative processes merely provide similar bond performances to the FPL etch, not necessarily similar surface characteristics. Studies of the morphology of the oxide films found on FPL etched surfaces led Kobayshi and Donnelly (325) to propose the structure shown in Fig. 5.4 (a), which features a thin barrier layer and an outer 400 Å thick porous cell structure. More recently Venables (312) using high resolution scanning transmission electron microscopy has proposed a morphology shown in Fig. 5.5 (a), which is characterised by a high concentration ($\sim 10^{10}$ cm^{-2}) of 50 Å thick, 400 Å long alumina whiskers which protrude from a thin barrier layer.

Although chromic-sulphuric acid etching has been the subject of a great many investigations, the mechanisms by which it confers good bond durability have not yet been elucidated.

5.3.2 Phosphoric acid anodising

Oxide films produced under the processing conditions specified in BAC 5555 for adhesive bonding applications have been investigated (312, 325) and the morphologies shown in Figs. 5.4 (b) and 5.5 (b) proposed.

The Kobayashi model is very similar to that he suggested for FPL etched surfaces, except that the porous layer in the anodic film is considerably thicker.

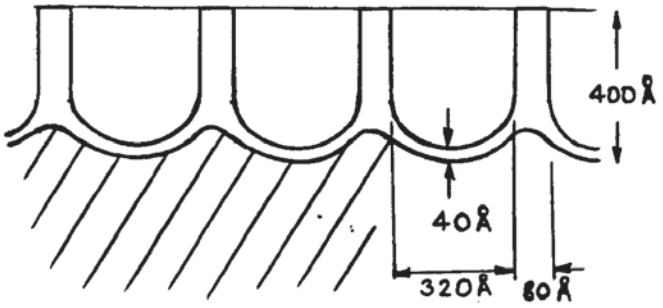

(a) F.P.L. etch.

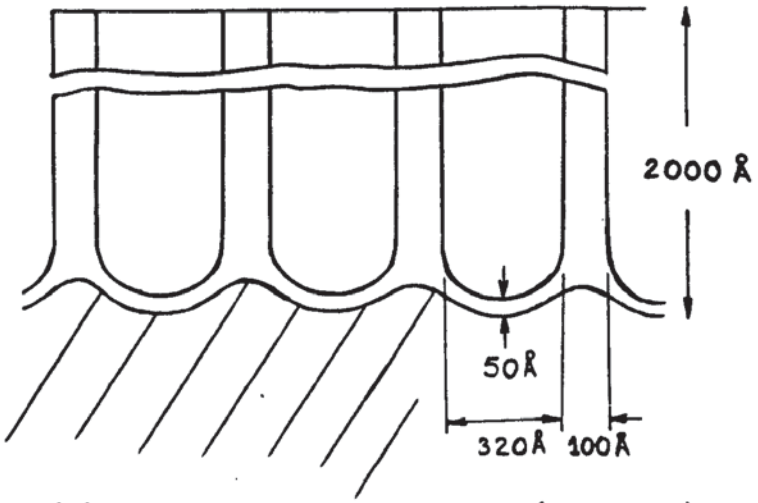

(b) Phosphoric acid anodise (BAC 5555)

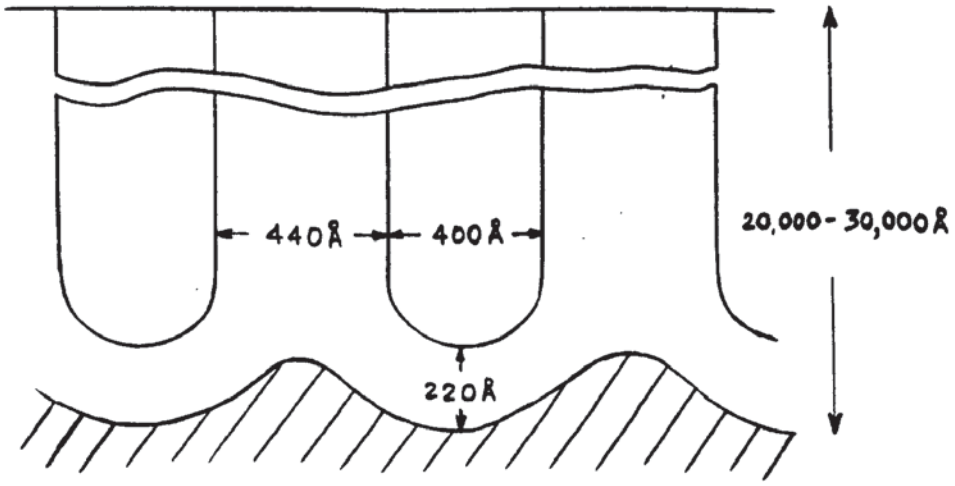

(c) Chromic acid anodise (22 volts)

Fig 5.4. Oxide structures (after Kobayashi, Donnelly [325], and McMillan [310])

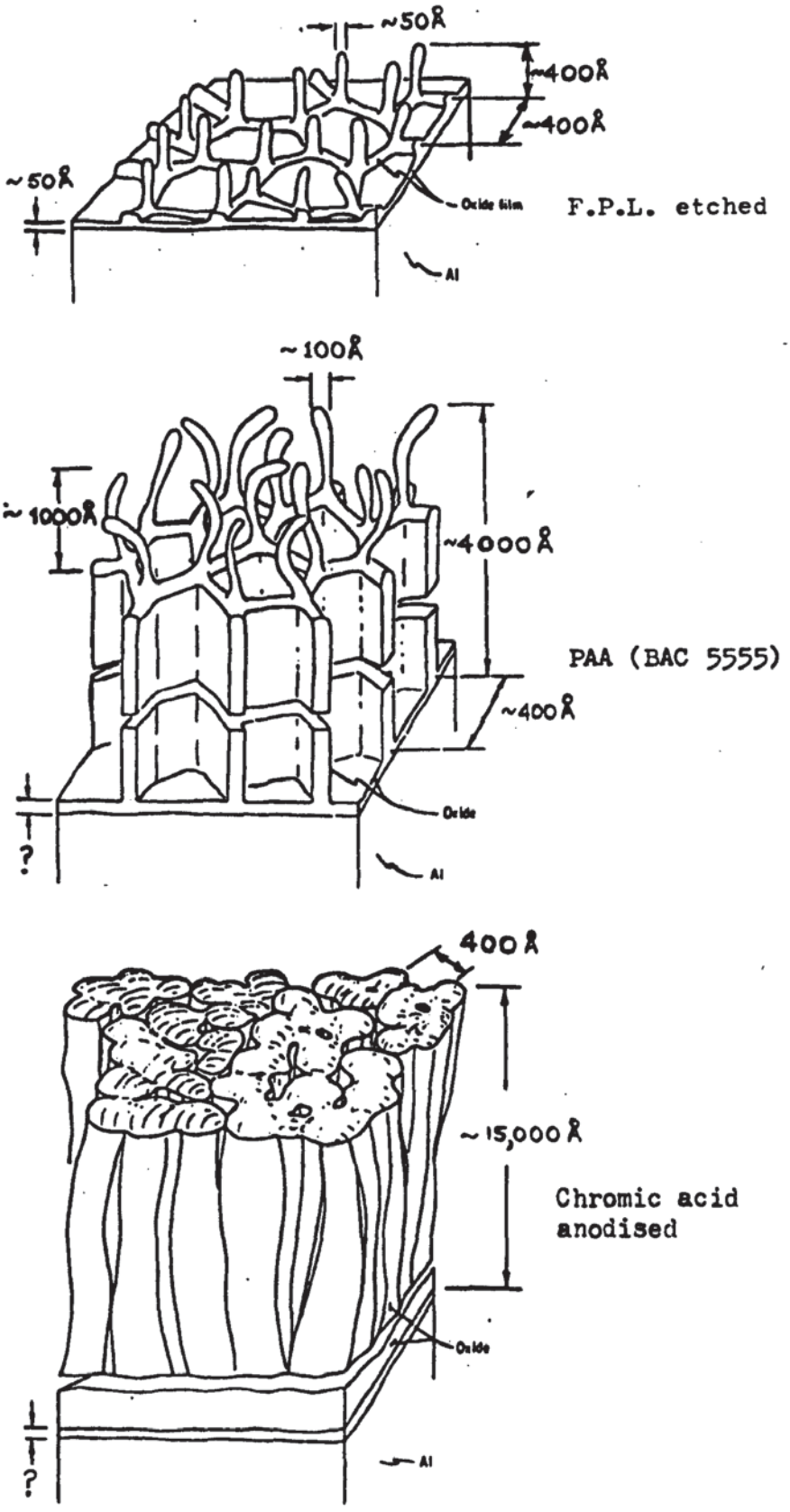

Fig. 5.5. Oxide structures (after Venables [312])

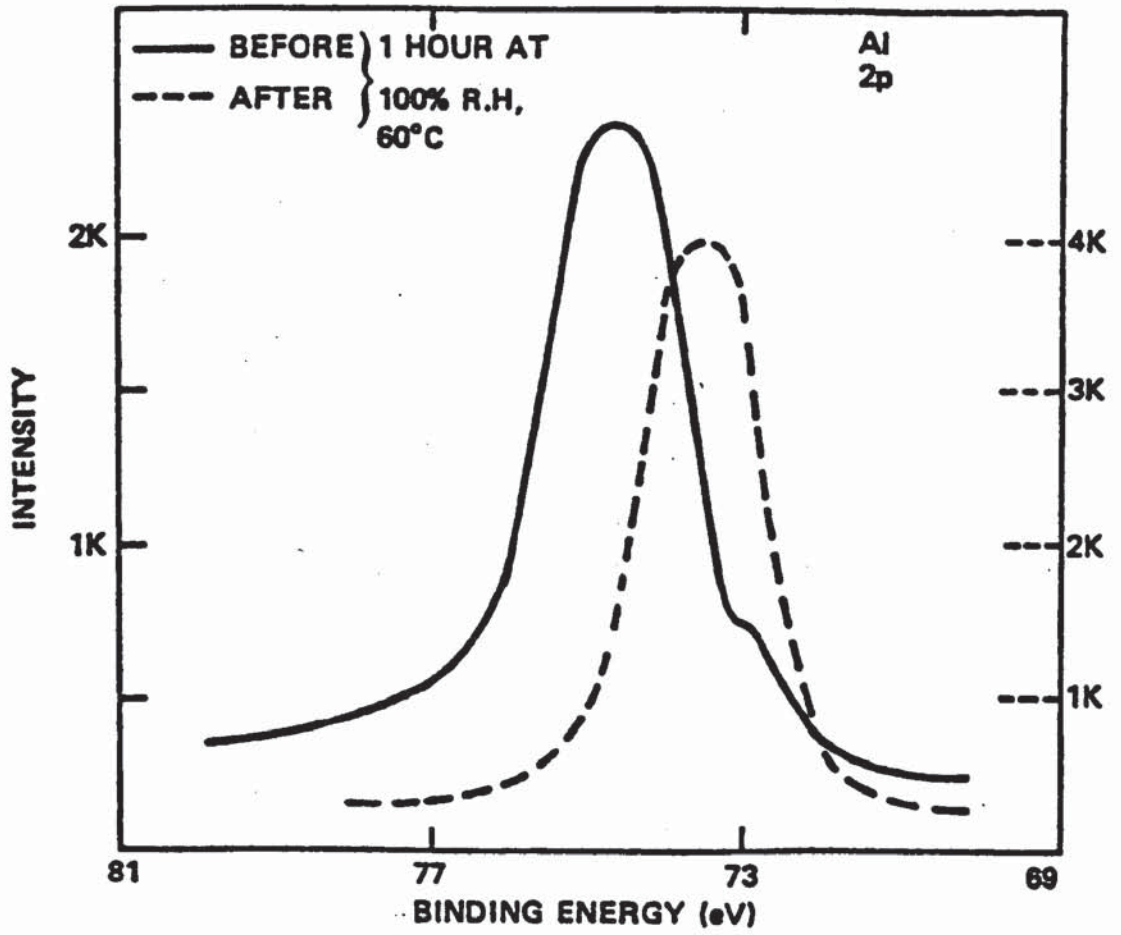

Fig. 5.6. X-ray photoelectron spectra of FPL etched 2024 aluminium alloy (after Noland [292])

Examinations [312] by STEM, however, has revealed the existence of 1000 Å long oxide whiskers protruding from a highly developed cellular oxide structure approximately 3000Å thick.

Thompson, Furneaux and Wood [326] studying comparable porous anodic films on aluminium, have established that the cell boundary bands consist of relatively pure alumina, whilst

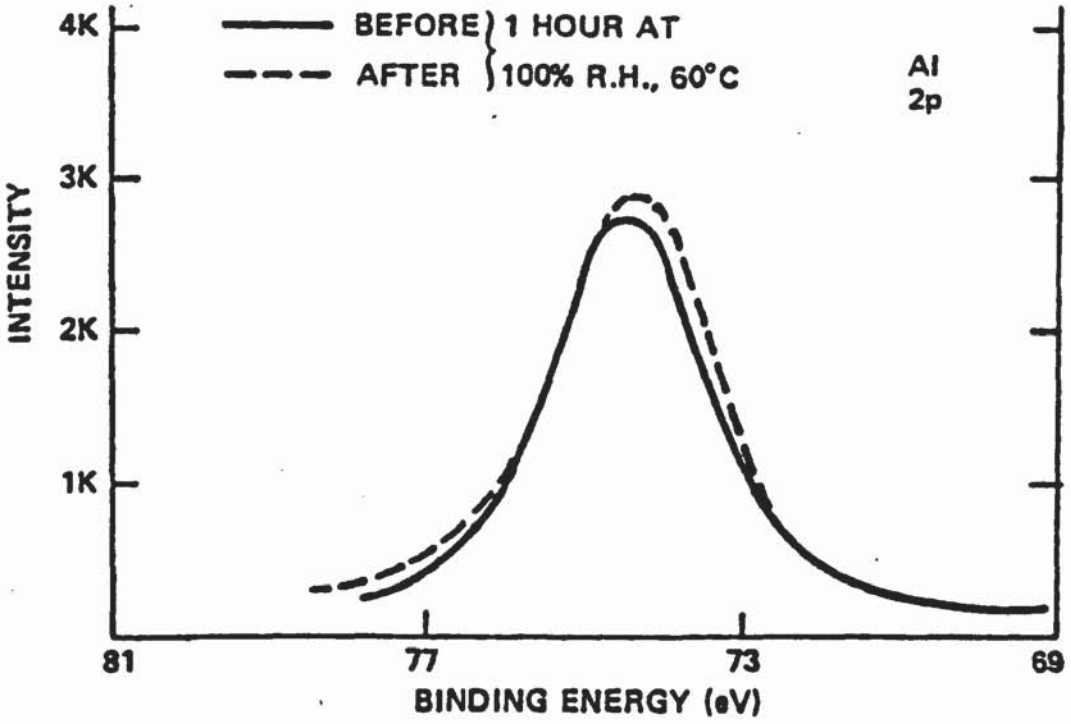

Fig. 5.7. X-ray photoelectron spectra of phosphoric acid anodised 2024 aluminium alloy. (after Noland [292])

adjacent cell material incorporates phosphate derived from the anodising electrolyte. The good durability of bonds to surfaces anodised by the BAC 5555 process is generally attributed to the high resistance of the anodic film to hydration conferred by the incorporation of phosphate ions into the oxide. Figs. 5.6 and 5.7 illustrate the differences in resistance to hydration of phosphoric acid anodised and FPL etched surfaces.

5.3.3 Chromic acid anodising

The chromic acid anodising process is favoured where, in addition to the need for durable bonds, a corrosion resistance requirement exists. McMillan et al [310] have suggested an oxide morphology of the type shown in Fig. 5.4. (c) i.e. a thick walled cellular structure formed over a substantial barrier layer. The dimensions quoted are for a film formed at 22 volts.

More recently Venables [312] has examined, using scanning transmission electron microscopy, films formed under anodising conditions which more closely approximates to the Stuart - Bengough process and reports the much denser structure shown in Fig. 5.5. (c).

The chromic acid anodic film originally studied lacked the oxide protrusions observed on FPL etched and PAA surfaces, but their existence on CAA films produced under different, unspecified conditions has since been claimed.

The incorporation of chromate ions into this oxide structure is probably very limited [326].

5.3.4 Bonding characteristics

5.3.4.1 Initial strengths

It has been suggested that the oxide protrusions observed on FPL etched and phosphoric acid anodised surfaces should provide a high degree of mechanical interlocking with the adhesive and enhanced bond strengths. Thompson and Heaton [327] using a room temperature curing epoxide and a variety of alloy types have measured peel strengths to PAA surfaces which were generally double those obtained by chromic acid anodising. Further evidence of the value of these protrusions has been reported [312]; reductions in peel strength by an order of magnitude were detected after the chemical removal of oxide whiskers from an FPL etched surface. It has also been proposed [312] that the more highly developed oxide structure of this type of anodic film should interlock even more effectively than the FPL etch morphology and result in higher bondstrengths. Comparisons based on lap shear joints however have shown identical strengths for FPL etched and PAA surfaces. Some of the initial strength data presented in Chapter 4 is reproduced in Table 5.2. Comparisons should strictly be confined to results within a given experiment to ensure freedom from the effects of adhesive batch variations and differences in test temperature. Nevertheless, the initial strengths exhibit a low sensitivity to surface treatment.

Generally, phosphoric acid anodising to the BAC 5555 specification yields bonds which are the equal to, or

Table 5.2. Initial strengths of bonds as a function of surface treatment.

Ref.Table No.	Alloy	Adhesive	Pretreatment	Initial strength, MPa
4.1.4	2117	EC 2214	Optimised FPL etch	19.0 ± 1.7
4.1.5	2117	EC 2214	CAA (Def. Std. 151)	20.2 ± 0.9
4.1.6	2117	EC 2214	PAA (BAC 5555)	16.4 ± 1.2
4.2.1	2117	EC 2214	PAA (BAC 5555)	18.6 ± 0.9
4.3.1	2117	EC 2214	Optimised FPL etch	19.1 ± 0.3
4.3.2	2117	EC 2214	PAA (30 sec. anodise)	18.2 ± 0.8
4.3.3	2117	EC 2214	PAA (1 min. anodise)	18.4 ± 0.3
4.3.4	2117	EC 2214	PAA (2 min. anodise)	18.5 ± 1.3
4.3.5	2117	EC 2214	PAA (2 min. anodise)	18.6 ± 0.3
4.3.6	2117	EC 2214	PAA (5 min. anodise)	18.3 ± 1.0
4.3.7	2117	EC 2214	PAA (10 min. anodise)	20.8 ± 1.8
4.3.8	2117	EC 2214	PAA (20 min. anodise)	21.1 ± 1.0
4.4.1	5251	ESP 105	Deoxidise	18.9 ± 0.4
4.4.3	5251	ESP 105	Opt.FPL. + 20 min. anodise (BAC 5555)	20.1 ± 0.4
4.4.5	5251	ESP 105	Deoxidise + 20 min. anodise (BAC 5555)	21.1 ± 0.3
4.4.7	5251	ESP 105	Deoxidise + 1 min. AC PAA	20.9 ± 0.4
4.4.8	5251	ESP 105	Deoxidise + 2 min. AC PAA	21.0 ± 0.6
4.4.9	5251	ESP 105	Deoxidise + 10 sec. AC SAA	21.0 ± 0.5
4.5.1	2117	EC 2214	PAA (BAC 5555)	18.6 ± 0.8
4.5.3	2117	EC 2214	Optimised FPL etch	18.0 ± 0.5
4.5.5	2117	EC 2214	PAA (2 min. anodise)	17.4 ± 0.7
4.5.7	2117	EC 2214	Deoxidise	16.9 ± 0.3

marginally stronger than, those associated with other treatments, though in Section 4.1 the trend is reversed. Possible reasons are that the PAA and FPL morphologies observed by Venables were not produced on the alloy used, or that effective wetting and penetration by the adhesive was not achieved. Differences in failure modes of unexposed bonds to phosphoric acid anodised and FPL etched 2117 alloy surfaces have been observed in this project, as shown in Figs. 4.3.22a and 4.3.17a respectively. Bonds to the anodised material were approximately 10% stronger than those to the etched surfaces, a finding which is consistent with the previously discussed mechanical interlocking view of Venables.

Failure of these bonds to FPL etched 2117 alloy has however occurred close to the interface and within the adhesive, in constrast to the locus of failure in the anodised joints which was closer to the substrate. This behaviour in unexposed joints suggests the possibility of an interaction between the adhesive the FPL etched surface leading to the formation of a weak boundary layer. The loci of failure of bonds to surfaces which had been anodised in phosphoric acid for shorter-than-specified times exhibited combinations of the features associated with the two extremes i.e. FPL etching and phosphoric acid anodising for 20 minutes.

5.3.4.2 Bond durability

The results presented in Section 4.1 demonstrate the superiority of these three well established surface treatments over simpler, faster processes, at least when applied to 2117 alloy and exposed to

salt-spray conditions. Phosphoric acid anodising in a 10% solution at room temperature for 20 minutes at 10 volts D.C. i.e. in accordance with the BAC 5555 specification produced the most durable adhesive bonds. A relatively small difference in performance was noted between the etching and anodising treatments in chromic acid. The superiority of the PAA process over FPL etching is confirmed at the higher salt-spray temperature of 43°C, as shown in Section 4.3.

The behaviour of the FPL etched joints is characterised by a rapid loss of strength and bond line corrosion, increasing in severity, after 3 months exposure to these conditions. Areas of the bond line which were free of signs of corrosion exhibited a locus of failure within the adhesive but very close to the interface, as in the unexposed specimens tested. In contrast, the loci of failure of bonds to phosphoric acid anodised surface could not be established by optical means and may have occurred at, or extremely close to, the adhesive/oxide interface or within the oxide itself. The possibilities of wicking along the interface, or the existence of water distributions along the z-axis, both of which are pretreatment dependent, must always be considered.

In the case of anodising to BAC 5555 and the FPL etch, the loci of failure did not appear to change during environmental exposure, and appreciable losses in retained strength were not discernible until bond line corrosion in the FPL etched specimens developed. The delay in the development of bond line corrosion implies that the effect follows, rather than precedes, the debonding process.

The initial loss of adhesion could be due to the desorption of the adhesive by water or the hydration of the aluminium oxide. The very rapid strength loss occurring after bond line corrosion is first observed suggests that the formation of corrosion products accelerates the debonding process. Although general adherend corrosion also occurred on PAA specimens, no visible signs of corrosion in the bond line were apparent. Durability testing of bonds to chromic acid anodised surfaces was limited to 2117 alloy and salt-spray at 35°C. Under these conditions this, the most corrosion-inhibiting treatment of the three established processes investigated, yielded the least durable bonds.

5.4 Rapid treatments

The proprietary chromate treatments described in Section 4.1 vary in reactivity to the aluminium oxide surface.

Bonderite 714 is the most aggressive of the three processes investigated, and contains hexavalent chromium, nitrate and fluoride ions.

Bonderite 1415 is more complex, containing both hexavalent and trivalent chromium, phosphate ions and silica.

Accomet C contains only hexavalent and trivalent chromium ions and silica.

These last two treatments are non-rinse types and are intended to produce an insoluble film on drying. Silica is present to provide the flow properties required to maintain a film on the surface.

The performances of these treatments for structural bonding purposes was found to be markedly inferior to those of the established processes previously discussed.

Tested on 2117 alloy, phosphoric acid anodising for times shorter than the 20 minutes specified in BAC 5555 resulted in serious losses in bond durability. Indeed, the bonding qualities of the FPL etch are impaired by subsequent anodising for up to 2 minutes. Nevertheless, although the process conditions described in the above specifications have been chosen for optimum bonding performance, some scope may exist for reducing anodising time if other process parameters are changed. The growth, and chemical modification, of oxide structures in separate process stages warrants further study. The results in Section 4.7. are encouraging in that the bonds to the triethyl phosphate treated anodic film always failed cohesively and retain higher levels of strength. Longer exposures are required, in conjunction with careful analysis of fracture surfaces, in order to determine whether the improvement in bond durability is due to the enhanced hydration resistance of the oxide or to a modification of the adhesive.

After this experi ment was initiated, a recently published patent [331] was received which describes a similar principle. It recommends the application of amino phosphonate compounds such as nitrilotris (methylene) triphosphonic acid $N\left[CH_2PO(OH)_2\right]_3$ to aluminium surfaces to inhibit hydration of the oxide.

5.5 Adhesive stability

Bonded joints, even in the absence of losses of interfacial adhesion, are subject to changes in strength as a result of water absorption by the adhesive.

Kerr et al [332] finding that joints recovered up to 85% of their original strength after drying under vacuum for 24 hours @ 90°C., postulated that this recovery was due to the reforming of hydrogen bonds. Irreversible strength losses were attributed to the hydrolysis of covalent bonds in a boundary layer. They suggested that the formation of a boundary layer was due to the orientation of polar groups near the adherend surfaces, resulting in a boundary layer with a higher concentration of unreacted or partly reacted functional groups than in the bulk polymer.

They then proposed a mechanism of failure whereby water accumulates at hydrophilic centres in the boundary layer and interferes with metal oxide/adhesive and adhesive/adhesive hydrogen bonds, thus weakening the boundary layer. Stress-hydrolysis of covalent bonds in the weakened boundary layer was then thought to occur. For example, the authors postulated that hydrolysis of C-N bonds was the most likely, as shown in Fig. 5.8. Comyn [301] has reported a good correlation of bond strength loss to fractional water uptake, as shown in Fig 5.9. Considering the non-uniformity of both the water concentrations and the applied stresses in single lap joints the correlation is remarkable.

The results presented in Section 4.4 show, in the test environments used, that the durability of bonds to 5251 alloy was almost independent of the type of pretreatment employed.

It is probable that the durability of these bonds is primarily a function of water uptake as in Fig. 5.9.

This simple approach cannot however be applied in the case of 2117 alloy in corrosive environments in view of the vastly differing performances that have been observed.

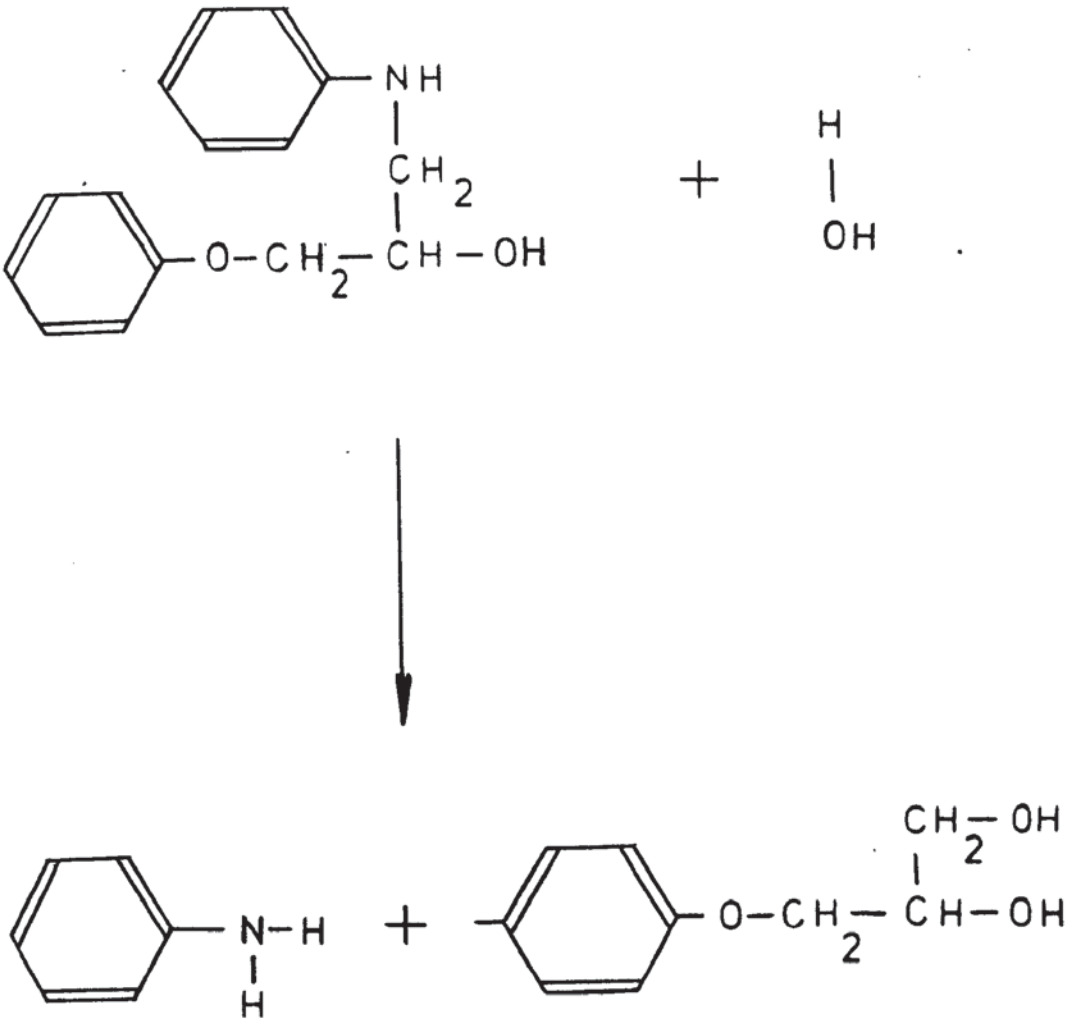

Fig. 5.8 Hydrolysis of an epoxide resin (after Kerr et al [332])

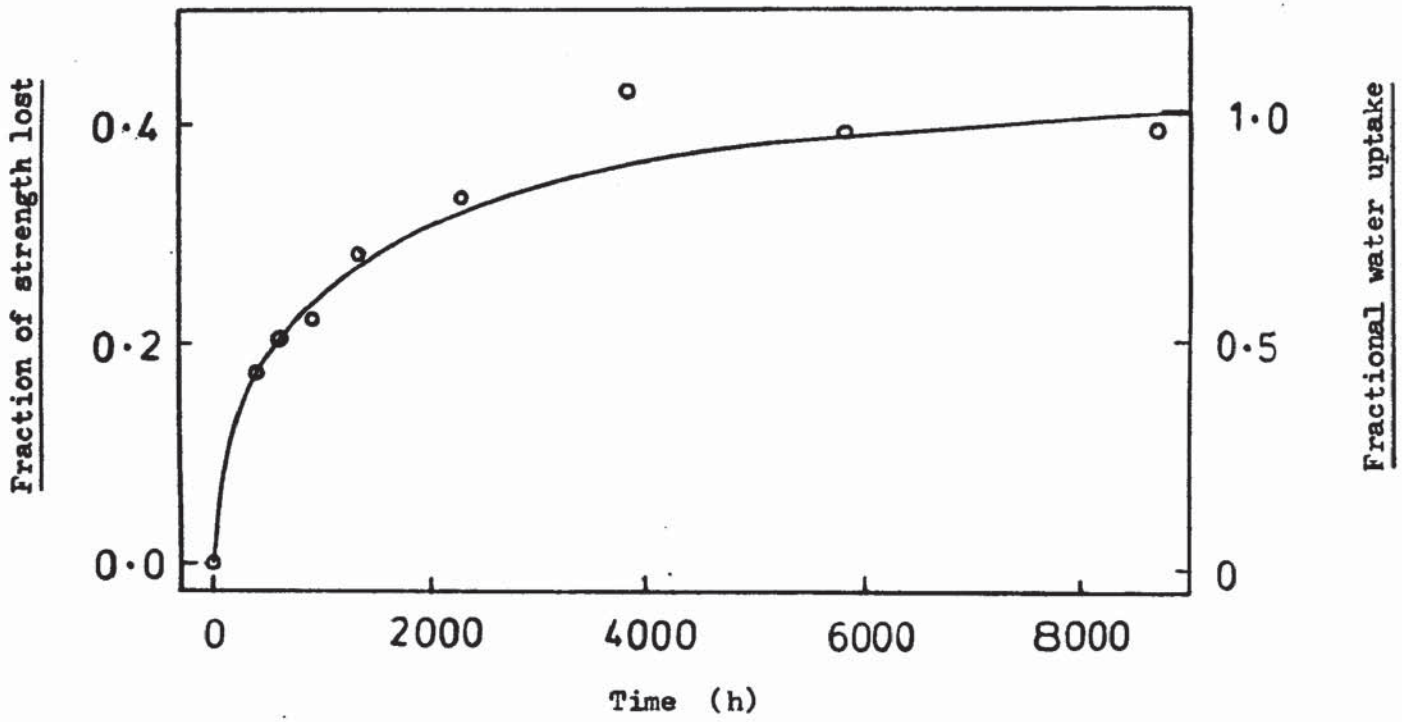

Fig. 5.9 Comparison of the strength of etched joints (301) (experimental points) with uptake of water (calculated line)

6. Conclusions

1. A new perforated lap shear test has been designed which considerably increases the rate of adhesive bond degradation, and which has been found to discriminate between different bonding systems in markedly shorter times.
2. Stress-humidity testing, using perforated lap shear specimens, has been developed and now achieves discrimination between bonding systems, where it was impossible in previous tests.
3. Loss of adhesive bond strength is primarily effected by water.
4. In some cases (e.g. with 2117 alloy) the presence of sodium chloride in solution influences the rate of bond failure after its initiation by water.
5. The pretreatment which gave the most durable bonds was the Boeing BAC 5555 process based on anodising in phosphoric acid.
6. Using the BAC 5555 pretreatment a structural bond will survive long periods of contact with many aqueous and organic fluids. Failure of the adhesive bond eventually occurs as a result of water absorption and the consequent reduction in cohesive strength of the adhesive.
7. Anodising times shorter than specified by BAC 5555 markedly reduce the durability of bonds to 2117 alloy using EC 2214 adhesive.

8. Rudimentary pretreatments are much more effective on 5251 alloy than on 2117 alloy in promoting bond durability in corrosive environments.

9. Rapid but effective pretreatments may be developed based on the growth and chemical modification of aluminium oxide in separate process stages.

7. Future work

1. Using the perforated lap shear joint configuration, establish the effects of stress combined with high relative humidity on adhesive bonds as a function of

   (i) applied stress

   (ii) surface treatment

   (iii) adhesive type

2. Establish a correlation between specific, severe, natural environments e.g. the hot-wet site at Innisfail, Australia, and high humidity accelerated laboratory conditions, using stressed and unstressed perforated lap shear joints.

3. Develop a perforated impact specimen configuration for the measurement of the energy absorption of degraded bonded joints.

4. Investigate alternative methods of producing perforated configurations e.g. by laser.

5. Study the long term durability effects of absorption of triethyl phosphate by anodic oxide films.

6. Establish the role of chromate, phosphate and fluoride ions in the surface treatment of aluminium. This research is already in progress supervised by Arrowsmith on a joint contract with Alcan, Blundell-Permoglaze and Metallic Protectives Limited.

7. To examine Arrowsmiths [333] novel surface treatment for aluminium and aluminium alloys prior to adhesive bonding without the need for anodising in phosphoric acid but using a controlled dip in a phosphoric acid based solution to obtain resistance to hydration and long term durability.

8. To establish the role of whisker-like structures on the surface of pretreated aluminium on the bond strength and durability of adhesive bonded joints using the techniques of Arrowsmith and Clifford [334].

REFERENCES

1. N.A.de Bruyne, Symposium on Adhesives for Structural Applications ed: M.J. Bodnar, Interscience, 1962, 1.
2. E.B. McMullon and E.W. Garnish, Metals and Materials, 1967, 1, 398.
3. P.K. Nelson and W.D. Sanders, Materials Overview for 1982, Proc. SAMPE Conf, May 1982, 967-977.
4. B.L.Technology Ltd and Permabond Adhesives Ltd, Int. J. Adhesion and Adhesives, 1983, 3, 65
5. A.J. Kinloch, J. Mat. Sci. 1980, 15, 2141.
6. A.J. Kinloch, J. Mat. Sci. 1982, 17, 617.
7. N.A. de Bruyne and R. Houwink (eds.), "Adhesion and Adhesives, Elsevier, 1951.
8. D.D. Eley (ed.), Adhesion, Oxford University Press, 1961.
9. R. Houwink and G. Salomon (eds.), Adhesion and Adhesives, Vol.1, Elsevier, 1965.
10. R. Houwink and G. Salomon (eds.), Adhesion and Adhesives, Vol.2, Elsevier, 1967.
11. J.J. Bikerman, The Science of Adhesive Joints, Academic Press, 1961 and 1968.
12. D.H. Kaelble, Physical Chemistry of Adhesion, Interscience, 1971.
13. W.C. Wake, Adhesion and the Formulation of Adhesives, Applied Science, 1976.
14. I. Skeist (ed.), Handbook of Adhesives, Van Nostrand, 1977.
15. R.L. Patrick (ed.) Treatise of Adhesion and Adhesives, Vol.1, Marcel Dekker, 1967.
16. Id., Vol.2, 1969.
17. Id., Vol.3, 1973.
18. Id., Vol.4, 1976.
19. W.D. Bascom and R.L Patrick, Adhesive Age, 1974, 17, (10), 25.
20. L.H. Sharpe and H. Schonhorn, Advances in Chemistry, 1964, 43, 189, Amer. Chem. Soc.
21. W.A. Dukes and A.J.Kinloch, Developments in Adhesives - 1, ed: W.C. Wake, Applied Science, 1977, 1, 251
22. K.L. Mittal, Adhesion Science and Technology, L.H. Lee (ed.), Plenum, 1975, 129.
23. K.L. Mittal, Polymer Eng. Sci. 1977, 17, 467.
24. Y. Iyengar and D.E. Erickson, J. Appl. Polymer Sci. 1967, 11, 2311.
25. Von G.A. Dyckerhoff and P.J. Sell, Die Angew. Makromol, Chemie, 1972, 21, 169
26. J.R. Huntsberger, Treatise on Adhesion and Adhesives, ed: R.L. Patrick, Marcel Dekker, 1967, 1, 119.
27. W.D. Bascom and R.L. Patrick, Adhesives Age, 1974, 17, (10), 25.
28. W.D. Bascom, R.L. Cottington and C.R. Singleterry, Advances in Chemistry, Amer.Chem.Soc. 1964, 43, 355.
29. R.L. Cottington, C.M. Murphy and C.R. Singleterry, Advances in Chemistry, Amer.Chem.Soc. 1964, 43, 341
30. G.D. Cheever, Interface Conversions for Polymer Coatings, Ed: P. Weiss and G.D. Cheever, Elsevier, 1968, 150.
31. R.N. Wenzel, Ind.Eng.Chem. 1963, 28, 988.
32. F.E. Bartell and J.W. Shepard, J.Phys.Chem. 1953, 57, 211.
33. Id., 1953, 57, 455.
34. R.E. Johnson and R.H. Dettre, Advances in Chemistry, Amer.Chem.Soc. 1964, 43, 112.
35. Id., 1964, 43, 137.

36. A.W.Neumann and R.J.Good, J.Colloid Interf. Sci. 1972, 38, 341.
37. J.C. Oliver,C.Huh and S.G. Mason, J.Adhesion 1977, 8, 223
38. N.A.deBruyne, Aero Research Technical Notes, 1956,(168), 1.
39. G.Z. Friz, Z. Angew. Phys, 1965, 19, 374.
40. A.M. Schwartz and S.B. Tegada, J. Colloid Interf.Sci.1972,38,359.
41. H. Schonhorn,C.Frisch and T.K.Kwei, J.Appl.Phys. 1966, 37, 4967.
42. B.W. Cherry and C.M. Holmes, J. Colloid Interf.Sci. 1969, 29, 174.
43. B.W. Cherry, S.El Muddaris and C.M. Holmes, J. Australian Inst. Met. 1969, 14, 174.
44. S. Newman, J. Colloid Interf.Sci. 1968, 26, 209.
45. B.W. Cherry and S.El Muddaris, J. Adhesion 1970, 2, 42.
46. W.D. Bascom and R.L. Cottington, J. Adhesion 1972, 4, 193.
47. F.P. Bowden and W.R. Throssell, Proc.Roy.Soc. 1951, A209, 297.
48. A.I. Bailey and S.M. Kay, Proc.Roy.Soc. 1967, A301, 47.
49. M. Gettings, F.S. Baker and A.J. Kinloch, J.Appl.Polymer Sci. 1977 21, 2375.
50. M.K. Bernett and W.A. Zisman, J. Colloid Interf.Sci. 1968, 28, 243.
51. R.A. Gledhill, A.J. Kinloch and S.J. Shaw, J. Adhesion 1977, 9, 81.
52. H. Schonhorn, J.Polymer Sci. 1963, A1,2343.
53. H. Schonhorn, J.Colloid Sci. 1963, 18,445.
54. H. Schonhorn and H.L. Frisch, J. Polymer Sci. Polymer Phys.Ed. 1973, 11, 1005.
55. W.C. Wake, Adhesion and the Formulation of Adhesives, Applied Science, 1976, 93.
56. A. Baszkin and L.Ter-Minassian-Saraga, Polymer, 1978, 19, 1083.
57. A. Baszkin, M. Nishino and L.Ter-Minassian-Saraga, J. Colloid Interf. Sci. 1977, 59, 516.
58. A. Baszkin, M. Nishino and L.Ter-Minassian-Saraga, J. Colloid Interf. Sci. 1967, 54, 317.
59. E.M. Borroff and W.C. Wake, Trans.Inst.Rubber.Ind. 1949, 25,190.
60. Id., 1949, 25, 199.
61. Id., 1949, 25, 210.
62. W.C. Wake, Adhesion and the Formulation of Adhesives, Applied Science, 1976, 272.
63. K. Kato, Polymer 1967, 8, 33.
64. Id., 1968, 9, 419.
65. M.Matsunaga, Y.Haguida and K.Ito, Met.Fin. 1968, 66, (11), 80.
66. K. Heynmann, Production Finish, 1966, 19, 38.
67. A. Rantell, Trans.Inst.Met.Fin. 1969, 47, 197.
68. J.M. Sykes and T.P. Hoar, J. Polymer Sci. 1969, A1, 1385.
69. I.A.Abu-Isa, J.Appl.Polymer Sci. 1971, 15, 2865.
70. R. Roberts, F.W. Ryan, H. Schonhorn, G.M. Sessler and J.E. West, J. Appl. Polymer Sci. 1976, 20, 255.
71. L.E. Perrins and K. Pettett, Plastics and Polymers 1971, 39, 391.
72. D.J. Arrowsmith, Trans.Inst.Met.Fin. 1970, 48, 88.
73. E.H. Andrews and A.J. Kinloch, Proc.Roy.Soc. 1973, A332, 385.
74. Id., 1973, A332, 401.
75. A.N. Gent and J. Schultz, J.Adhesion 1972, 3, 281.
76. W.C. Wake, Adhesion and the Formulation of Adhesives, Applied Science, 1976, 69.
77. D.E. Packham, K. Bright and B.W. Malpass, J.Appl.Polymer Sci. 1974, 18, 3237.
78. Id., 1974, 18, 3249.
79. J.R.Evans and D.E. Packham, Adhesion-1, Ed: K.W. Allen, Applied Science, 1977, 297.

80. J.R. Evans and D.E. Packham, J. Adhesion 1978, 9, 267.
81. Id., 1979, 10, 39.
82. Id., 1979, 10, 177.
83. C.E. Jennings, J.Adhesion 1972, 4, 25.
84. C.W. Jennings Appl.Polymer Symp. 1972, 19, 49.
85. W.D. Bascom, C.O. Timmons and R.L. Jones, J.Mat.Sci. 1975, 19,1037.
86. D.R. Mulville and R. Vaishnav, J.Adhesion 1975, 7, 215.
87. H.E. Bair, S. Matsuoka, R.G. Vadimsky and T.T. Wang, J.Adhesion, 1971, 3, 89.
88. T.T. Wang and H.N. Vazirani, J.Adhesion, 1972, 4, 353.
89. S.S. Voyutskii, Autohesion and Adhesion of High Polymers, Interscience, 1973.
90. J.N. Anand and H.J. Karam, J.Adhesion 1969, 1, 16.
91. J.N. Anand and R.Z. Balwinski, J.Adhesion 1969, 1, 24.
92. J.N. Anand, J.Adhesion 1969, 1, 31.
93. J.N. Anand and L. Dipzinski, J.Adhesion 1970, 2, 16.
94. J.N. Anand, J.Adhesion 1970, 2, 23.
95. R.M. Vasenin, Adhesion, Fundamentals and Practice, McLaren, 1969,29.
96. R.M. Vasenin, Adhesives Age 1965, 8, (5), 21.
97. R.M. Vasenin, Adhesives Age 1965, 8, ( ), 30.
98. R.P. Campion, J.Adhesion 1975, 7, 1.
99. R.P. Campion, Adhesion-1 Ed: K.W. Allen, Applied Science, 1977, 63.
100. F. Bueche, W.M. Cashin and P. Debye, J.Chem.Phys. 1952, 20, 1950.
101. S.E. Bresler, G.M. Zakharov and S.V. Kirillov, Vysok.Soed, 1961, 3, 1072.
102. S.S. Voyutskii, J.Adhesion 1971, 3, 69.
103. L.P. Morozova and N.A. Krotova, Dokl.Akod.Nauk.SSSR 1957,115,747.
104. L.P. Morozova and N.A. Krotova, Kolloid Zh. 1958, 20, 59.
105. N.A. Krotova and L.P.Morozova, DoklAkod,Nauk,SSSR 1959, 127, 141.
106. B.V. Deryaguin,Research 1955, 8, 70.
107. B.V. Deryaguin, N.A. Krotova, V.V. Karassev, Y.M. Kirillova and I.N. Aleinikova, Proc.2nd Int.Cong.Surface Activity, Butterworths, 1957, 417.
108. S.M. Skinner, R.L. Savages and J.E. Rutzler, J.Appl.Phys. 1953, 24, 439.
109. A. Roberts, Adhesion-1 Ed: K.W. Allen, Applied Science, 1977, 207.
110. D.M. Mattox, J.Vac.Sci.Technol. 1973, 10, 47.
111. C.T.H. Stoddart, D.R. Clarke, and C.J. Robbie, J.Adhesion 1970,2,241.
112. D.G.Teer, B.L.Delcea and A.J.Kirkham, J.Adhesion 1976, 8, 171.
113. D.G.Teer, J.Adhesion 1977, 9, 289.
114. W.C.Wake, Polymer 1978, 19, 291.
115. J. Krupp and W.Schnabel, J.Adhesion 1973, 5, 296.
116. W.Schnabel, Physics of Adhesion, Ed: R.Polke and P.Hohn, Universitat Karlsruhe, 1969, 102.
117. C.Kemball, Adhesion, Ed. D.D.Eley, OUP, 1961, 19.
118. A.J.Staverman, Adhesion and Adhesives, Ed: R. Houwink and G.Salomon, Elsevier, 1965, 1, 9.
119. W.C.Wake, Royal Institute of Chemistry Lecture Series, 1966, 4, 1.
120. J.R. Huntsberger, Adhesives Age, 1970, 13, (11), 43.
121. E.Orowan, J.Franklin Inst. 1970, 290, 493.
122. D.Tabor, Rep.Prog.Appl.Chem. 1951, 36, 621.
123. E.H.Andrews and A.J.Kinloch, J.Polymer Sci.Polymer Phys. 1973,11,269.
124. E.H.Andrews and A.J.Kinloch, J.Polymer Sci.Sympos. 1974, 46, 1.
125. A.N.Gent and A.J.Kinloch, J.Polymer Sci. 1971, A2, 659.
126. E.H.Andrews, J.Mat.Sci. 1974, 9, 887.
127. L.Pauling, The Nature of the Chemical Bond, Cornell, 1960.
128. R.J. Good, Treatise on Adhesion and Adhesives, Ed: R.L. Patrick, Marcel Dekker, 1967, 1, 15.

129. W.H.Pritchard, Aspects of Adhesion-6, Ed: D.J.Alner, University of London Press, 1970, 11.
130. R.A.Gledhill, A.J.Kinloch and S.J.Shaw, J.Adhesion 1977, 9, 81.
131. B.Leclerq, M.Sotton, A.Baszkin and L.Ter-Minassian-Saraga, Polymer 1977, 18, 675.
132. D.K.Owens, J.Appl.Polymer Sci. 1975, 19, 265.
133. Id., 1975, 19, 3315.
134. A.R. Blythe, D.Briggs, C.R.Kendall, D.G.Rance and V.J.I.Zichy, Polymer, 1978, 19, 1273.
135. A.Baszkin and L.Ter-Minassian-Saraga, Polymer 1978, 19, 1083.
136. F.M. Fowkes, Recent Advances in Adhesion, Ed: L.H. Lee, Gordon and Breach, London, 1973, 39.
137. J.C.Bolger and A.S.Michaels, Interface Conversions for Polymer Coatings, Ed: P.Weiss and G.D.Cheever, Elsevier, 1968, 3.
138. N.J.deLollis, Adhesives Age 1968, 11, (12), 21.
139. Id., 1969, 12, (1), 25.
140. J.E.Rutzler, Adhesives Age 1954, 2, (7), 28.
141. A.I.Vilenskii, E.E.Virlich and N.A.Krotova, Soviet Plastics 1973, 5, 68.
142. G.E.Koldunovich, V.G.Ephstein and A.A.Chekanova, Soviet Rubber Technol. 1970, 29, 22.
143. E.B.Trostyanskaya, G.S.Golovkin and G.V.Komarov, Soviet Rubber Technol. 1966, 25, 13.
144. R.B.Dean, Official Digest 1964, 36, 664.
145. A.Ahagon and A.N.Gent, J. Polymer Sci.Polymer Phys. 1975, 13, 1285.
146. A.N.Gent and E.C.Hsu, Macromolecules, 1974, 7, 933.
147. C.H.Lerchenthal, M.Brennan and N.Yits'haq, J.Polymer Sci. Polymer Chem. 1975, 12, 737.
148. C.H.Lerchenthal and M.Brennan, Polymer Eng.Sci. 1976, 16, 747
149. Id., 1976, 16, 760.
150. J.L.Koenig and P.T.K.Shih, J. Colloid Interf.Sci. 1971, 36, 247.
151. R.Bailey and J.E.Castle, J.Mat.Sci. 1977, 12, 2049.
152. M.Gettings and A.J.Kinloch, J.Mat.Sci. 1977, 12, 2511.
153. M.Gettings and A.J.Kinloch, Surf.Interference Analysis 1980, 1, 189.
154. F.Hauserman, Adv.Chem.Ser. 1959, 23, 338.
155. E.P. Plueddeman, J.Adhesion 1970, 2, 184.
156. P.E. Cassidy and B.J.Yager, J.Macromol.Sci.Revs.Polym.Technol. 1971, D1, 1.
157. P.E. Cassidy, J.M.Johnson and G.C.Rolls, Ind.Eng.Chem.Prod.Res. Devel. 1971, 11, 170.
158. W.A.Zisman, Ind.Eng.Chem.Prod.Res.Devel. 1969, 8, 99.
159. S.Sterman and J.G.Marsden, Ind.Eng.Chem. 1966, 58, 33.
160. M.C.Polniaszek and R.H.Schaufelberger, Adhesives Age 1968, 11, (7), 25.
161. F.O. Swanson and S.J.Price, Adhesives Age 1973, 16, ( ), 23.
162. W.D.Bascom, J.Colloid Interf.Sci. 1968, 27, 789.
163. W.D.Bascom, Macromolecules 1972, 5, 792.
164. W.A.Dukes, R.A.Gledhill and A.J.Kinloch, Adhesion Science and Technology, Ed: L.H.Lee, Plenum, 1975, 597.
165. H.T.Chu, N.K.Eib, A.N.Gent and P.N.Henriksen, Advances in Chemistry Series, Amer.Chem.Soc. 1979, 174, 87.
166. J.R.Huntsberger, J.Polymer Sci. 1963, A1, 1339.
167. S.S.Voyutskii, Mekhanika Polimerou 1966, 2, 728.
168. V.E.Gul, Vysokmol,Soed. 1962, 4, 294.
169. S.S.Voyutskii, Yu.I.Markin, V.M.Gorchavkoa and V.E.Gul, Adhesives Ages 1965, 8, (11), 24.

170. W.T.M.Johnson, Official Digest 1961, 33, 1489.
171. M.Toryama, T.Ito and H.Moriguchi, J.Appl.Polymer Sci. 1970,14,2295.
172. H. Foulkes, J. Shields and W.C. Wake, J.Adhesion 1970, 2, 254.
173. D. Briggs, D.M.Brewis and M.B.Konieczo, J.Mat.Sci., 1976, 11, 1270.
174. D.M.Brewis, M.B.Konieczo, and D.Briggs, Adhesion-2, Ed: K.W.Allen, Applied Science, 1978, 77.
175. R.J.Good, J.Adhesion 1972, 4, 133.
176. H.Schonhorn and R.H.Hansen, J.Polymer Sci. 1966, B4, 203.
177. H.Schonhorn and R.H.Hansen, J.Appl.Polymer Sci. 1967, 11, 1461.
178. H.Schonhorn, Adhesion, Fundamentals and Practice, McLaren and Son, London, 1969, 12.
179. H.Schonhorn and R.H.Hansen, Adhesion, Fundamentals and Practice, McLaren and Son, London, 1969, 22.
180. H.Schonhorn, F.W.Ryan and R.H.Hansen,J.Adhesion, 1970, 2, 93.
181. H.Schonhorn and F.W.Ryan, J.Polymer Sci. 1969, A27, 105.
182. H.Schonhorn, Polymer Surfaces, Ed: D.T.Clark and W.J.Feast, John Wiley, 1978, 213.
183. H.Schonhorn, J.Polymer Sci. 1968, A26, 231
184. K.Hara and H. Schonhorn, J.Adhesion 1970, 2, 100.
185. H. Schonhorn and R.H.Hansen, J.Appl.Polymer Sci. 1968,12,1231.
186. S.L.Vogel and H.Schonhorn, J.Appl.Polymer Sci. 1979, 23, 495.
187. B.W.Malpass and K.Bright, Aspects of Adhesion-5, Ed: D.J.Alner, University of London Press, 1969, 214.
188. R.R.Sowell, N.J.deLollis, J.N.Gregory and O.Montoya, J.Adhesion 1972, 4, 15.
189. N.J.deLollis, Rubber Chem.Technol. 1973, 46, 549
190. G.C.S.Collins, A.C.Lowe and D.Nicholas, Euto.Polym.J. 1973,9,1173.
191. D.W.Dwight and W.M.Riggs,J.Colloid Interf.Sci. 1974, 47, 650.
192. D.W.Dwight, J. Colloid Interf.Sci. 1977, 59, 447.
193. D.Briggs, D.M.Brewis and M.B.Konieczko, J.Mat.Sci. 1977, 12, 429.
194. D.Briggs, D.M.Brewis and M.B.Konieczko, Euro.Polym.J. 1978,14,1.
195. L.J.Hart-Smith, Developments in Adhesives-2, Ed: A.J.Kinloch, Applied Science, 1981, 1.
196. R.D.Adams, Developments in Adhesives-2, Ed: A.J.Kinloch, Applied Science, 1981, 45.
197. N.L.Harrison and W.J.Harrison, J.Adhesion 1972, 3, 195.
198. O.Volkersen, Luftfahrtforsch, 1938, 15, 41.
199. M.Goland and E.Reissner, J.Appl.Mech. 1944, 2, A-17.
200. C.Mylonas, Proc.Soc.Exp.Stress Anal. 1954, 12, 129.
201. I.Seddon, Adhesion, Ed: D.D.Eley, OUP, 1961, 207.
202. L.Greenwood, Aspects of Adhesion-5, Ed: D.J.Alner, University of London Press, 1970, 40.
203. R.D.Adams, S.H.Chambers, P.J.A.Del Strother and N.A.Peppiatt, J.Strain Anal. 1973, 8, 52.
204. R.D.Adams and N.A.Peppiatt, J.Strain Anal. 1973, 8, 134.
205. R.D.Adams and N.A.Peppiatt, J.Strain Anal. 1974, 9, 185.
206. R.D.Adams, J. Coppendale and N.A.Peppiatt, Adhesion-2. Ed: K.W.Allen, Applied Science, 1978, 105.
207. W.J.Renton and J.R.Vinson, J.Adhesion 1975, 7, 175.
208. W.J.Renton and J.R.Vinson, Eng.Fract.Mechs 1975, 7, 175.
209. W.J.Renton and J.R.Vinson, J.Appl. Mech. 1977, 44, 101.
210. D.J.Allman, Mechs.Appl.Maths, 1977, 30, 415.
211. D.W.Cherry and N.L.Harrison, J.Adhesion, 1970, 2, 125.
212. L.J.Hart-Smith, NASA Report No. CR-2218, 1974.

213. L.J.Hart-Smith, Douglas Aircraft Co. Report No. 6059A,1972.
214. L.J.Hart-Smith, Douglas Aircraft Co. Report No. 6224, 1974.
215. L.J.Hart-Smith, Douglas Aircraft Co. Report No. 6707, 1978.
216. L.J.Hart-Smith, Douglas Aircraft Co. Report No. 6922, 1980.
217. P.J.Grant, Jointing in Fibre Reinforced Plastics, IPC,1978,41.
218. C.Mylonas and N.A.deBruyne, Adhesion and Adhesives, Ed: N.A.deBruyne and R.Houwink, Elsevier, 1951, 91.
219. O.Ishai, D.Peretz and S.Gali, Expt.Mechs. 1977, 17, 265.
220. R.P.Penning, Engineering Sciences Data Unit, London, Report No. 78042, 1978.
221. C.Mylonas, Proc 7th Int.Cong.Appl.Mechanics, 1948, 4, 137.
222. N.J.Dellois and O. Montoya, Appl.Polym.Symp. 1972, 19, 417.
223. F.Swanson, Polym.Eng.Sci. 1977, 17, 122.
224. B.W.Cherry and K.W.Thomson, Adhesion-1, Ed: K.W.Allen, Applied Science, 1977, 251.
225. S.E.Garf, V.I.Myshko and R.A.Iuchenko, Sintez-I-Fizik-Khim-Polym. 1974, 13, 162.
226. Y.Inoue and Y.Kobatake, Appl.Sci.Res. 1958, A7, 53.
227. A.C.Elm, Official Digest 1956, 28, 752.
228. N.A.deBruyne, J.Appl.Chem. 1956, 6, 303.
229. Y.Inoue and Y.Kobatake, Appl.Sci.Res. 1958, A7, 314.
230. Y.Inoue and Y.Kobatake, Kolloid Z. 1958, 18, 18.
231. H.Danneberg, SPE J. 1965, 21, 669.
232. S.Gusman, Official Digest 1962, 34, 884.
233. J.J.Bikerman, The Science of Adhesive Joints, Academic Press, 1968, 192.
234. W.C.Wake, Trans.I.R.I. 1959, 35, 145.
235. J.A.Carlson and L.P.Sapetta, Adhesives Age 1967, 19, (12), 26.
236. M.H.Stone, Adhesion and Adhesives:Science Technology and Applications, Rubber and Plastics Institute, 1980, 101.
237. L.Greenwood, T.R.Boag and A.S.McLaren, Adhesion Fundamentals and Practice, McLaren, London, 1969, 273.
238. N.A.deBruyne, Aircraft Eng. 1944, 16, 115.
239. N.A.deBruyne, Aircraft Eng. 1944, 16, 140.
240. K. Wellinger and U.Rembold, VDI Zeitschrift, 1958,100,41.
241. J.J.Bikerman, The Science of Adhesive Joints, Academic Press, 1968, 273.
242. A.N.Gent and A.J.Kinloch, J.Polym.Sci. 1971, A29, 659.
243. E.H.Andrews and A.J.Kinloch, Proc.Roy.Soc. 1973, A332, 385.
244. E.H.Andrews and A.J.Kinloch, Proc.Roy.Soc. 1973, A332, 401.
245. E.H.Andrews and A.J.Kinloch, J.Polym.Sci.Symp. 1974, 46, 1.
246. E.H.Andrews and N.E.King, J.Mat.Sci. 1976, 11, 2004.
247. A.N.Gent, J.Polym.Sci. 1974, A2, 283.
248. D.H.Kaelble, J.Colloid Sci. 1969, 19, 102.
249. D.H.Kaelble and R.S.Reylek, J.Adhesion 1969, 1, 124.
250. A.N.Gent and R.P.Petrich, Proc.Roy.Soc. 1969, A310, 433.
251. D.W.Aubrey and M.Sherriff, J.Polym.Sci.Polym.Chem. Ed.1980, 18, 2597.
252. R.Bates, J.Appl.Polym.Sci. 1976, 20, 2941.
253. M.L.Williams, R.F.Landel and J.D.Ferry, J.Amer.Chem.Soc. 1955, 77, 3701.
254. D.W.Aubrey, Adhesion-3, Ed: K.W.Allen, Applied Science, 1979, 191.

255. J.L.Cotter, Revs.High Temp.Mat. 1973, 3, (4), 277.
256. R.E.Yaeger, Appl.Polym.Symp. 1969, 3, 369.
257. S.R.Sandler and F.R.Berg, J.Appl.Polym.Sci. 1965, 9, 3909.
258. R.A.Gledhill, A.J.Kinloch and S.J.Shaw, J.Mat.Sci. 1979, 14, 1769.
259. A.F.Lewis, R.A.Kinmonth and R.P.Kreahling, J.Adhesion 1972, 3, 249.
260. A.F.Lewis, Adhesives Age 1972, 15, (6), 38.
261. K.W.Allen and M.E.R.Shanahan, J.Adhesion 1975, 7, 161.
262. K.W.Allen and M.E.R.Shanahan, J.Adhesion 1976, 8, 43.
263. W.Spath, Adhesion 1973, 17, (10), 348.
264. V.Rayatskas and V.Pekarskas, J.Appl.Polym.Sci. 1976, 20, 1941.
265. J.P.Thomas, Appl.Polym.Symp. 1969, 3, 109.
266. W.C.Wake, K.W.Allen and S.M.Dean, Elastomers: Criteria for Engineering Design, Ed: C.Hepburn and R.J.W. Reynolds, Applied Science, 1979, 311.
267. R.A.Gledhill and A.J.Kinloch, Polymer 1976, 17, 727.
268. J.R.Romanko and W.G.Knauss, Developments in Adhesive-2, Ed: A.J.Kinloch, Applied Science, 1981, 173.
269. J.C.McMillan, Developments in Adhesives-2, Ed: A.J.Kinloch, Applied Science, 1981, 243.
270. N.J.deLollis, Adhesives Age, 1977, 20, (9), 41.
271. J.D.Minford, Adhesives Age, 1978, 21, (3), 17.
272. W.D.Bascom, Adhesives Age, 1979, 22, (4), 28.
273. R.J.Schliekelmann (Ed.), Bonded Joints and Preparation for Bonding, NATO-AGARD Lecture Series 102, 1979.
274. A.J.Kinloch, R.A.Gledhill and W.A.Dukes, Adhesion Science and Technology, Ed: L.H.Lee, Plenum, 1975, 597.
275. R.A.Gledhill and A.J.Kinloch, J.Adhesion, 1974, 6, 315.
276. M.Gettings, F.S.Baker and A.J.Kinloch, J.Appl.Polym.Sci. 1977, 21, 2375.
277. A.J.Kinloch and S.J.Shaw, Developments in Adhesives-2, Ed: A.J.Kinloch, Applied Science, 1981, 82.
278. S.Mostovoy and E.J.Ripling, J.Appl.Polym.Sci. 1979, 13, 1083.
279. R.A.Gledhill and A.J.Kinloch, Polym.Eng.Sci. 1979, 19, 82.
280. D.H.Kaelble, J.Appl.Polym.Sci. 1974, 18, 1869.
281. D.K.Owens, J.Appl.Polym.Sci. 1970, 14, 1725.
282. Y.W.Mai, J.Adhesion 1975, 7, 141.
283. A.N.Gent and J.Schultz, J.Adhesion 1972, 3, 281.
284. S.N.Zhurkov and E.E.Tomashevsky, Physical Basis of Yield and Fracture, Institute of Physics, 1966, 200.
285. S.N.Zhurkov and U.E.Korsukov, J.Polym.Sci.Polym.Phys. 1974, 12, 385.
286. D.W.Levi, R.F.Wegman, M.C.Ross and E.A.Garnish, SAMPE Q. 1971, 7, (3), 1.
287. R.A.Gledhill, A.J.Kinloch and S.J.Shaw, J.Adhesion, 1980, 11, 3.
288. W.D.Bascom, S.T.Gadomski, C.M.Henderson and R.L.Jones, J.Adhesion 1977, 8, 213.
289. F.J.Riel, SAMPE J. 1971, 7, 16.
290. J.L.Cotter, Developments in Adhesives-1, Ed: W.C.Wake, Applied Science, 1977, 1.
291. R.W.Shannon and E.W.Thrall, J.Appl.Polym.Sci. Appl.Polym. Symp. 1977, 32, 131.
292. J.S.Noland, Adhesion Science and Technology, Ed: L.H.Lee, Plenum, 1975, 413.

293. J.D.Venables, D.K.McNamara, T.S.Sun, B.Datchek and J.M.Chen, Structural Adhesives and Bonding Technology, Technical Conference Associates, El Segundo, California, 1979, 12.
294. T.S.Sun, J.M.Chen, J.D.Venables and R.Hopping, Appl.Surf. Sci. 1978, 1, 202.
295. A.J.Kinloch and N.J.Smart, J.Adhesion 1981, 12, 23.
296. J.D.Minford, Adhesives Ages 1974, 17, (7), 24.
297. J.A.Smith and W.E.Martinsen, Amer.Ceram.Soc.Bull. 1973,52,855.
298. J.Comyn, Developments in Adhesives-2, Ed: A.J.Kinloch, Applied Science,1981, 279.
299. D.M.Brewis, J.Comyn, B.C.Cope and A.C.Moloney, Polymer 1980, 21, 344.
300. J.Comyn, D.M.Brewis, R.J.A.Shalash and J.L.Tegg, Adhesion-3, Ed: K.W.Allen, Applied Science 1979, 13.
301. D.M.Brewis, J.Comyn and J.L.Tegg, Int.J.Adhes.Adhesives 1980, 1, 35.
301. D.M.Brewis, J.Comyn, B.C.Cope and A.C.Moloney, Polymer 1980, 21, 1477.
303. W.Althof, Nat. SAMPE Tech.Conf. 1979, 11, 309.
304. W.Althof, Aluminium, 1979, 55, 600.
305. D.M.Brewis, J.Comyn, A.C.Moloney and J.L.Tegg, Eur.Polym.J. 1981, 17, 127.
306. A.J.Kinloch and S.J.Shaw, Developments in Adhesives-2, Ed: A.J.Kinloch, Applied Science, 1981, 82.
307. B.W.Cherry and K.W.Thomson, Fracture Mechanics and Technology, Sijthoff and Nordoff, Netherlands, 1977, 723.
308. Y.W.Mai, J.Adhesion 1975, 7, 141.
309. E.H.Andrews and A.Stevenson, J.Adhesion 1980, 11, 17.
310. J.C.McMillan and J.T.Quinlivan, SAMPE Q. 1976, 7, (3), 13.
311. A.W.Bethune, SAMPE J. 1975, 11, (4), 4.
312. J.D.Venables, D.K.McNamara, J.M.Chen, T.S.Sun and R.L.Hopping, Appl.Surf.Sci. 1979, 3, 88.
313. W.Brockman and H.Kollek, Proc. 23rd SAMPE Symp. 1978, 1119.
314. C.J.Wood, B.L. Report MG/R 141 1978.
315. J.A.Marceau, Y.Moji, J.C.McMillan, Adhesive Age Oct.77. 28.
316. W.Brockmann, Adhesives Age, Jun.77. 30.
317. W.Brockmann, Int.J.Adhesion and Adhesives 1982, 2, 38.
318. T.Smith, J.App.Poly.Sc., 1977, 32, 11
319. J.Grant "The Mathematics of Diffusion" Oxf. Univ. Press 1967.
320. B.B.Bowen, Proc.7th Nat. SAMPE Conf. Oct 75.
321. W.T.McCarvill, J.P.Bell. J.App.Poly.Sc. 1974.18 335-349.
322. T.Smith, J.Adhesion 1977. 9 313.
323. W.J.Russell, J.App.Pol.Sc., App.Pol.Symp. 32, 105.
324. P.F.A. Bijlmer "Potentiostatic pickling as an alternative for sulfo-chromic pickling prior to adhesive bonding" Fokker VFW Report.
325. Kobayashi & Donnelly, Boeing Report DG-41517 Jan. 1974.
326. G.E.Thompson, R.C.Furneaux, G.C.Wood. Corr.Sci.1978, 18.481
327. P.J.Thompson, H.B.Heaton, Trans. I.M.F. 1980,58,81.
328. K.E.Weber, G.R.Gordon, SAMPE Qty. Oct. 1974.
329. A.Pattnaik, J.D.Meakin, Picatinny Arsenal Tech. Report 4699 July,1974.

330. W.J.Russell, SAMPE J., 1981, 17, 3, 20
331. U.S.Patent No. 4303079, Dec. 1981. Venables et al.
332. C.Kerr, N.C.MacDonald, S.Orman, Br.Poly.J.1970 2 67
333. D.J.Arrowsmith British Patent App. No. 8315203 Priority date 2.6.83.
334. D.J.Arrowsmith & A.W.Clifford. Int.J.Adhesion & Adhesives 1983, 3, 4, 193.